

DESIGN AND SYNTHESIS OF TUBULYSIN ANALOGS THAT STABILIZE AND MIMIC
A KEY ACETATE IMPORTANT FOR POTENT ANTIPROLIFERATIVE ACTIVITY
AGAINST MULTI-DRUG RESISTANT CANCERS

A DISSERTATION
SUBMITTED TO THE FACULTY OF
UNIVERSITY OF MINNESOTA
BY

MICHAEL THOMAS PETERSON

IN PARTIAL FULFILLMENT OF THE REQUIREMENTS
FOR THE DEGREE OF
DOCTOR OF PHILOSOPHY

ROBERT ANDREW FECIK, ADVISER

OCTOBER 2012

Acknowledgements

My first thanks go to my adviser, Prof. Robert Fecik, for accepting me into his lab, supporting me through his grants, and supplying me with a project that cemented my passion for the synthesis of interesting natural products for the treatment of cancer. His unending positive attitude and encouragement kept me going through many trying times. Robert's suggestions and discussions about my career direction, especially with respect to my industry internship, choice of postdoctoral appointment, and letters of reference, led to opportunities I never thought possible and that I most likely would not have attempted without his influence. The graduate students and postdocs I have shared lab space with have provided me with thoughtful discussion and companionship for many long days in front of the hood, for which I am grateful. I also thank Dr. Dan Sackett for his work determining the biological activity of my final compounds.

The faculty within the department of Medicinal Chemistry and beyond at the University of Minnesota have continuously assisted my growth as a scientist and as a person. My committee members, Profs. Gunda Georg, Rodney Johnson, and Chris Douglas, have patiently listened to my work presented throughout my tenure and have offered sound ideas for project direction. Most of the group meetings in the Fecik lab have been in conjunction with the Georg lab, where several critical issues were solved by helpful suggestions, and critical assessments of my practice talks very nicely honed my public speaking skills. Letters of reference from Profs. Georg and Johnson undoubtedly said something good, since they were highly influential in generating positive responses from my postdoctoral inquiries into top labs. All the successful HPLC purification of my final compounds was run using equipment from the lab of Prof. Rory Remmel, and I am indebted to him for this assistance. Prof. Dan Harki, whom the Fecik

lab shares lab space (and sometimes equipment), was a welcome mentor during instances of tough decisions where he was a continuously reliable source of good advice. Special thanks is extended to Prof. Patrick Hanna, who taught me an impactful lesson I will never forget about good intentions and how even the best ones can still be detrimental when teaching others. In his words, “You think you’re helping, but you’re not.”

The colleagues who I started grad school with are all extremely important and special people to me; they have helped and supported me during my entire time here. They are (in alphabetical order) Dr. Aaron Teitelbaum, Adam Benoit, Amy Doan, Bryant Gay, Dr. David Hermanson, Hailey Gahlon, and Katie Pietsch. Every one of these individuals is a friend to me in a way that is truly indescribable, and I hope to have close relationships and professional ties with them for the rest of our lives.

My wife Sarah has been incredible in believing in me, encouraging me, and putting up with me all through grad school; marrying her remains the best decision I have ever made by a vast margin. She has also given me the greatest gift of all, our beautiful son Dexter. My mom and dad have continued to be spectacular parents, always supporting me and listening to my problems well past my youth. My immediate and extended family has shown me unstopping love, and in return I hope to give them all the love I have.

This thesis and all of my graduate work was possible through laptops provided to me, out of the goodness of his heart and through God’s grace, by Charlie Neuhaus. Charlie has shown me the limitlessness of generosity, and he can be sure I will pay it forward the rest of my life.

Dedication

This thesis is dedicated to my wife Sarah. Her tireless support and sacrifice have enabled the completion of my graduate work, so it is with her that I share the accomplishments presented here.

I love you Sarah.

Abstract

Tubulysins are antimitotic natural products with potent anticancer activity against multidrug-resistant (MDR) cancer cells, acting by inhibition of tubulin polymerization. The marked difference in antiproliferative activity between tubulysins V and U exemplifies the importance of an acetate positioned alpha to the thiazole ring. However, this acetate has been shown to be labile under both acidic and basic conditions, so the effectiveness of this modification may be hindered due to this instability. Hence, the work presented here focuses on the synthesis of analogs that mimic and stabilize the acetate at this position.

Heteroatom exchange at the α -thiazole position of tubuvaline was hypothesized to increase molecular stability while maintaining observed activity by bioisosteric replacement of the tubuvaline oxygen with a nitrogen. The nitrogen-containing analogs of tubulysin V and U, N_t tubulysin V and U, were the most important targets to test the singular modification of heteroatom exchange on bioactivity and to survey molecular stability. The synthetically derived N_t tubuvaline amino acid residue was generated following a rigorously controlled Mitsunobu reaction, but difficult final stage deprotections to N_t tubulysin V suggests a lowered stability compared to tubulysin V. *N*-acylation of a penultimate tetrapeptide intermediate led to generation of N_t tubulysin U and other acylated N_t tubulysin analogs to establish a more robust SAR at the α -thiazole position. N_t Tubulysin U was found to be more stable than tubulysin U under strongly basic conditions, and upcoming biochemical evaluation will determine the effect that these modifications have on antiproliferative activity.

Investigations into the SAR at the tubuvaline α -thiazole position also included

oxygen-based analogs, where two methods for acylation of tubulysin V were exploited to generate *O*-acylated analogs with various alkyl groups. Biochemical evaluation of antiproliferative activity, along with the use of two electrophilic analogs to act as affinity labels, will survey important interactions within the tubulysin-tubulin binding site.

Table of Contents

Acknowledgements	i
Dedication	iii
Abstract	iv
Table of Contents	vi
List of Tables	viii
List of Figures	ix
List of Abbreviations	xi
Chapter 1: Background on Tubulysins, Antimitotic Natural Products with Potent Cytotoxicity Against Multi-Drug Resistant Cancer Cells	1
Discovery, Isolation, Structure Elucidation, and Biochemical Evaluation of Tubulysins 1 Established SAR for Tubulysins.....	8
Previous Work on Tubulysins from the Fecik Group	12
Thesis Goals.....	13
Chapter 2:	16
Introduction.....	16
Retrosynthetic Analysis of the Target ^N Tubulysin V (36)	17
Modified Syntheses of the Weinreb Amide 44 and Thiazole 45 Starting Materials	19
First Generation Synthesis to ^N Tubuvaline 40 : Synthesis and Transformation of Ketone 42	22
Second Generation Synthesis to ^N Tubuvaline 40 : Attempted Synthesis of Nitriles Electrophiles.....	25
Synthesis and Application of Dibenzyl Protected Nitrile 72	29
Third Generation Synthesis to ^N Tubuvaline 40 : Attempted Synthesis of Dibenzyl Protected Ketone 79 and Aldehyde 82 Leading to a Retro-Michael Reaction	32
Successful Regio- and Stereoselective Installation of the ^N Tubuvaline Nitrogen	36
Conclusion.....	39
Chapter 2 Experimentals:	41
Chapter 3: Synthesis of ^NTubulysin V (36), U (37), and <i>N</i>-acylated ^NTubulysin Analogs as Complements to Naturally Isolated Tubulysins.....	57
Introduction.....	57
Synthesis of the ^N Tubuvaline-Tubuphenylalanine Dipeptide 93 and Further Ligations	57
Attempts to Synthesize Amine 36 through Successional Deprotection of Tetrapeptide 98	62
Attempts to Synthesize Amine 36 through Milder Deprotection of Tetrapeptide 98 ...	64
Hydrolytically Stable Intermediates Used in a Modified Route to Amine 36	66
Investigation into Phthalimide Deprotection Conditions to Furnish Amine 36	70
Synthesis of ^N Tubulysin Analogs by Acylation of Tetrapeptide 100	73
Model Studies Examining Synthetic Routes to <i>N</i> -Alkylated ^N Tubulysin Analogs	79
Conclusion.....	81
Chapter 3 Experimentals:	83
Standard Procedure for ^N Tubulysin Analogs 109–111 from Amine 100	93
Standard Acylation Procedure:	93
Standard LiOH Hydrolysis Procedure:	93
Chapter 4: Synthesis of Unique Tubulysin U (11) Analogs with Various Oxygen-Based Functional Groups Replacing the Key Tubuvaline Acetate	100
Introduction.....	100

Evaluation and Modification of Precursor Synthesis towards Tubulysin V (12).....	101
Synthetic Efforts towards Tubulysin Analogs with O-Alkylation at the Tubuvaline Hydroxyl Group.....	105
Synthesis of Acylated Tubulysin Analogs using Anhydrides in Pyridine	113
Studies towards the Synthesis of Halogenated Analogs of Tubulysin U (11).....	118
Studies towards the Synthesis of Carbamate and Urea Analogs of Tubulysin U (11)	120
Synthesis of Acylated Tubulysin Analogs using DCC Pre-Activated Acids.....	122
Synthesis of Affinity Labels Modeled after Tubulysin U (11).....	126
Conclusion.....	128
Chapter 4 Experimentals:	130
Standard Procedure for Tubulysin V (12) Acylation using Anhydrides in Pyridine: ...	135
Standard Procedure for Tubulysin V (12) Acylation using DCC Activated Acids:	136
Chapter 5: Overview of Current and Future Studies Associated with Synthesis and Biochemical Evaluation of Stabilized Tubulysin Analogs	142
Review and Discussion of the Synthetic Efforts Associated with ^N Tubulysin Analogs	142
Review and Discussion of the Synthetic Efforts Associated with Tubulysin Analogs	149
Future Studies, Project Directions.....	153
References	159
Appendix A: NMR Spectra of Key Compounds	172

List of Tables

Table 1: Synthesis of acylated ^N tubulysin analogs 37 and 109–113	76
Table 2: Model studies for alkylated ^N tubulysin analogs 120–122	80
Table 3: Acylation reactions using an anhydride in a pyridine solution of hydroxyl 12 (pyridine/anhydride method).	116
Table 4: Attempted acylations of hydroxyl 12 with halogenated acyl groups.	119
Table 5: Attempted synthesis of tubulysin analogs with non-ester functional groups... ..	121
Table 6: Synthesis of acylated tubulysin analogs by DCC activation of simple acids (DCC pre-activation method).	125

List of Figures

Figure 1: Structures of naturally occurring tubulysins.....	2
Figure 2: Graphical representation of tubulysin biosynthesis.....	4
Figure 3: Representative examples of SAR trends at the <i>N</i> -methyl-D-pipecolinic acid residue.	9
Figure 4: Representative examples of SAR trends at the tubuvaline residue.....	10
Figure 5: Representative examples of SAR trends at the tubuphenylalanine/tubutyrosine residue.	12
Figure 6: Comparison of tubulysin U (11) and tubulysin V (12) IC ₅₀ values in 1A9 ovarian cancer cells.....	13
Figure 7: Proposed modification of ester 11 and hydroxyl 12 leading to ^N tubulysin V (36), ^N tubulysin U (37), and ^N tubulysin analogs.....	14
Figure 8: Retrosynthetic strategy to form ^N tubulysin V.	17
Figure 9: Retrosynthetic strategy to form ^N tubuvaline using the Weinreb amide 44	18
Figure 10: Established synthesis of thiazole 45	19
Figure 11: Detailed reactions in the new synthesis of thiazole 45	21
Figure 12: Synthesis of the Weinreb amide 44	22
Figure 13: Synthesis of the ketone 42 using a sacrificial base.	23
Figure 14: Attempted synthesis of the azide 56 as an intermediate towards ^N tubuvaline.	24
Figure 15: Retrosynthetic strategy to form ^N tubuvaline using the Boc protected nitrile 58	26
Figure 16: Attempted synthesis of the Boc protected nitrile 58	27
Figure 17: Poorly productive synthesis of the phthalimide protected nitrile 68	28
Figure 18: Productive synthesis of the dibenzyl protected nitrile 72	29
Figure 19: Synthesis of the amino mixture 74	30
Figure 20: Model reactions for manipulation of ^N tubuvaline fragments.	31
Figure 21: Routes to the unstable dibenzyl protected ketone 79	33
Figure 22: Routes to the unstable dibenzyl protected aldehyde 82	35
Figure 23: An alternative approach to the synthesis of alcohol 55	37
Figure 24: The successful Mitsunobu reaction and finishing steps to the ^N tubuvaline fragment 89	38
Figure 25: Reactions producing <i>N</i> -acylurea side products 94 and 96 with dipeptide 93 and tripeptide 95	59
Figure 26: Synthesis of pure samples of dipeptide 93 and <i>N</i> -acylurea side product 94 .60	60
Figure 27: Highly productive amide bond forming reactions to tetrapeptide 98	61
Figure 28: Initial deprotection strategy to synthesize amine 36	63
Figure 29: Potential alternative deprotection strategy to amine 36	66
Figure 30: A pertinent example of basic hydrolysis from the Astleford and Weigel paper.	67
Figure 31: Synthesis of the phthalimide protected, benzyl deprotected tetrapeptide 102 with intermediate isolation.	68
Figure 32: Synthesis of the phthalimide protected, benzyl deprotected tetrapeptide 102 without intermediate isolation.	70
Figure 33: The final deprotection step to synthesize amine 36	72
Figure 34: Synthesis of reagents 114 and 115 for generating ^N tubulysin urea analogs.78	78
Figure 35: New synthetic methods to tubuvaline 125	103
Figure 36: Use of old and new synthetic methods to generate hydroxyl 12	104

Figure 37: Attempted methylation of the tubuvaline hydroxyl in late-stage intermediates.	107
Figure 38: Revised strategy to install a methyl ether at the tubuvaline hydroxyl group.	108
Figure 39: Proposed steps to finish the synthesis of methyl ether 133 .	112
Figure 40: Synthesis of the methoxymethyl ether 142 and its comparison to ester 11 .	113
Figure 41: Resulting products of hydroxyl 12 acetylation under published conditions.	114
Figure 42: Cyclized lactams resulting from modification to the DCC pre-activation method.	125
Figure 43: Comparison of heteroatom exchange in tubulysins/ ^N tubulysins V and U.	143
Figure 44: First generation synthesis to ^N tubuvaline.	144
Figure 45: Second generation synthesis to ^N tubuvaline.	145
Figure 46: Third generation synthesis to ^N tubuvaline.	146
Figure 47: Synthesis of amine 36 under modified deprotection conditions.	148
Figure 48: Failed syntheses of acylated analogs of ester 11 .	152
Figure 49: Potential methods for larger scale generation of tubuvaline intermediates.	152
Figure 50: A potential alternative method to generate tetrapeptide 102 .	157
Figure 51: Important ^N tubulysin analogs for complete SAR analysis.	158

List of Abbreviations

[α]	specific rotation [expressed without units; the units = (deg□mL)/(g□dm)]
Ac	acetyl
AcOH	acetic acid
Bn	benzyl
BOC, Boc	<i>tert</i> -butoxycarbonyl
br	broad (spectral)
Bu, <i>n</i> -Bu	normal (primary) butyl
<i>t</i> -Bu	<i>tert</i> -butyl
°C	degrees Celsius
calcd	calculated
CBS	Corey-Bakshi-Shibata
CDI	1,1'-carbonyldiimidazole
CoA	Coenzyme A
CSA	camphorsulfonic acid
d	day(s); doublet (spectral)
DBU	1,8-diazabicyclo[5.4.0]undec-7-ene
DCC	<i>N,N'</i> -dicyclohexylcarbodiimide
DDQ	2,3-dichloro-5,6-dicyano-1,4-benzoquinone
DIAD	diisopropyl azodicarboxylate
DIBAL-H	diisobutylaluminum hydride
DMAP	4-(<i>N,N</i> -dimethylamino)pyridine
DMF	dimethylformamide
DMSO	dimethyl sulfoxide
dr	diastereomer ratio
<i>E</i>	entgegen (configurational)
ED ₅₀	dose effective in 50% of test subjects
equiv	equivalent
ESI	electrospray ionization
Et	ethyl
g	gram(s)
h	hour(s)
HATU	<i>O</i> -(7-azabenzotriazol-1-yl)- <i>N,N,N',N'</i> -tetramethyluronium hexafluorophosphate
HPLC	high-performance liquid chromatography
HRMS	high resolution mass spectrometry
Hz	hertz
IC ₅₀	inhibitory concentration in 50% of test subjects
Ile	isoleucine
<i>J</i>	coupling constant (in NMR spectrometry)
L	liter(s)
μ	micro
m	multiplet (spectral); meter(s); milli
M	molar (moles per liter)
MDR	multi-drug resistant
Me	methyl
Mep	<i>N</i> -methyl-D-pipecolinic acid
<i>N</i> -Me-D-Pip	<i>N</i> -methyl-D-pipecolinic acid

MHz	megahertz
min	minute(s); minimum
mL	milliliter
mM	millimolar (millimoles per liter)
μ M	micromolar (micromoles per liter)
mol	mole(s)
MOM	methoxymethyl
mp	melting point
Ms	methylsulfonyl (mesyl)
MS	mass spectrometry
ng	nanogram
NIH	National Institutes of Health
nM	nanomolar (nanomoles per liter)
NMR	nuclear magnetic resonance
NOESY	nuclear Overhauser effect spectroscopy
NRPS	nonribosomal peptide synthetase
OAc	acetate
ovlp	overlapping
PDC	pyridinium dichromate
pg	picogram
pH	power of hydrogen
Ph	phenyl
Phth	phthalimide
Pip	pipecolic acid
PKS	polyketide synthase
PPh_3	triphenylphosphine
ppm	part(s) per million
Pr	propyl
<i>i</i> Pr	isopropyl
q	quartet (spectral)
<i>R</i>	rectus (configurational)
R_f	retention factor (in chromatography)
rt:	retention time
s	singlet (spectral); second(s)
<i>S</i>	sinister (configurational)
SAR	structure-activity relationship(s)
S_N2	bimolecular nucleophilic substitution
t	triplet (spectral)
TBAF	tetrabutylammonium fluoride
TBDPS	<i>tert</i> -butyl
<i>tert</i>	tertiary
TFA	trifluoroacetic acid
TFAA	trifluoroacetic anhydride
THF	tetrahydrofuran
TLC	thin-layer chromatography
Ts	<i>para</i> -toluenesulfonyl
<i>p</i> -TsOH	<i>para</i> -toluenesulfonic acid
Tub	tubulysin
Tup	tubuphenylalanine

Tut	tubutyrosine
Tuv	tubuvaline
Z	zusammen (configurational)

Chapter 1:

Background on Tubulysins, Antimitotic Natural Products with Potent Cytotoxicity Against Multi-Drug Resistant Cancer Cells

Discovery, Isolation, Structure Elucidation, and Biochemical Evaluation of Tubulysins

Tubulysins are naturally occurring antimitotic tetrapeptides with potent anticancer activity against multidrug-resistant (MDR) cancer cells, acting by inhibition of tubulin polymerization. Their first report was in 2000, when they were identified through a screen of the culture broths from myxobacteria *Archangium gephyra* and *Angiococcus disciformis* against mammalian cell lines (Sasse *et al.* 2000). Tubulysins A (1), B (2), D (4), and E (5) possessed potent antiproliferative activity against L929 mouse fibroblasts, PtK₂ kidney cancer cells, and KB-3.1 cervix cancer cells (IC₅₀ = 20 pg/mL to 1 ng/mL, Sasse *et al.* 2000). Additionally, all retained their high potency against the MDR cervical cancer cell line KB-V1 (IC₅₀ = 80 pg/mL to 1 ng/mL, Sasse *et al.* 2000). Investigation into the cellular structure of treated cells showed that the tubulysins function through disruption of the microtubule network, where microtubule decay was followed by complete solubilization beginning after 2 and 24 hours, respectively (Sasse *et al.* 2000).

Tubulysins follow a standard tetrapeptide template with a few key modifications to the core structure (Figure 1). Starting at the N-terminus, the four amino acid residues are *N*-methyl-D-pipecolinic acid (Mep), L-isoleucine (Ile), tubuvaline (Tuv), and tubuphenylalanine or tubutyrosine (Tup or Tut). Variations exist at the oxygen and nitrogen of tubuvaline, where substitution of a rare *N,O*-acetal is present in certain members (1–10), and at the phenyl ring of the C-terminus residue based on either a phenylalanine or tyrosine source for this residue. Full stereochemical determination was

found by analysis of fragmentation following acidic hydrolysis of tubulysin D (**4**) (Höfle *et al.* 2003).

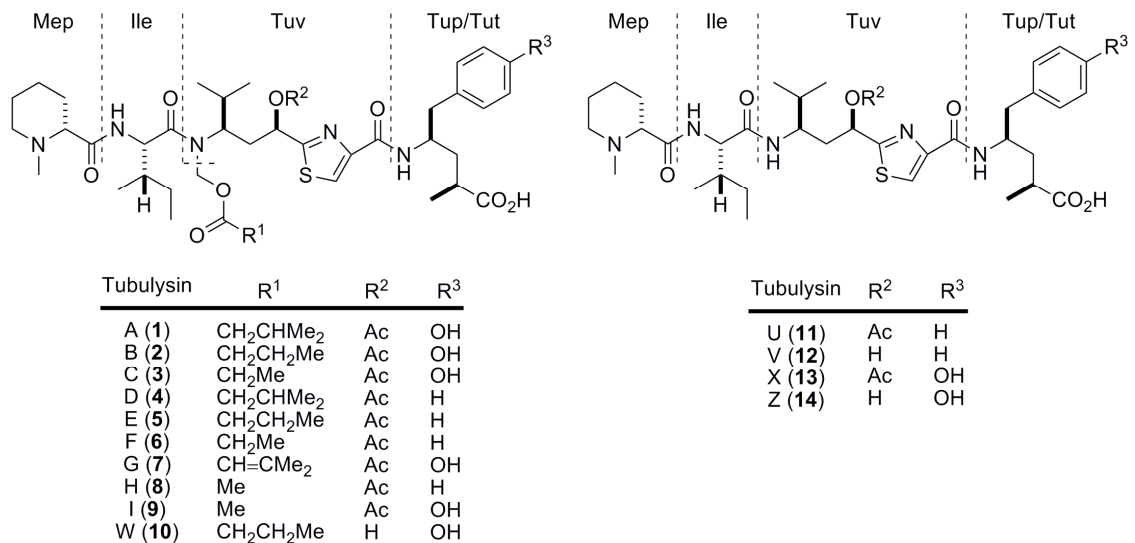


Figure 1: Structures of naturally occurring tubulysins.

Biosynthesis of the tubulysins is through a mixed nonribosomal peptide synthetase (NRPS)-polyketide synthase (PKS) system (Sandmann *et al* 2004), which contains 7 modules (2 PKS and 5 NRPS) on 5 proteins (Tub B–F) (Chai *et al* 2010, Figure 2). Initial loading of L-pipecolic acid derived from L-lysine onto module 1 forms the methylated pipecolic acid residue through an N-methyltransferase; the point at which pipecolic acid isomerization occurs providing the stereochemistry observed in the final analogs has yet to be determined. Further chain elongation occurs on modules 2–4 with L-isoleucine, L-valine, and malonyl-CoA, with the malonyl installed as part of the first PKS module. Module 5 is responsible for installation of the unique thiazole ring as a result of cysteine addition and heterocyclization. Addition of either phenylalanine or tyrosine on module 6 precedes the final chain elongation where another PKS module adds malonyl-CoA and following a C-methyltransferase, releases the molecule as

pretubulysin A (**15**) or D (**16**). Tailoring oxidations and acylations of these intermediates add the acylated functional groups at tubuvaline which finishes the tubulysin biosynthesis (Chai et al 2010). The specific enzymes that oxidize and acylate pretubulysins are difficult to determine since the tubulysin gene cluster does not express proteins with this potential (Chai et al. 2012).

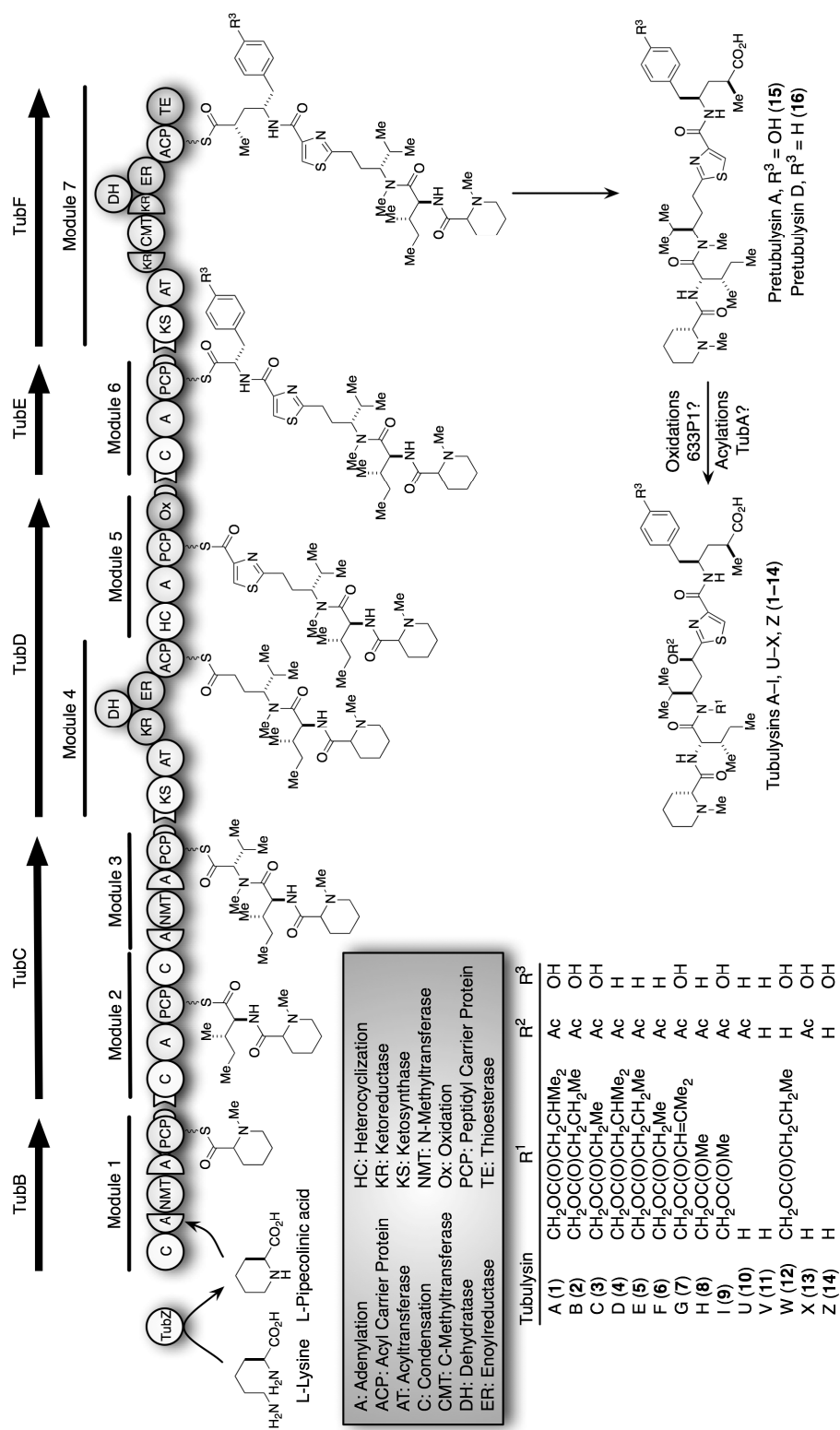


Figure 2: Graphical representation of tubulylin biosynthesis.

Tubulysins bind to β -tubulin at the peptide site of the *Vinca* alkaloid domain and exert their anticancer activity through inhibition and destabilization of microtubule polymerization (Khalil *et al.* 2006). Microtubules are long, polymeric cylinders made up of α - and β -tubulin heterodimers and are essential to normal cellular function. These functions include maintenance of the cellular structure and transportation of cellular components involved in cell signaling, mitosis and apoptosis. Microtubule cellular tasks are achieved through its frequent lengthening and shortening via polymerization/depolymerization of the heterodimeric tubulin subunits, termed 'dynamic instability' (Jordan and Wilson 2004). Agents that affect the dynamic instability of microtubules have found much success as anticancer agents. These include the taxanes and epothilones (inducing and stabilizing tubulin polymerization), and the *Vinca* alkaloids (disrupting and inhibiting microtubule polymerization).

The anticancer activity of both microtubule stabilizing and destabilizing molecules lies within their ability to suspend mitosis (Jordan and Wilson 2004). Mitosis is the multistage process of cell division, wherein a parent cell replicates into two genetically identical daughter cells. In contrast to the microtubule dynamics of interphase, the resting phase of the cell cycle, comparatively rapid dynamic instability is necessary for proper attachment and movement of the duplicated chromosomes through each stage of mitosis (Jordan and Wilson 2004). Studies have shown that drugs targeting microtubules cause incomplete delivery of chromosomes to the metaphase plate, a process critical to cell division (Jordan and Wilson 2004). Even one chromosome not aligned at the metaphase plate will stop forward mitotic progress, trapping the cell mid-mitosis and eventually causing programmed cell death, or apoptosis (Jordan and Wilson 2004). These agents' effectiveness against malignant cells can be partially explained by

the higher rate of mitosis cancer cells undergo compared to normal cells. An increased incidence of mitosis puts cancer cells in a position of vulnerability with drugs that arrest the mitotic cycle (Jordan and Wilson 2004).

Biochemical investigations into the tubulysin mode of action have revealed their ability to disrupt microtubule dynamics by depolymerizing or inhibiting the polymerization of the tubulin subunits onto microtubules (Sasse *et al.* 2000, Khalil *et al.* 2006). As a result, treated cells are halted mid-mitosis which leads to their eventual shift into apoptosis, as shown by classic markers such as DNA fragmentation and increased caspase-3 activity (Kaur *et al.* 2006, Khalil *et al.* 2006). Additionally, cell angiogenesis was severally hindered upon treatment with tubulysin A, which may prove to be another venue in which these compounds exert their effects. Competitive binding studies have shown non-competitive inhibition of vinblastine with tubulysin A, similarly to the peptide antimetotics dolastatin 10 and phomopsin A (Khalil *et al.* 2006). This, together with NMR conformation studies showing that tubulysin A and epothilone A share a common tubulin binding site (Kubicek *et al.* 2010), suggests that the tubulysins bind at the peptide site of the *Vinca* domain.

Naturally derived tubulysins have shown potent *in vitro* growth inhibitory activity against a variety of different cancer cell lines, including breast (Ranganathan *et al.* 2009), cervix (Sasse *et al.* 2000, Steinmetz *et al.* 2004), colon (Kaur *et al.* 2006), leukemia (Sasse *et al.* 2000), lung, (Ullrich *et al.* 2009b), melanoma (Kaur *et al.* 2006), ovarian (Ranganathan *et al.* 2009), and prostate (Kaur *et al.* 2006) carcinomas, with IC₅₀ values representing a 20-1000 fold improvement over the epothilones, vinblastine and paclitaxel (Steinmetz *et al.* 2004). A correlation exists between lipophilicity and *in vitro* activity, where tubulysins A through I follow a predictable trend of increased lipophilicity

showing more potent antiproliferative activity (Steinmetz *et al.* 2004). This trend may be explained by the observation that increased cellular uptake of the more lipophilic tubulysins resulted in higher cellular concentrations in mouse fibroblast cells. The question of whether the mechanism of cellular uptake is through diffusion or active transport is still unknown (Steinmetz *et al.* 2004).

Preliminary animal studies have shown limited success using low doses of tubulysin A in hollow fiber assays of 12 human cancer cell lines (Kaur *et al.* 2006), and no success in xenograft mouse models, where both tubulysins A and B show no therapeutic window (Leamon *et al.* 2008, Schluep *et al.* 2009, Reddy *et al.* 2009). Targeted delivery of tubulysins by conjugation to cancer-specific substrates, on the other hand, has seen limited success in mouse studies. Over-expression of the folate receptor in cancer cells was taken advantage of by conjugation of tubulysins to folate, where the drug is released for its anticancer action follow cancer cell selective absorption of the complex (Vlahov *et al.* 2008, Leamon *et al.* 2008, Reddy *et al.* 2009). This same strategy has also been used with cyclodextrin nanoparticle-tubulysin conjugates (Schluep *et al.* 2009) and prostate-specific antigen-tubulysin prodrugs (Kularatne *et al.* 2010). The folate and nanoparticle bound conjugates have both shown an increased therapeutic window and prolonged survival when compared to unbound tubulysins in mice (Leamon *et al.* 2008, Reddy *et al.* 2009, Schluep *et al.* 2009).

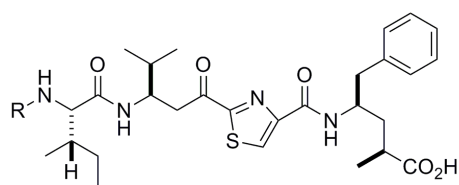
In short, tubulysins exhibit low nanomolar to picomolar inhibition against drug-sensitive cancer cell lines and their potency is retained against multidrug resistant (MDR) cancer cell lines, a claim their closely related clinical counterparts (paclitaxel, *Vinca* alkaloids) cannot make. These attractive qualities make the tubulysins potential

alternatives to the currently available small molecule treatments of MDR cancers, and represent the motivation for focusing on these molecules in the studies presented below.

Established SAR for Tubulysins

Many synthetic efforts have been put forth to generate both the naturally isolated and modified analogs of tubulysins. From these investigations, the minimum pharmacophore necessary for cytotoxicity have been established as structure-activity relationships (SAR) at several points on the tubulysin structure. In general, modifications and simplifications are additive (Patterson *et al.* 2007) and potency tends to increase with greater lipophilicity.

At the *N*-terminus of all the naturally isolated tubulysins lies an *N*-methyl-D-pipecolinic acid, which SAR studies have deemed the most favorable group for potent cytotoxicity. Stereochemistry of the ring is important as exemplified by comparing the observed IC₅₀ values in 1A9 ovarian cancer cells of **17** to **18** (Figure 3, Raghavan *et al.* 2008), but variation in ring size to *N*-methyl-D-proline causes an insignificant change in anticancer activity (**19**, Raghavan *et al.* 2008). Replacement with truncated residues is not well tolerated and causes significant loss of potency, as shown with the secondary amine **20** (Raghavan *et al.* 2008), non-cyclic amino acids such as the alanine derivative **21** (Balasubramanian *et al.* 2009), and acetamides (Patterson *et al.* 2007, not shown).



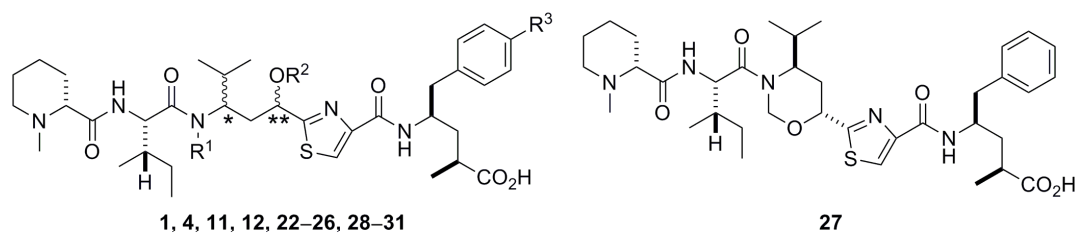
17–21

Compound	R	Activity (1A9 IC ₅₀ , μ M)
17	<i>N</i> -Me-D-Pipecolinic acid	0.2
18	<i>N</i> -Me-L-Pipecolinic acid	25
19	<i>N</i> -Me-D-Proline	0.8
20	D-Pipecolinic acid	23
21	<i>N,N</i> -DiMe-D-Alanine	>50

References: Raghavan et al. 2008, Balasubramanian et al. 2009

Figure 3: Representative examples of SAR trends at the *N*-methyl-D-pipecolinic acid residue.

SAR studies have been most heavily invested into the tubulysin residue since the synthetically derived nature of this fragment lends itself to analog synthesis and dramatic effects on activity occur as a consequence of structural changes. One of the most crucial aspects of this tubulysin portion is stereochemistry, which can be seen by comparing the antiproliferative activity of **4** and **22–24** in MCF-7 breast cancer cells (Figure 4). Significant decreases in activity are observed when either stereocenter is isomerized (**22** and **23**), and these changes are additive as seen with **24**. A minor one-fold loss of activity occurs with simplification of **4** to *N*-methyl **25** when dosed in L929 mouse fibroblast cells, and in separate studies, analogs **4** and **11** were shown to have comparable activity in the MCF-7 cell line with IC₅₀ values of 0.67 nM and 0.4 nM despite the simplification to a secondary amide. This leads to the conclusion that the *N,O*-acetal is not essential for potent cytotoxicity, and hence can be replaced with less labile groups.



Compound	R ¹	R ²	R ³	*	**	Activity (IC ₅₀)	Reference
tubulysin D (4)	CH ₂ OC(O)CH ₂ CHMe ₂	Ac	H	R	R	0.67 nM (MCF-7) 0.01–0.068 nM (L929)	Shibue <i>et al.</i> 2011 Patterson <i>et al.</i> 2007
22	CH ₂ OC(O)CH ₂ CHMe ₂	Ac	H	R	S	280 nM (MCF-7)	Shibue <i>et al.</i> 2011
23	CH ₂ OC(O)CH ₂ CHMe ₂	Ac	H	S	R	240 nM (MCF-7)	Shibue <i>et al.</i> 2011
24	CH ₂ OC(O)CH ₂ CHMe ₂	Ac	H	S	S	>10000 nM (MCF-7)	Shibue <i>et al.</i> 2011
25	Me	Ac	H	R	R	0.32 nM (L929)	Patterson <i>et al.</i> 2007
26	CH ₂ OC(O)CH ₂ CHMe ₂	H	H	R	R	0.32 nM (L929)	Patterson <i>et al.</i> 2007
tubulysin U (11)	H	Ac	H	R	R	0.4 nM (MCF-7)	Ranganathan <i>et al.</i> 2009
tubulysin V (12)	H	H	H	R	R	240 nM (MCF-7)	Ranganathan <i>et al.</i> 2009
tubulysin A (1)	CH ₂ OC(O)CH ₂ CHMe ₂	Ac	OH	R	R	1.0 nM (KB cells) 0.21 nM (PC-3, GI ₅₀)	Vlahov <i>et al.</i> 2011 Pando <i>et al.</i> 2011
28	CH₂C(O)NCHMe₂	Ac	H	R	R	0.29 nM (PC-3, GI ₅₀)	Pando <i>et al.</i> 2011
29	CH₂Oalkyl	Ac	OH	R	R	1.4–18 nM (KB cells)	Vlahov <i>et al.</i> 2011
30	CH₂Salkyl	Ac	OH	R	R	0.7–26 nM (KB cells)	Vlahov <i>et al.</i> 2011
31	CH₂NHC(O)CH₂CHMe₂	Ac	OH	R	R	8.0 nM (KB cells)	Vlahov <i>et al.</i> 2011

Figure 4: Representative examples of SAR trends at the tubuvaline residue.

A general paradigm at the acetate of tubuvaline is contentious since only a slight decrease of potency in L929 cancer cells occurs when comparing **4** to alcohol **26**, but this same change in **11** to **12** causes a drastic loss of activity in MCF-7 cells. This may be an outcome of additive effects from structural simplification at both the oxygen and nitrogen of the tubuvaline. Regardless of the source, the comparison of **11** and **12** clearly shows that the acetate at the α -thiazole position is crucial for potent antiproliferative effects in cancer cells when the tubuvaline secondary amide is not substituted. Cyclization between the oxygen and nitrogen of tubuvaline as in **27** results in equivalent potency to **11** when screened in HEP-2 epidermoid carcinoma cells (Shibue *et al.* 2010).

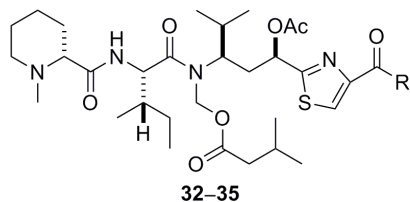
The difficulty in installing and maintaining the labile *N,O*-acetal group has led to several investigations into SAR at this position. Equivalent IC₅₀ values were observed in

PC-3 prostate cancer cells when an *N*-branched peptide-like functional group replaces the *N,O*-acetal at the tubuvaline residue (**28**). Semi-synthetic work with naturally isolated tubulysins gave access to analogs with ether, thioether, and amide replacement of the *N,O*-acetal (**29–31**); in KB cells, all of these were equally active in inhibiting growth of the cancerous cells. Based on these results and the positive correlation of lipophilicity with antiproliferative activity noted above, it appears that the determining factor for activity at this position is not the identity of the functional group but rather its contribution to overall molecule lipophilicity.

Some results not graphically represented here have established that activity equivalent to tubulysin V (**12**) is retained when replacing the α -thiazole hydroxyl with either a ketone (Balasubramanian *et al.* 2009) or a methylene (pretubulysin D (**16**), Ullrich *et al.* 2009a). Replacement of the thiazole ring with an oxazole does not affect activity (Shankar *et al.* 2011), while substitution with a phenyl ring causes a significant loss in IC₅₀ values (Burkhart *et al.* 2011).

Residing at the C-terminus of naturally occurring tubulysins is either tubuphenylalanine or tubutyrosine, resulting in a largely insignificant change in cytotoxicity; this general trend is highlighted by comparison of **1** and **4** cytotoxicity in L929 mouse fibroblasts (Figure 5). Simplification of tubuphenylalanine by removal of the carboxylate end results in a small loss of potency as shown by phenylethylamine **32** (IC₅₀ value = 0.33 nM). Alternatively, removal of the benzyl moiety results in a great loss of activity as shown in **33**, but potency is returned with replacement of the further simplified *N*-methyl amide **34**. This demonstrates that none of the functional groups of the tubuphenylalanine backbone are absolutely necessary to maintain activity. With addition of the poor activity resulting from full removal of all residues at the tubuvaline

carboxylate (**35**), this data again confirms the effect that lipophilicity has on tubulysin anticancer activity.



Compound	R	Activity (L929, IC ₅₀ , nM)
1	tubutyrosine	0.083–0.24
4	tubuphenylalanine	0.01–0.068
32	NHCH ₂ CH ₂ Ph	0.33
33	NH(CH ₂) ₃ CO ₂ H	4.8
34	NHMe	0.46
35	OH	3.4

References: Sasse *et al.* 2000, Steinmetz *et al.* 2004, Patterson *et al.* 2007

Figure 5: Representative examples of SAR trends at the tubuphenylalanine/tubutyrosine residue.

Previous Work on Tubulysins from the Fecik Group

Work in the Fecik lab has focused on the synthesis and biological evaluation of simplified tubulysin analogs to probe minimum structural requirements for cytotoxicity and the identification of a clinical candidate. The Fecik lab has synthesized and evaluated 2 natural tubulysins, tubulysins V and U (Figure 6), and approximately 75 analogs (Balasubramanian *et al.* 2008, Raghavan *et al.* 2008, Balasubramanian *et al.* 2009). The marked difference in antiproliferative activity between tubulysins V and U exemplifies the importance of an acetate positioned alpha to the thiazole ring. However, these acetates have been showed to be labile under both acidic and basic conditions (Höfle *et al.* 2003), so the *in vivo* effectiveness of this modification may be hindered due to this instability.

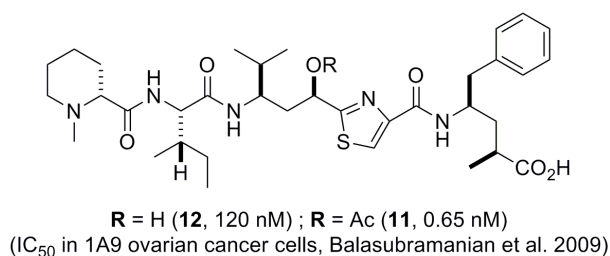


Figure 6: Comparison of tubulysin U (**11**) and tubulysin V (**12**) IC₅₀ values in 1A9 ovarian cancer cells.

Thesis Goals

The overall goal of these research projects was to synthesize and evaluate tubulysin analogs with structural modifications at the tubuvaline α -thiazole position which mimic and stabilize the crucial yet labile acetate seen in the most potent tubulysins. This was done by synthesizing analogs which replace the acetate with nitrogen based functional groups and with oxygen based functional groups which are less hydrolytically unstable. Following analog synthesis, biochemical evaluation will be performed by our collaborators at the NIH to test their activity against both normal and MDR cancer cell lines, in addition to their ability to inhibit tubulin polymerization. Based on the apparent effect that modifications to the acetate impose, an SAR will be developed, which can be used as a tool to more fully understand the interactions of tubulysins with their binding site on tubulin and assist with future development of these compounds as anticancer therapeutics.

Studies which replace the tubuvaline oxygen with a nitrogen have not yet been reported, so the first focus of the project was to synthesize the tubuvaline residue with installation of the key nitrogen. Previously established syntheses of tubulysins V and U reported by the Fecik lab were seen as a foundation for this work, where modifications to

these routes would modify the α -thiazole position without significant detriment in the rest of the transformations. Peptide couplings with the other tubulysin residues would then give access to N tubulysin V (**36**, Figure 7), a critical analog which will unequivocally judge the effect of heteroatom exchange at this position and function as a common precursor to the other N -substituted analogs.

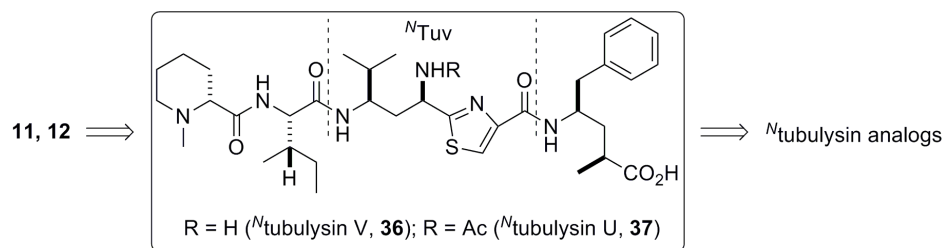


Figure 7: Proposed modification of ester **11** and hydroxyl **12** leading to N tubulysin V (**36**), N tubulysin U (**37**), and N tubulysin analogs.

Acetylation of **36** would then give access to N tubulysin U (**37**), which will survey whether stabilized acetylation at this position will result in increased activity as seen with comparison of **11** and **12**. Since all the other proposed N tubulysin V analogs will not have O -substituted analogs available for direct comparison, these compounds are crucial pieces to understand the singular modification to the heteroatom and will act as links to the SAR of other N -substituted analogs. By general substitution of **36** with other functional groups such as amides, amines, carbamates, ureas, and imides, insights will be given to the effect that space filling, hydrogen bonding, and polarity have on tubulin active site binding, and in turn cytotoxicity in cancer cells.

The established potency of the acetate-containing tubulysins has not been supplemented by investigations into the effect that other esters and various other oxygen based functional groups have at this position. Hence, with access to **12** from previous

synthetic efforts, another thesis objective was to attach various acyl and alkyl groups to this position. Various esters appended to **12** will determine the importance and limitations of the alkyl group at this position, while acylation resulting in non-ester functionality will gauge the effect that hydrogen binding and polarity have on tubulin binding. *O*-alkylation will replace the carbonyl with a more hydrolytically stable moiety while maintaining a hydrophobic presence, which will survey the importance of the acetate carbonyl. In addition to the SAR data gained through biochemical evaluation of these compounds, *O*-acylation of **12** also affords the opportunity to attach electrophilic groups at this position in order to develop affinity probes, which will covalently bind to tubulin and provide data on the specific interactions between tubulysins and the tubulin active site residues.

Chapter 2:

Studies Toward Design and Synthesis of ^NTubuvaline Fragments with Regio- and Diastereoselective Installation of the Key Nitrogen

Introduction

Testing the biochemical effect that replacement of the tubuvaline oxygen with a nitrogen has with regards to cytotoxicity in cancer cells first required access to the synthetically derived compounds **36** and **37**. Synthesis of the target tubulysin analogs starts with access to tubuvaline modified with regio- and stereoselective replacement of the hydroxyl oxygen. In order to generate this residue, the chemistry to an established ketone was reevaluated with improvements to reaction setup and purification. Addendums to a synthetic route pioneered by the Fecik lab led to exclusive formation of an unforeseen side product as a result of a Mitsunobu reaction which would have diastereoselectively installed the key nitrogen. An alternative strategy, which called upon the use of a nitrile electrophile, initially underwent similar side product formation and required survey of alternative protecting groups.

Following the successful regioselective installation of the nitrogen via a nitrile electrophile, this route was deemed problematic stemming from issues with stereoselectivity and purification. With the intention of circumventing both the previously seen side product formation and lack of selectivity, a hybrid approach was taken resulting in an unavoidable retro-Michael cleavage of the target molecules. Finally, after exhausting the usefulness of these alternative options, a working Mitsunobu reaction was established based upon the original synthetic pathway. With the nitrogen installed as a phthalimide, further functional group transformations which build upon established

methods led to the generation of the Boc protected N_t tubuvaline residue **89**.

Retrosynthetic Analysis of the Target N_t Tubulysin V (**36**)

Retrosynthetic analysis of the target **36** starts with amide bond disconnections into the four individual amino acid residues: *N*-methyl-D-pipecolic acid (Mep, **38**), L-isoleucine (Ile, **39**), N_t tubuvaline (N_t Tuv, **40**), and tubuphenylalanine (Tup, **41**, Figure 8). Of these fragments, Boc protected L-isoleucine is commercially available, *N*-methyl-D-pipecolic acid is easily generated in one step from commercial materials, and the synthesis of tubuphenylalanine has been reported by several groups including the Fecik lab (Raghavan *et al.* 2008). Conversely, the current syntheses of tubuvaline fragments have all contained either oxygen based functional groups or full saturation at the α -thiazole position. Hence, the initial synthetic focus to **36** concerned production of **40** with correct regio- and stereo-controlled installation of the key nitrogen. Production of the other target analog N_t tubulysin U (**37**) was predicted to be available by acetylation of **36**.

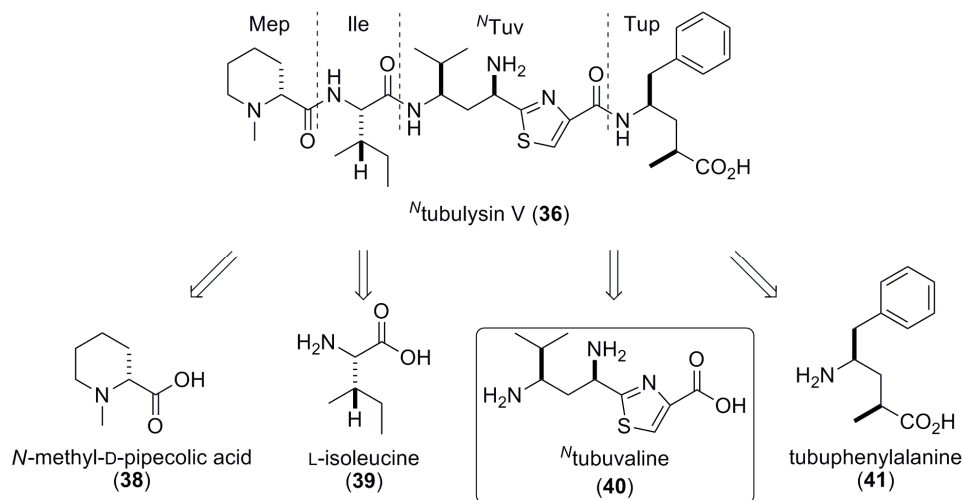


Figure 8: Retrosynthetic strategy to form N_t tubulysin V.

The route to N_t tubuvaline was envisioned to go through a convenient intermediate

ketone (**42**), made accessible using chemistry previously established in our lab towards the bis-Boc protected ketone **43** (Raghavan *et al.* 2008, Figure 9). In the forward sense, stereoselective reduction of other tubuvaline ketones has been shown to be selective and high yielding (Sani *et al.* 2007). Following diastereoselective reduction of **42**, production of the desired *N*_ttubuvaline diastereomer **40** was then predicted to be available through a Mitsunobu reaction and further functional group transformations of the resulting alcohol. The formation of ketone **42** was possible through arylation of the known Weinreb amide **44** with the known thiazole **45** (Raghavan *et al.* 2008).

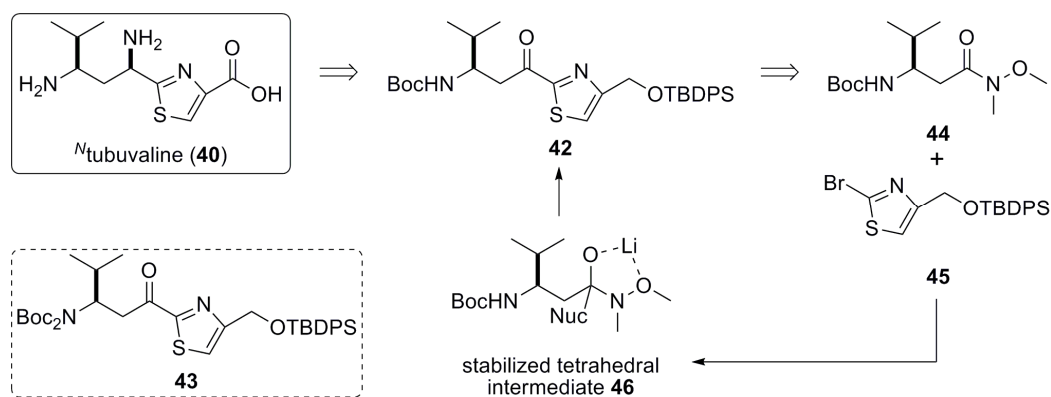


Figure 9: Retrosynthetic strategy to form *N*_ttubuvaline using the Weinreb amide **44**.

The advantage to using Weinreb amide **44** as the electrophilic precursor to ketone **42** lies in its resistance to excessive nucleophilic addition (Nahm and Weinreb 1981). Esters and acid chloride electrophiles contain leaving groups which can prematurely cleave following nucleophilic addition, causing collapse of the tetrahedral intermediate before the reaction is quenched. The resulting ketone is then susceptible to a second addition with the still present nucleophile, leading to production of an undesired tertiary alcohol byproduct. Alternatively, addition of the nucleophile into the carbonyl of Weinreb amides generates a stabilized tetrahedral intermediate supported by lithium chelation

(**46**, Figure 9). This intermediate is resistant to further nucleophilic addition even when several equivalents of the nucleophile are used, allowing for greater reaction control. Only upon work up is the carbon-nitrogen bond cleaved, freeing the desired ketone without fear of additional nucleophilic addition.

Modified Syntheses of the Weinreb Amide **44** and Thiazole **45** Starting Materials

Starting with synthesis of thiazole **45**, the established strategy calls for condensation of ethyl bromopyruvate (**47**) with thiourea (**48**) to form the thiazole ring. Bromination of the resulting thiazole **49**, followed by reduction of ethyl ester **50** and silyl ether protection of the alcohol **51** generates thiazole **45** in 44–61% overall yield over 4 steps (Figure 10, Kelly and Lang 1996, Raghavan *et al.* 2008). Despite the efficiency of this route, several aspects can still be improved since flash chromatography purification is required in 3 of the 4 steps, and the reaction scale is limited.

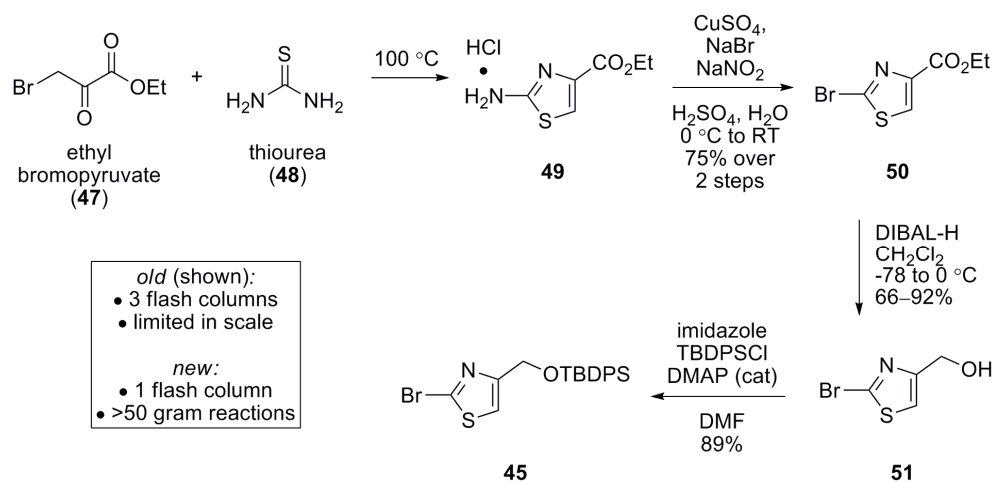


Figure 10: Established synthesis of thiazole **45**.

With several key modifications to reaction set up and purification, a scalable route to thiazole **45** which allows for fewer instances of chromatography was developed

(Figure 11). Previously, the condensation of ethyl bromopyruvate with thiourea was done neat, where careful heating and generous head space in the reaction container were necessary due to the violently exothermic reaction occurring upon reagent homogenization (Kelly and Lang 1996). By heating the starting materials as a solution in refluxing EtOH instead, the reaction can run safely at >50 gram scales. Following bromination of amino thiazole **49**, reaction purification has been flash chromatography, where bromine species are a common impurity. Alternatively, simple recrystallization in boiling hexanes gives pure bromo thiazole **50** without these impurities, and allows reaction scaling beyond what would be practical for silica-based purification.

Full reduction of the ethyl ester **50** was previously performed using 2 equivalents of a DIBAL-H solution (Figure 10). This reaction presents several challenges, including scale limitations based upon volume of available equipment, the difficulty in working up reactions with large amounts of aluminum salts, and the requirement for flash chromatography. The alternative route presented here uses simple reagents for *in situ* generation of LiBH_4 in a biphasic mixture of THF and H_2O (Figure 11). This route is preferable due to its reduced solvent volume supporting a large scale reaction, operational simplicity, and production of highly pure alcohol **51** after aqueous quench and organic extraction, making additional purification unnecessary.

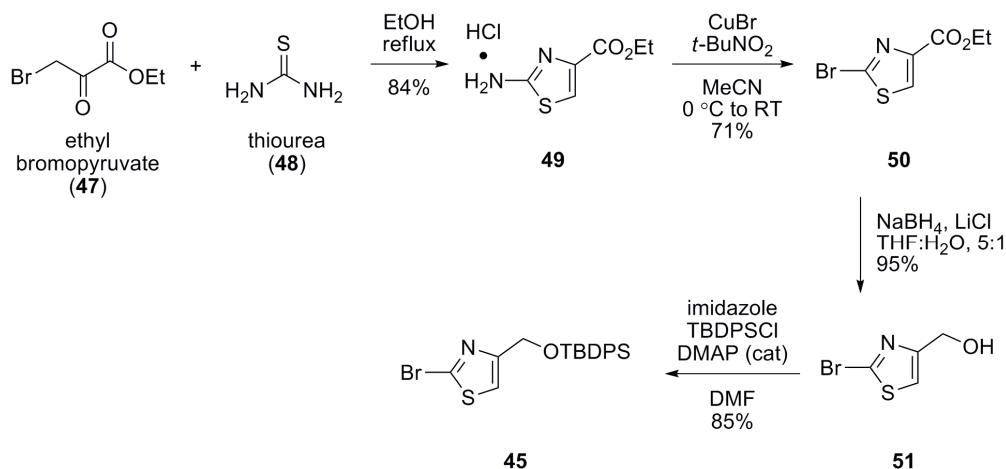


Figure 11: Detailed reactions in the new synthesis of thiazole **45**.

The other synthetically derived starting material towards the ketone **42** is Weinreb amide **44**. Weinreb amide **44** was synthesized through a one-pot Arndt–Eistert reaction, which furnishes the desired one carbon homologation at the Boc-L-valine carboxylate (Figure 12). Synthesis of the intermediate diazomethylketone begins with carboxylate activation as a mixed anhydride, followed by addition of diazomethane as a solution in ether. The true scale limitation of this route to the crucial ketone **42** lies in the scale that diazomethane can be safely generated, since it is explosive and therefore requires special equipment and handling considerations. Wolff rearrangement of the diazomethylketone in the presence of *N,O*-dimethylhydroxylamine and catalytic silver benzoate gives Weinreb amide **44**. Use of silver benzoate was preferable to the silver trifluoroacetate previously reported (Raghavan *et al.* 2008) since the benzoate salt is soluble in the Et₃N, making its transfer into the reaction more operationally simple.

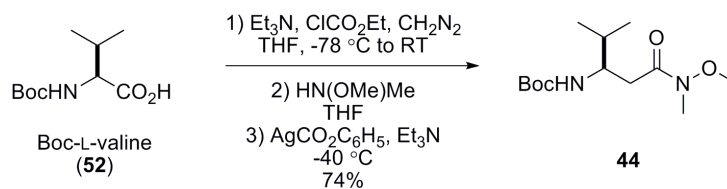


Figure 12: Synthesis of the Weinreb amide **44**.

First Generation Synthesis to ^NTubovaline **40**: Synthesis and Conversion of Ketone **42**

Arylation of the Weinreb amide previously relied on a bis-Boc protection of **42** to avoid N–H deprotonation by the lithiated thiazole nucleophile **53** (Figure 13, Raghavan *et al.* 2008). This extra protection was low yielding (55%) but necessary so as not to waste the precious thiazole intermediate **45**. Investigators at Merck (Liu *et al.* 2002) have reported a method where secondary *N*-carbamate protected electrophiles are first deprotonated by adding a simple, commercially available, non-nucleophilic Grignard reagent termed a “sacrificial base.” Instead of adding an extra equivalent of nucleophile to account for the acidic N–H proton, a near stoichiometric amount of any number of lithiated or Grignard based nucleophiles were added to electrophiles pre-deprotonated with a sacrificial base. High yields of the target molecules confirmed this method’s value for economic use of nucleophiles.

Such a procedure was adopted for the arylation of the singly Boc protected Weinreb amide **44** (Figure 13). The sacrificial base, *i*-PrMgCl, was added first to deprotonate **44**, while the thiazole **45** was separately lithiated using *n*-BuLi. After their respective exchanges, the two solutions were mixed, predominately resulting in the target ketone **42** and the bromine exchanged thiazole **54** as an impurity. Purification of the reaction was challenging due to the similar R_f values of **42** and **54** on silica gel, where slowly eluting flash chromatography with a very non-polar mobile phase was

necessary for complete purification. The yield of this reaction was modest at 51% (58% based on recovered starting material), but up to 5 grams of ketone **42** was generated and the overall yield of **42** from commercial starting materials was improved by eliminating the inefficient bis-Boc protection.

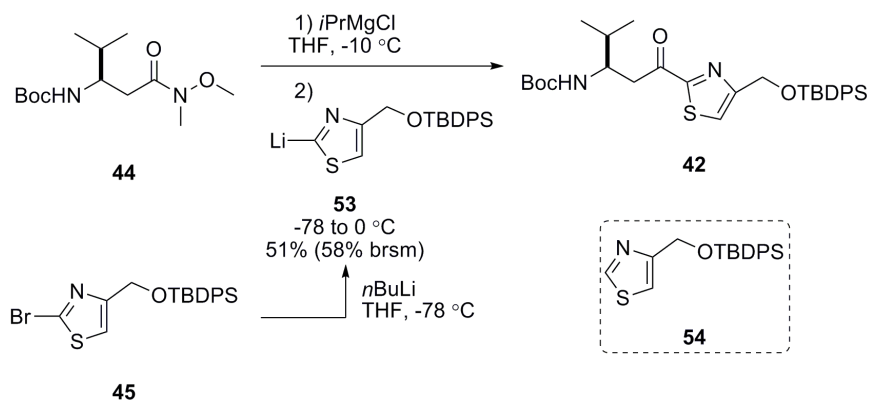


Figure 13: Synthesis of the ketone **42** using a sacrificial base.

Access to multi-gram quantities of ketone **42** set the stage for the second half of the ^Ntubuvaine synthesis: installation of the key nitrogen. A stereoselective reduction was performed using the (*R*)-CBS catalyst and borane to form the desired (*S*)-alcohol **55** (Figure 14). Reaction selectivity tended to fluctuate, and retrospective literature survey suggests that the CBS reduction may have been more reproducible if performed at elevated temperatures (Stone 2004). The stereochemical identity of the alcohol **55** was confidently assigned based upon precedent set by the Zanda group, where (*R*)-CBS reduction of a similar ketone led to the corresponding (*S*)-alcohol, which was unambiguously assigned by X-ray crystallography (Sani *et al.* 2007). The Fecik lab has also used the CBS catalysts for selective reduction of tripeptides towards the synthesis of tubulysin V and its epimer at the α -thiazole position (Balasubramanian *et al.* 2009). This study confirmed stereochemistry at this position both by Mosher ester analysis

(Dale and Mosher 1973) and comparison of the respective cytotoxicity of each epimer against naturally occurring tubulysin V.

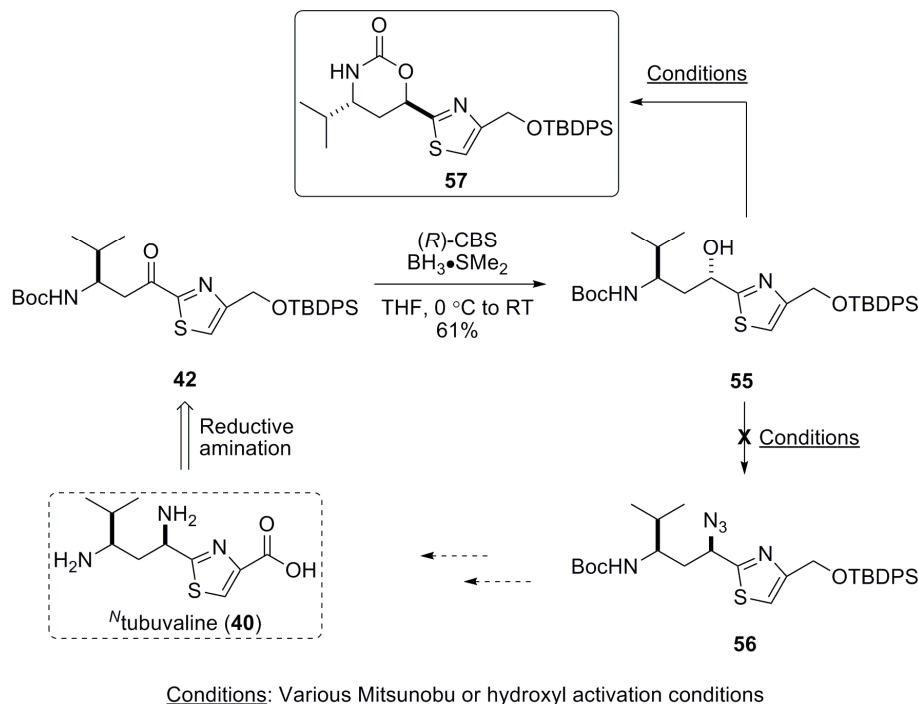


Figure 14: Attempted synthesis of the azide **56** as an intermediate towards *N*-tubuvaline.

With **55** in hand, stereospecific nucleophilic substitution through a Mitsunobu reaction was then performed to install the nitrogen as an azide. Under the many various Mitsunobu and hydroxyl activation conditions described below, however, conversion of **55** did not produce the desired azide compound **56**. Instead, an intramolecular cyclization of the Boc group resulted in the cyclized carbamate **57** as the exclusive product, where an $\text{S}_{\text{N}}2$ -type mechanism characteristic to Mitsunobu and nucleophilic displacement reactions is assumed. Along with standard Mitsunobu conditions (PPh_3 , NaN_3/DPPA , then DIAD), several modifications were attempted. These included 1) changing the order of reagent addition, 2) running the reaction at room temperature, 0 or

-15 °C, 3) using the oxidant DDQ in place of DIAD (Iranpoor *et al.* 2004), and 4) using conditions which were reported to be superior to standard Mitsunobu conditions in the case of a benzylic alcohols (Thompson *et al.* 1993). These modifications all resulted in either no reaction or production of **57** as the major product.

In preparation for an S_N2-type hydroxyl displacement with an azide nucleophile, alcohol **55** was activated as a mesylate or tosylate in the presence of amine bases at both 0 °C and room temperature. When kept to 0 °C, no reaction occurs; when the reaction was performed at room temperature, activation was presumed to occur followed immediately by intramolecular cyclization to form **57** exclusively. In hopes that this route could be salvaged, a reductive amination was performed on ketone **42** to non-diastereoselectively install the amine (Figure 14). This too failed by not progressing past the starting material.

Ultimately it was determined that regardless of reaction conditions, intramolecular cyclization would always be faster than intermolecular nucleophilic substitution in cases where the hydroxyl at the α-thiazole position was activated as a leaving group. Other members of the Fecik lab have noted the same reactivity occurs under these conditions using a tripeptide alcohol previously established for use towards the synthesis of tubulysins V and U (Balasubramanian *et al.* 2009).

Second Generation Synthesis to ^NTubuvaline **40**: Attempted Synthesis of Nitriles Electrophiles

Since side product production via an intramolecular cyclization dominated the first generation route to the ^Ntubuvaline analogs, a new method was developed. In order to preinstall the nitrogen and negate the need for activation of the α-thiazole position,

Weinreb amide **44** was replaced with a nitrile electrophile **58** (Figure 15).

Retrosynthetically, a diastereomeric mixture of amine **59** was to be accessible via arylation of nitrile **58** with thiazole **45** followed by non-diastereoselective reduction of the *in situ* imine. Following separation of the diastereomers and functional group transformations, **40** would then be available. This strategy was inspired by the reported route Wipf used to tubulylin analogs (Wipf and Wang 2007), where an aldehyde electrophile was used to non-diastereoselectively install the hydroxyl at the α -thiazole position of tubuvaline.

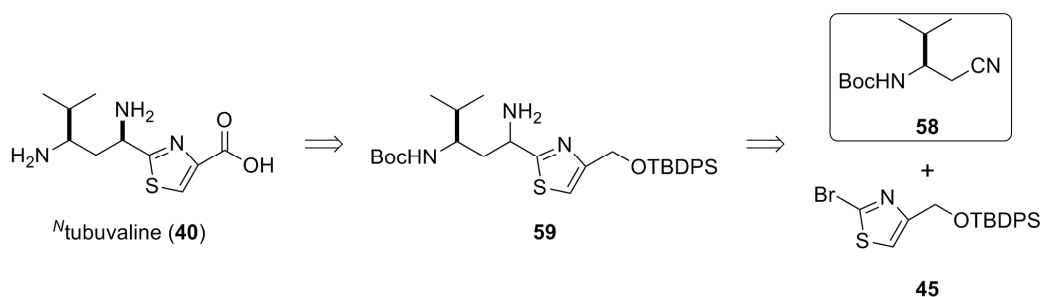


Figure 15: Retrosynthetic strategy to form *N*-tubuvaline using the Boc protected nitrile **58**.

Reduction of the Boc Weinreb amide **44** followed by conversion to nitrile **58** (Zhu *et al.* 2007) was successful, but was also low yielding and would require a substantial amount of precious Weinreb amide intermediate (Figure 16). Instead, synthesis of **58** was attempted by starting with the easily accessible Boc protected valinol **60**. This route proved to be problematic, since at both the halogenation of **60** and the cyanide addition into **62**, partial intramolecular cyclization occurred yielding the cyclized carbamate **61** as well as a low yield of the targeted molecules **62** and **58**. Little variation to this paradigm was found when changing the leaving group X (OTs, Br, or I) or reaction temperature (0 °C, room temperature, or 70 °C). This was surprising since, although one source reports similar yields of activated Boc-valinol (Veitía *et al.* 2009), most previous studies report

yields ranging from 80 to 95% at each step (Sott *et al.* 2005 and references within). This reactivity is not without precedent, however, with the intramolecular cyclization of Boc-alinanol occurring after its activation as a tosylate (van den Broek *et al.* 1989). These cyclized side products were accessible in part by the presence of a *tert*-butyl cationic leaving group at Boc.

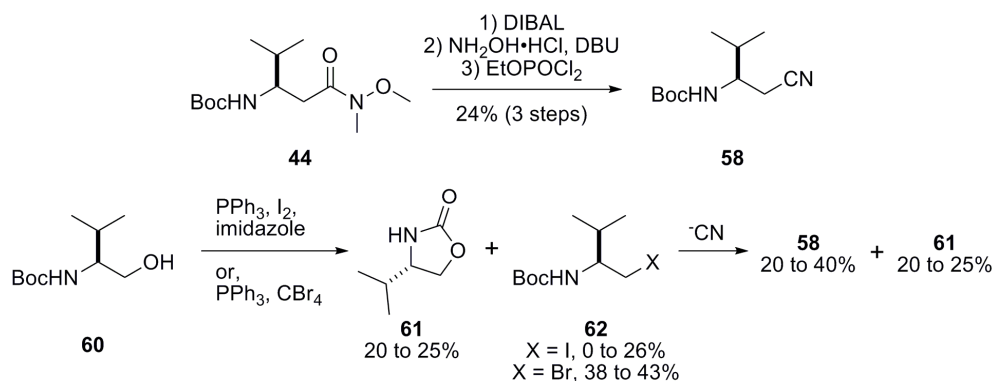


Figure 16: Attempted synthesis of the Boc protected nitrile **58**.

In order to fix the problem of cyclized product formation, it was hypothesized that by removing leaving groups or hydrogens within the protecting group, any cyclization that occurred would be reversible back to useful molecules. For this purpose phthalimide (Phth) protection was picked since any intramolecular cyclization at the proposed intermediates would result in an unstable, non-progressive cationic species **63** (Figure 17). Synthesis of phthalimide protected valinol was possible through subjecting L-valine to standard reduction (McKennon *et al.* 1993) and protection (Sheehan *et al.* 1952) conditions. This protecting group strategy did indeed improve the hydroxyl activation step, with both bromo- and tosyl-activated intermediates **67** synthesized in good yield without formation of cyclized side products.

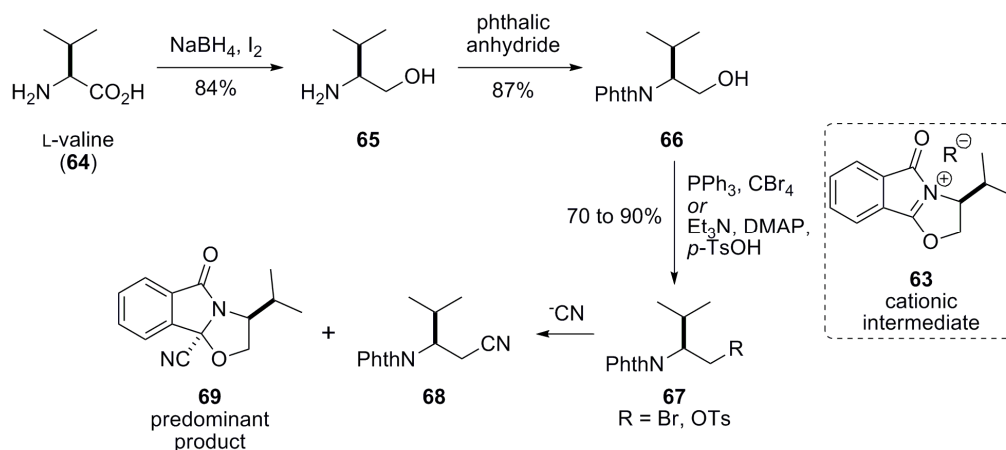


Figure 17: Poorly productive synthesis of the phthalimide protected nitrile **68**.

Unfortunately, cyanide addition gave a product mixture favoring the cyclized side product **69** over the intended nitrile **68**, indicating that an *in situ* equilibrium exists between the open form of **67** and the reversible, cyclized intermediate **63** made irreversible with cyanide addition. NMR analysis of **69** clearly shows only one diastereomer present, but simple experiments to determine relative stereochemistry such as NOESY would not be possible since the newly created stereocenter does not have a proton. For complete structural characterization, further chemical manipulations or X-ray crystallography will be necessary. A fair assumption would be that, due to the mostly planar nature of the cationic intermediate **63** and the apparent stereospecificity of nitrile addition, the steric effects of the isopropyl must strongly dictate the facial selectivity to the *re* face, resulting in the nitrile on the opposite face to the isopropyl. In retrospect, this route may have also been subject to undesired reactivity in later reactions based upon phthalimide base sensitivity, which will be discussed at length later.

Synthesis and Application of Dibenzyl Protected Nitrile **72**

Based upon the results using carbamate and imide based protecting groups, any protecting groups containing carbonyls were predicted to undergo undesired cyclization at some point during *N*-tubovaline fragment synthesis. With this consideration in mind, a dibenzyl protecting group strategy was picked to eliminate potential cyclization, along with the added advantage of removing the acidic N–H proton in preparation for the arylation step. The activation of dibenzyl protected L-valinol **70** (Reetz *et al.* 2004) resulted in the bromide **71** (Savithri *et al.* 1996, Figure 18), where the crude reaction was first filtered through Celite to remove the PPh₃ and triphenylphosphine oxide side products which tended to complicate flash chromatography. Nucleophilic substitution of **71** with a cyanide affords the nitrile **72** at either room temperature or 65 °C, but with a greater than 100 fold rate enhancement when run at the elevated temperature (completion within 1 hour versus 5 days). Each step in the synthesis to **72** efficiently gives its respective product in multi-gram quantities.

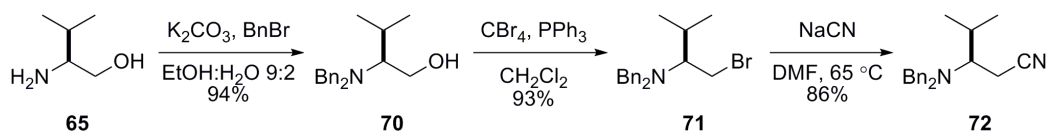


Figure 18: Productive synthesis of the dibenzyl protected nitrile **72**.

With the two precursors to **40** in hand, installation of the amine onto the *N*-tubulysin backbone was possible by activation of thiazole **45** as a Grignard reagent, nucleophilic addition into nitrile **72**, and *in situ* reduction of the resulting imine **73** (Figure 19). Activation of the thiazole as a nucleophile via Grignard reagents was necessary due to the instability of lithiated thiazoles at the relatively higher temperatures required for addition into the nitrile and their reported tendency to undergo double addition into

nitriles (Spieß *et al.* 2004). The bromine-magnesium exchange used to activate thiazole **45** originates from a commercially available Grignard reagent, as Grignard formation using elemental Mg turnings was non-productive. Prior to the NaBH₄ reduction, absolute EtOH was added to destroy any remaining Grignard species, a procedure which has been shown to improve the reaction outcome (Brussee *et al.* 1990). As noted above, this procedure is very similar to the protocol that Wipf used for oxygen based tubuvaline intermediates (Wipf and Wang 2007).

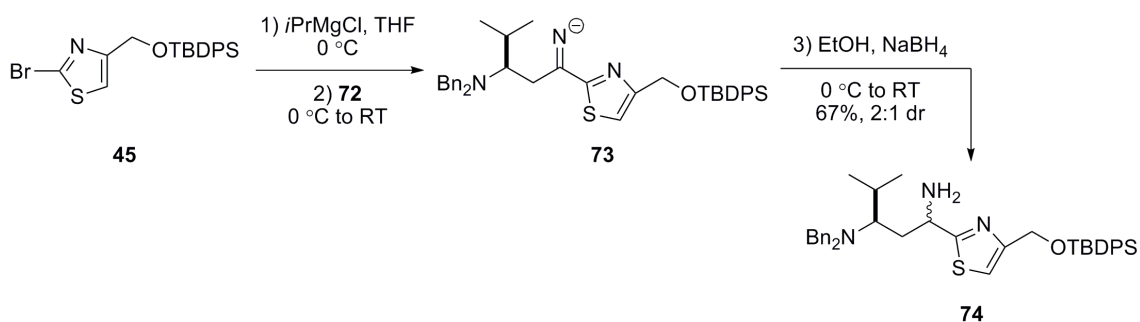


Figure 19: Synthesis of the amino mixture **74**.

While productive for the installation of the amine functionality within the ^{N₄}tubuvaline carbon framework, several significant issues exist in this synthetic strategy. This non-diastereoselective reduction gives a nearly equal mixture of (*R,R*)- and (*R,S*)-**74**, and since these types of tubuvaline analogs have not been reported, the identity of the major diastereomer would be pure conjecture. The mixture **74** was poorly separable by flash chromatography, a characteristic which persisted even after several functional group manipulations (*N*-acetylation, TBDPS deprotection, and oxidation, below). Finally, based upon the requisite peptide couplings towards the final tetrapeptide, the amine would have to undergo relatively early functionalization or protection. These options lack efficiency since late stage *N*-derivatization is desirable when generating many similar

compounds and a protection/deprotection strategy would add superfluous synthetic steps and reduce available material through yield loss.

What this route did offer was material to develop improved functional group transformations to *N*₄tubuvaline intermediates with model reactions. Following acetylation of the diastereomeric mixture **74**, TBDPS deprotection was found to be faster and very high yielding when using a solution of the fluoride salt tetrabutylammonium fluoride (TBAF, Figure 20). Procedures for oxidation of the alcohol **76** to the aldehyde **77** were scanned using standard conditions. Swern oxidation caused degradation of the starting material. Due to its location at a benzylic position, oxidation using MnO₂ successfully generated **77** in moderate yield (60–70%), with the advantage of convenient reaction set up and simple purification (filtration through Celite). Parikh-Doering oxidation gave the product but with a yield higher than theoretically possible; it was found that DMSO, SMe₂, and other impurities were trapped in the product mixture.

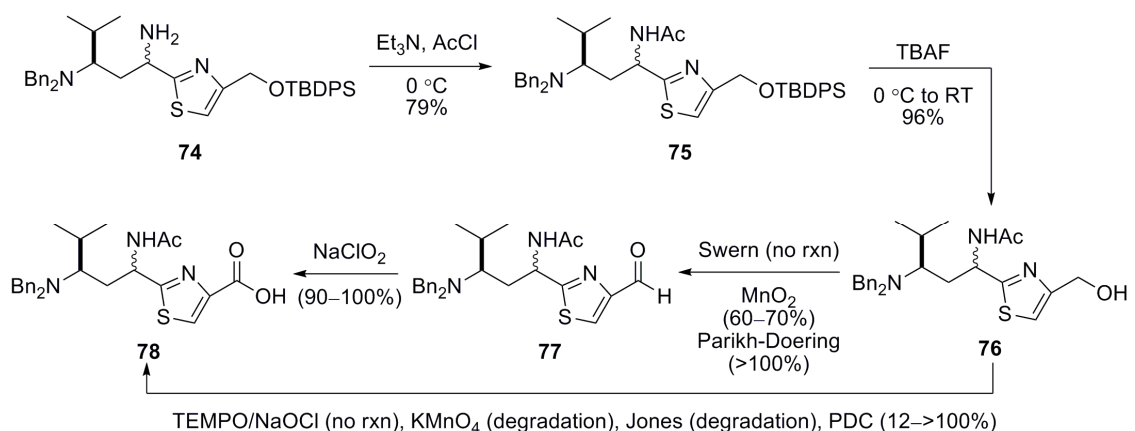


Figure 20: Model reactions for manipulation of *N*₄tubuvaline fragments.

Synthesis of the fully oxidized acid was also investigated with standard methods from either the alcohol **76** or aldehyde **77**. Full oxidation of **76** was more heavily

investigated since a successful route via the alcohol would eliminate redundant steps (Figure 20). Use of catalytic tempo/NaOCl in the presence of NaClO₂ (Zhao *et al.* 2005) was non-reactive with the alcohol, whereas Jones and KMnO₄ oxidations caused full degradation. PDC did produce aldehyde **77** and acid **78**, but multiple reaction variations could not give a consistent yield of each product or fix the problem of multiple impurities which hindered purification. The poor reaction outcomes with full oxidation of **76** showed that stepwise oxidation was superior. Alternative reactions to oxidize the aldehyde **77** were attempted, but the previously established oxidation system using NaClO₂ (Raghavan *et al.* 2008) was superior in reaction set up, yield, and ease of purification.

Third Generation Synthesis to ^NTubuvaline **40**: Attempted Synthesis of Dibenzyl Protected Ketone **79** and Aldehyde **82** Leading to a Retro-Michael Reaction

From this point, synthetic efforts were focused upon installation of the ^Ntubuvaline nitrogen stereoselectively but without the previously encountered intramolecular cyclization. Dibenzyl protected ketone **79** (Figure 21) was seen as a superior choice compared to the amino intermediate **74** under the prediction that a stereoselective nitrogen installation via the previously proposed Mitsunobu route would be possible while avoiding the pervasive cyclization endemic with Boc protection (Figure 14). Following the same nucleophilic addition of thiazole **45** into nitrile **72** used to generate imine **73** (Figure 19), hydrolysis of **73** was employed using acidic, neutral, or basic aqueous quenches (Figure 21). Instead of the expected dibenzyl ketone **79**, the reaction exclusively formed the retro-Michael products dibenzyl amine and α,β -unsaturated ketone **80**. A large coupling constant ($J = 15.7$ Hz) between the two alkene hydrogens of **80** establishes that the *E* isomer was formed based upon the established paradigm of *E/Z* proton splitting patterns in ¹H NMR and the report of a similar molecule (Dondoni *et*

al. 1994). This type of intermediate has been studied pertaining to tubuvaline synthesis before (Shankar *et al.* 2009).

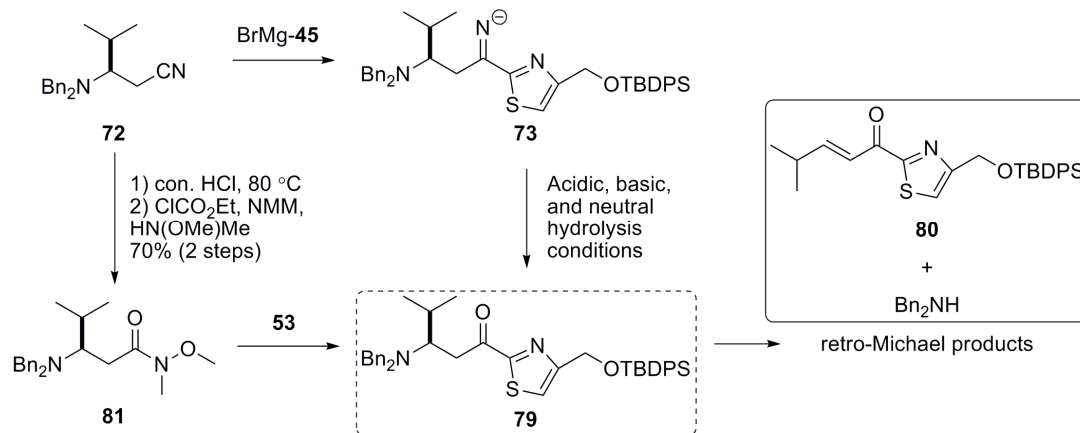


Figure 21: Routes to the unstable dibenzyl protected ketone **79**.

An alternative route based on the successful synthesis of ketone **42** through a Weinreb amide electrophile (Figure 13) was adapted for use in production of ketone **79** by first synthesizing the dibenzyl protected Weinreb amide **81** (Figure 21). Using nitrile **72**, hydrolysis was successful with minimal production of retro-Michael products using concentrated aqueous HCl at 80 °C; alternative acids (H_2SO_4), concentrations (6 M aqueous HCl), and temperatures (reflux) all resulted in partial or full production of the retro-Michael products. Standard peptide coupling supplied the Weinreb amide **81**, making the synthesis of this β -amino acid available from commercial starting materials without the need for anhydrous, oxygen free, or potentially explosive reaction conditions. This is unique when compared to standard procedures for one carbon homologations, where the Ardn-Eistert reaction (shown above), Kowalski ester homologation (Gray *et al.* 2004), Danheiser's diazotransfer modification (Danheiser *et al.* 1998), and Gmeimer's aspartic acid method (Gmeimer 1990) all require the use of a sensitive reagents.

Carbamate-protected amino acids have previously been used for β -amino acid synthesis through a nitrile intermediate (Caputo *et al* 1995), but as shown above, this method tends to be subject to intramolecular cyclization (Figure 14).

Unfortunately, arylation of the dibenzyl Weinreb amide **81** also underwent cleavage into the retro-Michael products (Figure 21). Based upon these results, the ketone **79** was clearly unstable under even mild conditions and was therefore a nonviable intermediate.

A general paradigm established by the work shown above can be summarized as such;

The N_t tubovaline intermediates will be susceptible to:

- 1) intramolecular cyclization upon α -thiazole activation if a carbonyl is present in the amine protecting group,
- 2) poor stereoselectivity with nucleophilic addition and reduction at a valine-derived nitrile, and
- 3) retro-Michael cleavage with dibenzyl amine protection β -positioned to a ketone.

With this in mind, the next route planned was to synthesize aldehyde **82**, which would be subjected to a non-stereoselective arylation using lithiated thiazole **53** towards the single desired diastereomer **84** (Figure 22). Despite the assured production of a diastereomeric mixture from this arylation, literature precedent will assist in determination of absolute stereochemistry of each alcohol. Following isolation of the pure (*S*)-alcohol **83**, diastereoselective installation of the key nitrogen via a Mitsunobu reaction was envisioned to run smoothly since intramolecular cyclization is not possible with the dibenzyl protection. This route agrees with the three criteria stated above: 1)

the nitrogen protecting group does not contain a carbonyl and hence **83** would not be subject to cyclization during a Mitsunobu reaction, 2) unlike the nitrile reactions, Mitsunobu reactions are well known to be stereoselective, and 3) at no point does a ketone exist at the α -thiazole position.

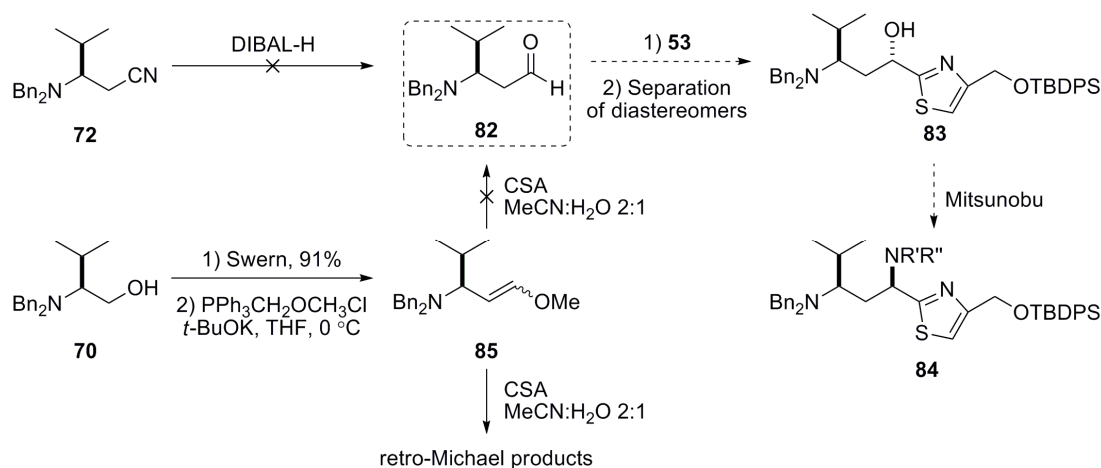


Figure 22: Routes to the unstable dibenzyl protected aldehyde **82**.

Synthesis of aldehyde **82** from nitrile **72** by DIBAL-H reduction proceeded to full consumption of the starting material by TLC analysis, but after aqueous workup, ^1H NMR analysis did not show any trace of the expected characteristic aldehyde peak. Instead, several peaks were present in the alkene region indicative of an elimination, so a less direct route starting with Swern oxidation of dibenzyl protected L-valinol **70** was used instead. A Wittig reaction at the aldehyde generated the methyl vinyl ether **85** which has been reported to provide a one carbon homologation to an aldehyde upon exposure to acidic conditions in aqueous solvents (Liu *et al.* 2009). When CSA was added to a solution of **85** in 2:1 MeCN:H₂O, TLC analysis of the crude reaction after 18 hours revealed starting material and dibenzyl amine. The reaction was deemed a failure due to the dibenzylamine's role as a marker for retro-Michael products and was not

investigated further. According to a report with an analogous aldehyde, the silica chromatography used to monitor the reaction may have been responsible for the retro-Michael product observed (Burke et al. 2004). This data shows that the dibenzyl protection is susceptible to elimination when positioned β to an aldehyde as well, which leads to the conclusion that the dibenzyl protection is too vulnerable to cleavage for use in diastereoselective routes to **40**.

Successful Regio- and Stereoselective Installation of the ^NTubovaline Nitrogen

Following extensive laboratory research and literature survey, a method in which to successfully perform a Mitsunobu reaction was eventually established using the Boc protected alcohol **55** previously synthesized using a (*R*)-CBS catalyzed reduction of the ketone **42** (Figure 14). The CBS reduction of **42** discussed above is stereospecific, but gives only a modest yield of the desired (*S*)-alcohol **55**. A non-stereoselective reduction of the ketone using NaBH₄ gives a 3:2 mixture of the two diastereomers favoring the target alcohol, but with a yield comparable to the CBS reduction and the opportunity to recover and convert the (*R*)-alcohol **86** back to **42** using MnO₂ oxidation (Figure 23). Overall, this route is preferable since it uses basic reagents in an operationally simple reaction that is equally productive as the diastereoselective reduction and easily separable by flash chromatography. In fact, with several rounds of **42** reduction and oxidation of recovered **86**, the overall yield of the desired alcohol **55** would surpass that of the diastereoselective CBS reduction. Work from this lab has previously featured the non-diastereoselective reduction of di-, tri-, and tetrapeptide ketones with approximately the same diastereomeric ratio (Balasubramanian *et al.* 2009).

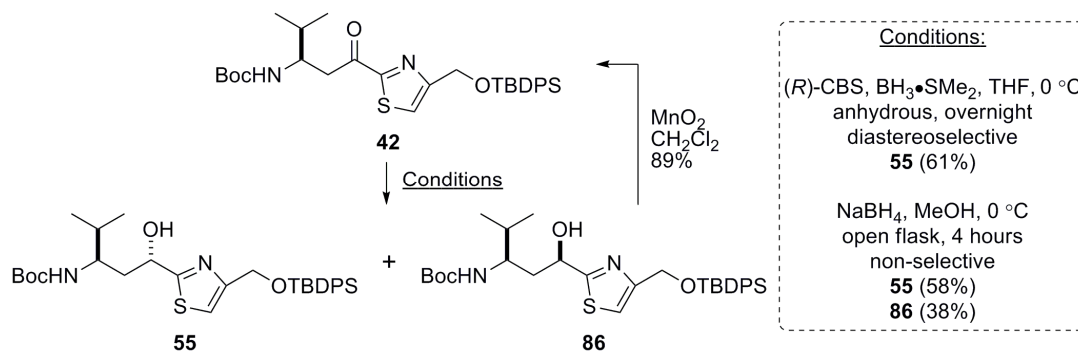
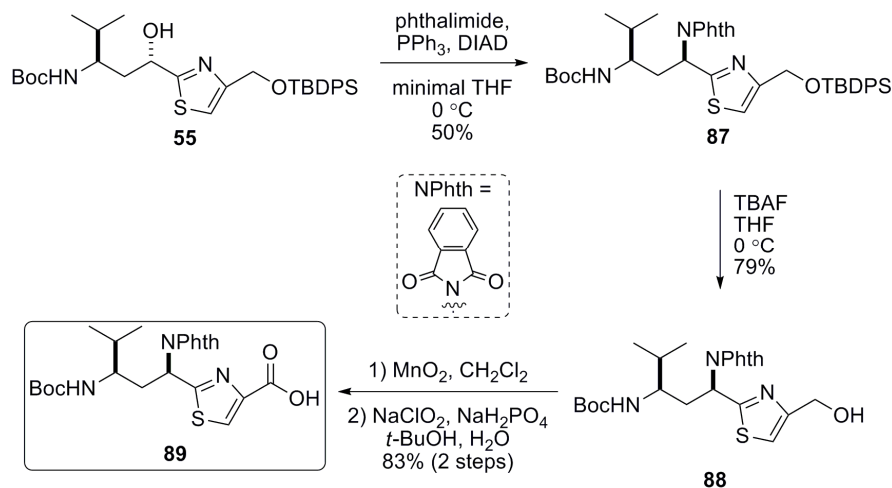


Figure 23: An alternative approach to the synthesis of alcohol **55**.

Under carefully controlled reaction conditions featuring the use of phthalimide as a nitrogen source, a successful Mitsunobu reaction was established with a reproducible yield of 50%, thus providing the means to stereoselectively install the nitrogen at the tubuvaline α -thiazole position (Figure 24). Unimportant factors for reaction success include the equivalents of reagents used as long as they are in a slight excess of **55**, and the reaction temperature, where lowering the temperature below 0 °C does not impact reaction yield or the time of reaction. A benzene:heptane solvent system does not change reaction outcome despite reports of improvements in systems with allylic alcohols (Lopez *et al.* 2005). A concentrated reaction (0.2 M) was important for reaction success, wherein the reagents were not fully dissolved until the addition of DIAD. The order of reagent addition should follow the standard for Mitsunobu reactions (alcohol, then PPh₃ and phthalimide, then slow addition of DIAD) and was crucial for any reaction progress. Compared to other organic solvents (EtOAc, CH₂Cl₂), post-reaction work up with ether extractions was superior by removing many of the impurities that complicate purification. Along with providing the desired product with regio- and stereo-controlled installation of the target nitrogen, this route is also advantageous by concurrently protecting the amine as a phthalimide. Phthalimides have unique deprotection

conditions which will allow for late-stage divergent synthesis via their selective deprotection, which will be discussed in detail later.



Previous Work: Raghavan *et al.*, 2008

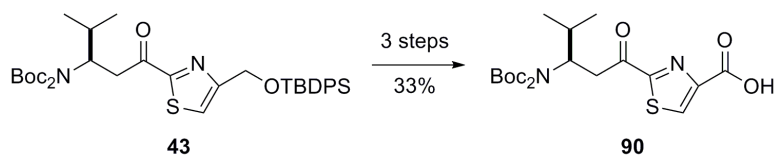


Figure 24: The successful Mitsunobu reaction and finishing steps to the ^Ntubuvaline fragment **89**.

Based upon the methods established through functional group transformations of the diastereomeric mixture of acetylated amino compounds **75–77**, modifications were made to the published procedures to finish the ^Ntubuvaline synthesis. In order to potentially improve the yield and reproducibility of the TBAF deprotection of **87**, different acid additives were screened with the intention of buffering the reaction, thereby avoiding the reactive anionic intermediate. In conjunction with TBAF, the addition of AcOH did not improve reaction yield but greatly increased reaction time, while the addition of *p*-TsOH caused a non-productive reaction. Deprotection through use of

H₂SiF₆ alone caused a mixture of products containing both the desired product and the Boc/TBDPS bis-protected amino alcohol. Ultimately, deprotection of the silyl ether was performed with the use of just TBAF.

Oxidation of the alcohol **88** would have previously been performed using the Dess-Martin periodinane, but MnO₂ oxidation was picked as an alternative due to its reproducibility, efficiency (80-90% yield typical), and the ease of purification. Full oxidation to the carboxylic acid went to nearly quantitative yield with NaClO₂, thus providing the bis-protected ^Ntubuvaline **89**. Purification of **89** by flash chromatography was not necessary according to ¹H NMR analysis, but more than a quantitative yield was obtained by crude weight, and the subsequent peptide coupling step ran more efficiently when purification was performed. This route to **89** improves on our previous work by increasing the yield from 33% to 66% over the final three steps to **90** (Raghavan *et al.* 2008, Figure 24).

Conclusion

After several synthetic iterations to circumvent side product formation and poor stereoselectivity, a method to regio- and stereoselectively install the key nitrogen of ^Ntubuvaline has been developed. Unavoidable intramolecular cyclization with use of established starting materials prompted changing the Weinreb amide electrophile to a nitrile for nitrogen pre-installation. Undesirable reactivity necessitated screening of different protecting groups towards the nitrile intermediate, wherein regioselective but non-stereoselective nitrogen installation was possible through use of a dibenzyl protected nitrile. This route presented a serious problem early on, and an alternative approach which hydrolyzed the *in situ* imine resulted in retro-Michael products

exclusively.

Following extensive laboratory and literature research, a method to properly run the Mitsunobu reaction through established intermediates was developed, where rigorously controlled reaction conditions reproducibly furnished phthalimide installation. As a supplement to target molecule synthesis, use of phthalimide as the nitrogen source will allow for selective deprotection, supporting an efficient late-stage divergence strategy. Addendums to the already established deprotection and oxidation steps improved overall yield to finish the ^Ntubuvaline fragment **89** synthesis. Availability of **89** and the other three amino acid residues of target compound **36** forms the material basis for generating ^Ntubulysin analogs following peptide couplings and deprotections, which will be discussed next.

Chapter 2 Experimentals:

General Procedures. All commercial reagents were used as provided unless otherwise indicated. THF and CH₂Cl₂ were dried by passage sequentially over 3Å molecular sieves followed by an alumina column. All reactions were performed under an inert atmosphere of dry Ar or N₂ in oven-dried (140 °C) glassware. Column chromatography was performed with silica gel 60 (43–60 Å). TLC was performed on Whatman silica gel (150 Å) F254 glass plates and spots visualized by UV, I₂, and KMnO₄ staining.

Ethyl 2-aminothiazole-4-carboxylate hydrochloride salt (49). A suspension of ethyl bromopyruvate (90%, 33 mL, 0.26 mol, 1 equiv), thiourea (30 g, 0.39 mol, 1.5 equiv) and absolute EtOH (500 mL) was heated to reflux. The resulting solution was refluxed for 18 h, concentrated under reduced pressure, and purified by recrystallization from EtOH/MeOH to afford the title compound as a white solid (56.0 g, 84% yield). ¹H and ¹³C NMR of the product matched those previously reported (Kelly and Lang 1996).

Ethyl 2-bromothiazole-4-carboxylate (50). To a solution of thiazole **49** (20.1 g, 0.0794 mol, 1 equiv) and CuBr (26.6 g, 0.119 mol, 1.5 equiv) in acetonitrile (400 mL) at 0 °C was added *t*-BuNO₂ (90%, 15.7 mL, 0.119 mol, 1.5 equiv) dropwise. After warming to room temperature over 1 h, the reaction was quenched with 1 M aqueous HCl (400 mL) and diluted with CH₂Cl₂ (400 mL). The layers were separated, and the aqueous layer was extracted with CH₂Cl₂ (2 x 200 mL). The combined organic layers were dried (Na₂SO₄), filtered, and concentrated under reduced pressure. Purification by recrystallization from hexanes afforded the title compound as a tan solid (13.2 g, 71% yield). *R*_f = 0.3 (SiO₂, 10% EtOAc:hexanes); ¹H and ¹³C NMR of the product matched those previously reported (Kelly and Lang 1996).

(2-Bromothiazol-4-yl)methanol (51). To a solution of ester **50** (10.0 g, 42.4 mmol, 1 equiv) in THF (200 mL) was added NaBH₄ (4.81 g, 127 mmol, 3 equiv), LiCl (5.4 g, 130 mmol, 3 equiv) and H₂O (40 mL). The resulting biphasic mixture was vigorously stirred for 2 h, after which TLC (20% EtOAc:hexanes) showed complete consumption of starting material. The reaction was quenched with saturated aqueous NH₄Cl (200 mL), diluted with EtOAc (200 mL), and the layers were separated. The aqueous layer was extracted with EtOAc (100 mL), and the organic layers were combined, dried (Na₂SO₄), filtered, and concentrated under reduced pressure to give the title compound as a yellow semi-solid (7.82 g, 95%). *R_f* = 0.2 (SiO₂, 20% EtOAc:hexanes); ¹H and ¹³C NMR of the product matched those previously reported (Wipf and Wang 2007).

2-Bromo-4-((tert-butyldiphenylsilyloxy)methyl)thiazole (45). To a solution of alcohol **51** (22.55 g, 0.116 mol, 1 equiv) in DMF (50 mL) was added imidazole (7.923 g, 0.116 mol, 1 equiv), DMAP (1.421 g, 0.0116 mol, 0.1 equiv), and TBDPSCI (30.5 mL, 0.116 mol, 1 equiv). After 48 h, TLC (20% EtOAc:hexanes) showed complete consumption of starting material. The reaction was quenched with H₂O (330 mL), diluted with EtOAc (300 mL), and the layers were separated. The aqueous layer was extracted with EtOAc (2 x 200 mL), and the combined organic layers were washed with H₂O (330 mL), 1 M aqueous HCl (330 mL), and saturated aqueous NaCl (330 mL), dried (Na₂SO₄), filtered, and concentrated under reduced pressure. Purification by flash chromatography (0–10% EtOAc:hexanes) afforded the title compound as a white solid (42.45 g, 85%). *R_f* = 0.8 (SiO₂, 20% EtOAc:hexanes); ¹H and ¹³C NMR of the product matched those previously reported (Raghavan *et al.* 2008).

(R)-tert-Butyl 1-(methoxy(methyl)amino)-4-methyl-1-oxopentan-3-ylcarbamate (44). To a solution of Boc-L-valine **52** (10.5 g, 48.3 mmol, 1 equiv) in THF (100 mL) at -78 °C

was added Et₃N (6.8 mL, 48 mmol, 1 equiv) and the reaction was stirred for 15 min. To this solution was added ethyl chloroformate (4.62 mL, 48.3 mmol, 1 equiv) causing a white precipitate to form. The reaction mixture stirred for 15 min, followed by removal of the stir bar. To the standing reaction mixture was added 75% of an ethereal diazomethane solution generated using Diazald (21.4 g, 100 mmol, 2 equiv) and KOH (16.8 g, 300 mmol, 6 equiv) (de Boer and Backer 1963). After 1 h, the remaining diazomethane solution and a stir bar were added to the reaction mixture, and the reaction stirred while warming to room temperature overnight. Separately, a mixture of (MeO)MeNH•HCl (14.4 g, 145 mmol, 3 equiv) and Et₃N (20.4 mL, 145 mmol, 3 equiv) in THF (100 mL) was stirred at room temperature overnight. After 18 h, the diazomethane reaction was quenched with 0.5 M aqueous AcOH solution (60 mL), and the resulting clear yellow mixture was stirred for 30 min. The layers were separated, and the organic layer was washed with saturated aqueous NaHCO₃ (100 mL) and saturated aqueous NaCl (100 mL), dried (Na₂SO₄), filtered, and concentrated under reduced pressure. The crude diazomethylketone was then dissolved in THF (100 mL), and the mixture containing the desalted (MeO)MeNH was added following salt removal by filtration through a fritted glass funnel. (**CAUTION:** Diazoketones have been reported to be explosive, and proper precaution should be used in the synthesis and handling of these compounds.) The resulting solution was cooled to -40 °C and the flask was wrapped in aluminum foil. To the reaction was added silver benzoate (1.6 g, 7.3 mmol, 0.15 equiv) as a solution in Et₃N (15 mL), and the reaction was stirred while warming to room temperature overnight. After 24 h, the reaction was diluted with CH₂Cl₂ (200 mL) and washed with 0.1 M aqueous HCl (100 mL). The aqueous layer was extracted with CH₂Cl₂ (3 x 200 mL), and the combined organic layers were dried (Na₂SO₄), filtered, and concentrated under reduced pressure. Purification by flash chromatography (30%

EtOAc:hexanes) afforded the title compound (9.8 g, 74%) as a colorless oil. $R_f = 0.6$ (SiO₂, 50% EtOAc:hexanes); ¹H and ¹³C NMR of the product matched those previously reported (Raghavan *et al.* 2008).

(R)-tert-Butyl 1-(4-((tert-butyldiphenylsilyloxy)methyl)thiazol-2-yl)-4-methyl-1-oxopentan-3-ylcarbamate (42). To a solution of bromo thiazole **45** (9.5 g, 22 mmol, 1.2 equiv) in THF (200 mL) at -78 °C was added *n*-BuLi (2.4 M in hexane, 11 mL, 26 mmol, 1.4 equiv) dropwise and the reaction was stirred for 90 min. Separately, to a solution of Weinreb amide **44** (5.0 g, 18 mmol, 1 equiv) in THF (200 mL) at -10 °C was added *i*-PrMgCl (1.7 M in THF, 11.2 mL, 19 mmol, 1.05 equiv) dropwise and the reaction stirred for 30 min. The Weinreb amide **44** solution was cooled to -78 °C and was added dropwise to the bromo thiazole **45** solution via cannula over 30 min. The reaction was stirred at -78 °C for 200 minutes, warmed to 0 °C, and stirred for an additional 90 min. TLC (10% EtOAc:hexanes) showed the reaction was no longer progressing, so the reaction was quenched with saturated aqueous NaHCO₃ (200 mL). The reaction mixture was diluted with Et₂O (200 mL) and the layers were separated. The organic layer was washed with saturated aqueous NaHCO₃ (100 mL) and the combined aqueous layers were extracted with Et₂O (2 x 100 mL). The combined organic layers were washed with H₂O (100 mL) and saturated aqueous NaCl (100 mL), dried (Na₂SO₄), filtered, and concentrated under reduced pressure. Purification by flash chromatography (5% EtOAc:hexanes, then 50% EtOAc:hexanes) afforded the title compound (5.245 g, 51%, 58% brsm) as a viscous orange oil and recovered Weinreb amide **44** (0.650 g). $R_f = 0.5$ (SiO₂, 20% EtOAc:hexanes); ¹H NMR (400 MHz, CDCl₃) δ 7.72–7.67 (m, 4H), 7.62 (s, 1H), 7.48–7.33 (m, 6H), 5.00–4.82 (m, 3H), 4.01–3.88 (m, 1H), 3.25 (dd, $J = 15.6, 7.4$ Hz, 1H), 3.16 (dd, $J = 15.6, 4.0$ Hz, 1H), 1.97–1.76 (m, 1H), 1.37 (s, 9H), 1.12 (s, 9H),

0.93 (d, $J = 6.4$ Hz, 3H), 0.92 (d, $J = 6.3$ Hz, 3H); ^{13}C NMR (101 MHz, CDCl_3) δ 192.9, 166.8, 159.3, 155.6, 135.7, 133.1, 130.1, 128.0, 121.7, 79.1, 63.0, 53.3, 40.9, 32.2, 28.5, 27.0, 19.4, 19.4, 18.6; HRMS calcd for $\text{C}_{31}\text{H}_{43}\text{N}_2\text{O}_4\text{SSi}^+$ [$\text{M} + \text{H}^+$] 567.2707, found 567.2714.

***tert*-Butyl (1*S*,3*R*)-1-(4-((*tert*-butyldiphenylsilyloxy)methyl)thiazol-2-yl)-1-hydroxy-4-methylpentan-3-ylcarbamate (55).** To a solution of (*R*)-CBS (20 mg, 0.072 mmol, 0.2 equiv) in THF (10 mL) at 0 °C was added $\text{BH}_3 \cdot \text{SMe}_2$ (2.0 M in THF, 0.21 mL, 0.42 mmol, 1.2 equiv) and the reaction stirred for 30 min. Ketone **42** (200 mg, 0.353 mmol, 1 equiv) was added as a solution in THF (6 mL, with 3 mL wash) dropwise. The reaction was stirred at 0 °C for 30 min and was then warmed to room temperature. After 3.5 h, TLC (20% EtOAc:hexanes) showed remaining starting material. The reaction was re-cooled to 0 °C and additional $\text{BH}_3 \cdot \text{SMe}_2$ (2.0 M in THF, 0.21 mL, 0.42 mmol, 1.2 equiv) was added. The reaction was slowly warmed to room temperature overnight. After 24 h total, TLC showed complete consumption of starting material. The reaction was quenched with slow addition of MeOH (CAUTION: generates hydrogen gas) and concentrated under reduced pressure. Purification by flash chromatography (20% EtOAc:hexanes) afforded the title compound as a clear oil (123 mg, 61% yield). $R_f = 0.2$ (SiO_2 , 20% EtOAc:hexanes); ^1H NMR (400 MHz, CDCl_3) δ 7.73–7.64 (m, 4H), 7.46–7.33 (m, 6H), 7.19 (s, 1H), 5.02 (ddd, $J = 7.5, 5.4, 4.5$ Hz, 1H), 4.85 (d, $J = 1.3$ Hz, 2H), 4.61–4.48 (m, 1H), 4.39 (d, $J = 5.7$ Hz, 1H), 3.68–3.59 (m, 1H), 2.28–2.17 (m, 1H), 1.97–1.86 (m, 1H), 1.86–1.76 (m, 1H), 1.41 (s, 9H), 1.10 (s, 9H), 0.93 (d, $J = 6.8$ Hz, 3H), 0.90 (d, $J = 6.8$ Hz, 3H); ^{13}C NMR (101 MHz, CDCl_3) δ 175.8, 156.9, 156.6, 135.7, 133.4, 129.9, 127.9, 113.7, 78.0, 71.3, 63.2, 53.7, 41.0, 32.6, 28.5, 27.0, 19.4, 19.1, 17.7; HRMS calcd for $\text{C}_{31}\text{H}_{45}\text{N}_2\text{O}_4\text{SSi}^+$ [$\text{M} + \text{H}^+$] 569.2863, found 569.2863.

(4R,6R)-6-(4-((*tert*-Butyldiphenylsilyloxy)methyl)thiazol-2-yl)-4-isopropyl-1,3-oxazinan-2-one (57). $R_f = 0.4$ (SiO₂, 50% EtOAc:hexanes); ¹H NMR (400 MHz, CDCl₃) δ 7.69 (t, $J = 6.4$ Hz, 4H), 7.48–7.33 (m, 6H), 7.28 (s, 1H), 6.17 (s, 1H), 5.64 (dd, $J = 4.6, 4.6$ Hz, 1H), 4.86 (s, 2H), 3.17–3.09 (m, 1H), 2.44 (ddd, $J = 14.0, 4.9, 4.9$ Hz, 1H), 2.16 (ddd, $J = 13.5, 8.8, 4.7$ Hz, 1H), 1.80–1.67 (m, 1H), 1.10 (s, 9H), 0.97 (d, $J = 6.7$ Hz, 3H), 0.94 (d, $J = 6.8$ Hz, 3H); ¹³C NMR (101 MHz, CDCl₃) δ 169.0, 157.4, 153.0, 135.7, 133.3, 130.0, 127.9, 115.2, 75.2, 63.0, 53.7, 32.6, 28.6, 27.0, 19.4, 18.15, 18.13.

(3S,9bR)-3-Isopropyl-5-oxo-2,3,5,9b-tetrahydrooxazolo[2,3-a]isoindole-9b-carbonitrile (69). White solid; $R_f = 0.5$ (SiO₂, 20% EtOAc:hexanes); ¹H NMR (400 MHz, CDCl₃) δ 7.85–7.64 (m, 4H), 4.64 (dd, $J = 9.1, 7.5$ Hz, 1H), 4.32 (dd, $J = 9.1, 7.5$ Hz, 1H), 3.82 (dt, $J = 9.2, 7.4$ Hz, 1H), 2.15–1.95 (m, 1H), 1.20 (d, $J = 6.6$ Hz, 3H), 1.02 (d, $J = 6.7$ Hz, 3H); ¹³C NMR (101 MHz, CDCl₃) δ 172.1, 139.8, 134.3, 132.5, 131.5, 125.1, 123.8, 116.1, 90.4, 76.3, 62.4, 32.9, 20.5, 18.9.

(S)-2-(Dibenzylamino)-3-methylbutan-1-ol (70). (Reetz *et al.* 2004) To a solution of L-valinol (9.457 g, 91.7 mmol, 1 equiv) and K₂CO₃ (25.34 g, 183 mmol, 2 equiv) in EtOH (180 mL) and H₂O (40 mL) at reflux was added BnBr (27.4 mL, 229 mmol, 2.5 equiv) slowly over 15 min. After refluxing for 24 h, TLC (10% EtOAc:hexanes) showed complete consumption of starting material. The reaction was cooled to room temperature and the reaction was quenched with addition of saturated aqueous NaHCO₃ (20 mL) and H₂O (10 mL). The aqueous layer was extracted with Et₂O (3 x 100 mL), and the combined organic layers were washed with saturated aqueous NaCl (100 mL), dried (Na₂SO₄), filtered, and concentrated under reduced pressure. Purification by flash chromatography (10% EtOAc:hexanes) afforded the title compound (24.411 g, 94% yield) as a yellow oil. $R_f = 0.3$ (SiO₂, 10% EtOAc:hexanes); ¹H and ¹³C NMR of the

product matched those previously reported (Métro *et al.* 2006).

(S)-N,N-Dibenzyl-1-bromo-3-methylbutan-2-amine (71). (Savithri *et al.* 1996) To a solution of the alcohol **70** (5.022g, 17.7 mmol, 1 equiv) in CH₂Cl₂ (150 mL) at 0 °C was added CBr₄ (7.346 g, 22.2 mmol, 1.25 equiv) in one portion. After 5 min stirring, PPh₃ (6.972 g, 26.6 mmol, 1.5 equiv) was added portionwise over an additional 5 min. After an additional 5 min, TLC (10% EtOAc:hexanes) showed complete consumption of starting material. Celite was added to the reaction mixture and the slurry was concentrated under reduced pressure. To the resulting free flowing powder was added hexanes (150 mL), and the slurry was filtered through a tightly packed plug of Celite and washed with hexanes (3 x 50 mL). The solution was concentrated under reduced pressure, and this method of Celite filtration was repeated until all the PPh₃ and triphenylphosphine oxide were removed by TLC. Purification by flash chromatography (10% EtOAc:hexanes) afforded the title compound (5.701 g, 93% yield) as a clear oil. *R*_f = 0.7 (SiO₂, 10% EtOAc:hexanes); ¹H NMR (400 MHz, CDCl₃) δ 7.31–7.13 (m, 10H), 4.00 (ddd, *J* = 8.5, 6.2, 2.4 Hz, 1H), 3.62 (d, *J* = 13.5 Hz, 2H), 3.40 (d, *J* = 13.5 Hz, 2H), 2.81 (dd, *J* = 13.5, 8.5 Hz, 1H), 2.74 (dd, *J* = 13.5, 6.2 Hz, 1H), 2.03–1.90 (m, 1H), 0.85 (d, *J* = 6.7 Hz, 3H), 0.51 (d, *J* = 6.5 Hz, 3H); ¹³C NMR (101 MHz, CDCl₃) δ 139.3, 129.3, 128.5, 127.4, 63.7, 59.42, 59.37, 30.5, 22.0, 16.6.

(R)-3-(Dibenzylamino)-4-methylpentanenitrile (72). To a solution of bromide **71** (1.952 g, 5.64 mmol, 1 equiv) in DMF (70 mL) was added NaCN (0.829 g, 16.9 mmol, 3 equiv) and the reaction was heated to 65 °C. After 1 h, TLC (10% EtOAc:hexanes) showed complete consumption of the starting material. The reaction was cooled to room temperature and was partitioned between H₂O (350 mL) and Et₂O (350 mL). The aqueous layer was extracted with Et₂O (2 x 350 mL), and the combined organic layers

were washed with H₂O (3 x 350 mL), dried (Na₂SO₄), filtered, and concentrated under reduced pressure. Purification by flash chromatography (5–10% EtOAc:hexanes) afforded the title compound (1.411 g, 86% yield) as a clear oil. $R_f = 0.4$ (SiO₂, 10% EtOAc:hexanes); ¹H NMR (400 MHz, CDCl₃) δ 7.37–7.09 (m, 10H), 3.84 (d, $J = 13.7$ Hz, 2H), 3.39 (d, $J = 13.7$ Hz, 2H), 2.55–2.44 (m, 2H), 2.41–2.32 (m, 1H), 2.10–1.91 (m, 1H), 0.98 (d, $J = 6.6$ Hz, 3H), 0.84 (d, $J = 6.6$ Hz, 3H); ¹³C NMR (101 MHz, CDCl₃) δ 139.1, 129.0, 128.5, 127.3, 119.5, 60.6, 54.0, 29.9, 20.9, 20.4, 14.3.

***N*³,*N*³-Dibenzyl-1-(4-((*tert*-butyldiphenylsilyloxy)methyl)thiazol-2-yl)-4-**

methylpentane-1,3-diamine (74). (Spieß *et al.* 2004) To a solution of thiazole **45** (1.98 g, 4.58 mmol, 2.5 equiv) in THF (25 mL) at 0 °C was added *i*-PrMgCl (2.0 M in THF, 1.9 mL, 4.8 mmol, 2.5 equiv) dropwise. The resulting yellow solution was stirred for 1 h, after which nitrile **72** (0.535 g, 1.83 mmol, 1 equiv) was added as a solution in THF (10 mL, with 5 mL wash) dropwise. The reaction was immediately warmed to room temperature, and a dark orange color formed after 1 h. After an additional 21 h, TLC (10% EtOAc:hexanes) showed complete consumption of **72**, so the reaction was cooled to 0 °C, the Grignard species were quenched with absolute EtOH (10 mL), and NaBH₄ (0.208 g, 5.50 mmol, 3 equiv) was added in one portion. The reaction was stirred while warming to room temperature overnight, and after 24 h the reaction was quenched with slow addition of saturated aqueous NH₄Cl (30 mL). The reaction was diluted with Et₂O (40 mL) and H₂O (10 mL), the layers were separated, and the organic layer was washed with saturated aqueous NH₄Cl (20 mL), dried (Na₂SO₄), filtered, and concentrated under reduced pressure. Purification by flash chromatography (5–30% EtOAc:hexanes) afforded a 2:1 mixture of the title compounds (0.80 g, 67% yield) as a yellow oil. Less polar diastereomer: clear oil, $R_f = 0.25$ (SiO₂, 30% EtOAc:hexanes); ¹H NMR (400 MHz,

CDCl₃) δ 7.65 (d, *J* = 7.0 Hz, 4H), 7.42–7.27 (m, 8H), 7.26–7.04 (m, 8H), 4.81 (d, *J* = 0.9 Hz, 2H), 4.38 (dd, *J* = 10.0, 3.3 Hz, 1H), 3.80 (d, *J* = 13.2 Hz, 2H), 3.49 (d, *J* = 13.2 Hz, 2H), 2.54 (dt, *J* = 10.8, 3.7 Hz, 1H), 2.28–2.11 (m, 2H), 1.44–1.28 (m, 3H), 1.06 (s, 9H), 0.97–0.92 (m, 3H), 0.91 (d, *J* = 6.8 Hz, 3H); ¹³C NMR (101 MHz, CDCl₃) δ 178.4, 156.9, 140.6, 135.7, 133.5, 129.8, 129.4, 128.4, 127.8, 127.1, 113.0, 63.4, 58.2, 54.1, 51.3, 37.0, 27.1, 27.0, 22.8, 20.0, 19.5. More polar diastereomer: yellow oil, *R*_f = 0.18 (SiO₂, 30% EtOAc:hexanes); ¹H NMR (400 MHz, CDCl₃) δ 7.63 (dd, *J* = 7.8, 1.3 Hz, 4H), 7.39–7.23 (m, 10H), 7.23–7.15 (m, 4H), 7.15–7.02 (m, 3H), 4.77 (s, 2H), 4.09 (t, *J* = 6.2 Hz, 1H), 3.61 (d, *J* = 13.6 Hz, 2H), 3.55 (d, *J* = 13.6 Hz, 2H), 2.55–2.42 (m, 1H), 1.99 (s, 3H), 1.91–1.76 (m, 2H), 1.11–0.96 (m, 9H), 0.94–0.80 (m, 6H); ¹³C NMR (101 MHz, CDCl₃) δ 177.7, 156.7, 140.3, 135.7, 133.5, 129.9, 129.2, 128.4, 127.9, 127.0, 113.0, 63.3, 61.0, 54.4, 53.8, 36.3, 28.9, 27.0, 22.1, 20.1, 19.5.

(*E*)-1-(4-((*tert*-Butyldiphenylsilyloxy)methyl)thiazol-2-yl)-4-methylpent-2-en-1-one (80). To a solution of the thiazole **45** (146 mg, 0.338 mmol, 1.2 equiv) in THF (3.0 mL) at -78 °C was added *n*-BuLi solution (2.5 M in hexanes, 0.16 mL, 0.40 mmol, 1.4 equiv) dropwise. The resulting deep orange solution was stirred for 1.5 h, followed by addition of Weinreb amide **81** (100 mg, 0.282 mmol, 1 equiv) as a solution in THF (2.0 mL, with 1 mL wash) dropwise. The reaction was stirred at -78 °C for 1 h and warmed to 0 °C over an additional 105 min, after which TLC (5% EtOAc:hexanes) showed complete consumption of starting material. The reaction was quenched with saturated aqueous NaHCO₃ (6 mL) and the THF was removed under reduced pressure. The resulting aqueous mixture was extracted with Et₂O (3 x 20 mL), and the combined organic layers were washed with H₂O (15 mL) and saturated aqueous NaCl (15 mL), dried (Na₂SO₄), filtered, and concentrated under reduced pressure. Purification by flash chromatography

(3% EtOAc:hexanes) afforded the title compound (0.114 g, 90% yield) as a yellow oil. R_f = 0.3 (SiO₂, 3% EtOAc:hexanes); ¹H NMR (400 MHz, CDCl₃) δ 7.75–7.70 (m, 4H), 7.64 (s, 1H), 7.50–7.37 (m, 6H), 7.30 (dd, J = 15.7, 6.5 Hz, 1H), 7.19 (dd, J = 15.7, 1Hz, 1H), 4.99 (d, J = 0.9 Hz, 2H), 2.66–2.51 (m, 1H), 1.15 (ovlp s, 9H), 1.15 (ovlp s, 3H), 1.13 (s, 3H); ¹³C NMR (101 MHz, CDCl₃) δ 182.2, 168.1, 159.2, 157.5, 135.7, 133.2, 130.1, 128.0, 121.8, 121.5, 63.1, 31.9, 27.0, 21.4, 19.5.

(R)-3-(Dibenzylamino)-4-methylpentanoic acid (Supplemental 1, S1). A solution of nitrile **72** (0.907 g, 3.10 mmol) in concentrated HCl (16 mL) was heated to 80 °C and stirred for 1.5 h, after which TLC (50% EtOAc:hexanes) showed complete consumption of starting material. The reaction was adjusted to pH 6–8 with 10% aqueous NaOH, resulting in a white precipitate. The aqueous mixture was extracted with Et₂O (4 x 30 mL) to give the title compound as a clear oil (0.870 g, 90% yield) in sufficient purity for the next reaction. R_f = 0.2 (SiO₂, 50% EtOAc:hexanes); ¹H NMR (400 MHz, CDCl₃) δ 11.25 (br s, 1H), 7.38–7.27 (m, 10H), 3.95 (d, J = 13.0 Hz, 2H), 3.55 (d, J = 13.0 Hz, 2H), 3.00 (dt, J = 11.3, 4.0 Hz, 1H), 2.61 (dd, J = 16.8, 11.3 Hz, 1H), 2.31 (dd, J = 16.8, 4.2 Hz, 1H), 2.27–2.19 (m, 1H), 0.98 (dd, J = 6.8, 0.9 Hz, 6H); ¹³C NMR (101 MHz, CDCl₃) δ 174.6, 136.1, 129.8, 128.9, 128.2, 59.5, 53.6, 30.3, 25.9, 22.5, 18.9.

(R)-3-(Dibenzylamino)-N-methoxy-N,4-dimethylpentanamide (81). To a solution of **S1** (125 mg, 0.40 mmol, 1 equiv) in CH₂Cl₂ (15 mL) at -10 °C was added NMM (0.20 mL, 1.8 mmol, 4.5 equiv) and ethyl chloroformate (60 μL, 0.62 mmol, 1.5 equiv). After 15 min, HCl•HN(OMe)Me was added resulting in a white precipitate, and the reaction stirred while warming to room temperature overnight. After 16 h, TLC (50% EtOAc:hexanes) of the resulting yellow/orange mixture showed complete consumption of starting material. The reaction was concentrated under reduced pressure and

purification by flash chromatography (20% EtOAc:hexanes) afforded the title compound (100 mg, 70% yield) as a clear oil. $R_f = 0.3$ (SiO₂, 20% EtOAc:hexanes); ¹H NMR (400 MHz, CDCl₃) δ 7.39 (d, $J = 7.3$ Hz, 4H), 7.30 (t, $J = 7.5$ Hz, 4H), 7.21 (t, $J = 7.2$ Hz, 2H), 3.76 (d, $J = 13.6$ Hz, 2H), 3.66 (s, 3H), 3.42 (d, $J = 13.6$ Hz, 2H), 3.19 (s, 3H), 3.05–2.94 (m, 1H), 2.68–2.52 (m, 2H), 1.91–1.74 (m, 1H), 0.99 (d, $J = 6.6$ Hz, 3H), 0.80 (d, $J = 6.7$ Hz, 3H); ¹³C NMR (101 MHz, CDCl₃) δ 174.6, 140.3, 129.3, 128.2, 126.8, 61.3, 60.9, 54.5, 32.6, 31.5, 29.7, 21.2, 20.0.

(S)-2-(Dibenzylamino)-3-methylbutanal (Supplemental 2, S2). (Reetz *et al.* 2004) To a solution of (COCl)₂ (0.74 mL, 8.5 mmol, 1.2 equiv) in CH₂Cl₂ (40 mL) cooled to -78 °C was added DMSO (1.00 mL, 14.1 mmol, 2 equiv) dropwise. After 5 min, valinol **70** (1.995 g, 7.06 mmol, 1 equiv) was added as a solution in CH₂Cl₂ (20 mL, with 5 mL wash) via cannula, resulting in a light yellow solution. After 30 min, Et₃N (4.0 mL, 28 mmol, 4 equiv) was added and the reaction was warmed to room temperature resulting in formation of a white precipitate. After 15 min, TLC (5% EtOAc:hexanes) showed complete consumption of starting material. The reaction was quenched with H₂O (40 mL), the layers were separated, and the aqueous layer was extracted with CH₂Cl₂ (3 x 20 mL). The combined organic layers were washed with 0.1 M aqueous HCl (20 mL), H₂O (20 mL), and 5% aqueous NaHCO₃ (20 mL), dried (Na₂SO₄), filtered, and concentrated under reduced pressure. Purification by flash chromatography (5% EtOAc:hexanes) afforded the title compound (1.807 g, 91% yield) as a yellow oil. $R_f = 0.5$ (SiO₂, 5% EtOAc:hexanes); ¹H NMR of the product matched that previously reported (Cooke *et al.* 1996).

(S)-N,N-Dibenzyl-1-methoxy-4-methylpent-1-en-3-amine (85). (Liu *et al.* 2009) To a suspension of (methoxymethyl)triphenylphosphonium chloride (276 mg, 0.782 mmol, 2.2

equiv) in THF (5 mL) at 0 °C was added *t*-BuOK (84 mg, 0.71 mmol, 2 equiv) in one portion. The resulting red-orange suspension stirred for 75 min, after which **S2** (100 mg, 0.355 mmol, 1 equiv) was added as a solution in THF (1 mL with 0.5 mL wash) dropwise. The resulting yellow suspension was stirred at 0 °C for 75 min, and was then stirred while warming to room temperature overnight. After 48 h, the reaction was quenched with saturated aqueous NH₄Cl (10 mL) and H₂O was added until full solvation of the precipitates. The layers were separated, the aqueous layer was extracted with EtOAc (3 x 20 mL), and the combined organic layers were washed with saturated aqueous NaCl (30 mL), dried (Na₂SO₄), filtered, and concentrated under reduced pressure. Purification by flash chromatography (2% EtOAc:hexanes) afforded a 10:1 *E:Z* mixture (according to ¹H NMR analysis at room temperature) of the title compound as a yellow oil. *R*_f = 0.6 (SiO₂, 5% EtOAc:hexanes); *E* isomer: ¹H NMR (400 MHz, CDCl₃) δ 7.32 (d, *J* = 7.5 Hz, 4H), 7.21 (t, *J* = 7.4 Hz, 4H), 7.12 (t, *J* = 7.2 Hz, 2H), 6.08 (d, *J* = 12.7 Hz, 1H), 4.49 (dd, *J* = 12.5, 10.4 Hz, 1H), 3.71 (d, *J* = 13.7 Hz, 2H), 3.51 (s, 3H), 3.16 (d, *J* = 13.8 Hz, 2H), 2.31 (t, *J* = 10.2 Hz, 1H), 1.82–1.68 (m, 1H), 1.00 (d, *J* = 6.5 Hz, 3H), 0.67 (d, *J* = 6.6 Hz, 3H); ¹³C NMR (101 MHz, CDCl₃) δ 149.9, 140.7, 128.9, 128.3, 126.7, 98.7, 64.1, 56.2, 53.7, 30.3, 21.4, 20.7.

tert-Butyl (1*R*,3*S*)- and *tert*-Butyl (1*R*,3*R*)-1-(4-((*tert*-butyldiphenylsilyloxy)methyl)thiazol-2-yl)-1-hydroxy-4-methylpentan-3-ylcarbamate (55 and 86). To MeOH (45 mL) at 0 °C was added NaBH₄ (0.268 g, 7.1 mmol, 15 equiv) resulting in gas evolution. After 20 min, ketone 42 (0.268 g, 0.473 mmol, 1 equiv) was added as a solution in MeOH (35 mL, with 10 mL wash) precooled to 0 °C. After 4 h, TLC showed complete consumption of starting materials (20% EtOAc:hexanes). The reaction was quenched with saturated aqueous NH₄Cl (50 mL) and MeOH was removed under reduced pressure. The

remaining aqueous reaction mixture was diluted with enough H₂O to dissolve all solids and was extracted with EtOAc (3 x 30 mL). The combined organic layers were dried (Na₂SO₄), filtered, and concentrated under reduced pressure. ¹H NMR of the crude reaction mixture showed a 1.6:1 dr of the *R,S* and *R,R* diastereomers, respectively. Purification by flash chromatography (20% EtOAc:hexanes) afforded the title compounds as a yellow oil (*R,R* diastereomer **86**, 0.102 g, 38% yield) and a clear oil (*R,S* diastereomer **55**, 0.156 g, 58% yield). **55**: ¹H and ¹³C NMR of the product matched those reported above. **86**: *R_f* = 0.4 (SiO₂, 20% EtOAc:hexanes); ¹H NMR (400 MHz, CDCl₃) δ 7.72–7.64 (m, 4H), 7.45–7.31 (m, 6H), 7.18 (s, 1H), 5.07–4.95 (m, 1H), 4.91 (d, *J* = 9.8 Hz, 1H), 4.85 (s, 2H), 4.57 (d, *J* = 9.6 Hz, 1H), 3.78–3.66 (m, 1H), 1.97–1.86 (m, 1H), 1.83–1.75 (m, 1H), 1.75–1.66 (m, 1H), 1.43 (s, 9H), 1.10 (s, 9H), 0.94 (d, *J* = 4.2 Hz, 3H), 0.92 (d, *J* = 4.3 Hz, 3H); ¹³C NMR (101 MHz, CDCl₃) δ 175.4, 158.0, 156.5, 135.7, 133.4, 129.9, 127.8, 113.4, 80.4, 69.2, 63.2, 52.5, 46.2, 42.1, 32.3, 28.5, 27.0, 19.4, 18.5; HRMS calcd for C₃₁H₄₅N₂O₄SSi⁺ [*M* + H⁺] 569.2863, found 569.2859.

(*R*)-*tert*-Butyl 1-(4-((*tert*-butyldiphenylsilyloxy)methyl)thiazol-2-yl)-4-methyl-1-oxopentan-3-ylcarbamate (42**)**. The ketone **42** (42.5 mg, 89% yield) was obtained from alcohol **86** (48 mg, 0.084 mmol) in an identical fashion to that of **S1** after purification by flash chromatography (10% EtOAc:hexanes). ¹H and ¹³C NMR of the product matched those reported above.

tert-Butyl (1*R*,3*R*)-1-(4-((*tert*-butyldiphenylsilyloxy)methyl)thiazol-2-yl)-1-(1,3-dioxoisindolin-2-yl)-4-methylpentan-3-ylcarbamate (**87**). To a solution of alcohol **55** (0.590 g, 1.04 mmol, 1 equiv) in THF (5.0 mL) at 0 °C was added PPh₃ (0.345 g, 1.35 mmol, 1.3 equiv) and phthalimide (0.199 g, 1.35 mmol, 1.3 equiv) with only partial dissolution of solutes. To this mixture was added DIAD (94%, 0.28 mL, 1.4 mmol, 1.3

equiv) dropwise which resulted in an orange reaction solution. After 2 h, the reaction had turned yellow and TLC (20% EtOAc:hexanes using an aliquot partitioned between H₂O and ether) showed complete consumption of starting material. The reaction was quenched with ice cold H₂O (20 mL) and THF was removed under reduced pressure. The remaining aqueous reaction mixture was extracted with Et₂O (2 x 20 mL), and the combined organic layers were dried (Na₂SO₄), filtered, and concentrated under reduced pressure. Purification by flash chromatography (10% EtOAc:hexanes) afforded the title compound as a white solid (0.316 g, 50% yield). $R_f = 0.4$ (SiO₂, 20% EtOAc:hexanes); ¹H NMR (400 MHz, CDCl₃) δ 7.83 (dd, $J = 5.4, 3.1$ Hz, 2H), 7.71 (dd, $J = 5.4, 3.1$ Hz, 2H), 7.68–7.63 (m, 4H), 7.45–7.30 (m, 6H), 7.17 (s, 1H), 5.76 (dd, $J = 12.2, 4.5$ Hz, 1H), 4.83 (s, 2H), 4.37 (d, $J = 10.5$ Hz, 1H), 3.51–3.40 (m, 1H), 3.14–3.04 (m, 1H), 2.13 (ddd, $J = 14.3, 12.3, 4.5$ Hz, 1H), 1.77–1.63 (m, 1H), 1.39 (s, 9H), 1.08 (s, 9H), 0.89 (d, $J = 6.9$ Hz, 3H), 0.87 (d, $J = 6.9$ Hz, 3H); ¹³C NMR (101 MHz, CDCl₃) δ 169.5, 167.9, 156.8, 155.7, 135.7, 134.1, 133.4, 132.1, 129.9, 127.9, 123.6, 114.1, 79.4, 63.2, 52.3, 50.2, 34.2, 33.3, 28.5, 27.0, 19.4, 19.2, 18.1; HRMS calcd for C₃₉H₄₈N₃O₅SSi⁺ [M + H⁺] 698.3084, found 698.3099.

***tert*-Butyl (1*R*,3*R*)-1-(1,3-dioxisoindolin-2-yl)-1-(4-(hydroxymethyl)thiazol-2-yl)-4-methylpentan-3-ylcarbamate (88).** To a solution of silyl ether **87** (202 mg, 0.290 mmol, 1 equiv) in THF (2.0 mL) at 0 °C was added TBAF (1.0 M in THF, 0.32 mL, 0.32 mmol, 1.1 equiv). After 1.5 h, TLC (50% EtOAc:hexanes) showed complete consumption of starting material. The solvent was removed under reduced pressure, and the reaction was purified by flash chromatography (50% EtOAc:hexanes) affording the title compound as a clear oil (105 mg, 79% yield). $R_f = 0.3$ (SiO₂, 50% EtOAc:hexanes); ¹H NMR (400 MHz, CDCl₃) δ 7.83 (dd, $J = 5.4, 3.1$ Hz, 2H), 7.71 (dd, $J = 5.4, 3.1$ Hz, 2H),

7.10 (s, 1H), 5.79 (dd, $J = 12.2, 4.4$ Hz, 1H), 4.70 (s, 2H), 4.52 (d, $J = 10.5$ Hz, 1H), 3.52–3.38 (m, 1H), 3.16–3.02 (m, 1H), 2.77 (br s, 1H), 2.23–2.10 (m, 1H), 1.77–1.63 (m, 1H), 1.39 (s, 9H), 0.88 (apparent t, $J = 7.5$ Hz, 6H); ^{13}C NMR (101 MHz, CDCl_3) δ 170.3, 167.9, 156.2, 155.8, 134.2, 132.0, 123.6, 115.2, 79.4, 61.0, 52.3, 50.1, 34.2, 33.2, 28.5, 19.2, 18.1; HRMS calcd for $\text{C}_{23}\text{H}_{30}\text{N}_3\text{O}_5\text{S}^+$ [$\text{M} + \text{H}^+$] 460.1906, found 460.1925.

***tert*-Butyl (1*R*,3*R*)-1-(1,3-dioxoisindolin-2-yl)-1-(4-formylthiazol-2-yl)-4-**

methylpentan-3-ylcarbamate (Supplemental 3, S3). To a solution of alcohol **88** (53 mg, 0.12 mmol, 1 equiv) in CH_2Cl_2 (5 mL) was added MnO_2 (88% activated, 114 mg, 1.15 mmol, 10 equiv) and the reaction was stirred vigorously overnight. After 20 h, TLC (50% EtOAc:hexanes) showed complete consumption of starting material. The solvent was removed under reduced pressure, and the crude solid was mixed with EtOAc (10 mL). The resulting slurry was filtered through a tightly packed plug of Celite and washed with EtOAc (3 x 10 mL). The combined washings were concentrated under reduced pressure to give the title compound as a white/yellow solid (45 mg, 0.098 mmol, 85% yield) in sufficient purity for the next reaction. An analytically pure sample can be prepared by flash chromatography (20% EtOAc:hexanes). $R_f = 0.6$ (SiO_2 , 50% EtOAc:hexanes); ^1H NMR (400 MHz, CDCl_3) δ 9.96 (s, 1H), 8.10 (s, 1H), 7.84 (dd, $J = 5.4, 3.0$ Hz, 2H), 7.72 (dd, $J = 5.4, 3.0$ Hz, 2H), 5.87 (dd, $J = 12.2, 4.6$ Hz, 1H), 4.45 (d, $J = 10.5$ Hz, 1H), 3.52–3.40 (m, 1H), 3.19–3.04 (m, 1H), 2.22 (ddd, $J = 14.2, 12.2, 4.7$ Hz, 1H), 1.78–1.64 (m, 1H), 1.38 (s, 9H), 0.89 (apparent t, $J = 7.3$ Hz, 6H); ^{13}C NMR (101 MHz, CDCl_3) δ 184.9, 171.5, 167.8, 155.8, 154.7, 134.5, 132.0, 128.0, 123.8, 79.6, 52.3, 50.2, 34.4, 33.3, 28.5, 19.3, 18.2; HRMS calcd for $\text{C}_{23}\text{H}_{28}\text{N}_3\text{O}_5\text{S}^+$ [$\text{M} + \text{H}^+$] 458.1750, found 458.1769.

2-((1*R*,3*R*)-3-(*tert*-Butoxycarbonylamino)-1-(1,3-dioxoisindolin-2-yl)-4-

methylpentyl)thiazole-4-carboxylic acid (89). To a solution of **S3** (0.138 g, 0.302 mmol, 1 equiv) and 2-methyl-2-butene (1.76 mL, 16.6 mmol, 55 equiv) in *t*-BuOH (12 mL) was added a solution of NaClO₂ (80%, 0.306 g, 2.71 mmol, 9 equiv) and NaH₂PO₄•H₂O (0.291 g, 2.11 mmol, 7 equiv) in H₂O (6 mL) dropwise. The reaction color changed from yellow to colorless over 2 h and TLC (50% EtOAc:hexanes) showed complete consumption of starting material. *t*-BuOH was removed under reduced pressure, and the resulting slurry was partitioned between H₂O (30 mL) and CH₂Cl₂ (30 mL). The layers were separated, and the aqueous layer was acidified to pH 3 with 5% aqueous KHSO₄ and extracted with CH₂Cl₂ (2 x 30 mL). The combined organic layers were dried (Na₂SO₄), filtered, and concentrated under reduced pressure. Purification by flash chromatography (10% MeOH:CH₂Cl₂ with 0.5% AcOH), followed by removal of AcOH by addition and removal of benzene (3 x 20 mL) under reduced pressure, afforded the title compound as a white solid (0.138 g, 98%). *R*_f = 0.4 (SiO₂, 10% MeOH:CH₂Cl₂ with 0.5% AcOH); ¹H NMR (400 MHz, CDCl₃) δ 8.20 (s, 1H), 7.86 (dd, *J* = 3.1, 5.4 Hz, 2H), 7.75 (dd, *J* = 3.1, 5.4 Hz, 2H), 5.87 (dd, *J* = 4.7, 11.9 Hz, 1H), 4.40 (d, *J* = 10.5 Hz, 1H), 3.56–3.44 (m, 1H), 3.15–3.01 (m, 1H), 2.28–2.15 (m, 1H), 1.78–1.63 (m, 1H), 1.40 (s, 9H), 0.92 (d, *J* = 6.8 Hz, 3H), 0.89 (d, *J* = 6.9 Hz, 3H); ¹³C NMR (101 MHz, CDCl₃) δ 175.5, 170.9, 167.7, 161.3, 155.8, 134.5, 131.9, 128.5, 123.8, 79.7, 52.3, 50.0, 34.6, 33.2, 28.5, 19.3, 18.0; HRMS calcd for C₂₃H₂₆N₃O₆S⁻ [M - H] 472.1548, found 472.1549.

Chapter 3:

Synthesis of ^NTubulysin V (**36**), U (**37**), and *N*-acylated ^NTubulysin Analogs as Complements to Naturally Isolated Tubulysins

Introduction

With the crucial ^Ntubuvaline fragment **89** in hand, the stage has been set for peptide couplings with the other amino acid residues of ^Ntubulysin V (**36**) to form a common tetrapeptide intermediate. Procedures for the ^Ntubuvaline-tubuphenylalanine coupling based upon literature precedence resulted in undesirable *N*-acyl transfer impurities which poisoned the desired product. Modifications to this route have supported high yielding reactions to supply the protected tetrapeptide **98** as a common intermediate. This molecule allows for efficient final compound synthesis through late-stage modifications.

Consecutive deprotections of the phthalimide and benzyl ester groups caused reaction material degradation, so a strategy wherein final stage tetrapeptides more robust under the necessary deprotection conditions was used. These changes eventually proved successful in the total synthesis of amine **36**. Acylation of the ^Ntubuvaline nitrogen was ran as the penultimate step through the late stage primary amine **100**, where subsequent hydrolysis furnished a range of compounds which will support an initial SAR profile. The stage has also been set for the synthesis of various derivatives of ^Ntubulysin V.

Synthesis of the ^NTubuvaline-Tubuphenylalanine Dipeptide **93** and Further Ligations

The precedent set in the Fecik lab (Raghavan *et al.* 2008) calls for peptide

coupling of the tubuvaline and tubuphenylalanine residues by carboxylate activation using an electron withdrawing phenol, itself installed by DCC activation of the carboxylate. When this was performed on ^Ntubuvaline residue **89** and the benzyl protected tubuphenylalanine **92** (from Boc deprotection of tubuphenylalanine fragment **91**, Raghavan *et al.* 2008), the reaction was seemingly high yielding, albeit with some excessive proton integration in the aliphatic region of dipeptide **93** by ¹H NMR (Figure 25). While this dipeptide coupling was high yielding, its use as starting material in the synthesis of tripeptide **95** proved to be far less efficient, where coupling to Boc-L-isoleucine generated the desired product in 50% yield or less under the same conditions which had furnished the analogous coupling in 78% yield previously (Raghavan *et al.* 2008). Full characterization of the individual components of the reaction using ¹H and ¹³C NMR, and low resolution MS, revealed that two products had been formed from the reaction: the desired tripeptide **95** and *N*-acylurea **96** (Figure 25). Production of **96** from pure **93** would require the cleavage and reformation of the ^Ntubuvaline-tubuphenylalanine amide bond under the relatively mild conditions of the tripeptide coupling. Hence, the source of the impurity must have been from an *N*-acylurea **94** impurity in the starting material, a fact that was not initially discovered since **93** and **94** are inseparable by flash chromatography.

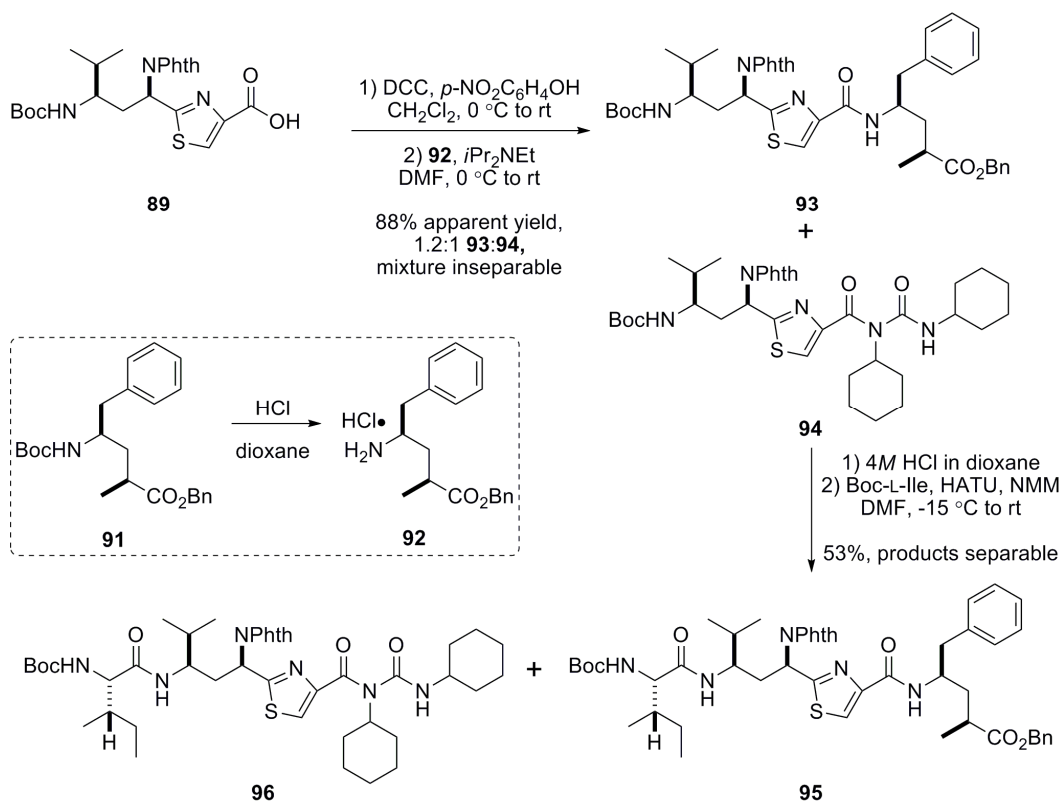


Figure 25: Reactions producing *N*-acylurea side products **94** and **96** with dipeptide **93** and tripeptide **95**.

This theory was confirmed by activation of **89** with DCC and *para*-nitro phenol. Purification of the reaction mixture before addition of the tubophenylalanine fragment **92** supplied the activated ester **97** and **94** as separable entities, allowing for their isolation as pure samples (Figure 26). Tubophenylalanine fragment **92** was then added to the purified activated ester **97**, and dipeptide **93** was isolated from this reaction without impurity **94**. Full ¹H NMR characterization of each product allowed comparison to the NMR of the previously generated mixture of **93**:**94** and showed that a 1.2:1 molar ratio existed based upon relative integration, translating to approximately a 50% yield of dipeptide **93** and 40% yield of the *N*-acylurea **94**. This provides a clear explanation for

the poor yield in the tripeptide synthesis and the incorrect integration in the aliphatic region of the dipeptide mixture. An *N*-acyl shift occurring with DCC activation of carboxylates has been studied previously (DeTar and Silverstein 1966), but has not been reported pertaining to tubulysin synthesis.

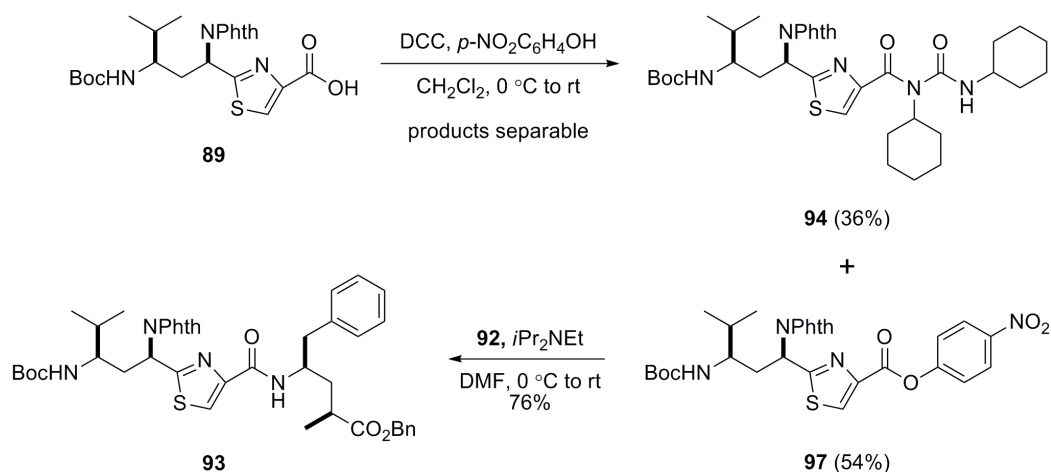


Figure 26: Synthesis of pure samples of dipeptide **93** and *N*-acylurea side product **94**.

Such a significant loss of these synthetically derived intermediates prompted investigation into alternative methods of *N*_ttubuvaline-tubuphenylalanine amide bond formation. By simply activating the carboxylate of *N*_ttubuvaline **89** as a mixed anhydride with ethyl chloroformate, diepeptide **93** was obtained following addition of a small excess of the tubuphenylalanine fragment **92**. The reaction resulted in moderate yields of **93** (60–70%) with use of crude **89**, but a high yield of 92% when using purified **89** (Figure 27). In addition to the efficiency of this reaction, chromatographic purification proved to be much simpler with no *N*-acylurea side product impurities formed. The same strategy was used previously to form the tubuvaline-tubuphenylalanine amide bond during tubulysin analog synthesis (Wipf and Wang 2007).

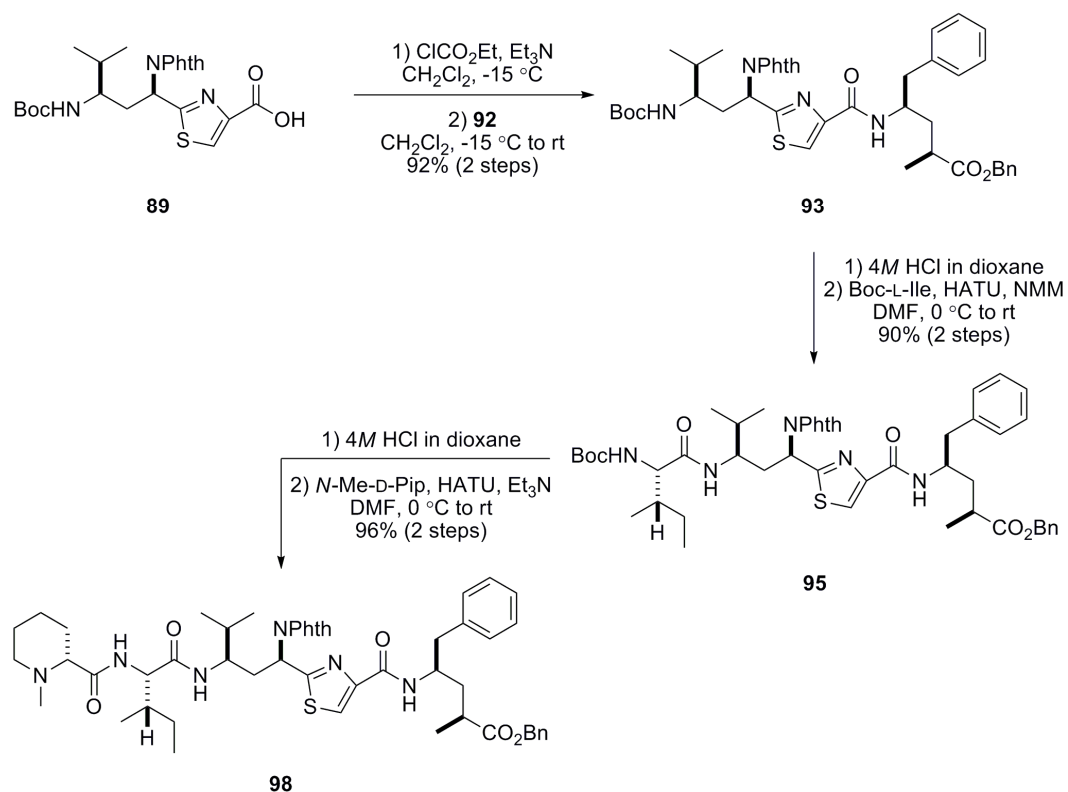


Figure 27: Highly productive amide bond forming reactions to tetrapeptide **98**.

With access to pure dipeptide **93**, coupling to Boc-L-Isoleucine using the HATU peptide coupling reagent generated the tripeptide **95** exclusively following the protocol of our previously established syntheses (Raghavan *et al.* 2008, Balasubramanian *et al.* 2008). Amide bond formation to furnish tetrapeptide **98** was only somewhat successful using the phenol-activated ester of *N*-methyl-D-pipecolinic acid, but ran with nearly quantitative yield using HATU. Based upon the work described here, tetrapeptide **98** is available from the 4 individual N_t tubulyisin residues in 6 steps with a 79% overall yield (Figure 27) and thus represents an extremely productive method to a common late-stage intermediate.

Attempts to Synthesize Amine **36** through Successive Deprotection of Tetrapeptide **98**

The strategy to quickly generate many *N*-tubulysin analogs was contingent on the selective deprotection of the phthalimide and benzyl ester protecting groups of **98**. Selective functionalization of the resulting molecules would provide a range of products to establish an initial SAR at the α -thiazole position of *N*-tubuvaline. Phthalimides have long been known to be selectively deprotected with the use of hydrazine in the presence of other common functional groups (Ing–Manske procedure, Ing and Manske 1926). Adding excess hydrazine to a solution of **98** in methanol fully converts the phthalimide ring into partially cleaved intermediate **99** after 3 hours reaction, where hydrazine has added into one of the carbonyls of the imide (Figure 28). For conversion of **99** to the primary amine **100**, the reaction is refluxed overnight; the intermediate **99** is long lived at room temperature, and will not proceed to the target molecule **100** unless heated. A convenient workup, starting with removal of MeOH under reduced pressure, has the reaction taken up in 0.1 M aqueous HCl and extracted with 3 portions of diethyl ether, which effectively separates **100** from the excess hydrazine and most of the other impurities that make purification challenging. Interestingly, when the reaction is performed in absolute EtOH, it progresses from the intermediate to the product slowly at 50 °C, but significant degradation is observed by TLC and a 52% yield of the amine **100** is obtained when the reaction is heated to the temperature at which MeOH refluxes (65 °C).

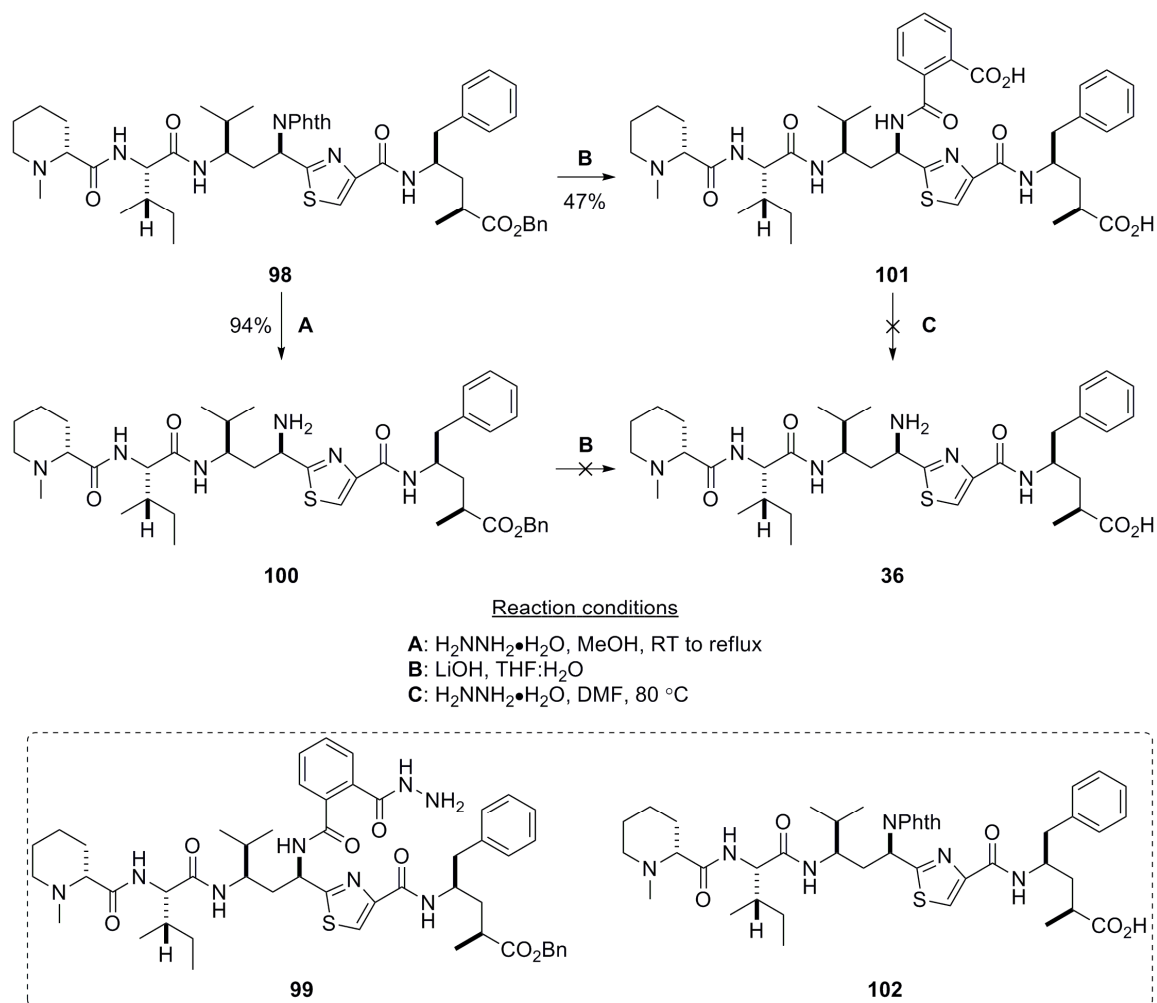


Figure 28: Initial deprotection strategy to synthesize amine **36**.

Standard LiOH hydrolysis based upon our previous benzyl ester deprotections of tubulysin analogs (Raghavan *et al.* 2008) was performed on **100** in order to obtain **36**. When two separate hydrolysis reactions were performed using **100** generated from different sources, both reactions resulted in complete degradation of the starting material (Figure 28). The materials resulting from the reaction were a white solid which was insoluble in a range of polar and non-polar solvents, and an orange oil that was indistinguishable by ¹H NMR, ¹³C NMR, and MS analysis.

Final stage deprotection of tetrapeptide **98** was also attempted by first hydrolyzing the benzyl ester in the presence of the phthalimide protected amine. Since phthalimide rings are susceptible to base hydrolysis in environments with pH as low as 7.4 (Astleford and Weigel 1991 and references therein), LiOH caused both removal of the ester and partial hydrolysis of the phthalimide ring to benzoic acid **101** (Figure 28). With full cleavage of the now opened phthalimide ring in mind, **101** was heated in the presence of hydrazine, resulting in the same type of degradation as seen with hydrolysis of the amine. Unexpectedly, a purified and dried sample of this bis-hydrolyzed side product at room temperature had partially transformed into both the recycled phthalimide ring **102** and **36** after 6 months according to low resolution MS. Unfortunately, the sample was so small that not nearly enough of this product mixture could have been used for complete characterization upon repurification.

Attempts to Synthesize Amine **36** through Milder Deprotection of Tetrapeptide **98**

Benzyl ester deprotection using milder palladium catalyzed hydrogenation was attempted on several model systems in an attempt to overcome the reaction degradation seen with LiOH hydrolysis. Using di, tri, and tetrapeptide tubulysin intermediates, the reaction outcomes were erratic and ranged from no reaction to full starting material degradation into several products. In general, if excess Pd/C was used in anhydrous EtOAc under high hydrogen gas pressure, progress of starting material occurred given several days reaction. The lack of desired reactivity under metal-catalyzed hydrogenation of tubulysin intermediates bearing a thiazole ring has been observed several times before (Wipf and Wang 2007, Ullrich *et al.* 2009b, Burkhart and Kazmaier 2012), and this limitation is apparent through this work as well. On the other hand, plenty of successful hydrogenations with tubulysin intermediates not containing thiazoles

have also been reported (Peltier *et al.* 2006, Patterson *et al.* 2007, Pando *et al.* 2009, Pando *et al.* 2011, Shibue *et al.* 2011, Vlahov *et al.* 2011).

Replacing the primary amine of **100** with an azide to stabilize the molecule for LiOH hydrolysis was considered a viable option, since a mild Staudinger reaction could remove the azide following benzyl deprotection instead of relying on the standard yet problematic azide deprotection through hydrogenation. Azido transfer using a shelf stable azido transfer reagent (Goddard-Borger and Stick 2007) under conditions that have previously been used successfully with other tubulysin intermediates resulted in complete destruction of the starting material.

These reactions made apparent that the final stage tetrapeptide intermediates **98**, **100**, and **101** are sensitive to the standard deprotection conditions to remove the benzyl ester, but are also resistant to alternative means to perform this transformation. The options moving forward then were to either use these intermediates in a less direct route to ^Ntubulysins, or to use modified versions of these intermediate which are not sensitive to basic conditions. One strategy using an available intermediate was to recycle the hydrolyzed phthalimide ring of **101** into phthalisoimide **103** using DCC, followed by hydrazine cleavage to the primary amine (Figure 29). This route is reported to increase the deprotection strength of hydrazine, thereby allowing for transformation to the amine under milder conditions more amenable to compounds with acid and base sensitive functionalities (Kukolja and Lammert 1975, Hemenway *et al.* 2010). Due to the presence of the crucial carboxylate at the C-terminus and a suspicion that side product formation would occur as seen in the early dipeptide coupling strategy (Figure 25), this route was not used. Work that will be discussed later confirms that in the presence of DCC, this carboxylate undergoes undesirable reactivity.

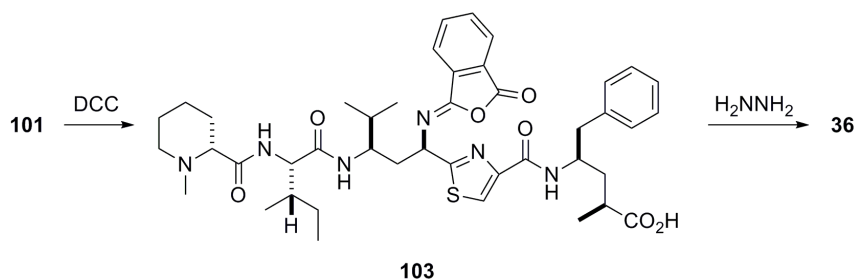


Figure 29: Potential alternative deprotection strategy to amine **36**.

Hydrolytically Stable Intermediates Used in a Modified Route to Amine **36**

After much work with unproductive and destructive routes to *N*-tubulysin V (**36**), the means by which to synthesize this molecule was eventually possible based upon work reported from investigators at Lilly (Astleford and Weigel 1991). Their publication showed that β -lactams appended with phthalimides can be selectively reacted with pyrrolidine in the presence of other reactive functionalities, not the least of which is the electrophilic lactam. The resulting open-chain intermediate has a reversal of reactivity: whereas phthalimide rings undergo hydrolysis in basic conditions but are robust under acidic conditions, opening the phthalimide ring by addition of a pyrrolidine causes the functional group to become very stable under basic or nucleophilic conditions, but cleavable back to the phthalimide ring under acidic conditions. A crucial example from this report featured the hydrolysis of the ethyl ester **105** using NaOH without disturbing the pyrrolidine-opened phthalimide (**106**, Figure 30). Hence this system is well suited to solve the problems seen with these late-stage deprotections, since an intact phthalimide ring following benzyl ester hydrolysis was predicted to be cleaved with hydrazine under more mild conditions than shown above (Figure 28). While it is not an obvious factor in the success of this reaction, the presence of the pyrrolidine salt in **105** may be critical based upon the discussions below.

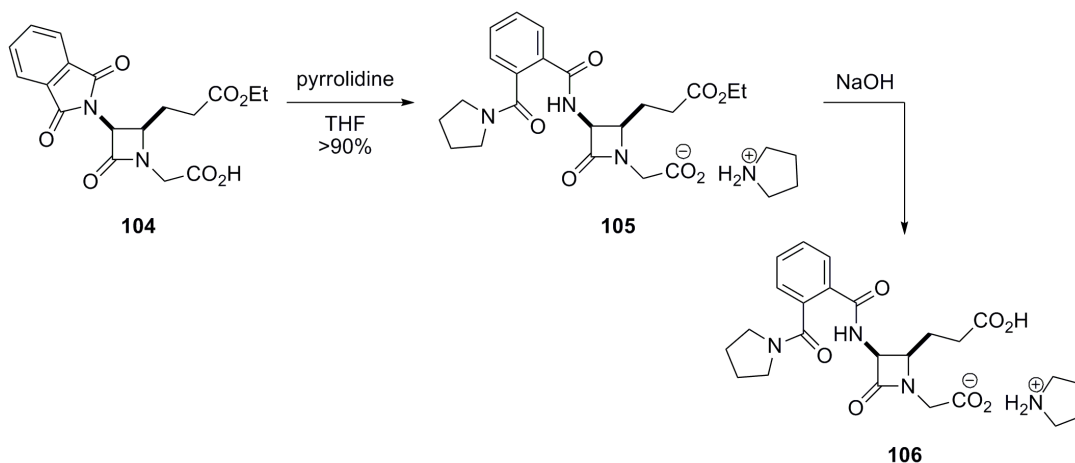


Figure 30: A pertinent example of basic hydrolysis from the Astleford and Weigel paper.

Pyrrolidine mediated phthalimide ring opening of **98** was initially performed using 1.2 equivalents of pyrrolidine in THF as reported (Astleford and Weigel 1991), but even after an additional 2.5 equivalents of pyrrolidine was added with 3 days reaction time, progression beyond the starting material had not occurred. When a large excess of pyrrolidine was added to the THF solution, the reaction was finally pushed to completion within 6 hours; subsequently it was found that the reaction can be run in neat pyrrolidine for full production of **107** in 5 hours without side product formation or product degradation (Figure 31). Steric bulk at the phthalimide may be the factor which necessitates the use of a large excess of pyrrolidine for reaction progress. Reaction workup through simple concentration resulted in a crude product with sufficient purity to move forward to the next step. An analytically pure sample can be made by aqueous work up and chromatographic purification of crude **107** to give 92% yield of pure **107**.

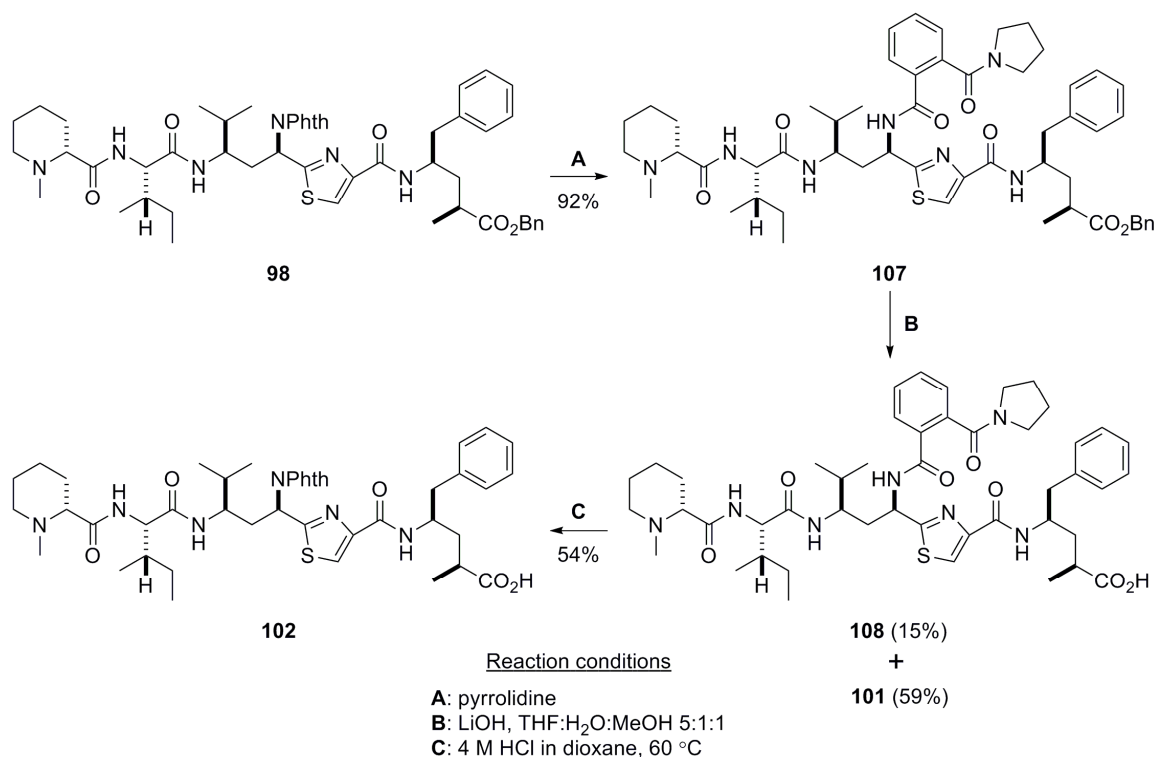


Figure 31: Synthesis of the phthalimide protected, benzyl deprotected tetrapeptide **102** with intermediate isolation.

Based upon the observations noted in the parent paper (Figure 30), base hydrolysis was expected to generate the desired benzyl ester deprotection of **107** without pyrrolidine hydrolysis. When performed on a sample of crude **107**, LiOH hydrolysis of the benzyl ester required additional equivalents (20 equivalents) of base beyond the standard protocol (10 equivalents) for complete progress to the acid **108**, where no significant hydrolysis of the pyrrolidine was observed. After acidic quench and CH₂Cl₂ extraction of the resulting aqueous phase, the crude product can be brought forward unpurified or an analytically pure sample can be obtained through flash chromatography.

When this same reaction was run on purified **107**, extensive hydrolysis of the

pyrrolidine was seen with production of **101** as the major product (Figure 31). Based upon the need for excess hydroxide to fully deprotect crude **107**, and the significant side product formation when using purified **107** under the same conditions, it is hypothesized that residual pyrrolidine carried over with the crude product buffers the reaction, providing for the observed selective hydrolysis. Valuable future studies should measure product formation under a range of buffered hydrolysis conditions in order to optimize this reaction. While seemingly innocuous, the potential role of the pyrrolidine salt as a buffer in the NaOH hydrolysis of **105** reported in the parent paper cannot be ignored, especially in light of **105** as the singular example of this type of modification subjected to basic hydrolysis (Astleford and Weigel 1991) and the results presented here.

Reclosure of the phthalimide ring was reported to run smoothly in acidic MeOH (Astleford and Weigel 1991, McCormick *et al.* 2006); however, previous studies from our lab have noted transesterification at the carboxylate of tubuphenylalanine occurring with use of an acidic H₂O/MeOH HPLC solvent system (Balasubramanian *et al.* 2009). In order to avoid methyl ester formation after the crucial benzyl ester hydrolysis, other acidic reaction media were investigated. No reaction progress was observed when **108** was stirred for extended periods in either 4 M HCl in dioxane or 3 M aqueous HCl at room temperature. Partial reaction occurred with 4 M HCl in dioxane at 50 °C, with full consumption of either crude or pure starting material at 60 °C after 48 hours to produce the closed phthalimide **102**. The more extreme reaction conditions necessary for pyrrolidine cleavage compared to those reported (slight excess of HCl in MeOH, room temperature) may again be attributed to steric bulk at this position.

While each intermediate in this pathway can be isolated as a pure entity, performing these 3 steps without intermediate purification is also possible. Simple

aqueous workups between steps and a final purification of **102** generates the desired molecule in 48% yield over the 3 steps, and is in fact the desirable choice due to yield efficiency and the elimination of unnecessary purifications (Figure 32).

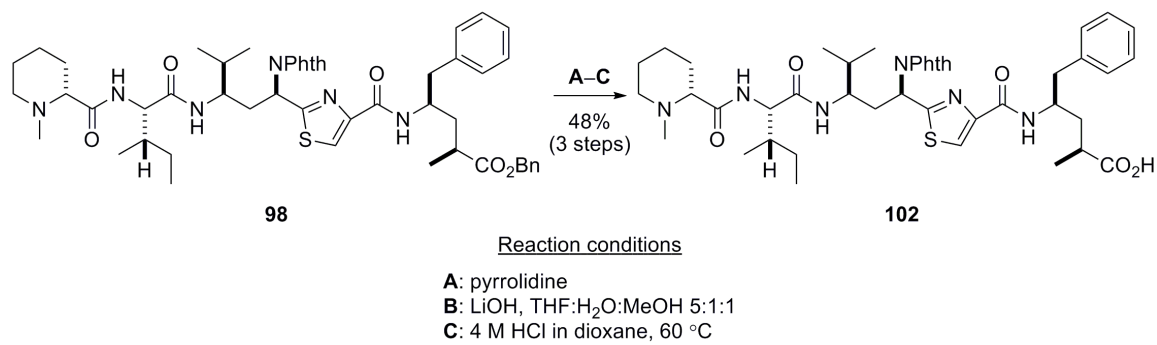


Figure 32: Synthesis of the phthalimide protected, benzyl deprotected tetrapeptide **102** without intermediate isolation.

Investigation into Phthalimide Deprotection Conditions to Furnish Amine **36**

With a method to selectively deprotect the benzyl ester and maintain the phthalimide established, milder transformations to generate **36** were attempted with a focus on reducing the hydrazine equivalents, reagent concentration, and temperature of the **102** deprotection. Since standard protocol calls for use of absolute EtOH in phthalimide deprotections (Ing–Manske procedure) and since the previously mentioned transesterification had been seen with use of MeOH as a solvent, initial reactions were performed using EtOH with a reduced hydrazine loading (10 equivalents compared to the 50 equivalents used previously). After an overnight reaction, the starting material **102** was shown by TLC to have been consumed and low resolution MS showed the production of both the partially cleaved benzamide and **36**.

Attempts to push the reaction to full product formation led to a change to aprotic

solvents and heating of the crude mixture. After removal of EtOH, the crude product was taken up in either CH₂Cl₂ or MTBE to test the effect of an aprotic solvent. When CH₂Cl₂ was used, most of the intermediate had proceeded to product after 48 hours, resulting in a higher product:intermediate ratio as shown by TLC and low resolution MS. Very little of the crude reaction mixture dissolved in the non-polar MTBE, so the mixture was heated to 60 °C, and after 48 hours some reaction progress had taken place. Despite the reaction progress seen in both cases, this strategy also caused significant degradation of reaction material as indicated by TLC.

After HPLC purification with an aqueous NH₄OAc (buffered with AcOH):MeCN solvent system, **36** was isolated in pure product fractions as confirmed by HPLC trace analysis and low resolution MS. To avoid isolating **36** by heated concentration of the fractions and risk potential degradation, the aqueous solutions were extracted with either CH₂Cl₂ or EtOAc. Upon organic solvent removal, impure samples of insufficient scale for characterization were isolated, where degradation may have occurred as a result of co-extraction and concentration of AcOH with the product. Thus, these final deprotections of the phthalimide ring in EtOH served as proof of concept, but additional modifications were needed for successful synthesis of **36**.

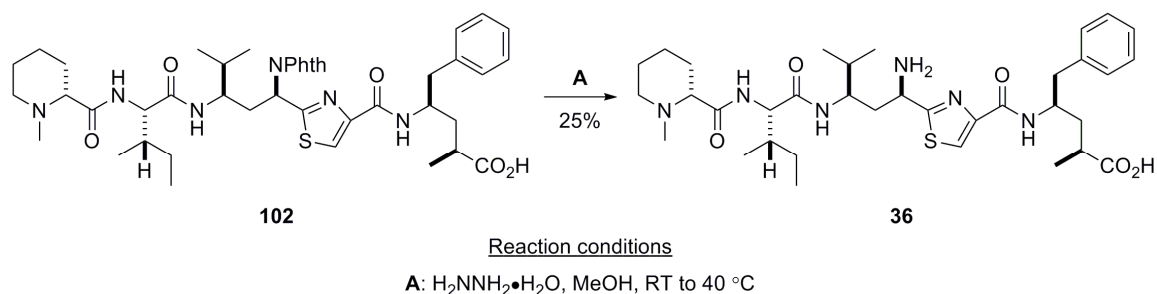


Figure 33: The final deprotection step to synthesize amine **36**.

By running the tetrapeptide **102** hydrazine deprotection as a dilute MeOH solution instead of in EtOH, a more mild reaction occurred as evidenced by only partial reaction of **102** after 72 hours stirring with hydrazine at room temperature according to low resolution MS; somewhat expectedly, the peak corresponding to the ^Ntubulysin V methyl ester was present to a small extent by MS analysis. With heating to 40 °C, no reaction progress was observed after 48 hours, so additional hydrazine was added to the heated solution. After an additional 24 hours, starting material had been consumed with production of the partially cleaved intermediate and desired product, favoring **36**. No reaction progress was observed after an additional day's reaction according to low resolution MS, but the degradation observed in the EtOH reactions had also not occurred as shown by TLC, so the reaction was concentrated and purified by HPLC despite remaining benzamide intermediate. MeOH solvated hydrazine deprotection of **102** is therefore preferable due to the formation of fewer degradation products compared to EtOH, with the caveat that minimal product loss occurs through transesterification.

Noting the stability of **36** at 40 °C, the HPLC fractions containing product were removed under high vacuum at 40 °C by way of a centrifugal evaporator. These dried HPLC fractions were combined with MeOH transfer to furnish the product as an acetate salt. NMR analysis was run as a solution in *d*₄-MeOH, a deuterated solvent that had

been used with other ^Ntubulysins to give superior spectra when compared to use of CDCl₃, without incidence of transesterification. Additionally, the increased volatility of CD₃OD served as a more convenient feature compared to the D₂O previously used for NMR analysis of Fecik lab final molecules. Despite the precedent for use of CD₃OD in earlier analogs, observations of more complicated splitting patterns than were expected in the ¹H NMR spectra and a doubling of the peaks in the ¹³C NMR spectra led to doubts of product purity. Upon MS analysis, mass peaks for **36** were dominant, but peaks representative of a methyl added to **36** were also observed, and it was hypothesized that transesterification had occurred with the catalytic acid provided by the acetate salt. Although the ¹H NMR was too populated to show clear peaks correlating to the methyl ester to establish a relative ratio of the two products, minor peaks matched nearly every significant peak in the ¹³C spectra. Comparison of the **36** ¹³C spectra to that of tubulysin V in *d*₄-MeOH (Shibue *et al.* 2010 and this work) assisted in assigning the major ¹³C peaks by taking into consideration the upfield shift of the α-thiazole carbon (approximately 70 ppm for tubulysin V (**12**) to approximately 53 ppm for **36**). Unrelated to the purity issues as a consequence of the solvents chosen to analyze **36**, this purification protocol shows that removal of HPLC solvents by high vacuum and mild heating is superior to extraction.

Synthesis of ^NTubulysin Analogs by Acylation of Tetrapeptide **100**

Previous syntheses towards natural tubulysins and tubulysin analogs containing a hydroxyl on the tubuvaline residue were free to acetylate and deacetylate this oxygen due to the susceptibility of acetates to hydrolytic cleavage. Strategies have included either late stage acetylation to avoid undesired hydrolysis in preceding reactions, or careful control of reaction conditions in order to not disturb an early stage acetylation.

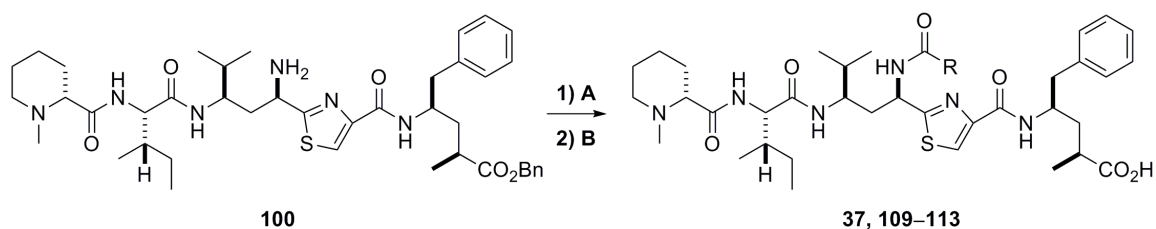
The Fecik lab and several others have used conditions wherein tubulysin V (**12**) is acetylated by adding an excess of acetic anhydride to a concentrated solution of **12** in pyridine, thus providing the tubulysin U (**13**) acetate in the last step to this natural product (Balasubramanian *et al.* 2009).

Since the nitrogen-containing tubulysins presented here make an amide bond instead of an ester bond following acylation, the reactivity at this position and reaction planning are very different. Amide bonds are not easily broken under even extreme conditions, and are certainly not broken under the standard conditions used for synthesis of tubulysin intermediates based on the sustainability of the molecule's other amide bonds. Reaction planning must be done strategically because of this stability, since early stage *N*-acylation would result in processing each analog individually through the remaining synthetic steps. Hence, the functionalization at this position should be done as late in the synthesis as possible for maximum output from synthetic efforts. Based upon the stability of amide bonds to basic hydrolysis and the need for divergence at a common late-stage intermediate, tetrapeptide **100** was used as the penultimate intermediate to several acylated ^Ntubulysin analogs.

Comparison of the *N*-acetate analog **37** to tubulysin U (**13**) will directly demonstrate the effect that the oxygen to nitrogen heteroatom exchange at the α -thiazole position has on biological activity, so *N*-acetylation of **100** was investigated first. With the reaction conditions previously set by the Fecik group for acetylation of **12** described above, a low yield of the product was observed with several strange impurities by MS analysis of HPLC fractions. By taking advantage of the increased nucleophilicity of the amine, less strongly electrophilic conditions gave an equal mixture of mono- and di-acetylated product. As predicted, LiOH hydrolysis of the monoacetylated benzyl ester

intermediate under our standard conditions gave **37** cleanly. This demonstrates a general method to generate the target molecule **37** and other *N*-acylated analogs, and confirms the stability of *N*-acetylated compounds to basic hydrolysis (Table 1).

This 2 step procedure was used to acylate the penultimate intermediate **100** leading to final compounds with a range of differing functional groups. A general procedure was followed where a solution of the acylating agent and an amine base in CH₂Cl₂ at 0 °C consumed the starting material in less than 2 hours to generate compounds **109–111**. The acylated benzyl esters were subject to an aqueous work up, and the resulting crude samples were run through a standard procedure for LiOH hydrolysis. Peaks corresponding to the TFA carbonyl and trifluoromethyl are absent in the ¹³C NMR spectra of **110**, an observation seen with other trifluoromethyl acetamides (Merritt and Bagley 2007).



Reaction conditions

A: acylating agent, base, solvent, temp

B: LiOH, THF:H₂O:MeOH 5:1:1

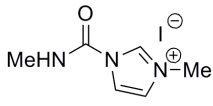
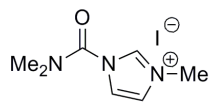
<u>Compound</u>	<u>R=</u>	<u>acylating agent</u>	<u>base</u>	<u>solvent, temp</u>	<u>yield (2 steps)</u>
37	Me	AcCl	Et ₃ N	CH ₂ Cl ₂ , 0 °C to rt	27%
109	<i>t</i> Bu	<i>t</i> BuCOCl	pyridine	CH ₂ Cl ₂ , 0 °C	33%
110	CF ₃	TFAA	pyridine	CH ₂ Cl ₂ , 0 °C	10%
111	OMe	ClCO ₂ Me	Et ₃ N/pyridine	CH ₂ Cl ₂ , 0 °C	15%
112	NHMe		Et ₃ N	MeCN, rt	17%
113	NMe ₂		Et ₃ N	MeCN, reflux	10%

Table 1: Synthesis of acylated *N*₁tubulysin analogs **37** and **109–113**.

The standard procedure for bis-substituted methyl urea installation at a primary amine is with the use of methyl isocyanate. This method was not used due to its inherent danger as a lachrymator (methyl isocyanate caused the Bhopal disaster), its lack of availability from common commercial sources, and the difficulty in its synthesis. Additionally, the dimethyl urea would be unavailable via this route. Acylation of the amine using CDI, a shelf stable alternative to phosgene, had low reactivity and the products produced from the reaction were not clear based upon MS analysis.

These issues with regard to urea formation at amines or carbamate formation at alcohols were confronted in a report published in *Tetrahedron* (Grzyb *et al.* 2005). CDI-based reagents with increased electrophilic character at the central carbonyl were described, wherein a simple amine is preinstalled onto one side of CDI followed by *N*-methylation of the remaining imidazole ring to increase its leaving group potential (Figure 34). The resulting iodo salt is reported to be over a hundred fold more reactive than CDI due to the enhanced stability of the charged imidazole unbound to the carbonyl. Synthesis of these reagents using primary amines preinstalled onto CDI, as in the case of **114**, were not described in the original paper or publications citing that work.

Surprisingly, extrapolation of this work to the synthesis of the 2 target molecules **112** and **113** resulted in drastically different results under the same reaction conditions. Addition of either methylamine (**116**) or desalted dimethylamine hydrochloride (**117**) into CDI followed by H₂O workup gave crude mixtures of imidazole and the uncharged intermediates **118** and **119** (Figure 34). When these crude samples were subjected to MeI in acetonitrile, a complicated reaction mixture was formed which did not contain the desired product. Conversely, the literature procedure notes pure compound isolation upon reaction concentration, albeit without imidazole impurity at either step.

In order to generate pure starting materials for the *N*-methylation step, both samples were separately partitioned between saturated aqueous NH₄Cl solution and CH₂Cl₂ to remove the imidazole impurity. Even after multiple extractions, a significant portion of **118** was trapped in the aqueous layer according to TLC. Alternatively, **119** was lipophilic enough to remain in the organic layers with its imidazole impurity stripped away into the aqueous phase. Once these purified intermediates were methylated, CH₂Cl₂ trituration removed any impurities, leaving the pure carbamoylimidazolium salts.

In the case of the methylamine-based reagent **114**, a minute 7% yield was isolated from this reaction, seemingly from extensive side product reactivity or degradation based upon TLC and ^1H NMR analysis of the titrant. Alternatively, the dimethylamine-based reagent **115** was synthesized in nearly quantitative yield. This difference in reactivity and stability between the primary and secondary amine based reagents gives credence to the absence of primary amines included in the parent paper.

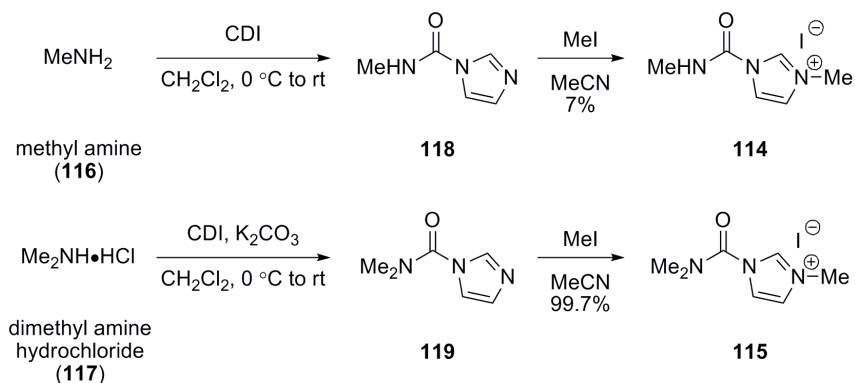


Figure 34: Synthesis of reagents **114** and **115** for generating N -tubulysin urea analogs.

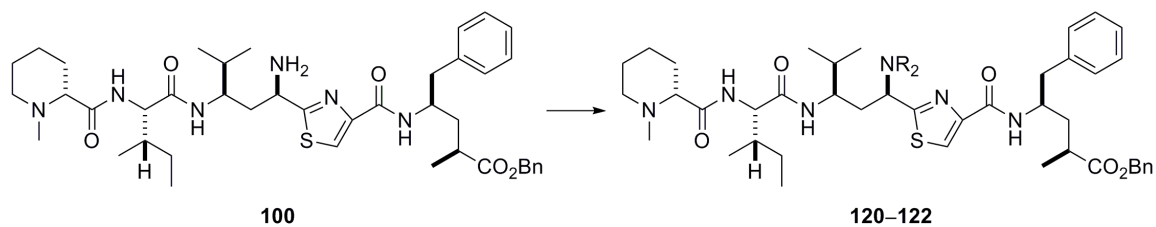
As was described in the Grzyb paper, addition of the methylamine-based carbamoylimidazolium salt **114** with Et_3N at room temperature gave full conversion of amine **100** to the acylated product overnight. Following an aqueous workup, the impure reaction was put through standard LiOH hydrolysis, which fully converted the benzyl ester intermediate to **112** by MS. When this same procedure was applied using **115**, no conversion of the starting material was seen after 48 hours. Multiple days of heating the reaction to reflux with addition of DMAP and a large excess of **115** was necessary to finally consume **100** with production of the acylated benzyl ester intermediate as shown by TLC and low resolution MS. Ester hydrolysis ran as expected, and both **112** and **113** were purified by HPLC. An explanation of the vast difference in reactivity between the 2

salts may be the additional bulk of the dimethylamine-based reagent **115**, along with its increased stability as observed with more productive synthesis of **115** compared to **114**.

Model Studies Examining Synthetic Routes to *N*-Alkylated ^NTubulysin Analogs

As part of a full SAR profile for *N*-substitution at the α -thiazole position of ^Ntubuvaline, probing the significance of the carbonyl at this position was of interest and led to model studies concerned with alkylation of the amine. The goal was to install functional groups that mimic the previously synthesized molecules above; the methyl, ethyl, and methoxymethyl appended amines were picked as logical starting points due to their close homology to **37**. Tetrapeptide **100** was picked as a close representation of **36**, but its use as a starting material for these compounds was dismissed due to the unfavorable reactivity observed with benzyl ester hydrolysis of **100**. Future implementation of this chemistry will require synthesis of additional **36** starting material.

With the intention of generating both secondary and tertiary methylated amines concurrently, a reaction was ran using 1.5 equivalents of iodomethane in the presence of a nitrogen base and **100** (Table 2). No reaction occurred with the use of Et₃N as the amine base, whereas the use of pyridine and additional iodomethane gave a complicated reaction mixture as shown by HPLC and MS. Both of these results can be explained by the non-selective alkylation of amines characteristic of iodomethane. When a nearly stoichiometric amount of iodomethane was used with an excess of Et₃N, the base was preferentially alkylated before the amines of **100**. Competitive alkylation of the *N*-methyl-D-pipecolinic acid tertiary amine with the ^Ntubuvaline primary amine in the presence of excess methylating agent has the potential to generate 5 different products, thus resulting in a complicated mixture of reaction products.



<u>compound</u>	<u>R=</u>	<u>reaction conditions</u>	<u>outcome</u>
120	Me	MeI, Et ₃ N, CH ₂ Cl ₂	no reaction
		MeI, pyridine, CH ₂ Cl ₂	complicated reaction mixture
		paraformaldehyde, NaBH(OAc) ₃ , DCE	mono- and di-alkylated product and unreacted 100 by MS
121	Et	AcOH, acetaldehyde, NaBH(OAc) ₃ , DCE	productive for di-alkylated product with full consumption of 100
122	CH ₂ OMe	MeOCH ₂ Cl, pyridine, CH ₂ Cl ₂ , 0 °C	productive for di-alkylated, methyl ester with full consumption of 100

Table 2: Model studies for alkylated ^Ntubulysin analogs **120–122**.

Reductive amination does not easily allow for stoichiometric control in alkylation, but it is a well established method to alkylate only primary and secondary amines, and thus was used towards the dimethyl and diethyl analogs **120** and **121** (Table 2). The use of excess paraformaldehyde and sodium triacetoxyborohydride (NaBH(OAc)₃), a reagent selective for mild reduction of imines in the presence of other reducible functional groups, partially consumed the starting material, and mass peaks for both the mono- and di-alkylated products were seen in low resolution MS. This method of reductive amination is not optimal, and future work should use the better established aqueous formaldehyde/NaBH(OAc)₃ system. The use of excess acetaldehyde, AcOH, and NaBH(OAc)₃ gave spot to spot conversion of the tetrapeptide to a less ninhydrin active product by TLC, where ninhydrin stain is active in the presence of amines but is less intense upon increasing amine substitution. Although low resolution MS analysis

showed this to be the dialkylated product **121**, HPLC purification did not produce enough material for proper characterization.

The methoxymethyl alkylated analog **122** is a homolog of **37** with *N,O*-acetal replacement of the carbonyl. Surprising results came after full consumption of **100** with excess methoxymethyl chloride (MOMCl) and pyridine, where the formula weight representative of the target molecule as a methyl ester was the only prominent product by low resolution MS (Table 2). One possible explanation for the observed transesterification of the benzyl ester lies in the apparent old age of the MOMCl reagent, where gradual degradative build up of MeOH and HCl within the reagent would supply the necessary conditions for this reactivity. As predicted by the instability of *N,O*-acetals and the previously observed degradation of **100** under basic conditions, LiOH hydrolysis of this molecule resulted in complete material degradation. Future work should take advantage of the reaction of formaldehyde with **36** in MeOH, which has been shown to regioselectively install MOM *N,O*-acetals at amines through imine intermediates (Padwa and Dent 1993).

Conclusion

Peptide couplings of the now synthetically available ^Ntubuvaline residue **89** to the other amino acid moieties, followed by late stage deprotections and acylations, have furnished several nitrogen-containing ^Ntubulyisin analogs. The amide bond formation between ^Ntubuvaline and tubuphenylalanine was modified from the literature precedent to avoid undesired *N*-acylurea side product formation. Subsequent coupling reactions efficiently yielded more than 90% product at each step to a common tetrapeptide intermediate **98**. Where direct deprotection of **98** failed to yield ^Ntubulyisin V (**36**), a

strategy which generates more robust intermediates insensitive to standard deprotection conditions successfully led to the target molecule.

By taking advantage of the stable amide bond formed through *N*-acylation of the benzyl protected amine **100**, the previously destructive basic hydrolysis used to remove the benzyl ester completed the synthesis of several ^Ntubulysin analogs. Urea formation at the nitrogen of ^Ntubuvaline presented unique challenges, where synthesis of **112** and **113** was possible through use of specialized reagents and appeared to be greatly affected by steric interactions. The methods to synthesize *N*-alkylated ^Ntubulysin analogs have been investigated and await the production of additional **36** starting material.

Chapter 3 Experimentals:

Dipeptide 93. A solution of benzyl ester **91** (160 mg, 0.40 mmol, 1.4 equiv) in HCl (4.0 M in dioxane, 5.0 mL) was stirred at room temperature for 2 h, after which TLC (50% EtOAc:hexanes) showed complete consumption of starting material. The reaction solution was concentrated under reduced pressure, and the resulting solid was dissolved in CH₂Cl₂ (5 mL) and concentrated under reduced pressure; this was repeated twice to afford the crude HCl salt as a white solid. Separately, to a solution of acid **89** (138 mg, 0.29 mmol, 1 equiv) in CH₂Cl₂ (10 mL) at -15 °C was added Et₃N (0.12 mL, 0.87 mmol, 3 equiv) and ethyl chloroformate (33 μL, 0.35 mmol, 1.2 equiv), and the resulting solution stirred for 35 min. To this was added a solution of the crude HCl salt in CH₂Cl₂ (10 mL) at -15 °C via cannula. After 1 h, TLC (10% MeOH:CH₂Cl₂ with 0.5% AcOH) showed complete consumption of starting material. The reaction was quenched with saturated aqueous NH₄Cl (15 mL), the layers were separated, and the aqueous layer was extracted with CH₂Cl₂ (2 x 15 mL). The combined organic layers were dried (Na₂SO₄), filtered, and concentrated under reduced pressure. Purification by flash chromatography (30% EtOAc:hexanes) afforded the title compounds as a white solid (202.4 mg, 92% yield). *R*_f = 0.3 (SiO₂, 40% EtOAc:hexanes); ¹H NMR (400 MHz, CDCl₃) δ 7.98 (s, 1H), 7.83 (dd, *J* = 5.4, 3.1 Hz, 2H), 7.72 (dd, *J* = 5.4, 3.1 Hz, 2H), 7.35–7.07 (m, 11H), 5.76 (dd, *J* = 12.1, 4.7 Hz, 1H), 5.10 (d, *J* = 12.5 Hz, 1H), 5.05 (d, *J* = 12.4 Hz, 1H), 4.48–4.35 (m, 2H), 3.54–3.42 (m, 1H), 3.14–3.03 (m, 1H), 2.91 (A of ABX, dd, *J* = 13.7, 6.0 Hz, 1H), 2.85 (B of ABX, dd, *J* = 13.7, 6.6 Hz, 1H), 2.69–2.57 (m, 1H), 2.11 (ddd, *J* = 14.1, 12.4, 4.8 Hz, 1H), 2.00 (ddd, *J* = 13.7, 9.2, 4.2 Hz, 1H), 1.77–1.65 (m, 1H), 1.60 (ddd, *J* = 14.2, 9.8, 4.6 Hz, 1H), 1.40 (s, 9H), 1.16 (d, *J* = 7.1 Hz, 3H), 0.92 (d, *J* = 6.8 Hz, 3H), 0.89 (d, *J* = 6.8 Hz, 3H); ¹³C NMR (101 MHz, CDCl₃) δ 176.1, 169.6, 167.8, 160.5,

155.8, 149.8, 137.7, 136.3, 134.4, 132.0, 129.7, 128.7, 128.6, 128.22, 128.18, 126.7, 123.9, 123.7, 79.6, 66.5, 52.3, 49.9, 48.6, 41.4, 37.8, 36.8, 34.4, 33.3, 28.5, 19.4, 18.1, 17.8; HRMS calcd for C₄₂H₄₉N₄O₇S⁺ [M + H⁺] 753.3322, found 753.3311.

Tripeptide 95. A solution of dipeptide **93** (95.6 mg, 0.127 mmol, 1 equiv) in HCl (4.0 M in dioxane, 4.0 mL) was stirred at room temperature for 2 h, after which TLC (50% EtOAc:hexanes) showed complete consumption of starting material. The reaction solution was concentrated under reduced pressure, and the resulting solid was dissolved in CH₂Cl₂ (5 mL) and concentrated under reduced pressure; this was repeated twice to afford the crude HCl salt as a white solid. Separately, to a solution of Boc-L-Ile (41 mg, 0.18 mmol, 1.4 equiv) in DMF (1.5 mL) at -15 °C was added HATU (68 mg, 0.18 mmol, 1.4 equiv) and *N*-methylmorpholine (56 µL, 0.51 mmol, 4 equiv), and the resulting solution was stirred for 20 min. To this solution was added a solution of the crude HCl salt in DMF (1.5 mL, with 0.5 mL wash) at -15 °C dropwise via pipette, and the reaction stirred while warming to room temperature overnight. After 18 h, the reaction was concentrated under reduced pressure and partitioned between CH₂Cl₂ (30 mL) and 5% aqueous KHSO₄ (15 mL). The aqueous layer was extracted with CH₂Cl₂ (15 mL), and the combined organic layers were washed with H₂O (15 mL), saturated aqueous NaHCO₃ (15 mL), H₂O (15 mL) and saturated aqueous NaCl (15 mL). The combined organic layers were dried (Na₂SO₄), filtered, and concentrated under reduced pressure. Purification by flash chromatography (30% EtOAc:hexanes) afforded the title compounds as a white solid (99 mg, 90% yield). *R*_f = 0.2 (SiO₂, 40% EtOAc:hexanes); ¹H NMR (400 MHz, CDCl₃) δ 7.96 (s, 1H), 7.86 (dd, *J* = 5.4, 3.1 Hz, 2H), 7.74 (dd, *J* = 5.4, 3.1 Hz, 2H), 7.36–7.07 (m, 10H), 6.09 (d, *J* = 9.9 Hz, 1H), 5.64 (dd, *J* = 11.7, 4.2 Hz, 1H), 5.10 (d, *J* = 12.4 Hz, 1H), 5.04 (d, *J* = 12.4 Hz, 1H), 4.97–4.78 (br m, 1H), 4.49–4.35 (m, 1H), 3.90–

3.75 (br m, 2H), 3.10 (ddd, $J = 14.5, 11.9, 2.9$ Hz, 1H), 2.91 (A of ABX, dd, $J = 13.7, 6.1$ Hz, 1H), 2.85 (B of ABX, dd, $J = 13.7, 6.6$ Hz, 1H), 2.68–2.57 (m, 1H), 2.22 (ddd, $J = 14.5, 11.6, 4.5$ Hz, 1H), 2.06–1.63 (m, 4H), 1.58 (ddd, $J = 14.3, 9.9, 4.5$ Hz, 2H), 1.42 (s, 9H), 1.16 (d, $J = 7.1$ Hz, 3H), 1.13–1.03 (m, 1H), 1.00 (d, $J = 6.7$ Hz, 3H), 0.95 – 0.84 (m, 9H); ^{13}C NMR (101 MHz, CDCl_3) δ 176.0, 171.9, 169.4, 167.7, 160.4, 149.9, 137.6, 136.3, 134.5, 131.8, 129.7, 128.59, 128.55, 128.3, 128.2, 128.0, 126.6, 123.83, 123.76, 80.4, 66.4, 59.8, 50.8, 50.0, 48.6, 41.4, 37.93, 36.8, 35.4, 34.2, 32.6, 28.4, 24.8, 19.2, 18.0, 16.0, 11.3; HRMS calcd for $\text{C}_{48}\text{H}_{60}\text{N}_5\text{O}_8\text{S}^+$ [$\text{M} + \text{H}^+$] 866.4163, found 866.3153.

Tetrapeptide 98. A solution of tripeptide **95** (41.5 mg, 0.0479 mmol, 1 equiv) in HCl (4.0 M in dioxane, 3.0 mL) was stirred at room temperature for 1 h, after which TLC (50% EtOAc:hexanes) showed complete consumption of starting material. The reaction solution was concentrated under reduced pressure, and the resulting solid was dissolved in CH_2Cl_2 (5 mL) and concentrated under reduced pressure; this was repeated twice to afford the crude HCl salt as a white/yellow solid. Separately, to a mixture of *N*-Me-D-Pip (20 mg, 0.14 mmol, 3 equiv) in DMF (4 mL) at 0 °C was added HATU (53 mg, 0.14 mmol, 3 equiv) and Et_3N (27 μL , 0.19 mmol, 4 equiv), and the resulting suspension was stirred for 1 h. To this suspension was added a solution of the crude HCl salt in DMF (2.0 mL, with 0.5 mL wash) at 0 °C dropwise via pipette, and the reaction stirred while warming to room temperature overnight. After 18 h, the reaction was concentrated under reduced pressure and partitioned between CH_2Cl_2 (30 mL) and H_2O (15 mL). The aqueous layer was extracted with CH_2Cl_2 (15 mL), and the combined organic layers were washed with saturated aqueous NaHCO_3 (15 mL), H_2O (15 mL) and saturated aqueous NaCl (15 mL). The combined organic layers were dried (Na_2SO_4), filtered, and concentrated under reduced pressure. Purification by flash chromatography (3.5%

MeOH:CH₂Cl₂) afforded the title compounds as a yellow solid (41.0 mg, 96% yield). $R_f = 0.3$ (SiO₂, 5% MeOH:CH₂Cl₂); ¹H NMR (400 MHz, CDCl₃) δ 7.96 (s, 1H), 7.86 (dd, $J = 5.5, 3.0$ Hz, 2H), 7.74 (dd, $J = 5.5, 3.1$ Hz, 2H), 7.36–7.09 (m, 9H), 7.03 (d, $J = 8.4$ Hz, 1H), 6.34 (d, $J = 10.0$ Hz, 1H), 5.65 (dd, $J = 11.7, 4.3$ Hz, 1H), 5.10 (d, $J = 12.4$ Hz, 1H), 5.04 (d, $J = 12.4$ Hz, 1H), 4.48–4.36 (m, 1H), 4.09 (t, $J = 8.4$ Hz, 1H), 3.90–3.78 (m, 1H), 3.08 (ddd, $J = 14.4, 11.9, 2.8$ Hz, 1H), 2.97–2.79 (m, 3H), 2.69–2.56 (m, 1H), 2.50 (dd, $J = 11.1, 3.0$ Hz, 1H), 2.22 (s, 3H), 2.09–1.29 (m, 15H), 1.19–1.12 (ovlp m, 1H), 1.16 (d, $J = 7.1$ Hz, 3H), 1.03 (d, $J = 6.7$ Hz, 3H), 0.95–0.81 (m, 9H); ¹³C NMR (101 MHz, CDCl₃) δ 176.1, 175.4, 171.3, 169.3, 167.7, 160.4, 150.0, 137.7, 136.3, 134.5, 131.8, 129.6, 128.6, 128.5, 128.3, 128.2, 126.6, 123.83, 123.78, 100.1, 69.8, 66.4, 58.1, 55.5, 50.7, 50.1, 48.7, 45.1, 41.4, 37.9, 36.8, 34.7, 33.9, 32.5, 31.0, 25.2, 25.0, 23.4, 18.9, 18.1, 18.0, 16.2, 10.9; HRMS calcd for C₅₀H₆₃N₆O₇S⁺ [M + H⁺] 891.4474, found 891.4481.

Tetrapeptide 100. To a solution of tetrapeptide **98** (14 mg, 0.016 mmol, 1 equiv) in MeOH (2.6 mL) was added hydrazine monohydrate (39 μL, 0.79 mmol, 50 equiv) and the solution was stirred for 3 h, after which TLC (10% MeOH:CH₂Cl₂) showed complete consumption of starting material to the intended product and the open chain intermediate **99**. The reaction was heated to reflux and stirred overnight. After 18 h, TLC showed full conversion to the desired product. The reaction was concentrated under reduced pressure, 0.1 M aqueous HCl (20 mL) was added and the resulting aqueous solution was extracted with Et₂O (3 x 10 mL). The combined organic layers were dried (Na₂SO₄), filtered, and concentrated under reduced pressure. Purification by flash chromatography (5% MeOH:CH₂Cl₂) afforded the title compound as a white/yellow solid (11.2 mg, 94% yield). An analytically pure sample can be prepared by removing residual grease using the following procedure: The crude sample is partitioned between MeCN (6 mL) and

hexanes (4 mL). The layers are separated, the hexanes layer is extracted with MeCN (3 x 3 mL), the combined MeCN layers are washed with hexanes (3 x 3 mL), and MeCN is removed under reduced pressure to yield the pure product. $R_f = 0.2$ (**99**), 0.4 (**100**) (SiO₂, 10% MeOH:CH₂Cl₂); ¹H NMR (400 MHz, MeOD) δ 8.01 (s, 1H), 7.36–7.12 (m, 10H), 5.08 (d, $J = 12.3$ Hz, 1H), 5.01 (d, $J = 12.3$ Hz, 1H), 4.44–4.33 (m, 1H), 4.19 (d, $J = 8.9$ Hz, 1H), 4.13 (dd, $J = 10.3, 3.3$ Hz, 1H), 4.04–3.95 (m, 1H), 2.99 (d, $J = 11.7$ Hz, 1H), 2.90 (dd, $J = 13.6, 7.2$ Hz, 1H), 2.84 (dd, $J = 13.7, 6.7$ Hz, 1H), 2.72 (dd, $J = 11.1, 1.8$ Hz, 1H), 2.69–2.59 (m, 1H), 2.26 (s, 2H), 2.25–2.15 (m, 1H), 2.03 (apparent dddd, $J = 27.7, 13.8, 9.9, 3.7$ Hz, 2H), 1.93–1.49 (m, 10H), 1.40–1.25 (m, 3H), 1.25–1.18 (m, 1H), 1.16 (d, $J = 7.1$ Hz, 3H), 0.95 (d, $J = 6.7$ Hz, 8H), 0.89 (t, $J = 7.4$ Hz, 3H); ¹³C NMR (101 MHz, MeOD) δ 178.1, 177.5, 174.8, 174.1, 163.1, 150.6, 139.4, 137.5, 130.5, 129.5, 129.4, 129.2, 129.1, 127.4, 124.5, 70.3, 67.4, 59.3, 56.6, 52.8, 52.5, 50.3, 44.5, 42.4, 42.0, 39.0, 38.0, 37.4, 33.8, 31.4, 26.0, 25.9, 24.1, 20.0, 18.7, 18.3, 16.2, 11.0; HRMS calcd for C₄₂H₆₁N₆O₅S⁺ [M + H⁺] 761.4424, found 761.4419.

Tetrapeptide 101. To a solution of tetrapeptide **98** (10.6 mg, 11.9 μ mol) in THF (1.5 mL) and H₂O (0.5 mL) was added LiOH•H₂O (20 mg, 0.48 mmol, 40 equiv) and the reaction was stirred overnight. After 72 h, HPLC showed complete consumption of starting material, and THF was removed under reduced pressure. The aqueous reaction mixture was acidified to pH 2 with 1.0 M aqueous HCl, extracted with CH₂Cl₂ (4 x 15 mL), and the combined organic layers were dried (Na₂SO₄), filtered, and concentrated under reduced pressure. Purification by HPLC (C₁₈, 150 x 10 mm, 32% MeCN/25 mM aqueous NH₄OAc, pH 4.78 for 10 min, 90% MeCN/25 mM aqueous NH₄OAc, pH 4.78 for 5 min, 5 mL/min) afforded the title compound as a white solid (4.6 mg, 47% yield). HPLC $t_r = 5.5$ min; $R_f = 0.1$ (SiO₂, 10% MeOH:CH₂Cl₂ with 1% AcOH); ¹H NMR (400

MHz, D₂O) δ 8.41 (d, J = 9.1 Hz, 1H), 8.00 (s, 1H), 7.70–7.52 (m, 4H), 7.30 (d, J = 4.3 Hz, 3H), 7.28–7.21 (m, 1H), 5.28 (dd, J = 11.3, 3.5 Hz, 1H), 4.33–4.25 (m, 1H), 4.22 (d, J = 8.5 Hz, 1H), 4.06–3.96 (m, 1H), 3.86 (d, J = 9.9 Hz, 1H), 3.54 (d, J = 12.8 Hz, 1H), 3.17–3.06 (m, 1H), 3.02 (dd, J = 13.2, 5.3 Hz, 1H), 2.84 (dd, J = 13.9, 8.7 Hz, 1H), 2.77 (s, 2H), 2.61–2.52 (m, 1H), 2.42–2.15 (m, 4H), 2.10–1.84 (m, 5H), 1.85–1.65 (m, 4H), 1.65–1.42 (m, 3H), 1.34–1.18 (m, 2H), 1.16 (d, J = 7.1 Hz, 3H), 0.95 (d, J = 6.7 Hz, 6H), 0.86 (t, J = 7.3 Hz, 3H); ¹³C NMR (214 MHz, D₂O) δ 183.2, 175.1, 173.6, 172.8, 172.4, 168.8, 162.8, 148.3, 138.4, 136.8, 133.8, 130.7, 129.7, 129.5, 128.4, 128.2, 127.6, 126.5, 124.5, 66.9, 59.0, 55.1, 51.9, 50.0, 49.8, 41.9, 40.7, 40.4, 38.1, 37.9, 35.6, 32.2, 28.7, 24.4, 22.6, 20.7, 18.1, 17.6, 17.5, 15.0, 9.9; HRMS calcd for C₄₃H₅₉N₆O₈S⁺ [M + H⁺] 819.4115, found 819.4137.

Tetrapeptide 107. A solution of tetrapeptide **98** (37.9 mg, 0.0425 mmol) in pyrrolidine (2.0 mL) was stirred for 5 h, after which TLC (5% MeOH:CH₂Cl₂, using an aliquot partitioned between 1.0 M aqueous HCl and EtOAc) showed complete consumption of starting material. The reaction was poured into 1.0 M aqueous HCl (75 mL) and the resulting aqueous solution was extracted with EtOAc (30 mL, then 2 x 20 mL). The combined organic layers were washed with 1.0 M aqueous HCl (2 x 25 mL) and saturated aqueous NaCl (25 mL), dried (Na₂SO₄), filtered, and concentrated under reduced pressure. Purification by flash chromatography (5%–10% MeOH:CH₂Cl₂) afforded the title compounds as an off white solid (37.8 mg, 92% yield). R_f = 0.4 (SiO₂, 10% MeOH:CH₂Cl₂); ¹H NMR (400 MHz, CDCl₃) δ 7.96 (s, 1H), 7.91–7.75 (m, 1H), 7.60–7.39 (m, 3H), 7.39–7.12 (m, 11H), 5.48 (s, 1H), 5.12 (d, J = 12.4 Hz, 1H), 5.06 (d, J = 12.4 Hz, 1H), 4.54–4.37 (m, 1H), 4.05 (d, J = 39.3 Hz, 2H), 3.70–3.58 (m, 1H), 3.57–3.48 (m, 1H), 3.29–3.13 (m, 2H), 3.09 (dd, J = 14.6, 7.3 Hz, 1H), 3.03–2.78 (m, 3H),

2.75–2.64 (m, 1H), 2.64–2.11 (m, 5H), 2.05 (ddd, $J = 13.7, 9.6, 4.0$ Hz, 2H), 1.99–1.31 (m, 15 H), 1.19 (d, $J = 7.1$ Hz, 3H), 1.15–1.01 (m, 2H), 0.93 (dd, $J = 14.7, 6.7$ Hz, 7H), 0.88–0.69 (m, 6H); ^{13}C NMR (101 MHz, CDCl_3) δ 176.6, 176.1, 174.9, 171.6, 171.3, 169.6, 167.7, 160.7, 150.4, 138.0, 136.3, 133.0, 131.0, 129.6, 129.5, 128.57, 128.55, 128.5, 128.2, 128.1, 128.0, 126.5, 123.1, 69.8, 66.4, 57.7, 55.5, 51.2, 49.6, 49.3, 48.8, 46.1, 45.1, 41.6, 38.0, 36.9, 36.8, 35.9, 32.1, 30.9, 26.0, 25.3, 24.6, 23.4, 22.8, 19.4, 18.1, 16.0, 14.3, 10.9; HRMS calcd for $\text{C}_{54}\text{H}_{72}\text{N}_7\text{O}_7\text{S}^+$ [$\text{M} + \text{H}^+$] 962.5214, found 962.5197.

Tetrapeptide 108. To a solution of the tetrapeptide **107** (37.8 mg, 0.0393 mmol) in THF (2.0 mL), H_2O (0.40 mL) and MeOH (0.40 mL) was added $\text{LiOH}\cdot\text{H}_2\text{O}$ (33 mg, 0.79 mmol, 20 equiv), and the resulting mixture was stirred overnight. After 18 h, the reaction had turned an orange color, and TLC (10% MeOH: CH_2Cl_2) showed complete consumption of starting material to the intended product and **101**. The organic solvents were removed under reduced pressure, and the resulting aqueous reaction mixture was diluted with H_2O (3 mL) and acidified to pH 2 with 1.0 M aqueous HCl. The resulting aqueous reaction solution was extracted with CH_2Cl_2 (5 x 5 mL), and the combined organic layers were dried (Na_2SO_4), filtered, and concentrated under reduced pressure. Purification by HPLC (C_{18} , 150 x 10 mm, 32% MeCN/25 mM aqueous NH_4OAc , pH 4.78 for 10 min, 90% MeCN/25 mM aqueous NH_4OAc , pH 4.78 for 5 min, 5 mL/min) afforded the title compound as a white solid (5.10 mg, 15%) and **101** (18.85 mg, 59%) as an acetate salt. HPLC $t_r = 8.4$ min; $R_f = 0.3$ (SiO_2 , 10% MeOH: CH_2Cl_2); ^1H NMR (400 MHz, D_2O) δ 8.51–8.35 (m, 1H), 8.02 (s, 1H), 7.81 (d, $J = 7.4$ Hz, 1H), 7.78–7.59 (m, 2H), 7.44 (d, $J = 7.1$ Hz, 1H), 7.41–7.17 (m, 4H), 5.24 (dd, $J = 11.0, 3.2$ Hz, 2H), 4.33 (br s, 1H), 4.21 (d, $J = 8.4$ Hz, 1H), 4.10 (br s, 1H), 3.97–3.66 (m, 3H), 3.55 (d, $J = 11.9$ Hz, 1H),

3.47–3.30 (m, 2H), 3.24–2.97 (m, 3H), 2.95–2.75 (m, 4H), 2.66 (br s, 1H), 2.46–2.33 (m, 1H), 2.33–2.16 (m, 2H), 2.14–1.42 (m, 13H), 1.40–1.26 (m, 2H), 1.20 (d, $J = 6.9$ Hz, 3H), 1.08–0.90 (m, 7H), 0.90–0.76 (m, 3H); ^{13}C NMR (214 MHz, D_2O) δ 185.1, 181.1, 172.8, 170.4, 168.8, 162.7, 158.7, 148.3, 138.3, 135.8, 132.1, 131.3, 129.8, 129.4, 128.4, 127.9, 127.0, 126.5, 124.6, 66.9, 59.0, 55.2, 51.6, 49.6, 49.5, 48.9, 45.9, 41.9, 40.7, 37.7, 36.7, 35.5, 35.0, 32.5, 28.7, 25.1, 24.3, 24.0, 22.6, 20.7, 18.2, 17.4, 17.1, 15.1, 9.9; HRMS calcd for $\text{C}_{47}\text{H}_{66}\text{N}_7\text{O}_7\text{S}^+$ [$\text{M} + \text{H}^+$] 872.4744, found 872.4738.

Tetrapeptide 102. A solution of tetrapeptide **108** (5.0 mg, 5.7 μmol) in HCl (4.0 M in dioxane, 3 mL) was heated to 60 °C and stirred for 48 h, after which TLC (10% MeOH: CH_2Cl_2) showed complete consumption of starting material. The reaction solution was concentrated under reduced pressure, and the resulting solid was dissolved in CH_2Cl_2 (5 mL) and concentrated under reduced pressure; this was repeated twice to afford the crude HCl salt as a white/yellow solid. Purification by flash chromatography (10% MeOH: CH_2Cl_2) afforded the title compounds as a white/yellow solid (2.5 mg, 54% yield). $R_f = 0.4$ (SiO_2 , 10% MeOH: CH_2Cl_2); ^1H NMR (400 MHz, D_2O) δ 8.31 (d, $J = 9.4$ Hz, 1H), 8.03 (s, 1H), 7.99–7.84 (m, 3H), 7.30–7.09 (m, 4H), 5.60 (dd, $J = 11.8, 3.2$ Hz, 1H), 4.24 (d, $J = 7.8$ Hz, 2H), 3.90–3.59 (m, 5H), 3.53 (d, $J = 12.2$ Hz, 1H), 3.36 (s, 1H), 3.12 (dd, $J = 28.8, 13.3$ Hz, 2H), 2.94 (dd, $J = 13.3, 4.2$ Hz, 1H), 2.74 (s, 3H), 2.59–2.45 (m, 1H), 2.45–2.32 (m, 1H), 2.28–2.15 (m, 1H), 1.99–1.45 (m, 10H), 1.36–1.16 (m, 2H), 1.11 (d, $J = 6.9$ Hz, 2H), 1.04 (d, $J = 6.7$ Hz, 2H), 0.90 (dd, $J = 14.4, 6.9$ Hz, 8H); ^{13}C NMR (214 MHz, D_2O) δ 181.0, 172.9, 169.8, 168.83, 168.76, 162.4, 147.9, 137.9, 135.4, 130.8, 129.4, 128.3, 126.5, 125.4, 123.8, 66.9, 59.0, 55.2, 52.1, 49.9, 49.4, 41.9, 40.5, 37.5, 36.6, 35.7, 32.6, 32.3, 28.7, 24.2, 22.5, 20.7, 18.1, 17.6, 17.1, 15.0, 10.0; HRMS calcd for $\text{C}_{43}\text{H}_{57}\text{N}_6\text{O}_7\text{S}^+$ [$\text{M} + \text{H}^+$] 801.4009, found 801.4000.

Tetrapeptide 36. To a solution of tetrapeptide **102** (9.5 mg, 0.012 mmol) in MeOH (5 mL) was added H₂NNH₂•H₂O (6.0 μL, 0.12 mmol, 10 equiv) and the reaction stirred at room temperature over 72 h, where crude MS showed major mass peaks for the starting material and the hydrazine added intermediate, and a minor product mass peak. The reaction was heated to 40 °C and stirred for an additional 48 h, where crude MS showed the reaction had not progressed significantly. The reaction was cooled to room temperature, additional H₂NNH₂•H₂O (30 μL, 0.62 mmol, 50 equiv) was added and the reaction was heated to 40 °C. After an additional 24 h, crude MS showed that starting material had been consumed and a small portion of the intermediate remained. After an additional 24 h, no significant reaction progress was observed, so the reaction was concentrated under reduced pressure. Purification by HPLC (C₁₈, 150 x 10 mm, 10–50% MeCN/25 mM aqueous NH₄OAc, pH 4.78 over 10 min, 90% MeCN/25 mM aqueous NH₄OAc, pH 4.78 for 5 min, 5 mL/min) afforded the acetate salt of the title compound as a white/yellow solid (1.99 mg, 25% yield) as a mixture with the methyl ester of the product. HPLC *rt* = 7.4 min; *R_f* = 0.2 (SiO₂, 10% MeOH:CH₂Cl₂); ¹H NMR (400 MHz, MeOD) δ 8.04 (s, 1H), 7.23 (d, *J* = 3.8 Hz, 4H), 7.19–7.10 (m, 1H), 4.41–4.29 (m, 1H), 4.26–4.14 (m, 2H), 4.02–3.93 (m, 1H), 3.16–3.05 (m, 1H), 3.03–2.82 (m, 3H), 2.63–2.48 (m, 1H), 2.46–2.31 (m, 4H), 2.16–2.06 (m, 1H), 1.95 (s, 3H), 2.05–1.52 (ovlp m, 12H), 1.41 (ddd, *J* = 16.3, 8.5, 3.8 Hz, 1H), 1.31–1.18 (m, 1H), 1.18–1.10 (m, 3H), 1.06–0.86 (m, 11H); ¹³C NMR (214 MHz, MeOD) δ 182.3, 177.4, 176.6, 174.2, 173.8, 162.9, 150.8, 139.7, 130.5, 129.3, 127.4, 124.5, 69.8, 59.6, 56.4, 53.0, 52.3, 51.0, 44.1, 42.6, 41.7, 41.6, 39.0, 37.4, 33.7, 31.1, 26.1, 25.5, 23.7, 22.2, 19.9, 18.8 (2C), 16.2, 11.0; HRMS calcd for C₃₅H₅₅N₆O₅S⁺ [M + H⁺] 671.3955, found 671.3960.

Tetrapeptide 37. To a solution of tetrapeptide **100** (2.9 mg, 3.8 μmol) in CH₂Cl₂ (1 mL)

at 0 °C was added Et₃N (4.2 μL, 30 μmol, 8 equiv) as a solution in CH₂Cl₂ (100 μL) and AcCl (1.1 μL, 15 μmol, 4 equiv) as a solution in CH₂Cl₂ (100 μL), and the reaction stirred while warming to room temperature overnight. After 18 h, TLC (2 x 5% MeOH:CH₂Cl₂ with 1% Et₃N) showed complete consumption of starting material. The reaction was concentrated under reduced pressure and purification by HPLC (C₁₈, 250 x 10 mm, 0–20% MeCN/0.04% aqueous HCl over 2 min, 20% MeCN/0.04% aqueous HCl for 2 min, 20–90% MeCN/0.04% aqueous HCl over 35 min, 90% MeCN/0.04% aqueous HCl for 5 min, 90–10% MeCN/0.04% aqueous HCl over 5 min, 3 mL/min) afforded the benzyl ester intermediate as a white solid (1.3 mg, 42 % yield) as confirmed by HRMS. The intermediate was brought forward without further characterization. HPLC *rt* = 21.9 min; *R_f* = 0.5 (SiO₂, 5% MeOH:CH₂Cl₂ with 1% Et₃N); HRMS calcd for C₄₄H₆₃N₆O₆S⁺ [M + H⁺] 803.4524, found 803.4511.

To a solution of the intermediate (1.3 mg, 1.6 μmol) in THF (1.2 mL) was added an aqueous LiOH solution (0.2 M in H₂O, 0.4 mL, 0.08 mmol, 50 equiv) and the reaction stirred overnight. After 18 h, HPLC trace analysis showed complete consumption of starting material, and a crude MS confirmed the presence of the product mass peak. The reaction mixture was acidified to pH 2 with 1.0 M aqueous HCl, and was concentrated under reduced pressure. Purification by HPLC (C₁₈, 250 x 10 mm, 0–20% MeCN/0.04% aqueous HCl over 2 min, 20% MeCN/0.04% aqueous HCl for 2 min, 20–90% MeCN/0.04% aqueous HCl over 35 min, 90% MeCN/0.04% aqueous HCl for 5 min, 90–10% MeCN/0.04% aqueous HCl over 5 min, 3 mL/min) afforded the title compound as a white solid (0.73 mg, 63 % yield, 27% yield over two steps). HPLC *rt* = 15.9 min; *R_f* = 0.2 (SiO₂, 10% MeOH:CH₂Cl₂); ¹H NMR (400 MHz, D₂O) δ 7.96 (s, 1H), 7.38–7.21 (m, 5H), 5.09 (dd, *J* = 11.3, 3.2 Hz, 1H), 4.35 – 4.25 (m, 1H), 4.22 (d, *J* = 8.4 Hz, 1H), 3.94–

3.82 (m, 2H), 3.55 (br d, $J = 13.3$ Hz, 1H), 3.20–3.07 (m, 1H), 3.00 (dd, $J = 13.5, 5.4$ Hz, 1H), 2.85 (dd, $J = 13.8, 8.3$ Hz, 1H), 2.78 (s, 3H), 2.72 – 2.61 (m, 1H), 2.28–2.13 (m, 2H), 2.10 (s, 3H), 2.07–1.69 (m, 8H), 1.67–1.45 (m, 3H), 1.26–1.16 (ovlp m, 1H), 1.19 (d, $J = 7.0$ Hz, 3H), 0.97 (d, $J = 6.7$ Hz, 3H), 0.92 (ovlp d, $J = 6.7$ Hz, 5H), 0.88 (ovlp t, $J = 7.5$ Hz, 4H); ^{13}C NMR (214 MHz, D_2O) δ 181.0, 174.2, 174.1, 172.8, 168.8, 162.8, 148.4, 138.3, 129.5, 128.4, 126.5, 124.3, 66.9, 59.0, 55.2, 51.5, 49.6, 49.4, 41.9, 40.8, 37.5, 36.6, 35.6, 32.4, 28.7, 24.3, 22.6, 21.7, 20.7, 18.3, 17.3, 17.0, 15.0, 9.9; HRMS calcd for $\text{C}_{37}\text{H}_{57}\text{N}_6\text{O}_6\text{S}^+$ [$\text{M} + \text{H}^+$] 713.4060, found 713.4055.

Standard Procedure for ^{14}N Tubulysin Analogs 109–111 from Amine 100

Standard Acylation Procedure:

To a solution of tetrapeptide **100** (1 equiv) in CH_2Cl_2 (5.0 mL) at 0 °C was added base (15–50 equiv) and acylating agent (10–25 equiv), and the reaction was stirred for up to 2 h. When TLC showed complete consumption of starting material, the reaction was quenched with 1.0 M aqueous HCl (3 mL), and the layers were separated. The aqueous layer was extracted with CH_2Cl_2 (3 x 3 mL), and the combined organic layers were dried (Na_2SO_4), filtered, and concentrated under reduced pressure. The crude intermediate was brought forward without purification.

Standard LiOH Hydrolysis Procedure:

To a solution of the intermediate in THF (2.5 mL), MeOH (0.5 mL), and H_2O (0.5 mL) was added $\text{LiOH}\cdot\text{H}_2\text{O}$ (21 mg) to make a 0.14 M reaction solution. If complete consumption of starting material was not observed by TLC after 18 h, additional $\text{LiOH}\cdot\text{H}_2\text{O}$ (21 mg) was added. After TLC and crude MS showed loss of starting material, the organic solvents were removed under reduced pressure and the remaining

aqueous mixture was diluted with additional H₂O (3 mL). The aqueous mixture was acidified to pH 2 with 1.0 M aqueous HCl solution and extracted with CH₂Cl₂ (5 x 3 mL). The combined organic layers were dried (Na₂SO₄), filtered, and concentrated under reduced pressure. Purification by HPLC afforded the title compounds.

Tetrapeptide 109. The title compound was obtained using **100** (5.2 mg, 6.8 μmol, 1 equiv), pyridine (14 μL, 0.17 mmol, 25 equiv) and trimethylacetyl chloride (21 μL, 0.17 mmol, 25 equiv) following the standard procedure for ^Ntubulysin analogs **109–111** and after purification by HPLC (C₁₈, 150 x 10 mm, 30–35% MeCN/25 mM aqueous NH₄OAc, pH 4.78 over 3 min, 35% MeCN/25 mM aqueous NH₄OAc, pH 4.78 for 7 min, 90% MeCN/25 mM aqueous NH₄OAc, pH 4.78 for 5 min, 5 mL/min). White solid (1.68 mg, 33% over 2 steps); HPLC rt = 8.6 min; *R*_f = 0.5 (SiO₂, 10% MeOH:CH₂Cl₂); ¹H NMR (601 MHz, MeOD with NH₄OAc) δ 7.98 (s, 1H), 7.25–7.19 (m, 4H), 7.17–7.11 (m, 1H), 5.14 (dd, *J* = 11.5, 3.3 Hz, 1H), 4.36–4.28 (m, 1H), 4.19 (d, *J* = 8.7 Hz, 1H), 3.93 (ddd, *J* = 11.5, 4.9, 3.0 Hz, 1H), 3.00–2.94 (m, 2H), 2.91 (dd, *J* = 13.6, 7.2 Hz, 1H), 2.67 (dd, *J* = 11.1, 2.8 Hz, 1H), 2.53–2.46 (m, 1H), 2.27 (ddd, *J* = 14.7, 11.7, 3.4 Hz, 1H), 2.22 (s, 3H), 2.20–2.11 (m, 2H), 2.00 (ddd, *J* = 14.2, 9.4, 4.7 Hz, 1H), 1.88–1.71 (m, 4H), 1.69–1.53 (m, 5H), 1.36–1.27 (m, 2H), 1.25 (s, 9H), 1.22–1.16 (m, 1H), 1.15 (d, *J* = 7.0 Hz, 3H), 0.97 (d, *J* = 6.8 Hz, 3H), 0.95 (d, *J* = 4.8 Hz, 3H), 0.94 (d, *J* = 4.8 Hz, 3H), 0.91 (t, *J* = 7.4 Hz, 3H); ¹³C NMR (226 MHz, MeOD with NH₄OAc) δ 184.3, 181.2, 179.9, 176.1, 175.1, 173.7, 162.8, 151.0, 139.8, 130.6, 129.2, 127.3, 123.9, 70.4, 59.5, 56.6, 52.3, 51.4, 50.7, 44.5, 41.5, 40.6, 39.8, 39.6, 37.4, 36.5, 34.1, 31.4, 27.8, 26.0, 24.1, 23.9, 19.5, 19.4, 18.5, 16.4, 11.0; HRMS calcd for C₄₀H₆₃N₆O₆S⁺ [M + H⁺] 755.4530, found 755.4546.

Tetrapeptide 110. The title compound was obtained using **100** (2.2 mg, 2.9 μmol, 1 equiv), pyridine (11 μL, 0.14 mmol, 50 equiv), and TFAA (4 μL, 0.03 mmol, 10 equiv)

following the standard procedure for ^Ntubulysin analogs **109–111** and after purification by HPLC (C₁₈, 150 x 10 mm, 10–50% MeCN/25 mM aqueous NH₄OAc, pH 4.78 over 10 min, 90% MeCN/25 mM aqueous NH₄OAc, pH 4.78 for 5 min, 5 mL/min). White solid (0.22 mg, 10% over 2 steps); HPLC *rt* = 9.9 min; *R_f* = 0.2 (SiO₂, 10% MeOH:CH₂Cl₂); ¹H NMR (900 MHz, MeOD) δ 8.08 (d, *J* = 3.0 Hz, 1H), 7.31–7.23 (m, 4H), 7.20–7.15 (m, 1H), 5.24 (dd, *J* = 11.3, 3.4 Hz, 1H), 4.41–4.35 (m, 1H), 4.23 (d, *J* = 8.4 Hz, 1H), 3.93 (ddd, *J* = 11.4, 5.4, 2.9 Hz, 1H), 3.28–3.25 (m, 1H), 3.19–3.10 (m, 1H), 2.98–2.92 (m, 2H), 2.62–2.47 (m, 2H), 2.44 (s, 3H), 2.32 (ddd, *J* = 14.6, 11.6, 3.4 Hz, 1H), 2.26 (ddd, *J* = 14.4, 11.4, 2.9 Hz, 1H), 2.02 (ddd, *J* = 13.9, 9.5, 4.3 Hz, 1H), 1.97–1.80 (m, 4H), 1.77 (d, *J* = 13.6 Hz, 1H), 1.72–1.59 (m, 4H), 1.50–1.41 (m, 1H), 1.26–1.20 (m, 1H), 1.18 (d, *J* = 7.1 Hz, 3H), 1.02 (d, *J* = 6.8 Hz, 3H), 0.98 (t, *J* = 7.3 Hz, 6H), 0.96–0.92 (m, 3H); ¹³C NMR (226 MHz, MeOD) δ 173.8, 172.9, 162.7, 160.7, 159.2, 151.2, 139.7, 130.5, 129.3, 127.4, 124.6, 69.6, 59.8, 56.3, 52.4, 51.1, 50.9, 43.9, 41.6, 38.9, 37.5, 36.7, 33.8, 31.0, 25.9, 25.3, 23.5, 19.5, 19.4, 18.9, 18.5, 16.2, 11.1; HRMS calcd for C₃₇H₅₄F₃N₆O₆S⁺ [*M* + H⁺] 767.3778, found 767.3776.

Tetrapeptide 111. The title compound was obtained using **100** (4.9 mg, 6.4 μmol, 1 equiv), Et₃N (13 μL, 0.094 mmol, 15 equiv) and methyl chloroformate (12 μL, 0.16 mmol, 25 equiv) following the standard procedure for ^Ntubulysin analogs **109–111** and after purification by HPLC (C₁₈, 150 x 10 mm, 20–25% MeCN/0.05% aqueous formic acid over 5 min, 25% MeCN/0.05% aqueous formic acid for 10 min, 90% MeCN/0.05% aqueous formic acid for 5 min, 5 mL/min). Off-white solid (0.69 mg, 15% over 2 steps); HPLC *rt* = 10.3 min; *R_f* = 0.3 (SiO₂, 10% MeOH:CH₂Cl₂); ¹H NMR (900 MHz, MeOD with NH₄OAc) δ 7.98 (s, 1H), 7.25–7.19 (m, 4H), 7.16–7.10 (m, 1H), 4.32–4.27 (m, 1H), 4.21 (d, *J* = 8.7 Hz, 1H), 4.00–3.92 (m, 1H), 3.66 (s, 3H), 2.98 (dd, *J* = 13.8, 5.6 Hz, 1H), 2.92

(dd, $J = 13.3, 8.1$ Hz, 2H), 2.55 (dd, $J = 11.2, 2.5$ Hz, 1H), 2.50–2.44 (m, 1H), 2.21–2.13 (ovlp m, 1H), 2.17 (s, 3H), 2.09–1.97 (m, 3H), 1.83–1.72 (m, 3H), 1.66–1.52 (m, 5H), 1.36–1.25 (m, 3H), 1.24–1.16 (m, 1H), 1.14 (d, $J = 7.0$ Hz, 3H), 1.00 (d, $J = 6.7$ Hz, 3H), 0.96–0.90 (m, 9H); ^{13}C NMR (226 MHz, MeOD with NH_4OAc) δ 185.0, 176.5, 175.7, 173.9, 162.8, 159.0, 151.4, 139.9, 130.6, 129.2, 127.2, 123.9, 70.7, 59.3, 56.7, 52.8, 52.4, 52.3, 51.8, 44.7, 41.3, 41.2, 39.8, 37.5, 34.1, 31.6, 30.8, 26.2, 26.0, 24.4, 19.6, 19.5, 18.5, 16.3, 11.0; HRMS calcd for $\text{C}_{37}\text{H}_{57}\text{N}_6\text{O}_7\text{S}^+$ [$\text{M} + \text{H}^+$] 729.4009, found 729.4013.

***N*-Methyl-1*H*-imidazole-1-carboxamide (118).** To a suspension of CDI (3.57 g, 22.0 mmol, 1.1 equiv) in CH_2Cl_2 (20 mL) at 0 °C was added a solution of methylamine **116** (2.0 M in THF, 10 mL, 20 mmol, 1 equiv) dropwise and the resulting orange solution was stirred while warming to room temperature overnight. After 72 h, the reaction was quenched with H_2O (20 mL) and the layers were separated. The aqueous layer (pH 8) was extracted with CH_2Cl_2 (4 x 10 mL), and the combined organic layers were dried (Na_2SO_4), filtered, and concentrated under reduced pressure. The resulting orange/white solid (1.363 g) was a 1:1 mixture of **118**:imidazole by ^1H NMR. A portion of this crude intermediate was purified by partitioning between CH_2Cl_2 (15 mL) and saturated aqueous NH_4Cl (15 mL), and the layers were separated. The aqueous layer was extracted with CH_2Cl_2 (3 x 10 mL), and the combined organic layers were dried (Na_2SO_4), filtered, and concentrated under reduced pressure. The resulting white solid was exclusively **118** by ^1H NMR and was used without further purification. ^1H NMR (400 MHz, CDCl_3) δ 8.20 (s, 1H), 7.34 (s, 1H), 7.10 (s, 1H), 5.92 (br s, 1H), 3.05 (d, $J = 4.8$ Hz, 3H).

***N,N*-Dimethyl-1*H*-imidazole-1-carboxamide (119).** To a suspension of CDI (3.57 g,

22.0 mmol, 1.1 equiv) in CH₂Cl₂ (20 mL) at 0 °C was added Na₂CO₃ (2.12 g, 20.0 mmol, 1 equiv) and dimethyl amine hydrochloride **117** (1.63 g, 20.0 mmol, 1 equiv), and the resulting suspension was stirred while warming to room temperature overnight. After 72 h, the reaction was quenched with H₂O (20 mL), diluted with CH₂Cl₂ (20 mL), and the layers were separated. The aqueous layer (pH 11) was extracted with CH₂Cl₂ (4 x 10 mL), and the combined organic layers were dried (Na₂SO₄), filtered, and concentrated under reduced pressure. The resulting yellow liquid (2.63 g) was a 2:1 mixture of **119**:imidazole by ¹H NMR. A portion of this crude intermediate was purified by partitioning between CH₂Cl₂ (15 mL) and saturated aqueous NH₄Cl (15 mL), and the layers were separated. The aqueous layer was extracted with CH₂Cl₂ (3 x 10 mL), and the combined organic layers were dried (Na₂SO₄), filtered, and concentrated under reduced pressure. The resulting orange liquid, which solidified to an orange solid upon standing, was exclusively **119** by ¹H NMR and was used without further purification. ¹H NMR (400 MHz, CDCl₃) δ 7.90 (s, 1H), 7.24 (br s, 1H), 7.09 (s, 1H), 3.11 (s, 6H).

3-Methyl-1-(methylcarbamoyl)-1*H*-imidazol-3-ium iodide (114). To a solution of **118** (39.8 mg, 0.318 mmol, 1 equiv) in MeCN (3 mL) was added MeI (80 μL, 1.3 mmol, 4 equiv) dropwise. After 72 h, the reaction was concentrated under reduced pressure, and the resulting crude was triturated with CH₂Cl₂ (3 x 3 mL) leaving the title compound (5.6 mg, 7% yield) as a yellow solid. ¹H NMR (400 MHz, CDCl₃) δ 10.97 (s, 1H), 9.21 (br s, 1H), 8.10 (s, 1H), 7.24 (s, 1H), 4.09 (s, 3H), 3.06 (d, *J* = 4.6 Hz, 3H).

1-(Dimethylcarbamoyl)-3-methyl-1*H*-imidazol-3-ium iodide (115). The same procedure for **114** was followed using **119** (161.5 mg, 1.16 mmol) to afford the title compound (325.1 mg, 99.7% yield) as an orange oil that solidified upon standing. ¹H NMR (400 MHz, CDCl₃) δ 10.72 (s, 1H), 7.65 (s, 1H), 7.33 (s, 1H), 4.30 (s, 3H), 3.32 (br

s, 6H).

Tetrapeptide 112. To a solution of tetrapeptide **100** (5.3 mg, 7.0 μ mol, 1 equiv) in MeCN (1.0 mL) was added imidazolium **114** (2.8 mg, 10 μ mol, 1.5 equiv) and Et₃N (1 drop) and the resulting solution was stirred overnight. After 18 h, TLC (5% MeOH:CH₂Cl₂) showed complete consumption of starting material. The reaction was concentrated under reduced pressure, partitioned between CH₂Cl₂ (3 mL) and 1.0 M aqueous HCl solution (3 mL), and the layers were separated. The aqueous layer was extracted with CH₂Cl₂ (3 x 1 mL), and the combined organic layers were dried (Na₂SO₄), filtered, and concentrated under reduced pressure. The resulting crude product was hydrolyzed using the standard LiOH hydrolysis procedure. Purification by HPLC (C₁₈, 150 x 10 mm, 10–50% MeCN/25 mM aqueous NH₄OAc, pH 4.78 over 10 min, 90% MeCN/25 mM aqueous NH₄OAc, pH 4.78 for 5 min, 5 mL/min) afforded the title compound as a white solid (0.86 mg, 17% yield over 2 steps). HPLC *rt* = 8.3 min; *R_f* = 0.2 (SiO₂, 10% MeOH:CH₂Cl₂); NMR studies are ongoing; HRMS calcd for C₃₇H₅₈N₇O₆S⁺ [M + H⁺] 728.4169, found 728.4164.

Tetrapeptide 113. To a solution of tetrapeptide **100** (5.6 mg, 7.4 μ mol, 1 equiv) in MeCN (1.0 mL) was added imidazolium **115** (4.1 mg, 15 μ mol, 2 equiv) and Et₃N (1 drop) and the resulting solution was stirred overnight. After 48 h, no reaction had occurred by TLC (3 x 5% MeOH:CH₂Cl₂) or crude MS. Additional **115** (21 mg, 75 μ mol, 10 equiv) was added as a solution in MeCN (1.0 mL) and the resulting solution was stirred overnight. After an additional 40 h, no reaction had occurred by crude MS, so a catalytic amount of DMAP was added and the resulting solution was heated to reflux and stirred overnight. After an additional 48 h, crude MS showed some reaction progress. Additional **115** (98 mg, 350 μ mol, 47 equiv) was added to the reaction and the solution

was heated to reflux and stirred overnight. After an additional 24 h, TLC showed complete consumption of starting material. The reaction was concentrated under reduced pressure, taken up in 1.0 M aqueous HCl (3 mL), and the resulting aqueous mixture was extracted with CH₂Cl₂ (3 x 3 mL). The combined organic layers were dried (Na₂SO₄), filtered, and concentrated under reduced pressure. The resulting crude product was hydrolyzed using the standard LiOH hydrolysis procedure. Purification by HPLC (C₁₈, 150 x 10 mm, 10–50% MeCN/25 mM aqueous NH₄OAc, pH 4.78 over 10 min, 90% MeCN/25 mM aqueous NH₄OAc, pH 4.78 for 5 min, 5 mL/min) afforded the title compound as a white solid (0.55 mg, 10% yield over 2 steps). HPLC *t*_r = 8.7 min; *R*_f = 0.2 (SiO₂, 10% MeOH:CH₂Cl₂); ¹H NMR (850 MHz, MeOD) δ 7.97 (s, 1H), 7.28–7.20 (m, 4H), 7.19–7.12 (m, 1H), 5.02 (dd, *J* = 11.1, 3.6 Hz, 1H), 4.38–4.30 (m, 1H), 4.19 (d, *J* = 8.7 Hz, 1H), 4.00 (ddd, *J* = 10.9, 5.0, 3.2 Hz, 1H), 3.95–3.69 (m, 2H), 3.03 (d, *J* = 11.8 Hz, 1H), 2.95 (s, 6H), 2.88–2.83 (m, 1H), 2.57 – 2.51 (m, 1H), 2.30 (s, 3H), 2.23 (ddd, *J* = 14.6, 11.2, 3.8 Hz, 1H), 2.13 (ddd, *J* = 14.3, 11.2, 3.1 Hz, 1H), 2.00 (ddd, *J* = 13.9, 9.3, 4.6 Hz, 1H), 1.90–1.54 (m, 10H), 1.40–1.31 (m, 1H), 1.24–1.17 (m, 1H), 1.15 (d, *J* = 7.1 Hz, 3H), 0.98 (d, *J* = 6.8 Hz, 3H), 0.95 (d, *J* = 6.9 Hz, 3H), 0.94 (d, *J* = 6.8 Hz, 3H), 0.91 (t, *J* = 7.4 Hz, 3H); ¹³C NMR (214 MHz, MeOD) δ 183.1, 178.9, 177.9, 174.3, 173.7, 163.0, 160.0, 150.9, 139.8, 130.5, 129.3, 127.3, 123.9, 70.1, 69.0, 59.6, 56.4, 52.5, 52.3, 51.3, 44.3, 41.6, 39.7, 39.2, 37.5, 37.4, 36.7, 33.8, 31.2, 26.1, 25.7, 23.9, 23.3, 19.6, 19.1, 18.4, 16.3, 11.0; HRMS calcd for C₃₈H₆₀N₇O₆S⁺ [M + H⁺] 742.4326, found 742.4310.

Chapter 4:

Synthesis of Unique Tubulysin U (**11**) Analogs with Various Oxygen-Based Functional Groups Replacing the Key Tubuvaline Acetate

Introduction

In addition to the nitrogen containing ^Ntubulysin compounds, analogs with an oxygen at the α -thiazole position of tubuvaline were synthesized to further test the SAR at this position with molecules that more closely resemble naturally isolated tubulysins. With the refined chemistry used towards synthesis of ^Ntubuvaline, production of the α -keto thiazole tubuvaline intermediate was improved. Adapted reactions also improved the tubuvaline-tubuphenylalanine peptide coupling, where *N*-acylurea side product formation was observed and removed similarly to ^Ntubulysin intermediate synthesis. Alkylated products of tubulysin V were the initially targeted molecules, where simple ethers would gauge the effect that the acetate carbonyl of **11** has on bioactivity. Installation of a methyl at late-stage tri- and tetrapeptide intermediates proved to be problematic, so a route which takes advantage of an early stage isoleucine-tubuvaline intermediate was successfully initiated using modified versions of materials previously synthesized (Peltier *et al.*, 2006). Alkylation as a methoxymethyl ether was regioselectively installed at the tubuvaline oxygen, and will be instrumental in early survey of alkylation at this position.

The method to synthesize tubulysin U by the conditions previously published in our lab (Balasubramanian *et al.* 2009) has been reinvestigated, leading to changes in the synthesis of this molecule and other *O*-acylated analogs. Experimentation has determined that the temperature of acylations performed in pyridine, as well as the

quenching methods to end these reactions, were determining factors in reaction outcome. A less problematic route to *O*-acylated tubulysin analogs lies in pre-activation of the pertinent acid with DCC, where full reaction of the reagents before addition into tubulysin V (**11**) was crucial to avoid reactivity at the tubuphenylalanine carboxylate. Success in acylation with a variety of functional groups was variable depending on the group being added, and will be discussed in greater detail below. With these new acylation conditions, two analogs which follow classic affinity label design were produced for covalent labeling of the tubulin binding pocket for in-depth analysis of substrate-target interactions.

Evaluation and Modification of Precursor Synthesis towards Tubulysin V (**12**)

Implementation of the modified synthetic methods used to generate ^Ntubuvaline fragments strengthened the α -keto thiazole tubuvaline finishing steps by increasing yields compared to previously published work. Not surprisingly, the single Boc protection at the *N*-terminus of **42** was an inconsequential factor in reaction success when these fragments were subjected to the standard functional group transformations previously used to produce bis-Boc protected intermediates (Raghavan *et al.* 2008). In the same respect, the reaction conditions which had efficiently generated the ^Ntubuvaline fragments **89** from **87** (Figure 24) were expected to undergo the same selective and efficient reactivity with the α -keto thiazole tubuvaline intermediates.

Implementation of the newly developed conditions discussed above resulted in more than doubling the overall yield in the final 3 functional group transformations to **125** (Figure 35). TBAF deprotection of **42** slightly enhanced the yield compared to an already efficient HF•pyridine deprotection of **43** (77% yield, Raghavan *et al.* 2008).

Previously, oxidation of **123** was run using Dess-Martin periodinane (DMP), an expensive reagent that is also synthetically available from cheaper 2-iodobenzoic acid via an explosive intermediate, 2-iodoxybenzoic acid (IBX, Frigerio *et al.* 1999). Both DMP and MnO₂ will oxidize the alcohol of **123**, but MnO₂ oxidation uses a stable, inexpensive reagent which does not require further purification beyond filtration and results in heightened production of aldehyde **124** (90% yield; a 65% yield was obtained using DMP on a similar alcohol, Raghavan *et al.* 2008). As was the case with ^Ntubuvaline **89** and earlier efforts, NaClO₂ oxidation efficiently converts **124** into acid **125**. During characterization of **125**, a 1:1 mixture of rotamers was present in both ¹H and ¹³C NMR spectra with use of CDCl₃, a phenomenon that did not occur with fragments **89** or **90** (Figure 24, Raghavan *et al.* 2008). Based upon literature precedence (Hu *et al.* 2012) and the significant difference in the N–H proton shift between rotamers (6.75 versus 4.83 ppm), one of the nitrogen-carbon bonds of the Boc protected amine is hypothesized to be slowly rotating, resulting in 2 distinct conformers. No change was observed in variable temperature NMR experiments, but by switching to CD₃OD, the splitting pattern ceased (Balasubramanian 2008). These procedures support production of tubuvaline fragment **125** in multi-gram quantities, and in 80% yield over 3 steps from an intermediate that is common to the ^Ntubuvaline route (**42**).

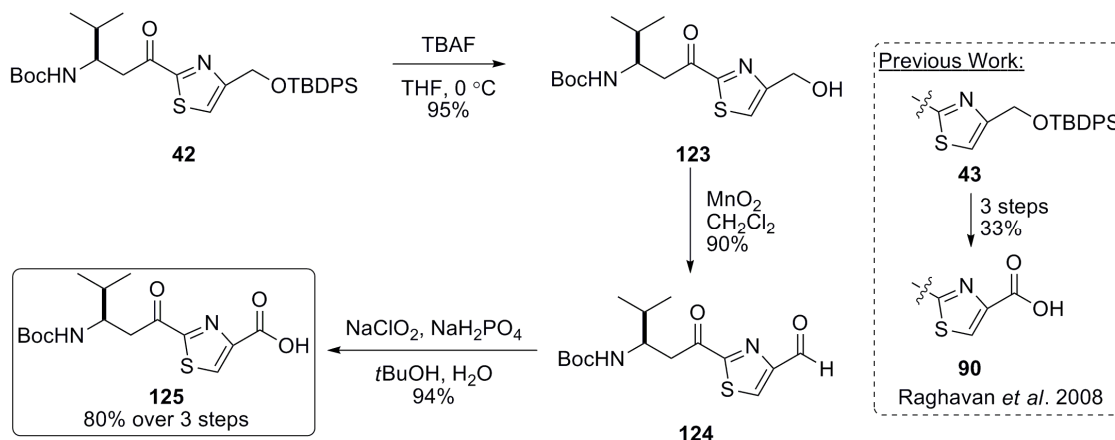


Figure 35: New synthetic methods to tubuvaline **125**.

In addition to the synthetic methods to tubuvaline fragment **125**, further peptide coupling conditions towards tetrapeptide **128** were also surveyed (Figure 36). As was the case with the dipeptide coupling furnishing the ^Ntubuvaline-tubuphenylalanine bond, **125**-tubuphenylalanine **92** coupling resulted in an inseparable *N*-acylurea side product **126** not previously reported. Identification of this impurity was only discovered upon coupling of the **126/127** mixture with Boc-L-isoleucine, where isoleucine-ligated **126** was separable from the keto tripeptide (not shown) under silica chromatography, furnishing both as pure samples for full characterization. With the aim of not wasting synthetically-derived intermediates, the operationally simpler mixed anhydride activation of **125** was a viable alternative to this reaction and cleanly led to the dipeptide **127**. Published methods proved to be the best option for synthesis of tetrapeptide **128** following the modified dipeptide coupling (Figure 36).

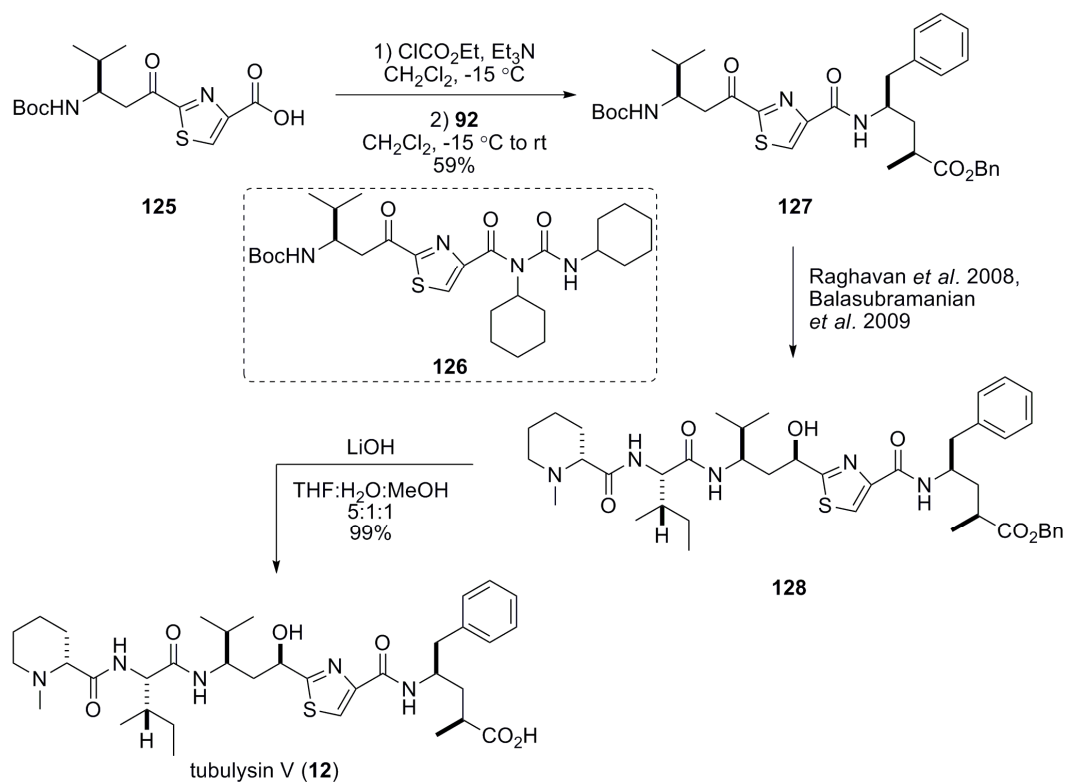


Figure 36: Use of old and new synthetic methods to generate tubulysin V.

Hydrolysis of the tetrapeptide **128** was run under conditions similar to those previously used, but with a key modification which became the standard for benzyl deprotections in all the tubulysin analogs. Previously, LiOH hydrolysis was performed in a 3:1 to 15:1 biphasic mixture of THF:H₂O. Despite the eventual production of the target molecule, these conditions were frequently subject to unpredictable reaction times ranging from 12 hours to 7 days and non-reproducible yields. The cause of these observations was hypothesized to be a separation of the LiOH dissolved in H₂O and the comparatively hydrophobic benzyl ester dissolved in THF, meaning reaction outcome is based on efficient solvent mixing. According to suggestions from Dr. Peter Dosa, MeOH was added to the THF:H₂O mixture in order to create a coalesced solution, with the presumption that any methyl ester formed would be hydrolyzed in the course of the

reaction. Indeed, hydrolyses run using a 5:1:1 THF:H₂O:MeOH solvent ratio saw a homogenous reaction solution with complete miscibility of the benzyl ester and LiOH. The results from this simple modification were astounding, since these unpredictable reactions now run in predictable reaction times of 12 to 48 hours and were high yielding for the target carboxylic acids. As predicted, a portion of methyl ester intermediate is generated during the course of the reaction, but these are short lived and are eventually fully hydrolyzed to the target molecule. The nearly quantitative production of >95% pure **12** possible through this protocol serves as a good example to the power of this modification (Figure 36).

Using the multi-gram stocks of individual amino acid residues along with the efficient couplings and late-stage reactions described above, access to greater than 100 mg quantities of **12** was possible, and served as the material basis for the ensuing modifications to the tubuvaline oxygen.

Synthetic Efforts towards Tubulysin Analogs with O-Alkylation at the Tubuvaline Hydroxyl Group

Initial tubulysin analog synthesis focused on etherification of the tubuvaline hydroxyl group, a change that would greatly increase the stability of the functional group at this position, and would also survey the importance of the **11** acetate carbonyl for cytotoxicity. The most productive starting point was to install a methyl group on the most mature intermediate possible. Following successful methyl group installation, the stage would then be set for alkylations using other groups, particularly the ethyl ether since it most closely mimics the acetate of **11** with a methylene replacement of the acetate carbonyl. Tripeptides **129** and **130** were initially picked since they exhibited the

maximum number of functional groups within **12** without the presence of the *N*-methyl-D-pipecolinic acid tertiary amine, which was deemed a liability by its potential to be alkylated.

Several routes to methyl ethers **131–133** based upon literature precedence were attempted, but ultimately this was a non-viable starting point to generate *O*-alkylated tubulysin analogs (Figure 37). The combination of iodomethane with silver (I) oxide has previously been used to selectively methylate secondary alcohols on other natural products, such as prostaglandins (Finch *et al.* 1975) and ribonucleosides (Hodge and Slnha 1995). Subjecting tripeptide **129** to the reaction conditions established in these papers resulted in no progress past the starting material (Figure 37). In retrospect, reaction productivity may have been improved by using freshly made Ag₂O along with molecular sieves to absorb water generated during the reaction (Reymond and Cossy 2007). A report from Evans had described a mild methylation of polyoxygenated natural products which was productive when the standard Ag₂O/MeI system had failed (Evans *et al.* 1994). An excess of 1,8-bis(dimethylamino)naphthalene, or proton sponge, and Meerwein's salt had selectively methylated secondary alcohols in complex molecules, but use on tripeptide **130** was unproductive and resulted in the recovery of starting material. This same paper also described selective methylation with use of the bulky base 2,6-di-*tert*-butyl-4-methylpyridine and methyl triflate. These reagents failed to methylate either the hydroxyl or the tertiary amine of the tetrapeptide **128**, a surprising conclusion based on the tendency of tertiary amines to be alkylated in the presence of such a strongly electrophilic alkylating agent (Table 2). Faced with a lack of even a small amount of progress in these procedures established to alkylate the alcohols of complex natural products, efforts were instead spent on earlier intermediates with more

established use in this type of transformation.

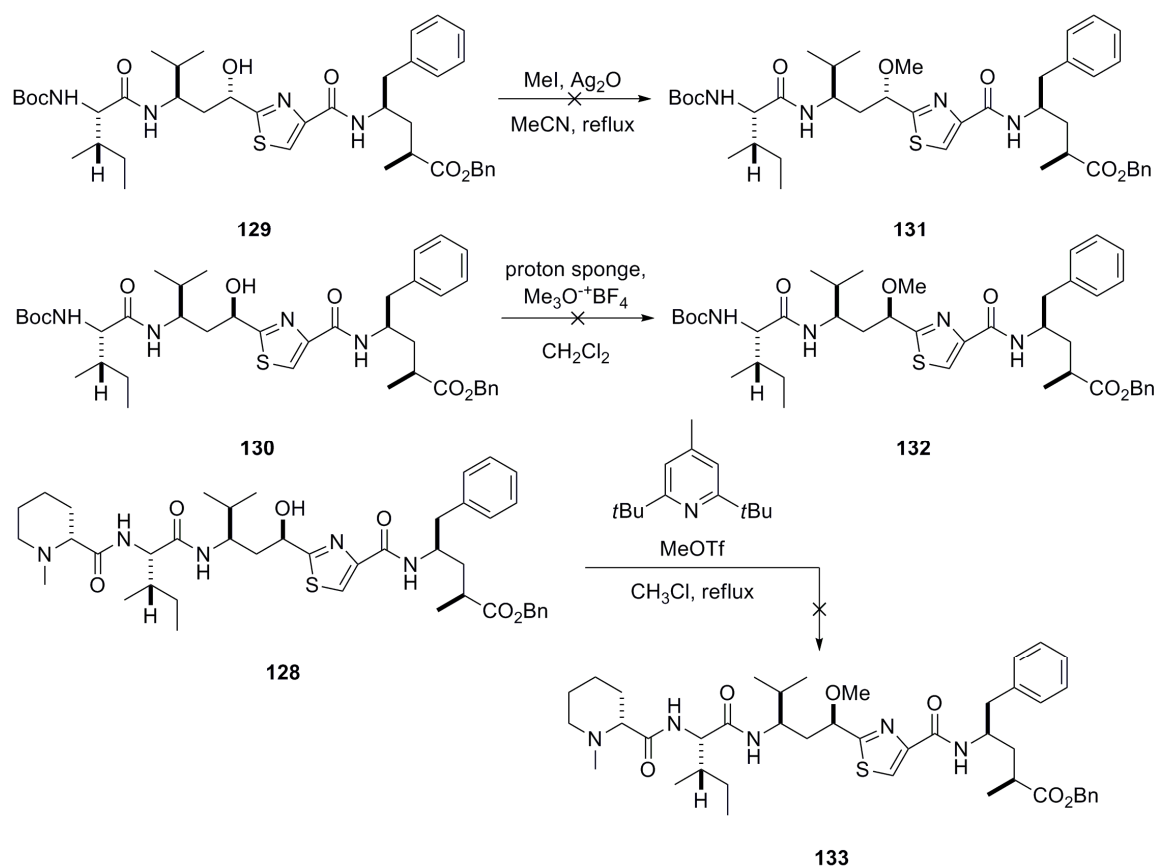


Figure 37: Attempted methylation of the tubuvaline hydroxyl in late-stage intermediates.

A route which is less efficient but better established for selective alkylation in tubulysin intermediates was explored next. In his synthesis of tubulysin D, Ellman described a strategy using an azido protected isoleucine-tubuvaline intermediate to install the labile *N,O*-acetal, which was strategically protected to mask all potentially nucleophilic sites excluding the position that was to be alkylated (Peltier *et al.* 2006). A version of this strategy was used to selectively install a methyl group at the tubuvaline hydroxyl group (Figure 38). Following Boc deprotection of **134**, azido protection was furnished by use of a purportedly shelf stable azido transfer reagent **136** (Goddard-

Borger and Stick 2007). As a safety note, a correction to the original article noted explosive potential of degraded **136** as an outcome of water absorption causing reagent hydrolysis to hydrazoic acid (Goddard-Borger and Stick 2011). Despite its issues with long-term storage, this reagent is simple to make and provided **137** in high yield according to the literature procedure.

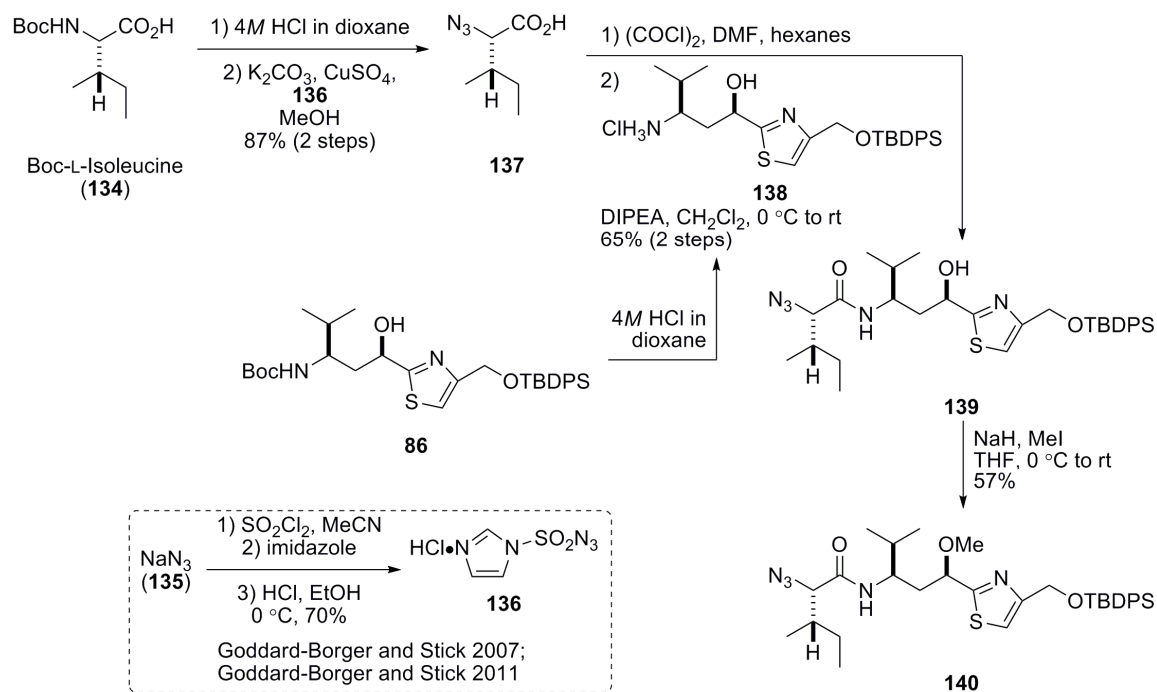


Figure 38: Revised strategy to install a methyl ether at the tubovaline hydroxyl group.

The isoleucine-tubovaline coupling started with activation of the **137** carboxylate as an acid chloride, a method which is usually discouraged for amino acids due to the tendency of amino acid chlorides to equilibrate as ketenes or oxazolones (Williams and Young 1964), thus destroying enantiopurity through racemization of the α stereocenter. In the case of azido protected amino acids, however, previous studies have noted their lack of racemization upon acid chloride activation (Meldal *et al.* 1997). This study also established their use in generating sterically encumbered peptide bonds, a characteristic

of the isoleucine-tubuvaline bond that has been noted (Sani *et al.* 2007). Selective deprotection of the **86** Boc group in the presence of its TBDPS silyl ether (Cavelier and Enjalbal 1997) afforded the tubuvaline free amine **138**, which was added into the acid chloride to furnishing the azido protected dipeptide **139**. The yield of this reaction could potentially be improved by use of an EtOAc/HCl deprotection of **86** according to the work of Cavelier and Enjalbal (Cavelier and Enjalbal 1997).

The choice of intermediate **139** for *O*-methylation was not a foregone conclusion, and was instead influenced by many factors from literature survey. Early tubulysin research noted that the tubuvaline nitrogen is sterically encumbered (Steinmetz *et al.* 2004), and commentary on the difficulty of synthetic transformations at this position have been made (Pando *et al.* 2011). Alkylation of the tubuvaline nitrogen has nonetheless been a heavily researched area due to the *N,O*-acetal at this residue in naturally isolated tubulysins, and the observation that picomolar antiproliferative activity is maintained by simple *N*-methylation of the tubuvaline amide (Wang *et al.* 2007). Syntheses involving tubuvaline *N*-methylation install this functionality before coupling to isoleucine, thereby avoiding this steric liability as a factor in reaction success. Previous works which install the *N,O*-acetal are the only examples where isoleucine-tubuvaline coupled intermediates are *N*-alkylated, where minimalist silyl ether protection of the tubuvaline hydroxyl is required to avoid both *O*-alkylation and poor reaction productivity due to restrictive crowding (Peltier *et al.* 2006). The overwhelming evidence regarding crowding at the tubuvaline amide and the difficulties reported in alkylation of this position led to the hypothesis that *N*-methylation would not occur under controlled reaction conditions for *O*-methylation of **139**.

Selective methylation at the hydroxyl of tubuvaline **139** using a nearly

stoichiometric amount of iodomethane following sodium hydride deprotonation gave the target **140** in moderate but unoptimized yield (Figure 38), where the position in which methylation occurred was confirmed by ^1H NMR. In both the compounds reported here and in our other publications (Raghavan *et al.* 2008, Balasubramanian *et al.* 2009), a paradigm exists where tubulysin intermediates containing a isoleucine-tubuvaline amide bond have a doublet in the >6.0 ppm range with a coupling constant (J) of approximately 9 Hz representative of the N–H proton at this position. Comparison of the ^1H spectra of **139** and **140** clearly shows the presence of the amide N–H proton as a doublet at 6.5 ppm ($J = 9.3$ Hz) and 6.5 ppm ($J = 9.6$ Hz), respectively. The typical tubuvaline O–H proton is a doublet between 4.5–5.5 ppm, which has been established by comparing tubulysin intermediates containing a ketone at the α -thiazole position to their products following ketone reduction. Within the 3.0–5.0 ppm range, two doublets appear in the **139** spectra (5.0 and 4.0 ppm), where azido protected isoleucine intermediates have typically shown a doublet at approximately 4.0 ppm representing the isoleucine backbone methine (Peltier *et al.* 2006). Upon methylation, the doublet at 5.0 ppm disappears in the **140** spectra while a doublet at 3.9 ppm remains, indicating the loss of the O–H proton.

Despite the consistency of these N–H and O–H protons in the ^1H NMR spectra of many tubulysin intermediates, the fact remains that heteroatom protons can be shifted drastically based on more factors than just their position within the molecule, such as sample concentration and temperature. Hence, the most convincing argument for O-methylation lies in analysis of a telltale methine proton between the two spectra. This methine is a multiplet at 4.8 ppm in the **139** spectra that shifts upfield to 4.45 ppm and simplifies to a doublet of doublets in the **140** spectra. Both of these changes would be

predicted for the α -thiazole methine proton upon O-methylation but would not be predicted for the γ -thiazole methine proton upon N-methylation. This overwhelming evidence strongly supports the claim of O-methylation, confirming the hypothesis that **139** will undergo selective methylation under non-specialized conditions, most likely as a result of the steric crowding around the amide nitrogen of tubuvaline.

Future work along this route would involve trivial functional group transformations and peptide couplings using established reactions. Previous work has demonstrated a one pot hydrogenation/peptide coupling strategy in which pre-activated N-methyl-D-pipecolinic acid and palladium on carbon were used to install the N-terminus residue on an azido deprotected isoleucine intermediate similar to **140** (Peltier *et al.* 2006). As previously discussed, metal-catalyzed hydrogenation of tubulyisin intermediates containing a thiazole ring have been problematic according to relevant literature. As an alternative strategy, a Staudinger reaction could be used to deprotect the azido group should issues with a lack of reactivity arise, followed by peptide coupling to generate **141** (Figure 39). Completion of the molecule would then involve the well established strategies presented in Figures 24 and 35 to give the carboxylate at the tubuvaline fragment, followed by coupling to tubuphenylalanine **92** to furnish the methyl ether analog **133**. While this route is certainly not optimized in step efficiency, it is the most viable option to generate alkylated tubulyisin analogs.

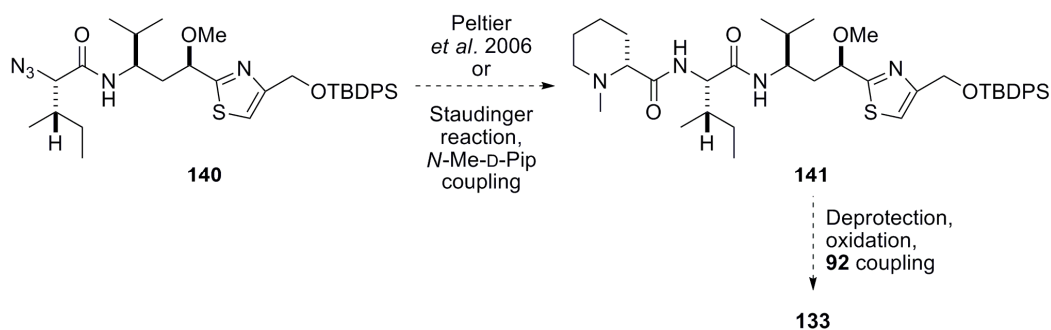


Figure 39: Proposed steps to finish the synthesis of methyl ether **133**.

Attachment of a methoxymethyl ether at the hydroxyl of **128** represents the singular successful alkylation of a late-stage intermediate towards alkylated analogs of **11** (Figure 40). The stability of this functional group under basic conditions is robust, so competitive alkylation of the free carboxylate of **12** was avoided by functionalizing the precursor **128**. Following benzyl ester hydrolysis and purification by HPLC, a low yield of the methoxymethyl protected analog **142** was isolated for full characterization and upcoming biochemical evaluation. Despite not appearing in the preceding low resolution MS, **12** was also isolated upon HPLC purification. The lability of methoxymethyl ethers under acidic conditions is well documented, so a less acidic aqueous phase for HPLC purification may be necessary in the future. As highlighted in Figure 40, a close structural comparison can be made between **11** and methoxymethyl ether **142**. Changes to the polarity and hydrogen bonding potential at this position, together with the resulting comparison in biological activity, will be a commentary on the interaction of these molecules with the tubulin binding pocket.

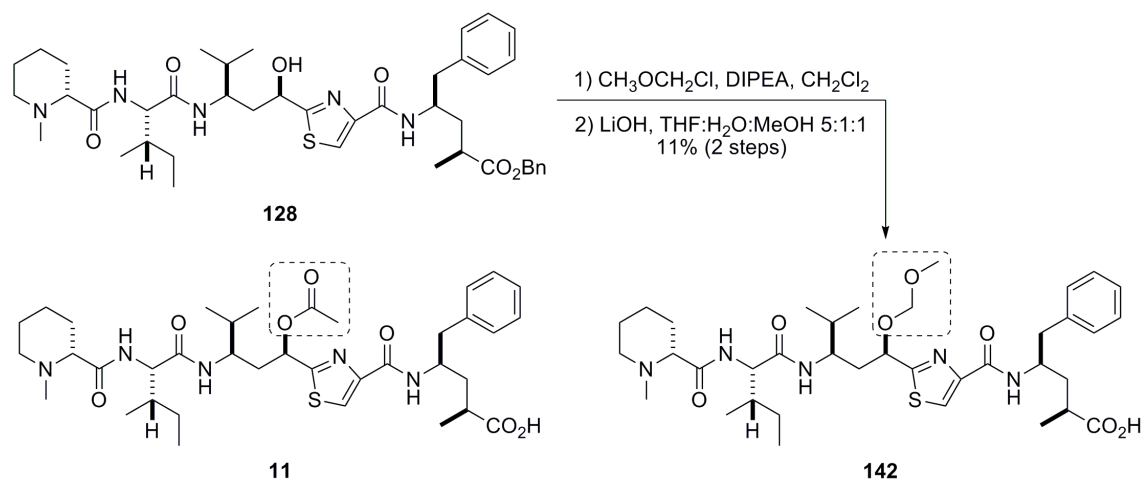


Figure 40: Synthesis of the methoxymethyl ether **142** and its comparison to ester **11**.

Synthesis of Acylated Tubulysin Analogs using Anhydrides in Pyridine

Acetylation of the tubovaline hydroxyl group in tubulysins has been shown to confer orders of magnitude increased anticancer activity, a trend supported by the 1000 fold increased potency of tubulysin U (**11**) compared to tubulysin V (**12**, Figure 6). Most established tubulysin syntheses acetylate the tubovaline residue with acetic anhydride in a pyridine solution containing the molecule of interest. Work in the Fecik lab is no different, where our total synthesis of **11** was completed by acetylation of **12** in pyridine using a large excess of acetic acid at room temperature (Balasubramanian *et al.* 2009). This reaction was reported to generate **11** in 65% yield following HPLC purification. Unexpectedly, reproducing the reported reaction conditions resulted in a 5:6 ratio of **11** and an unknown species. As predicted, **11** was formed as confirmed by comparison to its reported HPLC retention time, ¹H NMR, and low resolution MS (Balasubramanian *et al.* 2009). The other product of this reaction had a ¹H NMR spectra very similar to **11**, but was less polar than **11** judging by its increased HPLC retention time, and exhibited mass peaks correlating to dehydrated **11** exclusively.

Based upon analysis of the collected data and an understanding of tubulyisin reactivity, the identity of this side product was determined to be **11** with a lactam at the *N*-terminus created by intramolecular cyclization (**143**, Figure 41). Conversion of the carboxylic acid of **11** to the proposed lactam would certainly reduce the overall molecular polarity, as characterized by slower elution in reverse-phase HPLC. The ^1H NMR spectra of **11** and **143** in D_2O are expected to be similar due to the nearly unchanged structure between the molecules, and the removal of more distinguishing spectral changes from deuterium exchange at the acidic proton of the carboxylate and amide. Finally, the formula weight of **143** is that of dehydrated **11**, corresponding to the findings through low resolution MS. In addition to the data collected, a reasonable assessment of the possible outcomes of this reaction favors a scenario where activation of the tubuphenylalanine carboxylate as a mixed anhydride causes an intramolecular cyclization of this residue into a γ -lactam.

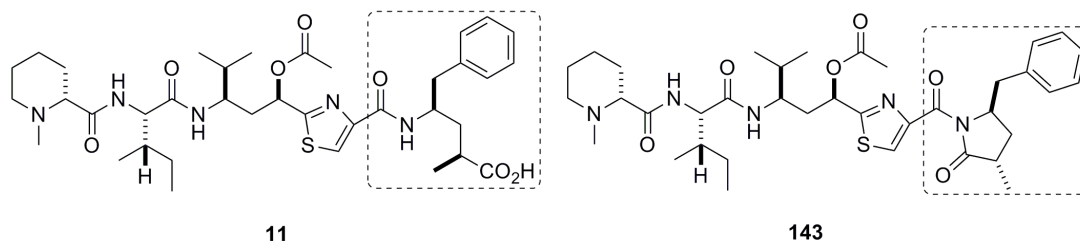
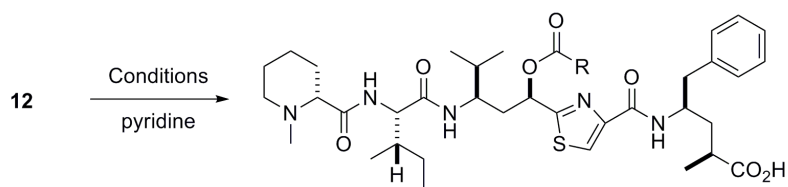


Figure 41: Resulting products of hydroxyl **12** acetylation under published conditions.

As further conformation of the side product identity, subjecting **143** to LiOH hydrolysis produced both **11** and **12** as confirmed by HPLC retention time and low resolution MS, where this procedure opens the tubuphenylalanine lactam during the synthesis towards **91** (Raghavan *et al.* 2008). The hydrolysis of the **143** lactam leading to **11** and **12** exemplifies the issue with this particular side product formation; there is not

a straightforward way in which to reopen the lactam ring without hydrolysis of the labile acetate. While this finding had not been noted in our previous publications, it was not completely unexpected due to the established formation of this lactam as an intermediate towards tubuphenylalanine and as a side product in the work published by other labs (Höfle *et al.* 2003, Wipf and Wang 2007, Ullrich *et al.* 2009b).

In order to avoid this side product formation, the reaction conditions for acetylation of **12** were reevaluated by lowering reaction temperature (Table 3). At 0 °C, the same reaction was much more selective for **11**, giving an 11:1 ratio of **11:143** according to HPLC trace analysis of the crude reaction mixture. Following purification, this unoptimized reaction yielded 47% of **11**. At -20 °C, **11** was essentially the sole product upon reaction workup with a >100:1 ratio of **11:143** by HPLC and with an overall purity of 90%; this slightly crude material was isolated in 91% yield. By simply lowering the reaction temperature, these model reactions have established a method to negate lactam formation while still forming the acetylated product. These acylation conditions have been applied to all further reactions where an excess of the acylating agent is added to a solution of **12** in pyridine. It should also be noted that tubulysin publications by Ellman and Shibue make special note of long H₂O:dioxane quenches following acetic anhydride/pyridine acetylation of the tubuvaline hydroxyl (Peltier *et al.* 2006, Patterson *et al.* 2007, Patterson *et al.* 2008, Shibue *et al.* 2010, Shibue *et al.* 2011). No mention of the significance of this procedure is made within these papers, but these reactions are reported to be high yielding and may be another viable method in which to prevent lactamization.



11, 144–146

<u>Conditions</u>	<u>R =</u>	<u>Outcome</u>
Ac ₂ O, rt	Me	11 (32% yield): 143 , 5:6 ratio
Ac ₂ O, 0 °C	Me	11 (47% yield): 143 , 11:1 ratio
Ac ₂ O, -20 °C	Me	11 (91% yield, 90% overall purity): 143 , >100:1 ratio
acetic formic anhydride, -20 °C	H	pure 144 by MS following reaction workup, full conversion to 12 following HPLC
benzoic anhydride, -20 °C	Ph	145 + 12 , mixture of side products
butyric anhydride, -20 °C	CH ₂ CH ₂ CH ₃	146 (58% yield) + 12

Table 3: Acylation reactions using an anhydride in a pyridine solution of hydroxyl **12** (pyridine/anhydride method).

Having established a productive means to acetylate tubulysin V (**12**) without undesired intramolecular cyclization, acylations were attempted using other anhydrides under the same conditions (Table 3). Generally, a solution of the natural product was dissolved in pyridine and placed in a -20 °C freezer, where upon addition of the anhydride and 48 hours reaction time, there was a spot to spot conversion of **12** to products **11** and **144–146** according to TLC analysis. The reaction quench was best performed by pouring the reaction solution directly into 1.0 M aqueous HCl and extracting with portions of EtOAc, which was effective in completely separating the pyridine and product. In the reactions using acetic anhydride or formic acetic anhydride, the reagent was completely hydrolyzed to its respective acids during the aqueous quench since no anhydride was present in the organic layers following extraction. Benzoic and butyric anhydrides, on the other hand, are not as quickly hydrolyzed and

significant amounts of these reagents were co-extracted into the organic layer. With the product mixture and excess anhydride present in the same ethyl acetate solution, solvent removal created a room temperature, concentrated mixture of these reactive species. Despite the clean reaction apparent from TLC analysis before reaction quench, these reactions resulted in complicated mixtures consisting of product, starting material, and to a varying extent the cyclized lactam versions of these molecules. Hence, any future work should use anhydrides which are destroyed upon aqueous quench or workup conditions which do not isolate the crude product mixtures along with anhydrides.

Unexpectedly, the nearly pure sample of formate ester **144** isolated after aqueous workup underwent full degradation to **12** upon HPLC purification and NMR analysis. Following the typical reaction setup using acetic formic anhydride in pyridine and finishing the reaction with an aqueous quench and organic extraction, immediate TLC and low resolution MS analysis showed production of **144** with an almost nonexistent presence of remaining **12**. Upon HPLC purification using the aqueous NH₄OAc (buffered with AcOH):MeCN solvent system typical for these tubulysin analogs, 2 prominent peaks were isolated separately and confirmed to be **144** and **12**. Centrifugal evaporator concentration of the pure **144** fractions resulted in complete degradation to **12** as confirmed by ¹H NMR, ¹³C NMR, and low resolution MS. This result is confusing since the formate ester group has been attached to natural products before, and has remained stable during purification and biochemical evaluation (Kumar *et al.* 2012). Although formate esters are sometimes used as a hydroxyl protecting group, indicating that there are non-demanding reaction conditions to cleave this group from the hydroxyl oxygen, formate deprotection is achievable under basic conditions, not the acidic HPLC

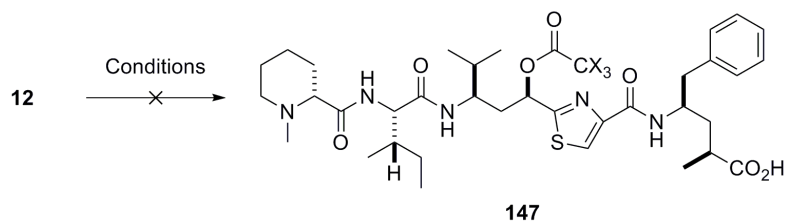
purification conditions presented here. Future work should manipulate **144** as little as possible after aqueous workup, and should purification be deemed necessary, flash chromatography should be used to generate purified **144**.

Studies towards the Synthesis of Halogenated Analogs of Tubulysin U (11)

As part of the SAR profile for oxygen based functional groups on the tubuvaline hydroxyl, we wished to investigate halogenated versions of tubulysin U (**11**). Fluorine acts as a bioisosteric replacement to hydrogen by exhibiting a similar Van der Waals radius; in this same way, chlorine acts as a bioisosteric replacement to methyl groups. The advantage of this sort of replacement comes in to play when metabolic processing of xenobiotics causes unfavorable loss in activity or change in pharmacokinetic properties. Strategic halogenation using fluorine or chlorine can help solve these weaknesses, since the structure of the modified drug is not drastically changed but the points of modification are not susceptible to the same metabolic processing. In this way, replacement of the acetate methyl with halogenated analogs would survey the feasibility of making these modifications for future drug applications. Further use of these analogs would take advantage of the halogen's increased electronegativity, where the additional electron withdrawing properties at this position would make these tubulysin analogs even more susceptible to deacylation. The increased tendency to cleave under nucleophilic conditions qualifies these compounds to gauge whether the tubulysin mode of action is at all based upon acylation of a nucleophilic site within the biological target, which would serve to explain the increased activity of acetylated analogs.

Unfortunately, the synthetic efforts towards these molecules were all non-productive or destructive (Table 4). Multiple iterations towards the trifluoroacetyl analog

of **11** under the conditions discussed above resulted in the complete destruction of the starting material **12**. Modifications intended to make this a more mild reaction, such as using a less concentrated solution of trifluoroacetic anhydride and pyridine in CH_2Cl_2 , or DCC activation of TFA, were simply not reactive enough to progress beyond **12**.



<u>Conditions</u>	<u>X =</u>	<u>Outcome</u>
TFAA, pyridine, rt	F	Degradation
TFAA, pyridine, -20 °C	F	Degradation
TFAA, DMAP, pyridine, CH_2Cl_2 -20 °C	F	No reaction
1) TFA, DCC, DMAP, CH_2Cl_2 , 0 °C 2) 12 , 0 °C to rt	F	No reaction
ClCOCCl_3 , pyridine, rt	Cl	product mass = 12 - mass units

Table 4: Attempted acylations of hydroxyl **12** with halogenated acyl groups.

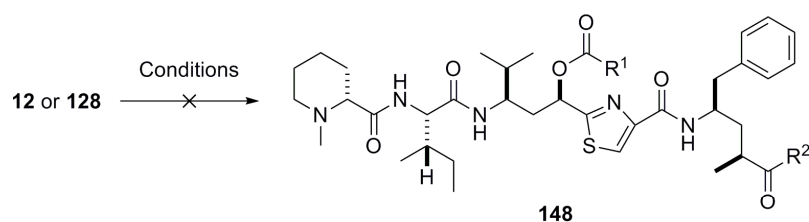
An unexpected outcome occurred under modified conditions using trichloroacetyl chloride as the acylating reagent (Table 4). After 48 hours, TLC showed loss of the product but no other UV active spots, an unusual observation since tubulysin analogs are typically visualized on TLC even at low concentration. HPLC trace analysis of the crude reaction showed a complicated mixture of many nearly equal peaks, where one peak was somewhat more significant than the others. Following isolation, low resolution MS of this peak gave a mass peak of 670, which correlates to the formula weight of tubulysin V minus 2 mass units. The ambiguous nature of this mass reading in addition to insignificant material for full NMR analysis led to inconclusive results, with the only definitive conclusion being that the isolated product was not the target molecule.

Studies towards the Synthesis of Carbamate and Urea Analogs of Tubulysin U (11)

In the realm of van der Waals forces that influence the strength of the substrate-biological target interaction, we wished to test the effect that hydrogen bonding and dipole-dipole interactions have at the space that the acetate of **11** interacts with in the tubulin binding pocket. In order to do this, the electronegativity of the atoms bonded at the tubuvaline hydroxyl group, and in turn the overall polarity and hydrogen bonding potential at this position, were to be changed by replacing the acetate with carbamate and carbonate based functional groups. So as to have the smallest impact on the other forces which dictate substrate binding such as hydrophobic effects and steric interactions with the binding pocket, the targeted compounds had only methyl groups appended at the new functional groups.

Initial focus was on installation of a methyl carbonate at the tubuvaline residue of **12** using a modified version of the procedure to synthesize **11**, which resulted in unforeseen reactivity (Table 5). Using either pyridine or Et₃N as base with or without the addition of DMAP, the reaction was solely productive for one product correlating with a methyl group added to **12** by low resolution MS. Any methyl carbonate containing product with this formula weight would be unreasonable considering the reaction conditions, and methylation of the tubuvaline hydroxyl is also very unlikely, so it can be safely assumed that the product from this reaction is the methyl ester of **12**. This product is not implausible based upon the reaction conditions, since methanol could easily add into the tubuphenylalanine carboxylate after its *in situ* activation as a mixed anhydride. However, ¹H NMR analysis of the methyl chloroformate reagent showed >95% purity with no trace of methanol formation, the reaction was kept under strictly anhydrous conditions, and reaction quench is through the addition of saturated, aqueous

salts, so the source of methanol as the driving force of this reaction is not clear.



Starting material	Conditions	R ¹ =	R ² =	Outcome
12	ClCO ₂ Me, pyridine, CH ₂ Cl ₂ , 0 °C	OMe	OH	12 , R ² = OMe
12	Et ₃ N, DMAP, ClCO ₂ Me, CH ₂ Cl ₂ , -20 °C	OMe	OH	12 , R ² = OMe
12	pyridine, DMAP, ClCO ₂ Me, CH ₂ Cl ₂ , -20 to 0 °C	OMe	OH	12 , R ² = OMe
12	1) Et ₃ N, ClCO ₂ Et, THF, 0 °C 2) CDI, 0 °C to rt	imidazole	OH	R ² = imidazole
128	CDI, DMAP, pyridine, toluene, rt to 75 °C	imidazole	OBn	no reaction
128	114 or 115 , Et ₃ N, MeCN, reflux	NHMe/NMe ₂	OBn	no reaction

Table 5: Attempted synthesis of tubulysin analogs with non-ester functional groups.

Carbamates appended to tubuvaline would also serve as simple functional groups useful to probe the electronic nature of the tubulin binding pocket, where CDI was picked to act as the carbonyl equivalent in the preparation of these molecules (Table 5). This reaction is complicated by the reactivity of CDI at the tubophenylalanine carboxylate, where carboxylates classically react with CDI to form a mixed anhydride, which is then subject to nucleophilic attack from the imidazole generated during the activation step. Since this reactivity was undesirable, a strategy to block this site was attempted through pre-formation of a mixed anhydride, which was postulated to limit the reactivity with CDI and in doing so reduce the *in situ* generation of imidazole. Not only was this mixed anhydride reactive with imidazole during the course of the reaction, a side product had also formed wherein lactam cyclization of the tubophenylalanine fragment occurred. CDI activation of the benzyl ester **128** was attempted instead, since the imidazole would assuredly not be reactive at the unactivated carboxylate, and under the assumption that

the resulting carbamate would not be susceptible to the hydrolytic cleavage used to remove the ester. Despite following literature precedent and running the reaction at high temperatures, the hydroxyl group was not reactive with CDI, even in the presence of DMAP.

A lack of reactivity at the hydroxyl group of tubuvaline prompted the use of a more electrophilic acylating agents, so the two imidazolium salts **114** and **115** were exploited based upon their success in the previous *N*-tubulysin urea syntheses when CDI had failed. Instead of hydroxyl group deprotonation using sodium hydride as noted in the parent paper (Grzyb *et al.* 2005), Et₃N was used with **128** (Table 5) in order to avoid deprotonation and reactivity of other acidic protons on **128**. Productivity of these reactions was questionable since these types of reagents are reported to be limited to O-acylation when installing carbamates at phenols and non-aromatic alkoxides. Not surprisingly, this reaction was not productive for the target molecule even after days of reflux by low resolution MS. The failure to produce the target carbamates underscores the difference in reactivity between the oxygen and nitrogen containing tubulysin analogs, where acylation at this position is more efficient with the increased nucleophilicity of the nitrogen. Future work towards these carbamates will focus on use of more established acylating agents, such as carbamoyls and isocyanates, with a special focus on the safe production of the non-commercially available *N*-methyl based reagents.

Synthesis of Acylated Tubulysin Analogs using DCC Pre-Activated Acids

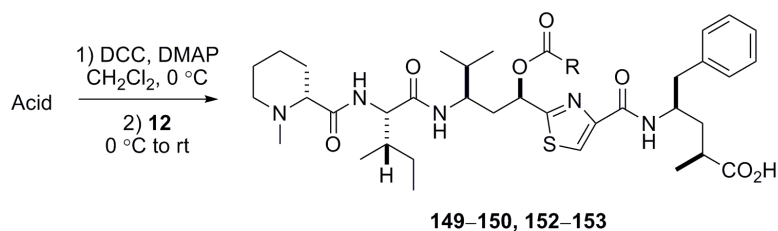
The problems with acylation of tubulysin V (**12**) described above led to the development of improved conditions for acylation of the tubuvaline hydroxyl group.

Rigorous survey of typical reagents and reaction conditions for installation of the ester eventually led to DCC activation of various acids. This is a common strategy to make ester bonds between an alcohol and acid, but tubulylin analogs such as **12** present certain structural features which make this method more complicated than normal. As was previously discussed, *N*-acylurea side products have been observed with DCC activation of the tubuvaline carboxylate. In this case, *N*-acyl shifting was not as pressing a concern since simple, commercially available acids would be used, allowing for an excess of these reagents compared to the far more precious tubulylin intermediates. Additionally, use of a catalytic portion of DMAP with this reaction has been shown to reduce the incidence of *N*-acyl shift (Neises and Steglich 1978).

DCC activation of simple acids for addition onto tubulylin analogs was subject to the more serious consideration of regioselectivity due to the persistence of the free carboxylate at the tubuphenylalanine residue. Under normal circumstances, DCC esterification between an acid and alcohol occurs by adding DCC to a solution containing both substrates. This would not be possible with acylation of **12** without risking undesired reactivity at the tubuphenylalanine carboxylate such as intramolecular cyclization, polymerization, or *N*-acylurea formation. Use of the benzyl protected precursor **128** would allow for selective reaction at the tubuvaline hydroxyl, but this strategy was dismissed based upon the problem of selectively deprotecting the benzyl ester under basic hydrolysis as was seen with **143**.

With consideration to the potential liabilities of this route, the acids were pre-activated in a separate solution of CH₂Cl₂ and allowed to fully react for more than 4 hours before their addition to **12**. To ensure complete consumption of DCC, a 10:5:1 molar ratio of acid:DCC:**12** was used in addition to one equivalent of DMAP, which

serves the dual purpose of reducing the incidence of *N*-acyl shifting and promoting efficient hydroxyl group acylation (Neises and Steglich 1985). Activation of acids with simple alkyl chains prior to their addition to **12** resulted in full conversion of the starting material after 20 to 48 hours with a high yield of the target molecule following simple filtration of the insoluble DCU byproducts and HPLC purification (**149** and **150**, Table 6). A critical aspect in the success of this reaction was the production of the desired product without *N*-acylurea or cyclized side products associated with activation of the tubuphenylalanine carboxylate, even when run at room temperature. In terms of reaction setup and reagent addition, this method for tubulysin acylation represents a more operationally complicated strategy when compared to the pyridine/anhydride method. However, the advantage of this method lies in its temperature independence resulting in no incidence of side product formation when using simple alkyl acids, whereas successful pyridine/anhydride reactions require carefully control of the reaction temperature and anhydride quench.



<u>Acid</u>	<u>Conditions</u>	<u>R =</u>	<u>Outcome</u>
Propionic acid	Complete after 48 h	CH ₂ CH ₃	149 (89% yield)
Isovaleric acid	Complete after 20 h	CH ₂ CH(CH ₃) ₂	Full conversion to 150
Pivalic acid	Additional acid and DCC used, reaction heated to 80 °C, complete after 36 h heating	<i>t</i> Bu	Full conversion to 151 (Figure 42)
Chloroacetic acid	Additional acid and DCC used, complete after 30 h	CH ₂ Cl	Full conversion to 152
Acrylic acid	Additional acid and DCC used, complete after 100+ h	CH=CH ₂	Full conversion to 153 and 154 (Figure 42)

Table 6: Synthesis of acylated tubulysin analogs by DCC activation of simple acids (DCC pre-activation method).

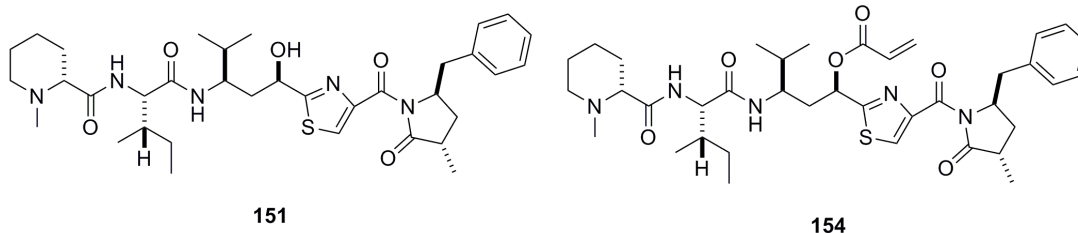


Figure 42: Cyclized lactams resulting from modification to the DCC pre-activation method.

Abnormal reactivity has occurred upon modification of the DCC pre-activation method with sterically demanding acids. Acylation of **12** with pivalic acid was attempted in order to probe the steric limitations at the tubulysin binding pocket in tubulin. Following reaction setup under the standard DCC pre-activation conditions followed by heating to 45 °C, no reaction progression had been made, so additional pivalic acid (50

equivalents) and DCC (25 equivalents) were combined with catalytic DMAP in a separate container, and the resulting mixture was added to the reaction solution after a relatively quick 15 minute activation. When still no progress had been made, the reaction was concentrated, taken up in DMF, and heated to 80 °C. After an additional 36 hours reaction time, the starting material was consumed and a new ninhydrin active spot formed as shown by TLC. Low resolution MS of the crude reaction gave a predominant mass peak correlating with the cyclized lactam **151** (Figure 42) without a peak corresponding to pivalate acylation. The lack of acylation in light of the successful production of the pivalic amide **109** and *O*-acylated products **149** and **150** is likely caused by the inability of **12** to overcome the additional steric bulk of the activated pivalic acid together with the lower nucleophilicity of the tubuvaline hydroxyl. Reactivity was instead dictated by activation of the tubuphenylalanine carboxylate in combination with increased energy supplied from reaction heating, resulting in intramolecular cyclization to the lactam **151**.

Synthesis of Affinity Labels Modeled after Tubulysin U (**11**)

Acylation of tubulysin V (**12**) with various acetate mimics affords the opportunity to synthesize molecules with a purpose beyond their use in further establishing SAR. By attaching electrophilic acyl groups at the hydroxyl group of **12**, structurally homologous analogs to **11** have the chance of creating a covalent bond with nucleophilic moieties within the tubulin binding pocket. These types of compounds are known as affinity labels and function as active site directed irreversible inhibitors. Covalently bound affinity labels that very closely mimic the structural elements of the substrate of interest can then be used to provide data critical to understanding the substrate binding mode through important interactions within the active site. This in turn provides insights into

deliberate structural changes to the substrate which may increase potency through improved binding. This data may be provided by digestion of the bound substrate-target complex followed by analysis of the resulting fragments, or more directly by providing an X-ray crystal structure of the complex. The advantage of a crystal structure is in obtaining a 3D picture of important binding interactions, and with modern computing software, the ability to quickly predict the effect of structural modifications before new analogs are made in the lab. Productive use of these compounds depends on sufficiently nucleophilic groups present at the tubulysin binding site and a low level of promiscuity with other nucleophilic areas on tubulin. Synthesis of the two affinity labels **152** and **153** follow classic affinity label design by installation of a chloromethyl ketone and a Michael acceptor as an α,β -unsaturated carbonyl (Table 6).

Syntheses of the two affinity labels **152** and **153** were at first run under the standard DCC pre-activation conditions, with the acylation using chloroacetic acid attempted first. Since no progress had occurred after 48 hours of reaction time, additional acid, DCC, and DMAP were added to the reaction solution following a quick pre-activation in the same manner as pivalic acid (above). Consideration was given to the previously seen cyclization of **12** to lactam **151** when addition reagents were added, but it was reasoned that this same reactivity would not occur if the reaction was not heated. After an additional 30 hours, low resolution MS analysis showed that the starting material had been consumed and the mass peak associated with **152** had been formed, but without cyclization at the carboxylate. The success of this reaction is in contrast to the previously attempted syntheses of halogenated tubulysin analogs (Table 4), and may represent an alternative method to generate these compounds.

In addition to its use as an affinity label functioning as a Michael acceptor, an

acrylic acid based analog of **11** was envisioned to also survey the effect of acetate replacement with an α,β -unsaturated carbonyl while minimizing steric debt. Reaction progress was slow under the standard DCC pre-activation conditions, with starting material remaining according to TLC and low resolution MS analysis after 78 hours. As was the case in the synthesis of **151** and **152**, a large excess of acid and DCC were added to a separate CH_2Cl_2 solution with catalytic DMAP. After a quick activation, this reagent mixture was transferred to the reaction, and complete consumption of starting materials was confirmed after an additional 36 hours. TLC analysis of the crude reaction revealed the presence of two ninhydrin active compounds, and low resolution MS gave peaks representative of **153** and lactam **154**. This indicates that both **153** and the intramolecular cyclized analog **154** were formed under these conditions, despite the lack of heat. The significantly different outcomes from these three reactions in which nearly the same modification to the standard procedure was employed suggests that DCC activation and reactivity of the tubuphenylalanine carboxylate is variable based upon subtle changes in reaction environment. HPLC purification, data acquisition, and biological evaluation of compounds **151–154** are currently underway.

Conclusion

Synthesis of oxygen based tubulysin analogs with various functional groups appended to the tubuvaline hydroxyl group have been investigated in order to generate a more complete understanding of the SAR at this position based upon changes in hydrogen bonding, polarity, and space filling properties. The materials necessary for this work are provided by improvements to the construction of the α -keto thiazole tubuvaline residue **125**, and a change in the conditions to form the tubuvaline-tubuphenylalanine bond which eliminates the occurrence of a wasteful *N*-acylurea side product. Due to the

failure in late-stage alkylation of tubulysin intermediates, an indirect route to the methyl ether analog was established by regioselective methylation of an azido protected isoleucine-tubuvaline fragment **139**. Biochemical evaluation of the methoxymethyl ether **142** and other alkylated tubulysins will provide insight into the effect of carbonyl removal at the crucial acetate of **11**.

Conditions to acylate the tubuvaline hydroxyl group have also been heavily investigated. Reevaluation of previously established reaction conditions to produce **11** received attention to reduce intramolecular cyclization, and a newly developed method based upon DCC activation of simple acids was successfully implemented. Attempts to acylate the tubuvaline hydroxyl to produce halogenated, carbonate, or carbamate functional groups resulted in nonproductive or degradative reactions when performed under established conditions. General trends in the reactivity of the hydroxyl group of tubuvaline and the carboxylate of tubuphenylalanine were strengthened by observations from these reactions: 1) Acylation of the hydroxyl group is more susceptible to steric effects when compared to the amino compounds due to its reduced nucleophilicity, and 2) electrophilic activation of the tubuphenylalanine carboxylate has the potential to undergo intramolecular cyclization to a γ -lactam under conditions with sufficient energy based on reaction temperature. In addition to the new *O*-tubulysin analogs subjected to antiproliferative assays against MDR cancer cell lines leading to a more robust SAR, compounds **152** and **153** have the potential to act as affinity labels for greater understanding of the interactions important to tubulysin-tubulin binding.

Chapter 4 Experimentals:

(R)-tert-Butyl 1-(4-(hydroxymethyl)thiazol-2-yl)-4-methyl-1-oxopentan-3-ylcarbamate (123). The same procedure to synthesize **88** was followed using **42** (298 mg, 0.526 mmol) and purification by flash chromatography (50% EtOAc:hexanes) to afford the title compound (164 mg, 95% yield) as a clear oil. $R_f = 0.3$ (SiO₂, 50% EtOAc:hexanes); ¹H NMR (400 MHz, CDCl₃) δ 7.56 (s, 1H), 4.92 (d, $J = 8.5$ Hz, 1H), 4.81 (s, 2H), 4.04–3.91 (m, 1H), 3.22 (d, $J = 5.4$ Hz, 2H), 3.39–2.94 (ovlp m, 1H), 1.93–1.74 (m, 1H), 1.34 (s, 9H), 0.96–0.88 (m, 6H); ¹³C NMR (101 MHz, CDCl₃) δ 192.6, 167.0, 159.0, 155.7, 122.3, 79.3, 61.0, 53.3, 41.4, 32.3, 28.4, 19.4, 18.4; HRMS calcd for C₁₅H₂₅N₂O₄S⁺ [M + H⁺] 329.1535, found 329.1528.

(R)-tert-Butyl 1-(4-formylthiazol-2-yl)-4-methyl-1-oxopentan-3-ylcarbamate (124). The same procedure to synthesize **S3** was followed using **123** (228 mg, 0.695 mmol) and purification by flash chromatography (20% EtOAc:hexanes) to afford the title compound (205 mg, 90% yield) as a white solid. $R_f = 0.25$ (SiO₂, 20% EtOAc:hexanes); ¹H NMR (400 MHz, CDCl₃) δ 10.10 (s, 1H), 8.44 (s, 1H), 4.77 (d, $J = 9.1$ Hz, 1H), 4.09–3.99 (m, 1H), 3.38 (dd, $J = 15.1, 3.9$ Hz, 1H), 3.22 (dd, $J = 15.0, 8.2$ Hz, 1H), 1.98–1.83 (m, 1H), 1.36 (s, 9H), 0.99 (d, $J = 1.7$ Hz, 3H), 0.97 (d, $J = 1.7$ Hz, 3H); ¹³C NMR (101 MHz, CDCl₃) δ 192.5, 184.9, 168.1, 155.9, 155.7, 132.3, 79.4, 53.3, 41.8, 32.4, 28.4, 28.4, 19.5, 18.5; HRMS calcd for C₁₅H₂₂N₂O₄SNa⁺ [M + Na⁺] 349.1193, found 349.1182.

(R)-2-(3-(tert-Butoxycarbonylamino)-4-methylpentanoyl)thiazole-4-carboxylic acid (125). The same procedure to synthesize **89** was followed using **124** (24.6 mg, 0.0754 mmol) and purification by flash chromatography (10% MeOH:CH₂Cl₂ with 0.5% AcOH) to afford the title compound (24.3 mg, 94% yield) as a white solid. $R_f = 0.2$ (SiO₂, 10%

MeOH:CH₂Cl₂ with 0.5% AcOH); ¹H and ¹³C NMR analysis showed a 1:1 mixture of rotamers using CDCl₃; ¹H NMR (400 MHz, CDCl₃) δ 8.51 (s, 1H), 8.33 (s, 1H), 6.75 (d, *J* = 9.5 Hz, 1H), 4.83 (d, *J* = 9.5 Hz, 1H), 4.18–3.88 (m, 3H), 3.37 (dd, *J* = 15.2, 4.6 Hz, 1H), 3.26 (dd, *J* = 15.2, 7.7 Hz, 1H), 2.78 (d, *J* = 12.7 Hz, 1H), 1.97–1.78 (m, 2H), 1.46 (s, 9H), 1.38 (s, 9H), 1.05–0.99 (m, 6H), 0.97 (d, *J* = 6.6 Hz, 6H); ¹³C NMR (101 MHz, CDCl₃) δ 193.4, 192.3, 167.6, 167.3, 163.1, 162.8, 158.5, 155.9, 148.9, 148.2, 134.4, 134.0, 81.7, 79.8, 55.6, 53.2, 42.3, 41.0, 33.4, 32.3, 28.4 (2 C), 19.5 (2 C), 18.3 (2 C); ¹H and ¹³C NMR analysis showed a single rotamer using *d*₄-MeOD; ¹H NMR (400 MHz, MeOD) δ 8.67 (s, 1H), 4.02–3.88 (m, 1H), 3.34–3.15 (ovlp m, 2H), 1.91–1.76 (m, 1H), 1.33 (s, 9H), 0.97 (t, *J* = 7.0 Hz, 6H); ¹³C NMR (101 MHz, MeOD) δ 193.7, 168.9, 163.8, 158.1, 150.0, 135.2, 79.8, 54.4, 42.3, 34.2, 28.7, 19.6, 18.5; HRMS calcd for C₁₅H₂₁N₂O₅S⁻ [M - H] 341.1177, found 341.1175.

Dipeptide 127. The same procedure to synthesize **93** was followed using **125** (250 mg, 0.730mmol) and purification by flash chromatography (20% EtOAc:hexanes) to afford the title compound (269 mg, 59% yield) as a clear oil that solidified to a white solid upon standing. *R*_f = 0.4 (SiO₂, 30% EtOAc:hexanes); ¹H NMR (400 MHz, CDCl₃) δ 8.32 (s, 1H), 7.37–7.16 (m, 10H), 5.10 (d, *J* = 12.4 Hz, 1H), 5.06 (d, *J* = 12.5 Hz, 1H), 4.80 (d, *J* = 9.3 Hz, 1H), 4.52–4.40 (m, 1H), 4.17–4.04 (m, 1H), 3.31–3.12 (m, 2H), 2.98 (dd, *J* = 13.6, 6.0 Hz, 1H), 2.89 (dd, *J* = 13.9, 6.7 Hz, 1H), 2.75–2.63 (m, 1H), 2.06 (ddd, *J* = 13.8, 9.3, 4.2 Hz, 1H), 1.96–1.81 (m, 1H), 1.75–1.61 (m, 2H), 1.39 (s, 9H), 1.20 (d, *J* = 7.1 Hz, 3H), 0.95 (t, *J* = 6.9 Hz, 6H); ¹³C NMR (101 MHz, CDCl₃) δ 192.1, 176.7, 176.1, 166.2, 160.0, 155.6, 151.7, 137.6, 136.1, 129.7, 129.6, 128.6, 128.2, 128.1, 126.7, 79.4, 66.5, 53.3, 48.8, 42.0, 41.3, 37.6, 36.8, 31.9, 28.4, 19.6, 18.3, 17.8; HRMS calcd for C₃₄H₄₄N₃O₆S⁺ [M + H⁺] 622.2951, found 622.2971.

(2S,3S)-2-Azido-3-methylpentanoic acid (137). (Goddard-Borger and Stick 2007) A solution of Boc-L-isoleucine (0.998 g, 4.31 mmol, 1 equiv) in HCl (4.0 M in dioxane, 15.0 mL) was stirred at room temperature for 18 h, after which TLC (50% EtOAc:hexanes) of the resulting mixture showed complete consumption of starting material. The reaction solution was concentrated under reduced pressure, and the resulting solid was dissolved in CH₂Cl₂ (5 mL) and concentrated under reduced pressure; this was repeated twice to afford the crude HCl salt as a white solid. To the HCl salt in MeOH (22 mL) was added K₂CO₃ (1.19 g, 8.6 mmol, 2 equiv), CuSO₄ (18 mg, 0.11 mmol, 0.026 equiv), and imidazole-1-sulfonyl azide hydrochloride (1.08 g, 5.17 mmol, 1.2 equiv, Goddard-Borger and Stick 2007) resulting in a bright blue solution with a white precipitate. **CAUTION:** An addition/correction to the Goddard-Borger and Stick paper notes the explosive potential of imidazole-1-sulfonyl azide hydrochloride and should be referred to for safety recommendations (Goddard-Borger and Stick 2011). After 44 h, TLC (5% MeOH:CH₂Cl₂ with 0.5% AcOH) showed partial consumption of starting material, so additional K₂CO₃ (0.42 g, 3.0 mmol, 0.7 equiv) was added, resulting in a green then grey reaction solution. After TLC showed complete consumption of starting material, the reaction was quenched with H₂O (60 mL), extracted with EtOAc (3 x 50 mL), and the combined organic layers were dried (Na₂SO₄), filtered, and concentrated under reduced pressure. Purification by flash chromatography (5% MeOH:CH₂Cl₂ with 0.5% AcOH), followed by washing the pooled fractions with saturated aqueous NaCl solution (3 x 30 mL) to remove AcOH, afforded the title compound (0.593 g, 87% yield) as an orange oil. *R*_f = 0.3 (SiO₂ with KMnO₄ stain, 5% MeOH:CH₂Cl₂ with 0.5% AcOH); ¹H NMR of the product matched that previously reported (Lundquist, IV and Pelletier 2001).

Dipeptide 139. (Peltier *et al.* 2006) A solution of alcohol **86** (102 mg, 0.18 mmol, 1

equiv) in HCl (4.0 M in dioxane, 5.0 mL) was stirred at room temperature for 1 h, after which TLC (50% EtOAc:hexanes) showed complete consumption of starting material. The reaction solution was concentrated under reduced pressure, and the resulting solid was dissolved in CH₂Cl₂ (5 mL) and concentrated under reduced pressure; this was repeated twice to afford the crude HCl salt as a white solid. Separately, to a solution of azide **137** (46 mg, 0.29 mmol, 1.6 equiv) in hexanes (12 mL) was added oxalyl chloride (0.11 mL, 1.3 mmol, 7.5 equiv) and DMF (22 μ L, 0.29 mmol, 1.6 equiv) resulting in a white/yellow precipitate which slowly turned orange. After 1 h, the mixture was filtered and the solution was concentrated under reduced pressure. To a solution of the hydrochloride salt in CH₂Cl₂ (5 mL) at 0 °C was added DIPEA (0.16 mL, 0.90 mmol, 5 equiv), followed by the acid chloride as a solution in CH₂Cl₂ (2 mL). After 1.5 h, the resulting yellow solution was quenched with saturated aqueous NaCl (10 mL), the layers were separated, and the aqueous layer was extracted with EtOAc (2 x 15 mL). The combined organic layers were dried (Na₂SO₄), filtered, and concentrated under reduced pressure. Purification by flash chromatography (10–20% EtOAc:hexanes) afforded the title compound (71.2 mg, 65% yield over 2 steps) as an off white solid. R_f = 0.25 (SiO₂, 20% EtOAc:hexanes); ¹H NMR (400 MHz, CDCl₃) δ 7.73–7.63 (m, 4H), 7.45–7.31 (m, 6H), 7.19 (s, 1H), 6.51 (d, J = 9.2 Hz, 1H), 5.03 (d, J = 4.3 Hz, 1H), 4.85 (s, 2H), 4.83–4.76 (m, 1H), 4.01 (d, J = 3.7 Hz, 1H), 4.05–3.95 (ovlp m, 1H), 2.23–2.10 (m, 1H), 2.07–1.96 (m, 1H), 1.93–1.71 (m, 2H), 1.50–1.22 (m, 3H), 1.10 (s, 9H), 1.14–1.05 (ovlp m, 2H), 0.95 (d, J = 6.9 Hz, 6H), 0.91 (d, J = 7.4 Hz, 3H); ¹³C NMR (101 MHz, CDCl₃) δ 174.9, 170.7, 156.5, 135.6, 133.4, 129.9, 127.8, 113.6, 69.9, 68.9, 63.2, 51.7, 41.5, 38.6, 32.0, 27.0, 24.3, 19.8, 19.4, 18.4, 16.1, 11.8; HRMS studies are ongoing.

Dipeptide 140. To a solution of **139** (43.8 mg, 0.072 mmol, 1 equiv) in THF (10 mL) at 0

°C was added NaH (60% dispersion in mineral oil, 9 mg, 0.2 mmol, 3 equiv) and the reaction was stirred for 1 h. To the resulting light yellow solution was added MeI (5.4 μ L, 0.086 mmol, 1.2 equiv), and the reaction stirred while warming to room temperature overnight. After 12 h, TLC (20% EtOAc:hexanes) showed complete consumption of starting material. The reaction was quenched with saturated aqueous NaCl (15 mL) and the THF was removed under reduced pressure. The aqueous mixture was diluted with H₂O (5 mL) to dissolve the resulting solids and was extracted with Et₂O (30 mL, then 2 x 10 mL), and the combined organic layers were dried (Na₂SO₄), filtered, and concentrated under reduced pressure. Purification by flash chromatography (10–20% EtOAc:hexanes) afforded the title compound (25.6 mg, 57% yield) as a clear oil/colorless semisolid. R_f = 0.3 (SiO₂, 20% EtOAc:hexanes); ¹H NMR (400 MHz, CDCl₃) δ 7.68 (d, J = 6.6 Hz, 4H), 7.46–7.32 (m, 6H), 7.23 (s, 1H), 6.49 (d, J = 9.6 Hz, 1H), 4.87 (s, 2H), 4.45 (dd, J = 10.0, 3.0 Hz, 1H), 4.20–4.10 (m, 1H), 3.89 (d, J = 4.2 Hz, 1H), 3.43 (s, 3H), 2.18–2.05 (m, 1H), 1.99–1.68 (m, 4H), 1.54–1.38 (m, 1H), 1.11 (s, 9H), 1.06 (d, J = 7.0 Hz, 3H), 0.91 (t, J = 7.3 Hz, 9H); ¹³C NMR (101 MHz, CDCl₃) δ 173.9, 168.5, 156.9, 135.7, 133.3, 129.9, 127.9, 114.0, 78.9, 70.4, 63.2, 58.6, 51.2, 40.1, 38.4, 32.1, 27.0, 24.4, 19.4, 19.1, 18.3, 16.2, 11.7; HRMS calcd for C₃₃H₄₈N₅O₃SSi⁺ [M + H⁺] 622.3247, found 622.3238.

Tubulysin V (12): ¹H NMR (600 MHz, MeOD with NH₄OAc) δ 8.01 (s, 1H), 7.27–7.18 (m, 4H), 7.18–7.09 (m, 1H), 4.40–4.26 (m, 1H), 4.20 (d, J = 8.8 Hz, 1H), 4.08 (ddd, J = 11.0, 5.9, 2.4 Hz, 1H), 3.03–2.98 (m, 1H), 2.97–2.88 (m, 2H), 2.79 (dd, J = 11.1, 2.7 Hz, 1H), 2.54–2.45 (m, 1H), 2.26 (s, 3H), 2.25–2.18 (m, 1H), 2.12 (ddd, J = 13.7, 11.3, 2.3 Hz, 1H), 2.03–1.96 (m, 1H), 1.89–1.54 (m, 10H), 1.32 (dd, J = 19.2, 15.2 Hz, 2H), 1.26–1.17 (m, 1H), 1.14 (d, J = 7.1 Hz, 2H), 1.11 (dd, J = 7.8, 6.9 Hz, 1H), 0.98 (d, J = 6.8 Hz,

3H), 0.96 (d, $J = 1.9$ Hz, 3H), 0.94 (d, $J = 1.8$ Hz, 3H), 0.91 (t, $J = 7.4$ Hz, 3H); ^{13}C NMR (151 MHz, MeOD with NH_4OAc) δ 179.3, 179.1, 174.7, 174.0, 163.0, 157.7, 151.0, 139.7, 130.6, 129.2, 127.3, 124.1, 70.2, 69.8, 59.6, 56.5, 52.6, 51.2, 44.4, 41.6, 40.9, 40.1, 39.5, 37.5, 33.8, 31.3, 26.1, 25.9, 24.0, 23.5, 19.6, 19.2, 18.8, 16.2, 11.0.

Tubulysin U (11): ^1H NMR and HPLC spectra of the product matched those previously reported (Balasubramanian *et al.* 2009).

Tetrapeptide 142. To a solution of the tetrapeptide **128** (5.1 mg, 6.7 μmol , 1 equiv) in CH_2Cl_2 (5 mL) at 0 °C was added chloromethyl methyl ether (20 μL , 0.27 mmol, 40 equiv) and DIPEA (50 μL , 0.29 mmol, 40 equiv). After 2 h, TLC (5% MeOH: CH_2Cl_2) showed complete consumption of starting material, and the reaction was quenched with 0.1 M aqueous HCl (5 mL) resulting in a biphasic mixture with a white precipitate. The layers were separated, the aqueous layer was extracted with CH_2Cl_2 (2 x 5 mL), and the combined organic layers were washed with saturated aqueous NaCl (2 x 5 mL). The resulting clear organic layer was dried (Na_2SO_4), filtered, and concentrated under reduced pressure. The crude intermediate was brought forward without purification and subjected to the standard LiOH hydrolysis procedure. Purification by HPLC (C_{18} , 150 x 10 mm, 10–50% MeCN/25 mM aqueous NH_4OAc , pH 4.78 over 10 min, 90% MeCN/25 mM aqueous NH_4OAc , pH 4.78 for 5 min, 5 mL/min) afforded the title compound (0.52 mg, 11% over 2 steps) as a white solid following grease removal following the procedure outlined for **100**. HPLC $r_t = 10.8$ min; $R_f = 0.2$ (SiO_2 , 10% MeOH: CH_2Cl_2); NMR studies are ongoing; HRMS calcd for $\text{C}_{37}\text{H}_{58}\text{N}_5\text{O}_7\text{Si}^+$ [$\text{M} + \text{H}^+$] 716.4057, found 716.4051.

Tetrapeptide 143. ^1H NMR (400 MHz, D_2O) δ 8.28 (d, $J = 9.7$ Hz, 1H), 7.96 (s, 1H), 7.34–7.10 (m, 5H), 5.85 (d, $J = 10.9$ Hz, 1H), 4.96 (q, $J = 6.8$ Hz, 1H), 4.24 (d, $J = 7.8$

Hz, 1H), 4.01–3.91 (m, 1H), 3.87 (dd, $J = 12.3, 2.7$ Hz, 1H), 3.55 (d, $J = 12.2$ Hz, 1H), 3.19–2.95 (m, 3H), 2.78 (s, 3H), 2.43–2.26 (m, 2H), 2.23 (s, 3H), 2.20–1.44 (m, 12H), 1.28–1.17 (m, 1H), 1.14 (d, $J = 6.9$ Hz, 3H), 1.00 (d, $J = 6.7$ Hz, 3H), 0.92 (t, $J = 5.8$ Hz, 9H); HPLC (C₁₈, 250 x 10 mm, 0–20% MeCN/0.04% aqueous HCl over 2 min, 20% MeCN/0.04% aqueous HCl for 2 min, 20–90% MeCN/0.04% aqueous HCl over 35 min, 90% MeCN/0.04% aqueous HCl for 5 min, 90–10% MeCN/0.04% aqueous HCl over 5 min, 3 mL/min) $rt = 21.3$ min; low resolution MS calcd for C₃₇H₅₄N₅O₆Si⁺ [M + H⁺] 696.38, found 696.31.

Standard Procedure for Tubulysin V (12) Acylation using Anhydrides in Pyridine:

To a solution of **12** (1 equiv) in pyridine (0.035 M) at -20 °C was added the anhydride (100 equiv) and the solution was placed in a -20 °C freezer overnight. After 24–48 h, TLC (10% MeOH:CH₂Cl₂, using an aliquot partitioned between 1.0 M aqueous HCl and EtOAc) showed complete consumption of starting material. The reaction was poured directly into 1.0 M aqueous HCl (30 mL) and extracted with EtOAc (15 mL). The layers were separated, and the aqueous layer was extracted with EtOAc (2 x 5 mL), and the combined organic layers were dried (Na₂SO₄), filtered, and concentrated under reduced pressure. Purification by HPLC afforded the title compound.

Standard Procedure for Tubulysin V (12) Acylation using DCC Activated Acids:

To a solution of the acid (10 equiv) in CH₂Cl₂ (5 mL) at 0 °C was added DMAP (1 equiv) and DCC (5 equiv) and the reaction was stirred while warming to room temperature over 4.5 h. The resulting mixture was re-cooled to 0 °C and cannulated into a flask pre-loaded with **12** (1 equiv) and the reaction stirred while warming to room temperature overnight. After 12–48 h, TLC (10% MeOH:CH₂Cl₂) showed complete consumption of

starting material. The reaction was concentrated under reduced pressure, the crude solid was mixed with MeCN (3 mL), and filtered through a plug of cotton. The solution was concentrated under reduced pressure and purified by HPLC to afford the title compound.

Tetrapeptide 144. After subjecting **12** (5.9 mg, 8.8 μ mol) and formic acetic anhydride (55 μ L, 0.88 mmol, Krimen 1988) to the standard procedure for tubulyisin V (**12**) acylation using anhydrides in pyridine, low resolution MS showed complete consumption of starting material after 24 h with exclusive production of the title compound following aqueous reaction workup. During HPLC purification (C_{18} , 150 x 10 mm, 32% MeCN/25 mM aqueous NH_4OAc , pH 4.78 for 10 min, 90% MeCN/25 mM aqueous NH_4OAc , pH 4.78 for 5 min, 5 mL/min), partial degradation back to **12** occurred, followed by full degradation of purified **144** back to **12** upon heated centrifugal evaporation of the HPLC fractions, as shown by 1H NMR, ^{13}C NMR and low resolution MS. HPLC r_t = 9.2 min; R_f = 0.25 (SiO_2 , 10% MeOH: CH_2Cl_2); low resolution MS calcd for $C_{36}H_{54}N_5O_7S^+$ [$M + H^+$] 700.37, found 700.21.

Tetrapeptide 145. After subjecting **12** (5.2 mg, 7.7 μ mol) and benzoic anhydride (175 μ L, 0.77 mmol) to the standard procedure for tubulyisin V (**12**) acylation using anhydrides in pyridine, TLC analysis showed complete consumption of starting material after 24 h. Following aqueous reaction workup using the standard protocol, the title compound was obtained as a mixture with **12** and the intramolecularly cyclized lactams of **145** and **12** according to low resolution MS. HPLC purification and structural characterization of **145** are currently underway. Low resolution MS calcd for $C_{42}H_{58}N_5O_7S^+$ [$M + H^+$] 776.41, found 776.24.

Tetrapeptide 146. The title compound was obtained using **12** (4.8 mg, 7.1 μmol) and butyric anhydride (0.12 mL, 0.71 mmol) after 18 h following the standard procedure for tubulysin V (**12**) acylation using anhydrides in pyridine and after purification by HPLC (C_{18} , 150 x 10 mm, 50% MeCN/25 mM aqueous NH_4OAc , pH 4.78 for 10 min, 90% MeCN/25 mM aqueous NH_4OAc , pH 4.78 for 5 min, 5 mL/min). White solid (3.10 mg, 58% yield); HPLC $r_t = 2.7$ min; $R_f = 0.35$ (SiO_2 , 10% MeOH: CH_2Cl_2); ^1H NMR (400 MHz, MeOD) δ 8.07 (s, 1H), 7.23 (d, $J = 4.2$ Hz, 4H), 7.19–7.11 (m, 1H), 5.92 (dd, $J = 10.8$, 2.7 Hz, 1H), 4.41–4.29 (m, 1H), 4.21 (d, $J = 8.4$ Hz, 1H), 3.96 (ddd, $J = 8.3$, 5.2, 2.7 Hz, 1H), 3.11 (d, $J = 11.8$ Hz, 1H), 3.05 (dd, $J = 11.2$, 2.6 Hz, 1H), 2.92 (d, $J = 6.7$ Hz, 2H), 2.60–2.37 (ovlp m, 4H), 2.40 (s, 3H), 2.24 (ddd, $J = 14.0$, 10.9, 2.9 Hz, 1H), 2.18–2.08 (m, 1H), 1.99 (ddd, $J = 13.9$, 9.7, 4.1 Hz, 1H), 1.93–1.53 (m, 11H), 1.48–1.34 (m, 1H), 1.26–1.18 (m, 1H), 1.16 (d, $J = 7.1$ Hz, 3H), 1.02–0.88 (m, 15H); ^{13}C NMR (101 MHz, MeOD) δ 174.2, 173.7, 173.4, 171.9, 162.7, 151.0, 139.7, 130.5, 129.3, 127.4, 124.9, 71.2, 69.7, 59.6, 56.4, 52.0, 51.1, 44.0, 41.7, 39.1, 38.0, 37.6, 36.8, 33.8, 31.1, 25.9, 25.4, 23.5, 22.4, 19.4, 19.3, 18.5, 16.2, 14.1, 11.1; HRMS calcd for $\text{C}_{39}\text{H}_{60}\text{N}_5\text{O}_7\text{S}^+$ [$\text{M} + \text{H}^+$] 742.4213, found 742.4198.

Tetrapeptide 149. The title compound was obtained using **12** (4.5 mg, 6.7 μmol), propionic acid (5 μL , 67 μmol), DMAP (1 mg, 8 μmol) and DCC (6.8 mg, 33 μmol) after 48 h following the standard procedure for tubulysin V (**12**) acylation using DCC activated acids and after purification by HPLC (C_{18} , 150 x 10 mm, 50% MeCN/25 mM aqueous NH_4OAc , pH 4.78 for 10 min, 90% MeCN/25 mM aqueous NH_4OAc , pH 4.78 for 5 min, 5 mL/min). White solid (4.3 mg, 89% yield); HPLC $r_t = 2.4$ min; $R_f = 0.3$ (SiO_2 , 10% MeOH: CH_2Cl_2); ^1H NMR (600 MHz, MeOD with NH_4OAc) δ 8.07 (s, 1H), 7.23 (d, $J = 4.2$ Hz, 4H), 7.18–7.12 (m, 1H), 5.92 (dd, $J = 11.0$, 2.5 Hz, 1H), 4.38–4.31 (m, 1H), 4.22 (d,

$J = 8.3$ Hz, 1H), 3.99–3.94 (m, 1H), 3.12 (d, $J = 12.0$ Hz, 1H), 3.05 (dd, $J = 11.1, 2.6$ Hz, 1H), 2.92 (d, $J = 6.8$ Hz, 2H), 2.57–2.41 (m, 4H), 2.40 (s, 3H), 2.24 (ddd, $J = 13.9, 11.2, 2.7$ Hz, 1H), 2.13 (ddd, $J = 14.4, 11.9, 2.6$ Hz, 1H), 2.00 (ddd, $J = 13.8, 9.4, 4.2$ Hz, 1H), 1.91–1.53 (m, 9H), 1.45–1.36 (m, 1H), 1.24–1.18 (m, 1H), 1.18–1.12 (m, 6H), 0.99 (d, $J = 6.7$ Hz, 3H), 0.95 (d, $J = 7.0$ Hz, 6H), 0.92 (d, $J = 7.4$ Hz, 3H); ^{13}C NMR (151 MHz, MeOD with NH_4OAc) δ 182.3, 177.8, 175.0, 173.7, 173.4, 171.9, 162.7, 151.0, 139.7, 130.5, 129.3, 127.3, 124.8, 71.2, 69.7, 59.6, 56.3, 52.0, 51.1, 44.1, 42.5, 41.8, 39.2, 38.0, 37.6, 33.8, 31.1, 28.3, 25.9, 25.4, 23.5, 22.5, 19.5, 19.0, 18.6, 16.3, 11.1, 9.3; HRMS calcd for $\text{C}_{38}\text{H}_{58}\text{N}_5\text{O}_7\text{S}^+$ [$\text{M} + \text{H}^+$] 728.4057, found 728.4076.

Tetrapeptide 150. After subjecting **12** (4.8 mg, 7.1 μmol), isovaleric acid (7.9 μL , 71 μmol), DMAP (0.9 mg, 7 μmol) and DCC (7.4 mg, 36 μmol) to the standard procedure for tubulysin V (**12**) acylation using DCC activated acids, TLC analysis showed complete consumption of starting material after 24 h and low resolution MS showed exclusive production of the title compound. HPLC purification and structural characterization of **150** are currently underway. Low resolution MS calcd for $\text{C}_{40}\text{H}_{62}\text{N}_5\text{O}_7\text{S}^+$ [$\text{M} + \text{H}^+$] 756.44, found 756.52.

Tetrapeptide 151. Modification to the standard procedure for tubulysin V (**12**) acylation using DCC activated acids was performed with **12** (4.7 mg, 7.0 μmol), pivalic acid (7.1 mg, 70 μmol), DMAP (0.85 mg, 7 μmol) and DCC (7.2 mg, 35 μmol):

After 24 h, no reaction progress had occurred by low resolution MS, so the reaction was heated to 45 °C. After an additional 24 h, no reaction progress had occurred by low resolution MS. To a separate container with a solution of pivalic acid (36 mg, 50 equiv) in CH_2Cl_2 (1.5 mL) at 0 °C was added DMAP (1 mg, 1 equiv) and DCC (36 mg, 25

equiv), resulting immediately in a white precipitate. After 15 min, to this mixture was added the heated **12** mixture. After an additional 30 h, no reaction progress had occurred by low resolution MS, so DMF (6 mL) was added to the reaction and the mixture was heated to 80 °C. After an additional 36 h, TLC analysis showed complete consumption of starting material and low resolution MS showed exclusive production of the title compound. HPLC purification and structural characterization of **151** are currently underway. Low resolution MS calcd for $C_{35}H_{52}N_5O_5S^+$ [M + H⁺] 654.37, found 654.

Tetrapeptide 152. Modification to the standard procedure for tubulysin V (**12**) acylation using DCC activated acids was performed with **12** (5.2 mg, 7.7 μmol), chloroacetic acid (7.3 mg, 77 μmol), DMAP (0.94 mg, 7.7 μmol) and DCC (7.9 mg, 39 μmol):

After 48 h, no reaction progress had occurred by TLC analysis. To a separate container with a solution of chloroacetic acid (37 mg, 50 equiv) in CH₂Cl₂ (3 mL) at 0 °C was added DMAP (1 mg, 1 equiv) and DCC (40 mg, 25 equiv), resulting in a white precipitate and effervescence to immediately form. After 15 min, to this mixture was added the **12** mixture. After an additional 30 h, TLC analysis showed complete consumption of starting material and low resolution MS showed exclusive production of the title compound. HPLC purification and structural characterization of **152** are currently underway. Low resolution MS calcd for $C_{37}H_{55}ClN_5O_7S^+$ [M + H⁺] 748.35, found 748.42.

Tetrapeptides 153 and 154. Modification to the standard procedure for tubulysin V (**12**) acylation using DCC activated acids was performed with **12** (6.5 mg, 9.7 μmol), acrylic acid (6.6 μL, 97 μmol), DMAP (1.2 mg, 9.7 μmol) and DCC (9.9 mg, 48 μmol):

After 72 h, partial reaction progress had occurred by low resolution MS, which showed

peaks corresponding to the starting material and **153** exclusively. To a separate flask with a solution of acrylic acid (6.6 μL , 10 equiv) in CH_2Cl_2 (1.5 mL) at 0 $^\circ\text{C}$ was added DMAP (1 mg, 1 equiv) and DCC (9.9 mg, 5 equiv), and after 15 min, to this solution was added the **12** mixture. After an additional 36 h, TLC analysis showed complete consumption of starting material and low resolution MS showed production of the title compounds. HPLC purification and structural characterization of **153** and **154** are currently underway. Low resolution MS calcd for $\text{C}_{38}\text{H}_{56}\text{N}_5\text{O}_7\text{S}^+$ [**153** + H^+] 726.39, found 726.47; low resolution MS calcd for $\text{C}_{38}\text{H}_{54}\text{N}_5\text{O}_6\text{S}^+$ [**154** + H^+] 708.38, found 708.

Chapter 5:

Overview of Current and Future Studies Associated with Synthesis and Biochemical Evaluation of Stabilized Tubulysin Analogs

Review and Discussion of the Synthetic Efforts Associated with ^NTubulysin Analogs

Tubulysins are antimitotic natural products with potent antiproliferative activity against multidrug-resistant cancer cells, with the most cytotoxic members containing a crucial acetate. Application of these molecules as treatments of MDR cancers is important since the current standards of therapy are ineffective in these cases, but the hydrolytic instability of the important acetate may diminish the effectiveness of this pharmacophore. The study presented here aimed to synthesize and evaluate stabilized tubulysin analogs which mimic the tubuvaline acetate, and in doing so supplement the known SAR at this position. Nitrogen based functional group replacements of the tubuvaline oxygen received the most attention, where syntheses of the two analogs which are directly comparable to tubulysin V and U (**12** and **11**) by heteroatom exchange were most crucial to fairly judge the effect of this replacement (**36** and **37**, Figure 43). Synthesis of the other nitrogen based functional groups presented here will provide for a more robust SAR according to changes in polarity, hydrogen bonding, space filling, and aromaticity within the tubulin binding pocket, as evaluated by changes in cytotoxicity.

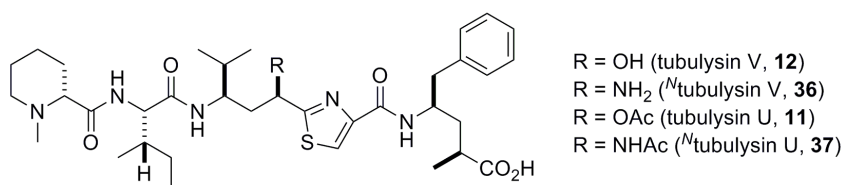


Figure 43: Comparison of heteroatom exchange in tubulysins/^Ntubulysins V and U.

With the other three amino acid residues (**38**, **39**, and **41**, Figure 8) of **36** available commercially or through established syntheses, initially synthetic work focused on regio- and diastereoselective nitrogen installation at ^Ntubuvaline (**40**). According to an established route to a crucial α -keto thiazole **42**, the syntheses of thiazole **45** and Weinreb amide **44** starting materials were reevaluated. Operational improvements to the synthesis of **45** were made through fewer instances of chromatography, reaction scalability, and replacement of a DIBAL-H reduction with *in situ* generated LiBH₄ (Figure 11). A low yielding bis-Boc protection of **44** (Raghavan *et al.* 2008) was avoided by first deprotonating **44** with a sacrificial base during the thiazole coupling, which led to formation of the ketone **42** with a nearly stoichiometric amount of the lithiated thiazole (Figure 44). Following a stereoselective reduction of **44**, a Mitsunobu reaction or hydroxyl group activation/nucleophilic displacement was envisioned to properly install the key nitrogen; unfortunately, intramolecular cyclization (**57**) precluded product formation and forced investigation into alternative methods.

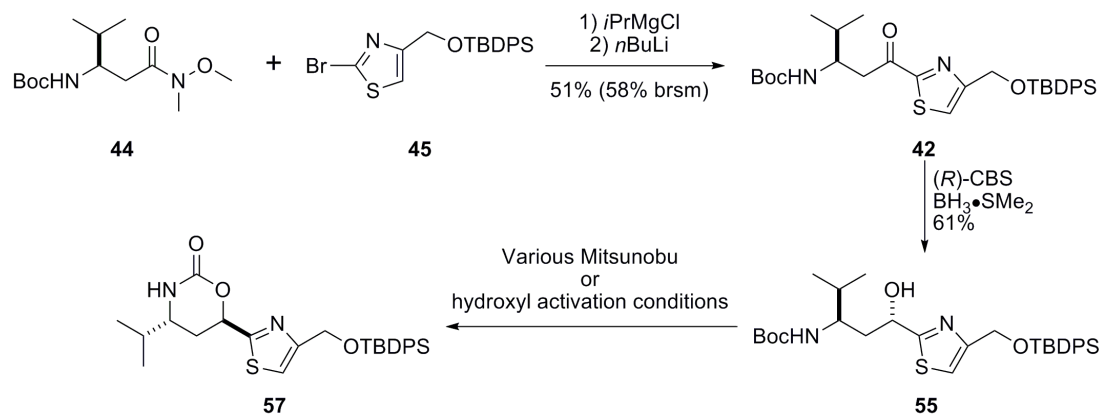


Figure 44: First generation synthesis to N_t tubuvaline.

Since the new goal towards synthesis of the N_t tubuvaline fragment was to avoid the intramolecular cyclization seen with α -thiazole activation of **55**, nitrogen pre-installation was attempted by alternating to a nitrile electrophile (Figure 45). Synthesis of the Boc protected nitrile **58** led to the same cyclization seen under Mitsunobu conditions, so phthalimide protection was used instead to promote reversible cyclization. Undesired side product formation occurred when a reversible phthalimide cyclized intermediate was trapped in the presence of nucleophilic cyanide (**69**, Figure 45), leading to the conclusion that cyclization was inevitable when using oxygen containing protecting groups. As predicted, dibenzyl protection led cleanly to the desired nitrile **72**. Arylation of **72** and *in situ* reduction of the resulting imine led to regioselective nitrogen installation, but low diastereoselectivity, poor separation of the product mixture **74**, the necessity for early N -functionalization made this route unnecessarily problematic.

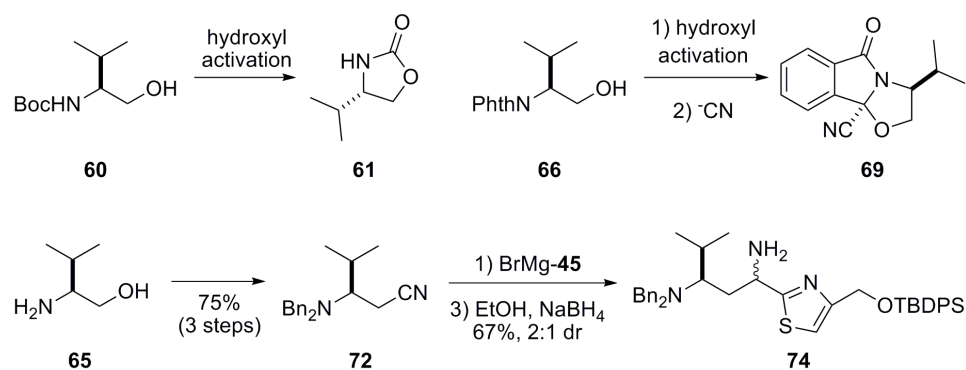


Figure 45: Second generation synthesis to *N*₄tubuvaine.

With regioselective nitrogen installation established, the next focus was on controlling the stereoselectivity of this transformation without the previously seen cyclization. Since the absence of a carbonyl at the benzyl protecting group negates the possibility for intramolecular cyclization as demonstrated by the synthesis of nitrile **72**, a Mitsunobu reaction following the diastereoselective reduction of ketone **79** became the premier strategy. Under the nitrile arylation conditions, hydrolysis of the *in situ* imine was attempted but led exclusively to retro-Michael products **80** and Bn₂NH, presumably through the desired product **79**. This paradigm was reproducible for both arylation of the Weinreb amide **81** and synthesis of aldehyde **82** as well. These experiments made clear that dibenzyl protection is susceptible to elimination when positioned β to a carbonyl, and is therefore not usable for diastereoselective production of **40**.

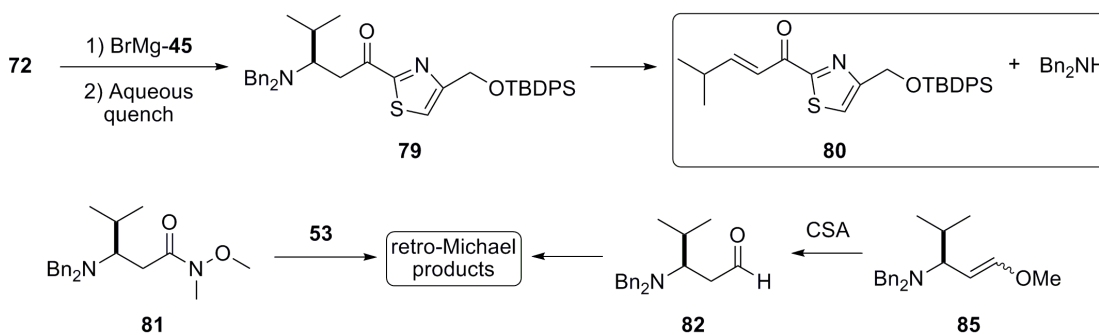


Figure 46: Third generation synthesis to N_4 tubuvaline.

In spite of the consistent cyclization problems observed under the first generation synthesis to **40**, extensive laboratory research and literature survey eventually led to a successful Mitsunobu reaction using phthalimide as the nitrogen source, which simultaneously protects the amine for later deprotection (Figure 24). After extensive survey of various classic conditions to perform silyl ether deprotections and oxidations of allylic alcohols, TBDPS deprotection using TBAF and MnO_2 oxidation of the resulting alcohol complimented the previously reported finishing steps to improve overall yield of the N_4 tubuvaline fragment **89** (Figure 24).

When established conditions for coupling of the N_4 tubulysin amino acid residues caused *N*-acylurea side product formation that poisoned the desired dipeptide product, simple mixed anhydride activation of N_4 tubuvaline fragment **89** was instead employed (Figure 25). This modification improved reaction yield and purification by avoiding side product formation. Subsequent peptide couplings using the HATU coupling reagent gave the bis-protected tetrapeptide **98** (Figure 27) as a common intermediate to the N_4 tubulysin analogs.

Following smooth phthalimide deprotection of **98** to **100** (Figure 28), the benzyl ester deprotection of **100** caused full material degradation under the basic hydrolysis

conditions which had previously supplied **12** (Balasubramanian *et al.* 2009). Alternatively, by removing the **98** benzyl ester first, phthalimide base sensitivity became a factor by leading to partial hydrolysis of the heterocycle (**101**). Subjecting this intermediate to comparable conditions used successfully to generate **100** resulted in complete molecule degradation. Observing the lowered stability of **36** and its precursors under conditions which were amenable to naturally isolated tubulysin analogs, such as tubulysin V (**12**), weakens the hypothesis that nitrogen containing ^Ntubulysin analogs will serve as stabilized alternatives to oxygen containing tubulysins.

Since the standard conditions for benzyl ester deprotection of the above intermediates resulted in material destruction and milder alternative methods for this transformation were non-productive, a compromise using intermediates insensitive to basic hydrolysis became necessary (Figure 47). By partially opening the phthalimide ring of **98** with addition of pyrrolidine, a reversal of reactivity occurs where this new functional group remains stable under basic conditions. Subsequent removal of the benzyl ester runs smoothly under buffered LiOH hydrolysis, resulting in minimal hydrolysis of pyrrolidine. Reclosure of the phthalimide ring is possible under heated acidic conditions to furnish **102**. Successful phthalimide ring opening and closing of **98** required harsher versions of the transformations previously reported in other phthalimide based molecules (Aistleford and Weigel 1991), which provides evidence of significant steric bulk at the amino position of **36**. As predicted, the closed phthalimide ring was cleaved under less harsh conditions, where minimal heating in methanolic hydrazine produced the target molecule **36** with minimal material degradation. Along with providing a route to **36**, this route supplies ^Ntubulysin analogs with benzamide-based functional groups which will provide insight into the effect of conformationally free

aromaticity at this position.

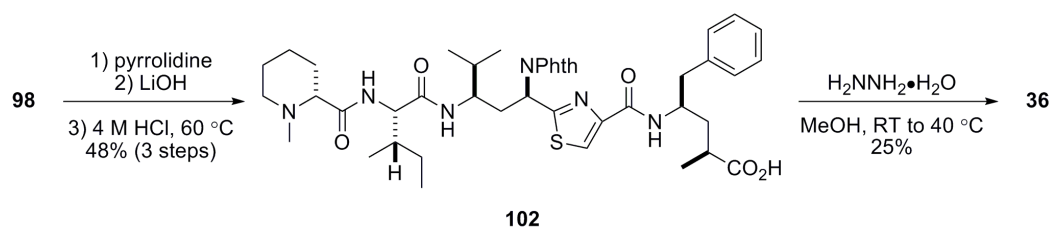


Figure 47: Synthesis of amine **36** under modified deprotection conditions.

In contrast to the *O*-acylated tubulysins and the amino compounds described above, *N*-acylated tubulysin intermediates are resilient to the basic hydrolysis conditions used to cleave the benzyl ester, which supported use of a common late-stage intermediate **100**. Common acylating reagents provided acetamide and carbamate based modifications to the free amine of **100**, while synthetically derived CDI-based reagents provided urea functional groups. Slower reactivity was seen at higher temperatures when the precursor to the dimethyl urea analog **113** was synthesized, indicating the effect that steric hindrance has at this position.

Following acylation, these intermediates were subjected to hydrolysis, providing compounds which will support a diverse functional group SAR at this position. This non-destructive benzyl deprotection of the *N*-acylated compounds constitutes a dichotomy with regards to the stability of *N*-tubulysin intermediates. Whereas **12** is stable under basic hydrolysis, **36** is unstable, resulting in degradation (Figure 28). On the other hand, the acylated analogs of **36** are stable under these same conditions, whereas the acetate of **11** is cleaved. This dependence on stability is important, since it confirms the hypothesis that *N*-acylated analogs of naturally isolated tubulysins are more stable, but with the caveat that the free amine is more prone to degradation.

The synthetic work presented here has provided compounds **36** and **37** for direct comparison with tubulysin analogs V and U (**12** and **11**), where any changes in biological activity can be attributed to the singular modification of the tubuvaline heteroatom. Limitations of steric bulk at the tubulysin-tubulin binding site will be tested to its extremes with the pivalamide **109**. Replacement of the acetamide with its trifluoromethyl analog **110** will evaluate the use of this bioisostere. Although similar in their steric bulk, the methyl carbamate **111** and ureas **112** and **113** will evaluate the nuances of H-bonding and polarity at this position in the binding pocket. Finally, the benzamides **101**, **102**, and **108** will test an element of conformationally-free aromaticity that has not been present before in tubulysin analogs. All put together, the biological activity of these 10 ^Ntubulysin analogs will support a robust initial SAR of tubulysins with nitrogen-based functional groups on ^Ntubuvaline.

Review and Discussion of the Synthetic Efforts Associated with Tubulysin Analogs

In conjunction with the use of ^Ntubulysin analogs to survey the effect that heteroatom exchange has at the crucial acetate, oxygen containing analogs also serve an important role in gauging the role of the acetate carbonyl and methyl groups. With this information, a full understanding of the acetate pharmacophore will be available to define the SAR at this position and influence the types and limitations to future modifications. Previous work showing retention of potency with replacement of the acetate with a cyclized methylene (**27**, Figure 27, Shibue *et al.* 2010) gives evidence that the carbonyl may not be essential for bioactivity.

Generating the materials necessary for oxygen containing analogs of **11** and **12** prompted reevaluation of the established synthetic methods towards these molecules in light of the success producing the precursors to **36**. These modifications built upon the

previously established methods by more than doubling the overall yield in the final three functional group transformations to the tubuvaline fragment **125** (Figure 35).

Unexpected *N*-acylurea side product formation during the dipeptide coupling was avoided under the same protocol applied to ^Ntubuvaline coupling (Figure 36).

Alkylation of late stage intermediates to **12** into simple ether and *N,O*-acetal analogs was not straight forward and required addendums to expected reactivity. The singular successful alkylation of **12** was by installation of a methoxymethyl ether (**142**, Figure 40); the activity of this compounds will be a commentary on the effect that polarity and hydrogen bonding have on tubulin binding at this position. Despite the well established methods to selectively *O*-alkylate complex natural products, direct methylation of late stage tubulysin analogs were not productive, so a less direct route was necessary. A strategy using an azido protected isoleucine-tubuvaline dipeptide gave regioselective methylation under non-specialized conditions as confirmed by analysis of the ¹H NMR spectra of **139** and **140** (Figure 38). Selective methylation gives additional evidence of the highly steric environment at the tubuvaline amide, while preferential reactivity at the α -thiazole position is in spite of the observed steric hindrance in the ^Ntubulysin intermediates. Established conditions to generate the full methyl ether tetrapeptide should be performed to finish this molecule.

Marked differences in antiproliferative activity between **11** and **12** exemplifies the importance of an acetate at the α -thiazole position, so scanning different hydroxyl group acylations was of interest to further understand the effect of this modification. By repeating the reported procedure to acetylate **12** in preparation for generalized acylation, lactamization of the tubuphenylalanine residue (**143**, Figure 41) occurred with more than half of the product when the reaction was performed at room temperature. Lacking a

method to preferentially open the lactam without disturbing the newly formed ester, methodology work was undertaken and found that lowering reaction temperature eliminated intramolecular cyclization while still providing acylation. During synthesis of other ester derivatives under the same protocol, non-hydrolyzed anhydride co-extracted with the product mixture caused partial intramolecular cyclization after reaction quench as predicted by the observation of intramolecular cyclization at room temperature. Conditions for destruction of the excess anhydride during aqueous quench will supplement the general utility of this protocol.

Analogs of **11** with halogenation at the key acetate are predicted to test the viability of these modifications as bioisosteres and the effect that increased acylation of tubulin has on bioactivity. As described above for the ^Ntubulysin analogs, carbonate and carbamate replacement of the acetate will survey polarity and hydrogen bonding at the acetate binding pocket within tubulin-tubulysin active site. All efforts to generate these molecules under the established conditions and modifications to these conditions to accommodate the observed reactivity were unsuccessful (Figure 48). Considering the successful modification of the nitrogen containing tubulysin intermediates with these same acyl groups, the lack of nucleophilicity typically seen with alcohols when compared to amines clearly runs true in tubulysin synthesis.

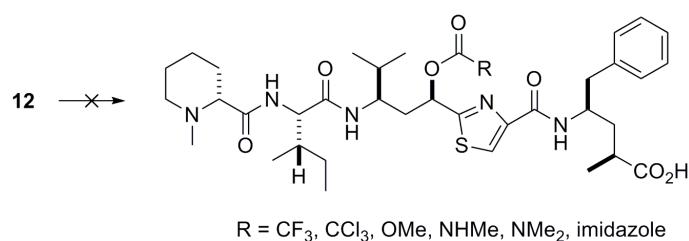


Figure 48: Failed syntheses of acylated analogs of ester **11**.

The issues described above led to development of an alternative method for acylation of **12**. By DCC pre-activation of acids with simple alkyl chains prior to their reaction with **12**, full conversion to the desired products was possible (Table 6). This more operationally involved process offers the advantage of a lowered incidence of side product formation under less strict adherence to variable reaction conditions such as reaction temperature and aqueous quench. Acylation of **12** by DCC pre-activation of sterically hindered alkyl groups or non-alkyl functional groups required modification to the standard paradigm, where excess acid was added following a quick pre-activation with DCC. Pivalic acid was non-reactive with the hydroxyl group of **12**, and instead underwent intramolecular cyclization to give the lactam **151** upon heating. Chloroacetic acid was exclusively productive for the desired product when no productivity had occurred following the standard procedure, while acrylic acid was slowly productive for product before excess reagents were added but underwent cyclization at room temperature following their addition. The significantly different outcome from these three reactions, in which nearly the same modification to the standard procedure was employed, suggests that DCC activation and reactivity of the tubuphenylalanine carboxylate is variable based upon subtle changes in reaction environment.

Comparing the reactions presented above pertaining to manipulation of the α -

thiazole position of tubuvaline residues, reactivity is clearly dependent on steric interactions. In cases of *O*-acylation, the reactions run well until a hindered substrate is to be added, wherein no acylation occurs (see DCC pre-activated pivalic acid). With consideration to *N*-acylation, the increased nucleophilicity of the amine outweighs any steric debts that must be paid with bulkier substrates. Thus, there is a clear point when the steric debt of the added substrate outweighs the nucleophilicity of the heteroatom at this position. Alternatively, when phthalimide based functional groups are appended to ^Ntubuvaline, the steric environment at this position requires harsher reaction conditions than usually necessary for these types of transformations. From these observations, a general paradigm can be established with consideration to the effect that sterics play on reactivity at the α -thiazole position: Manipulation of amino intermediates is controlled by the sterics of parent molecule, whereas the alcohol intermediates are controlled by the sterics of the substrate to be added.

Future Studies, Project Directions

The future goals for this project will be based on the outcome of ongoing biochemical evaluation. The synthetic endeavors presented here are unique in being the first to replace the hydroxyl group of the tubuvaline residue with a nitrogen, and the impact of this change on antiproliferative activity is still in question. A fair hypothesis predicts that these compounds will retain at least partial activity since heteroatom exchange is a staple of medicinal chemistry and has been used widely in order to increase potency and change pharmacokinetic properties. By comparing the relative activity of these compounds with tubulysins with established cytotoxicity, a new tool will be available for the understanding of tubulin polymerization inhibition by tubulysins and general SAR at the α -thiazole position. New work is expected to build upon this SAR for

a greater understanding of the important interactions at this position and lead to identification of an analog suitable for *in vivo* studies.

Biochemical evaluation of these tubulysin analogs will be performed by our collaborator at the NIH, Dr. Dan L. Sackett. Antiproliferative activity will be determined initially in drug-sensitive 1A9 human ovarian carcinoma cells and MCF-7 human breast cancer cells, both of which have drug-sensitive and drug-resistant sublines, and have been used by our lab as standard antiproliferative assays. Tubulin polymerization inhibition will be performed by observing the *in vitro* inhibition of purified tubulin polymerization. A hemisaterlin analog, HTI-286, is used as a positive control in these assays since it has close structural homology to tubulysins and also binds to the peptide site of the *Vinca* alkaloid domain.

Compounds with promising antiproliferative activity in drug-sensitive 1A9 and MCF-7 cells, generally in the 0.1–100 nM (IC₅₀ value) range, will be tested against additional drug-resistant cell lines. Resistance in MCF-7/Tax400 cells is a result of P-glycoprotein (P-gp) over expression (Giannakakou *et al.* 1997), whereas additional 1A9 sublines with β -tubulin mutations confer drug resistance; activity against these cells will be examined with the requisitely potent compounds. Preliminary data from the Fecik and Sackett labs has established that tubulysin analogs retain antiproliferative activity against cells with both mechanisms of drug resistance (unpublished results). Results from these secondary assays will determine if select analogs warrant further biochemical evaluation.

Upon confirmation of the affinity probes **152** and **153** antiproliferative activity in the primary assays described above, covalent modification of β -tubulin by these agents

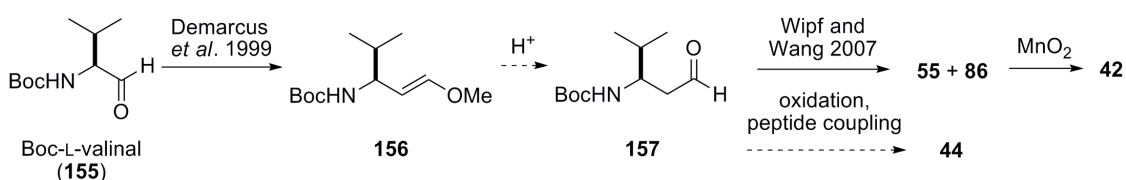
will need to be established. Unlike non-covalent inhibitors which establish a perpetual equilibrium between bound and unbound states, covalent inhibition is permanent and time-dependent. Experiments which measure compound activity as a function of time will therefore determine if covalent inhibition is occurring. The permanence of bound substrate will also preclude displacement by other substrates which bind to this site. Hence, use of a radio-labeled substrate established to bind in the same site of tubulysins (such as HTI-286) will not displace any bound affinity label and will show the same signal regardless of increased substrate concentration.

Once covalent inhibition is confirmed, collaboration with an X-ray crystallographer will then become necessary to implement the probes for their intended purpose. Several groups are involved in this sort of work within the University of Minnesota; however, previous studies with other tubulin binding drugs such as taxol (Nogales *et al.* 1998) and vinblastine (Gigant *et al.* 2005) have shown the difficulty in the crystallization of tubulin. With that in mind, principle investigators with a history of successful tubulin crystallization may be the best choice.

Several critical analogs that have yet to be developed will be accessible once a larger scale of the material towards **36** is accessible. Arguably the most crucial reaction of this synthetic sequence is the Mitsunobu reaction which installs the key nitrogen modification. While the 50% yield presented above does supply a means to generate final molecules, it also significantly reduces the already limited diazomethane-based material available due to yield loss. Hence, improvements to this transformation, or greater access to its starting materials, would further support final molecule generation. Of the several methods used for one carbon homologations, the enol ether method (Figure 49) is potentially the most scalable route since it is not susceptible to the safety

concerns seen with use of diazomethane. Following hydrolysis of enol ether **156** (Demarcus *et al.* 1999), an established non-diastereoselective arylation of **157** (Wipf and Wang 2007) supplies the desired alcohol **55**, with recovery of **86** by MnO₂ oxidation to the α-keto thiazole **42** (Figure 23). Alternatively, the β-valinal could be oxidized and subject to peptide coupling to form the Weinreb amide **44**, which would then be subjected to the established transformations.

Enol ether approach:



Danheiser's method: Based on Danheiser *et al.* 1998

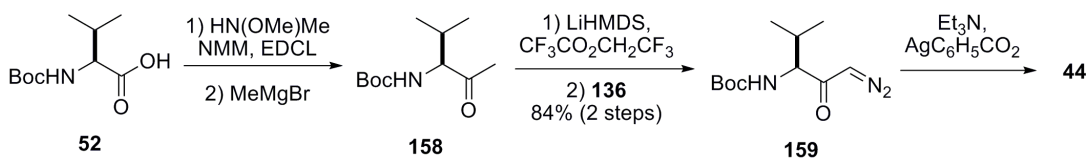


Figure 49: Potential methods for larger scale generation of tubuvaline intermediates.

Danheiser has developed a diazotransfer reaction to generate diazoketones, such as **159** (Danheiser *et al.* 1998). Preliminary work has generated **158** by trivial reactions with Boc-L-valine (**52**) (Figure 49). Modifications to the reported diazotransfer reaction starts with deprotonating the carbamate and methyl ketone of **158**, followed by diazotransfer using the reagent described above (Figure 38). The critical diazotransfer was done in high yield (84% over 2 steps) and constitutes a safer alternative compared to diazomethane. Established Wolff rearrangement of **159** then supplies the Weinreb amide **44** for use in generation of the ^Ntubuvaline fragment **89**.

Another challenge in synthesis of **36** has been the full deprotection of tetrapeptide **98**, where sequential deprotection resulted in degradation (Figure 28). After several alternative routes failed, a strategy in which the phthalidamide was masked to allow for benzyl deprotection successfully led to ^Mtubulysin V precursor **102**. A close examination of the pertinent literature (Peltier *et. al.* 2006) shows that **102** could be produced by instead installing fully deprotected tubuphenylalanine **41** on to the phthalimide protected tripeptide **160** (Figure 50), itself available through standard couplings. This route would save step economy and negate the troubles seen under hydrolysis of the benzyl ester.

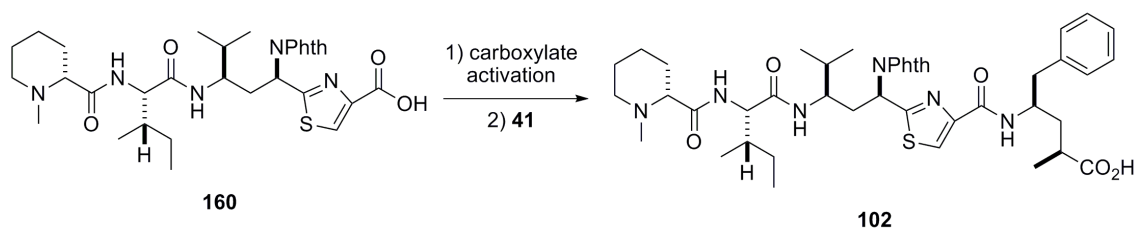


Figure 50: A potential alternative method to generate tetrapeptide **102**.

Upon the generation of additional **36**, important analogs to test the significance of substitution at this position will be the *N,N*-dimethyl, *N,N*-diethyl, and *N*-formylated analogs **161–163** (Figure 51). Amines **161** and **162** will probe the importance of the carbonyl and chain length as it pertains to *N*-acylation, while the formyl group of **163** will retain the carbonyl and lose the hydrocarbon component. These modifications most closely resemble the acetamide of **37** while still removing individual components to test their significance in the pharmacophore, and are thus important pieces to a full SAR.

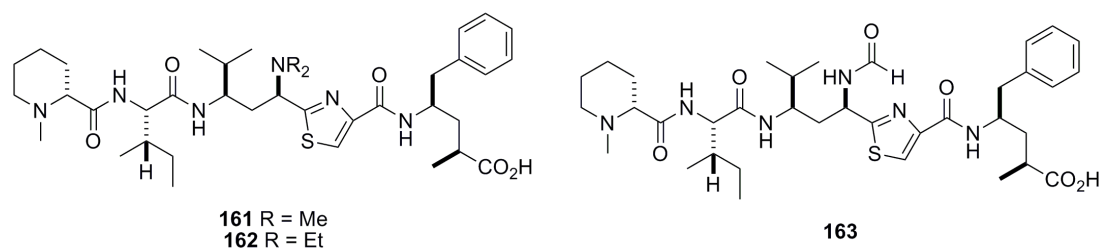


Figure 51: Important ^Ntubulysin analogs for complete SAR analysis.

In conclusion, several nitrogen and oxygen containing tubulysin analogs have been synthesized as stabilized and cytotoxic alternatives to the naturally isolated tubulysins. The critical ^Ntubuvaline residue is generated by reaction conditions not susceptible to the frequently seen intramolecular cyclization in tubuvaline intermediates. Following peptide couplings, a common tetrapeptide intermediate led to the target molecules ^Ntubulysin V, ^Ntubulysin U, and other *N*-acylated ^Ntubulysin analogs. Additionally, modification to an established method and a new DCC pre-activated method offer improvements in the acylation of tubulysin V. Several tubulysin U analogs with various alkyl groups at the tubuvaline acetate have been made. The usefulness of these compounds as cytotoxic agents will be determined by biochemical evaluation, which will lead to a better understanding of the SAR at the α -thiazole position.

References

- Astleford, B.; Weigel, L. O. Scope of Phthalamido Chemistry I. Extension of Utility by Conversion to the OPCB Protecting Group. *Tetrahedron Lett.* **1991**, *32*, 3301–3304.
- Balasubramanian, R. Part I. Design and synthesis of CYP7B1 inhibitors for the chemoprevention of prostate cancer. Part II. Synthesis and structure-activity relationships of tubulysins. Ph.D. Dissertation, University of Minnesota, Minneapolis, MN, **2008**.
- Balasubramanian, R.; Raghavan, B.; Begaye, A.; Sackett, D. L.; Fecik, R. Total Synthesis and Biological Evaluation of Tubulysin U, Tubulysin V, and Their Analogues. *J. Med. Chem.* **2009**, *52*, 238–240.
- Balasubramanian, R.; Raghavan, B.; Steele, J. C.; Sackett, D. L.; Fecik, R. A. Tubulysin Analogs Incorporating Desmethyl and Dimethyl Tubophenylalanine Derivatives. *Bioorg. Med. Chem. Lett.* **2008**, *18*, 2996–2999.
- Brussee, J.; Dofferhoff, F.; Kruse, C. G.; van der Gen, A. Synthesis of Optically Active Ethanolamines. *Tetrahedron* **1990**, *46*, 1653–1658.
- Burke, A. J.; Davies, S. G.; Garner, A. C.; McCarthy, T. D.; Roberts, P. M.; Smith, A. D.; Rodriguez-Solla, H.; Vickers, R. J. Asymmetric Synthesis and Applications of β -Amino Weinreb Amides: Asymmetric Synthesis of (S)-Coniine. *Org. Biomol. Chem.* **2004**, *2*, 1387–1394.
- Burkhart, J. L.; Kazmaier, U. A Straightforward Click-Approach Towards Pretubulysin-Analogues. *RSC Advances* **2012**, *2*, 3785–3790.

- Burkhart, J. L.; Müller, R.; Kazmaier, U. Synthesis and Evaluation of Simplified Pretubulysin Analogues. *Eur. J. Org. Chem.* **2011**, 3050–3059.
- Caputo, R.; Cassano, E.; Longobardo, L.; Palumbo, G. Synthesis of Enantiopure *N*- and *C*-Protected Homo- β -Amino Acids by Direct Homologation of α -Amino Acids. *Tetrahedron* **1995**, *51*, 12337–12350.
- Cavelier, F.; Enjalbal, C. Studies of Selective Boc Removal in the Presence of Silyl Ethers. *Tetrahedron Lett.* **1996**, *37*, 5131–5134.
- Chai, Y.; Pistorius, D.; Ullrich, A.; Weissman, K. J.; Kazmaier, U.; Müller, R. Discovery of 23 Natural Tubulysins from *Angiococcus disciformis* An d48 and *Cystobacter* SBCb004. *Chem. Biol.* **2010**, *17*, 296–309.
- Chai, Y.; Shan, S.; Weissman, K. J.; Hu, S.; Zhang Y., Müller, R. Heterologous Expression and Genetic Engineering of the Tubulysin Biosynthetic Gene Cluster Using Red/ET Recombineering and Inactivation Mutagenesis. *Chem. Biol.* **2012**, *19*, 361–371.
- Cooke, J. W. B.; Davies, S. G.; Naylor, A. Stereoselective Synthesis of (3*R*,4*S*)-Statine Utilising the Iron Acetyl Complex $[(\eta^5\text{-C}_5\text{H}_5)\text{Fe}(\text{CO})(\text{PPh}_3)\text{COMe}]$ as a Chiral Acetate Enolate Equivalent. *Tetrahedron* **1993**, *49*, 7955–7966.
- Dale, J. A.; Mosher, H. S. Nuclear Magnetic Resonance Enantiomer Regents. Configurational Correlations via Nuclear Magnetic Resonance Chemical Shifts of Diastereomeric Mandelate, *O*-Methylmandelate, and α -Methoxy- α -Trifluoromethylphenylacetate (MTPA) Esters. *J. Am. Chem. Soc.* **1973**, *95*, 512–519.

- Danheiser, R. L.; Miller, R. F.; Brisbois, R. G. Detrifuoroacetylative Diazo Group Transfer: (E)-1-Diazo-4-phenyl-3-buten-2-one. *Org. Synth.* **1996**, *73*, 134–143.
- de Boer, Th. J.; Backer, H. J. Diazomethane. *Org. Synth.* **1956**, *36*, 16–19.
- Demarcus, M.; Filigheddu, S. N.; Mann, A.; Taddei, M. Stereoselective Addition of Phenyl Selenyl Chloride to Methoxy Alkenes Derived from *N*-Protected Chiral α -Amino Acids. *Tetrahedron Lett.* **1999**, *40*, 4417–4420.
- DeTar, D. F. Silverstein, R. Reactions of Carbodiimides. I. The Mechanisms of the Reactions of Acetic Acid with Dicyclohexylcarbodiimide. *J. Am. Chem. Soc.* **1966**, *88*, 1013–1019.
- Dondoni, A.; Marra, A.; Merino, P. Installation of the Pyruvate Unit in Glycidic Aldehydes via a Wittig Olefination-Michael Addition Sequence Utilizing a Thiazole-Armed Carbonyl Ylide. A New Stereoselective Route to 3-Deoxy-2-Ulosonic Acids and the Total Synthesis of DAH, KDN, and 4-epi-KDN. *J. Am. Chem. Soc.* **1994**, *116*, 3324–3336.
- Evans, D. A.; Ratz, A. M.; Huff, B. E.; Sheppard, G. S. Mild Alcohol Methylation Procedure for the Synthesis of Polyoxygenated Natural Products. Applications to the Synthesis of Ionomycin A. *Tetrahedron Lett.* **1994**, *35*, 7171–7172.
- Finch, N.; Fitt, J. J.; Hsu, I. H. S. Total Synthesis of *dl*-9-Deoxyprostaglandin E₁. *J. Org. Chem.* **1975**, *40*, 206–215.
- Frigerio, M.; Santagostino, M.; Sputore, S. A User-Friendly Entry to 2-Iodoxybenzoic Acid (IBX). *J. Org. Chem.* **1999**, *64*, 4537–4538.

- Giannakakou, P.; Sackett, D. L.; Kang, Y.-K.; Zhan, Z.; Buters, J. T. M.; Fojo, T.; Poruchynsky, M. S. Paclitaxel-resistant Human Ovarian Cancer Cells Have Mutant β -Tubulins That Exhibit Impaired Paclitaxel-driven Polymerization. *J. Biol. Chem.* **1997**, *272*, 17118–17125.
- Gigant, B.; Wang, W.; Ravelli, R. B. G.; Roussi, F.; Steinmetz, M. O.; Curmi, P. A.; Sobel, A.; Knossow, M. *Nature* **2005**, *435*, 519–522.
- Goddard-Borger, E. D.; Stick, R. V. An Efficient, Inexpensive, and Shelf-Stable Diazotransfer Reagent: Imidazole-1-sulfonyl Azide Hydrochloride. *Org. Lett.* **2007**, *9*, 3797–3800.
- Goddard-Borger, E. D.; Stick, R. V. An Efficient, Inexpensive, and Shelf-Stable Diazotransfer Reagent: Imidazole-1-sulfonyl Azide Hydrochloride. *Org. Lett.* **2011**, *13*, 2514–2514.
- Gmeimer, P. General Synthesis of Enantiomerically Pure β -Amino Acids. *Tetrahedron Lett.* **1990**, *31*, 5717–5720.
- Gray, D.; Concellón, C.; Gallagher, T. Kowalski Ester Homologation. Application to the Synthesis of β -Amino Esters. *J. Org. Chem.* **2004**, *69*, 4849–4851.
- Grzyb, J. A.; Shen, M.; Yoshina-Ishii, C.; Chi, W.; Brown, R. S.; Batey, R. A. Carbamoylimidazolium and Thiocarbamoylimidazolium Salts: Novel Reagents for the Synthesis of Ureas, Thioureas, Carbamates, Thiocarbamates and Amides. *Tetrahedron* **2005**, *61*, 7153–7175.

- Hemenway, J. N.; Jarho, P.; Henri, J. T.; Nair, S. K.; Vandervelde, D.; Georg, G. I.; Stella, V. J. Preparation and Physicochemical Characterization of a Novel Water-Soluble Prodrug of Carbamazepine. *J. Pharm. Sci.* **2010**, *99*, 1810–1825.
- Hodge R. P.; Slnha, N. D. Simplified Synthesis of 2'-O-Alkyl Ribopyrimidines. *Tetrahedron Lett.* **1995**, *36*, 2933–2936.
- Höfle, G.; Glaser, N.; Leibold, T.; Karama, U.; Sasse F.; Steinmetz, H. Semisynthesis and Degradation of the Tubulin Inhibitors Epothilone and Tubulysin. *Pure Appl. Chem.* **2003**, *75*, 167–178.
- Hu, D. X.; Grice, P.; Ley, S. V. Rotamers or Diastereomers? An Overlooked NMR Solution. *J. Org. Chem.* **2012**, *77*, 5198–5202.
- Ing, H. R.; Manske, R. H. F. A Modification of the Gabriel Synthesis of Amines. *J. Chem. Soc.* **1926**, 2348–2351.
- Iranpoor, N.; Firouzabadi, H.; Akhlaghinia, B.; Nowrouzi, N. A Novel and Highly Selective Conversion of Alcohols, Thiols, and Silyl ethers to Azides using the Triphenylphosphine/2,3-dichloro-5,6-dicyanobenzoquinone(DDQ)/*n*-Bu₄NN₃ System. *Tetrahedron Lett.* **2004**, *45*, 3291–3294.
- Jordan, M. A.; Wilson, L. Microtubules as a Target for Anticancer Drugs. *Nat. Rev. Cancer* **2004**, *4*, 253–265.
- Kaur, G.; Hollingshead, M.; Holbeck, S.; Schauer-Vukašinović, V.; Camalier, R. F.; Dömling, A.; Agarwal, S. Biological Evaluation of Tubulysin A: A Potential Anticancer and Antiangiogenic Natural Product. *Biochem. J.* **2006**, *396*, 235–242.

- Kelly, T. R.; Lang, F. Total Synthesis of Dimethyl Sulfomycinamate. *J. Org. Chem.* **1996**, *61*, 4623–4633.
- Khalil, M. W.; Sasse, F.; Lünsdorf, H.; Elnakady, Y. A.; Reichenbach, H. Mechanism of Action of Tubulysin, an Antimitotic Peptide from Myxobacteria. *ChemBioChem* **2006**, *7*, 678–683.
- Krimen, L. I. Acetic Formic Anhydride. *Org. Synth.* **1970**, *50*, 1–3.
- Kubicek, K.; Grimm, S. K.; Orts, J.; Sasse, F.; Carlomagno, T. The Tubulin-Bound Structure of the Antimitotic Drug Tubulysin. *Angew. Chem. Int. Ed.* **2010**, *49*, 4809–4812.
- Kukulja, S.; Lammert, S. R. Azetidinone Antibiotics. XIV. Removal of a Phthaloyl Protective Group from Acid and Base Sensitive Compounds. *J. Am. Chem. Soc.* **1975**, *97*, 5582–5583.
- Kularatne, S. A.; Venkatesh, C.; Santhapuram, H.-K. R.; Wang, K.; Vaitilingam, B.; Henne, W. A.; Low, P. S. Synthesis and Biological Analysis of Prostate-Specific Membrane Antigen-Targeted Anticancer Prodrugs. *J. Med. Chem.* **2010**, *53*, 7767–7777.
- Kumar, A.; Shah, B. A.; Singh, S.; Hamid, A.; Singh, S. K.; Sethi, V. K.; Saxena, A. K.; Singh, J.; Taneja, S. C. Acyl Derivatives of Boswellic Acids as Inhibitors of NF- κ B and STATs. *Bioorg. Med. Chem. Lett.* **2012**, *22*, 431–435.
- Leamon, C. P.; Reddy, J. A.; Vetzal, M.; Dorton, R.; Westrick, E.; Parker, N.; Wang, Y.; Vlahov, I. Folate Targeting Enables Durable and Specific Antitumor Responses

from a Therapeutically Null Tubulysin B Analogue. *Cancer Res.* **2008**, *68*, 9839–9844.

Liu, D.; Acharya, H. P.; Yu, M.; Wang, J.; Yeh, V. S. C.; Kang, S.; Chiruta, C.; Jachak, S. M.; Clive D. L. J. Total Synthesis of the Marine Alkaloid Halichlorine: Development and Use of a General Route to Chiral Piperidines. *J. Org. Chem.* **2009**, *74*, 7417–7428.

Liu, J.; Ikemoto, N.; Petrillo, D.; Armstrong, III, J. D. Improved Syntheses of α -BOC-Aminoketones from α -BOC-amino-Weinreb Amides using a Pre-deprotonation Protocol. *Tetrahedron Lett.* **2002**, *43*, 8223–8226.

Lopez, R.; Poupon, J.-C.; Prunet, J.; Férézou, J. P.; Ricard, L. Diastereocontrolled Synthesis of Highly Functionalized Spiroketal: Application to the Synthesis of a Precursor of the C-12-C-25 Fragment of Bafilomycin A₁. *Synthesis*, **2005**, *4*, 644–661.

Lundquist, IV, J. T.; Pelletier, J. C. Improved Solid-Phase Peptide Synthesis Method Utilizing α -Azide-Protected Amino Acids. *Org. Lett.* **2001**, *3*, 781–783.

McCormick, J. E.; McElhinney, R. S.; McMurry, T. B. H.; O'Brien, J. E. *N,N'*-Transphthaloylation in a Monoprotected Diamine. *Synthesis* **2006**, *6*, 983–988.

McKennon, M. J.; Meyers, A. I.; Drauz, K.; Schwarm, M. A Convenient Reduction of Amino Acids and Their Derivatives. *J. Org. Chem.* **1993**, *58*, 3568–3571.

Meldal, M.; Juliano, M. A.; Jansson, A. M. Azido Acids in a Novel Method of Solid-Phase Peptide Synthesis. *Tetrahedron Lett.* **1997**, *38*, 2531–2534.

- Merritt, E. A.; Bagley, M. C. Holzapfel–Meyers–Nicolaou Modification of the Hantzsch Thiazole Synthesis. *Synthesis* **2007**, *22*, 3535–3541.
- Métro, T.-X.; Appenzeller, J.; Pardo, D. G.; Cossy, J. Highly Enantioselective Synthesis of β -Amino Alcohols. *Org. Lett.* **2006**, *8*, 3509–3512.
- Nahm, S.; Weinreb, S. M. *N*-methoxy-*N*-methylamides as Effective Acylating Agents. *Tetrahedron Lett.* **1981**, *22*, 3815–3818.
- Neises N.; Steglich, W. Simple Method for the Esterification of Carboxylic Acids. *Angew. Chem. Int. Ed.* **1978**, *17*, 522–524.
- Neises N.; Steglich, W. Esterification of Carboxylic Acids with Dicyclohexylcarbodiimide/4-Dimethylaminopyridine: *tert*-Butyl Ethyl Fumarate. *Org Synth.* **1985**, *63*, 183–187.
- Nogales, E.; Wolf, S. G.; Downing, K. H. Structure of the $[[\alpha]][[\beta]]$ Tubulin Dimer by Electron Crystallography. *Nature* **1998**, *391*, 199–203.
- Padwa A.; Dent, W. *N*-benzyl-*N*-methoxymethyl-*N*-(trimethylsilyl)methylamine as an Azomethine Ylide Equivalent: 2,6-Dioxo-1-phenyl-4-benzyl-1,4-diazabicyclo[3.3.0]octane. *Org. Synth.* **1989**, *67*, 133–140.
- Pando, O.; Dörner, S.; Preusentanz, R.; Denkert, A.; Porzel, A.; Richter, W.; Wessjohann, L. A. First Total Synthesis of Tubulysin B. *Org. Lett.* **2009**, *11*, 5567–5569.
- Pando, O.; Stark, S.; Denkert, A.; Porzel, A.; Preusentanz, R.; Wessjohann, L. A. The Multiple Multicomponent Approach to Natural Product Mimics: Tubugis, *N*-

- Substituted Anticancer Peptides with Picomolar Activity. *J. Am. Chem. Soc.* **2011**, *133*, 7692–7695.
- Patterson, A. W.; Peltier, H. M.; Ellman, J. A. Expedient Synthesis of *N*-Methyl Tubulysin Analogues with High Cytotoxicity. *J. Org. Chem.* **2008**, *73*, 4362–4369.
- Patterson, A. W.; Peltier, H. M.; Sasse, F.; Ellman, J. A. Design, Synthesis, and Biological Properties of Highly Potent Tubulysin D Analogues. *Chem. Eur. J.* **2007**, *13*, 9534–9541.
- Peltier, H. M.; McMahon, J. P.; Patterson, A. W.; Ellman, J. A. The Total Synthesis of Tubulysin D. *J. Am. Chem. Soc.* **2006**, *128*, 16018–16019.
- Raghavan, B.; Balasubramanian, R.; Steele, J. C.; Sackett, D. L.; Fecik, R. A. Cytotoxic Simplified Tubulysin Analogues. *J. Med. Chem.* **2008**, *51*, 1530–1533.
- Reddy, J. A.; Dorton, R.; Dawson, A.; Vetzal, M.; Parker, N.; Nicoson, J. S.; Westrick, E.; Klein, P. J.; Wang, Y.; Vlahov, I. R.; Leamon, C. P. *In Vivo* Structural Activity and Optimization Studies of Folate-Tubulysin Conjugates. *Mol. Pharm.* **2009**, *6*, 1518–1525.
- Reetz, M. T.; Drewes, M. W.; Schwickardi, R. Preparation of Enantiomerically Pure α -*N,N*-Dibenzylamino Aldehydes: *S*-2-(*N,N*-Dibenzylamino)-3-Phenylpropanal. *Org. Synth.* **1999**, *76*, 110–122.
- Reymond, S.; Cossy, J. Synthesis of Migrastatin and its Macrolide Core. *Tetrahedron* **2007**, *63*, 5918–5929.

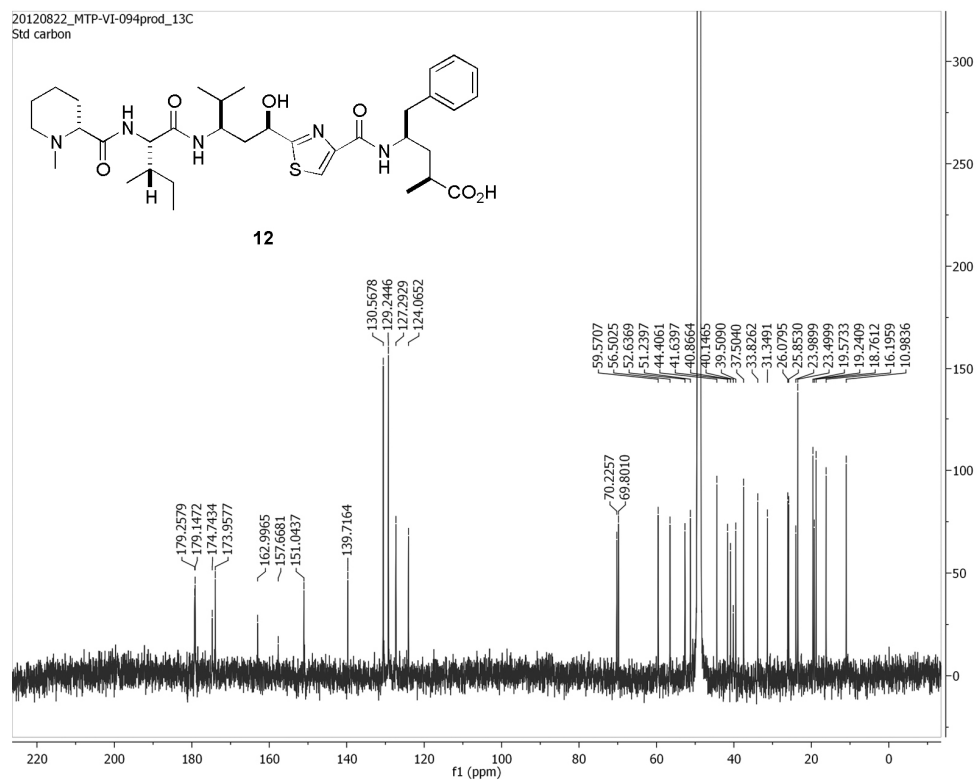
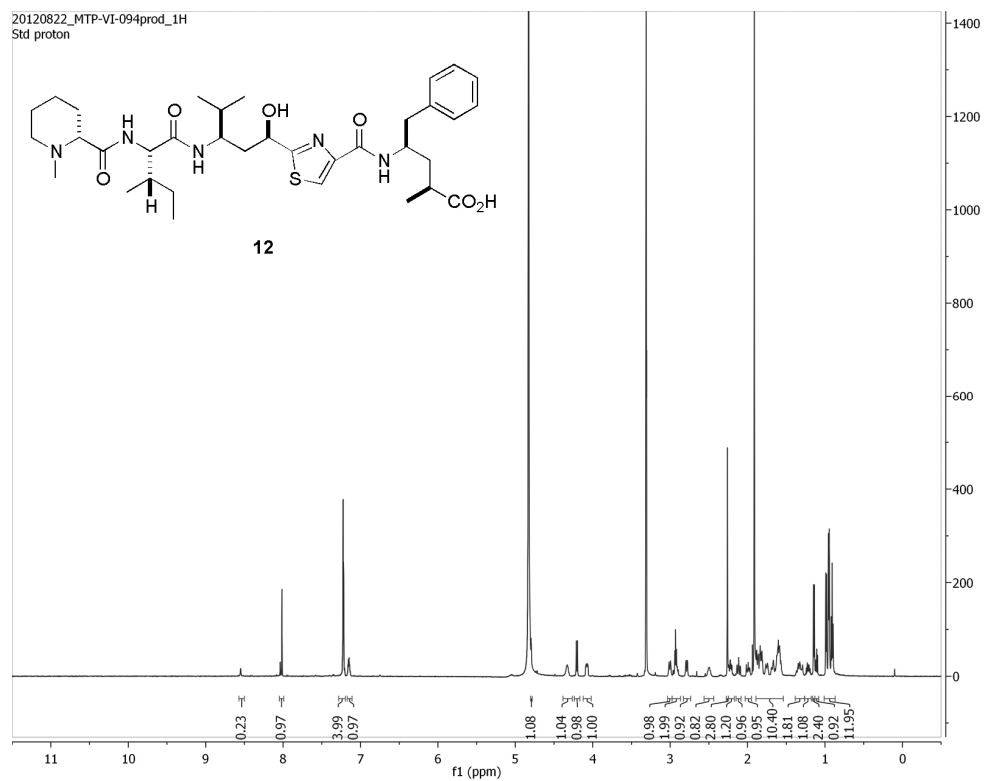
- Sandmann, A.; Sasse, F.; Müller, R. Identification and Analysis of the Core Biosynthetic Machinery of Tubulysin, a Potent Cytotoxin with Potential Anticancer Activity. *Chem. Biol.* **2004**, *11*, 1071–1079.
- Sani, M.; Fossati, G.; Huguenot, F.; Zanda, M. Total Synthesis of Tubulysins U and V. *Angew. Chem. Int. Ed.* **2007**, *46*, 3526–3529.
- Savithri, D.; Leumann, C.; Scheffold, R. Synthesis of a Building Block for a Nucleic-Acid Analog with a Chiral, Flexible Peptide Backbone. *Helv. Chim. Acta* **1996**, *79*, 288–294.
- Schluep, T.; Gunawan, P.; Ma, L.; Jensen, G. S.; Düringer, J.; Hinton, S.; Richter, W.; Hwang, J. Polymeric Tubulysin-Peptide Nanoparticles with Potent Antitumor Activity. *Clin. Cancer Res.* **2009**, *15*, 181–189.
- Shankar, S.; Sani, M.; Terraneo, G.; Zanda, M. Studies towards a Novel Synthesis of Tubulysins: Highly Asymmetric Aza-Michael Reactions of 2-Enoylthiazoles with Metalated Chiral Oxazolidinones. *Synlett* **2009**, *8*, 1341–1345.
- Sasse, F.; Steinmetz, H.; Heil, J.; Höfle, G.; Reichenbach, H. Tubulysins, New Cytostatic Peptides from Myxobacteria Acting on Microtubuli Production, Isolation, Physico-chemical and Biological Properties. *J. Antibiot.* **2000**, *53*, 879–885.
- Shankar, S.; Sani, M.; Saunders, F. R.; Wallace, H. M.; Zanda, M. Total Synthesis and Cytotoxicity Evaluation of an Oxazole Analogue of Tubulysin U. *Synlett*, **2011**, *12*, 1673–1676.

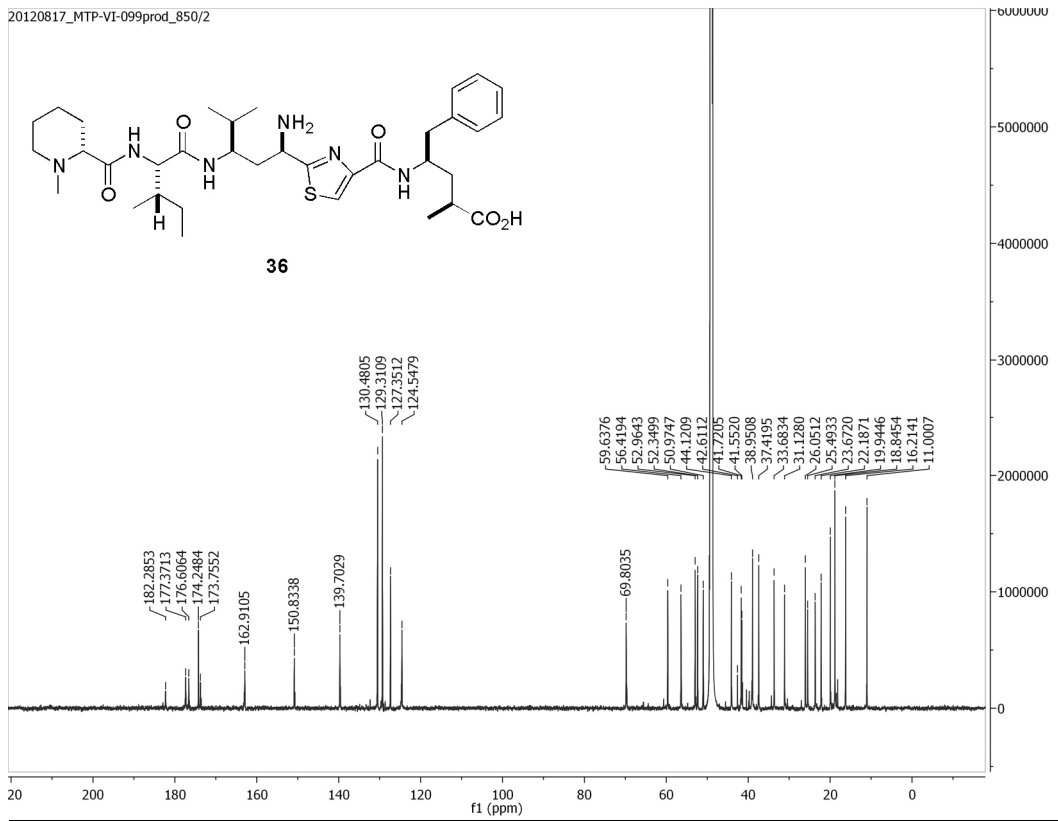
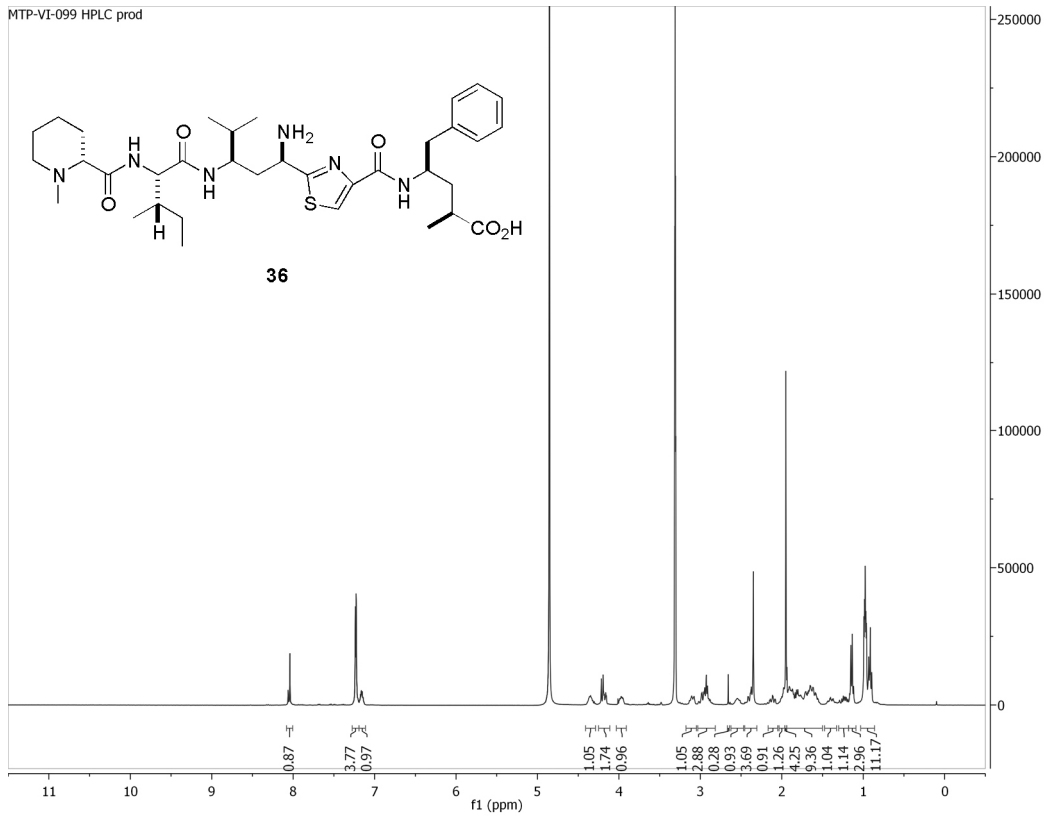
- Sheehan, J. C.; Chapman, D. W.; Roth, R. W. The Synthesis of Stereochemically Pure Peptide Derivatives by the Phthaloyl Method. *J. Am. Chem. Soc.* **1952**, *74*, 3822–3825.
- Shibue, T.; Hirai, T.; Okamoto, I.; Morita, N.; Masu, H.; Azumaya, I.; Tamura, O. Total Syntheses of Tubulysins. *Chem. Eur. J.* **2010**, *16*, 11678–11688.
- Shibue, T.; Okamoto, I.; Morita, N.; Morita, H.; Hirasawa, Y.; Hosoya, T.; Tamura, O. Synthesis and Biological Evaluation of Tubulysin D Analogs Related to Stereoisomers of Tubuvaline. *Bioorg. Med. Chem. Lett.* **2011**, *21*, 431–434.
- Sott, R.; Granander, J.; Williamson, C.; Hilmersson, G. Kinetic and NMR Spectroscopic Studies of Chiral Mixed Sodium/Lithium Amides Used for the Deprotonation of Cyclohexene Oxide. *Chem. Eur. J.* **2005**, *11*, 4785–4792.
- Spieß, A.; Heckmann, G.; Bach, T. Regio- and Stereoselective Synthesis of α -Chiral 2-Substituted 4-Bromothiazoles from 2,4-Dibromothiazole by Bromine–Magnesium Exchange. Building Blocks for the Synthesis of Thiazolyl Peptides and Dolabellin. *Synlett* **2004**, *1*, 131–133.
- Steinmetz, H.; Glaser, N.; Herdtweck, E.; Sasse, F.; Reichenbach, H.; Höfle, G. Isolation, Crystal and Solution Structure Determination, and Biosynthesis of Tubulysins—Powerful Inhibitors of Tubulin Polymerization from Myxobacteria. *Angew. Chem. Int. Ed.* **2004**, *43*, 4888–4892.
- Stone, G. B. Oxazaborolidine Catalyzed Borane Reductions of Ketones: a Significant Effect of Temperature on Selectivity. *Tetrahedron Asymm.* **2004**, *3*, 465–472.

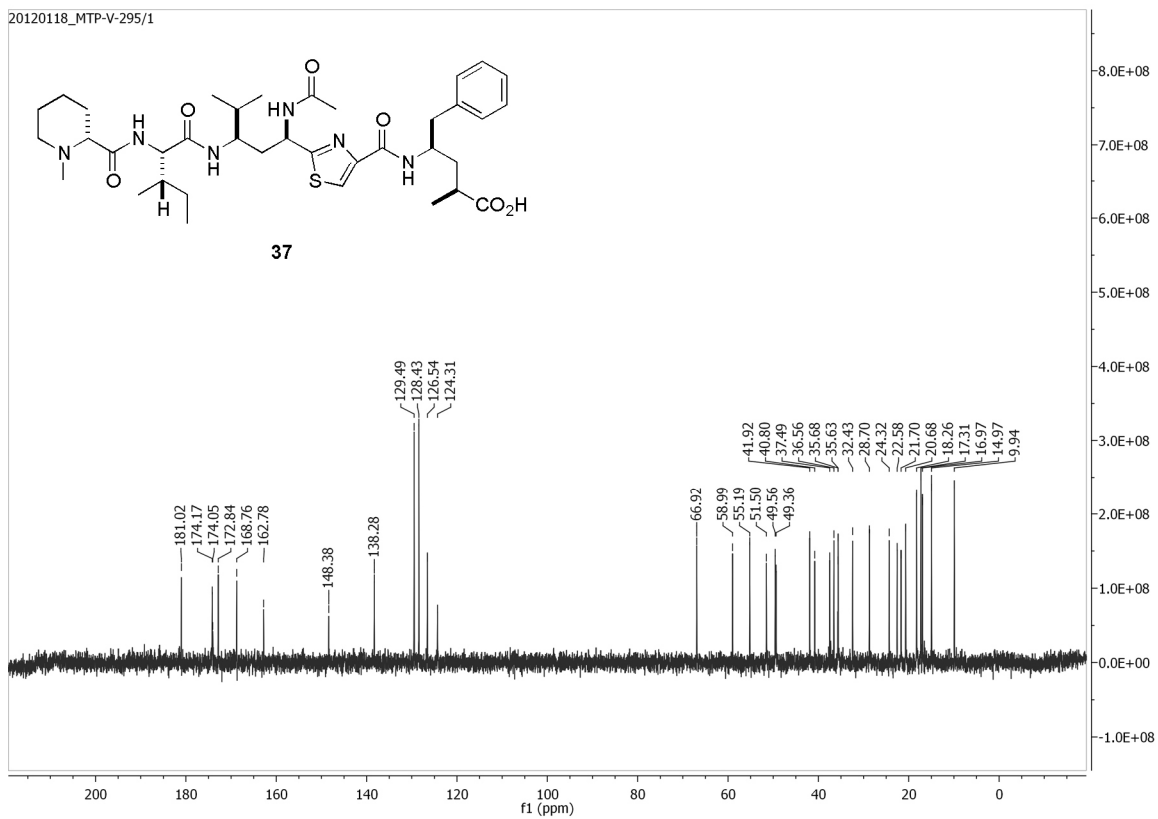
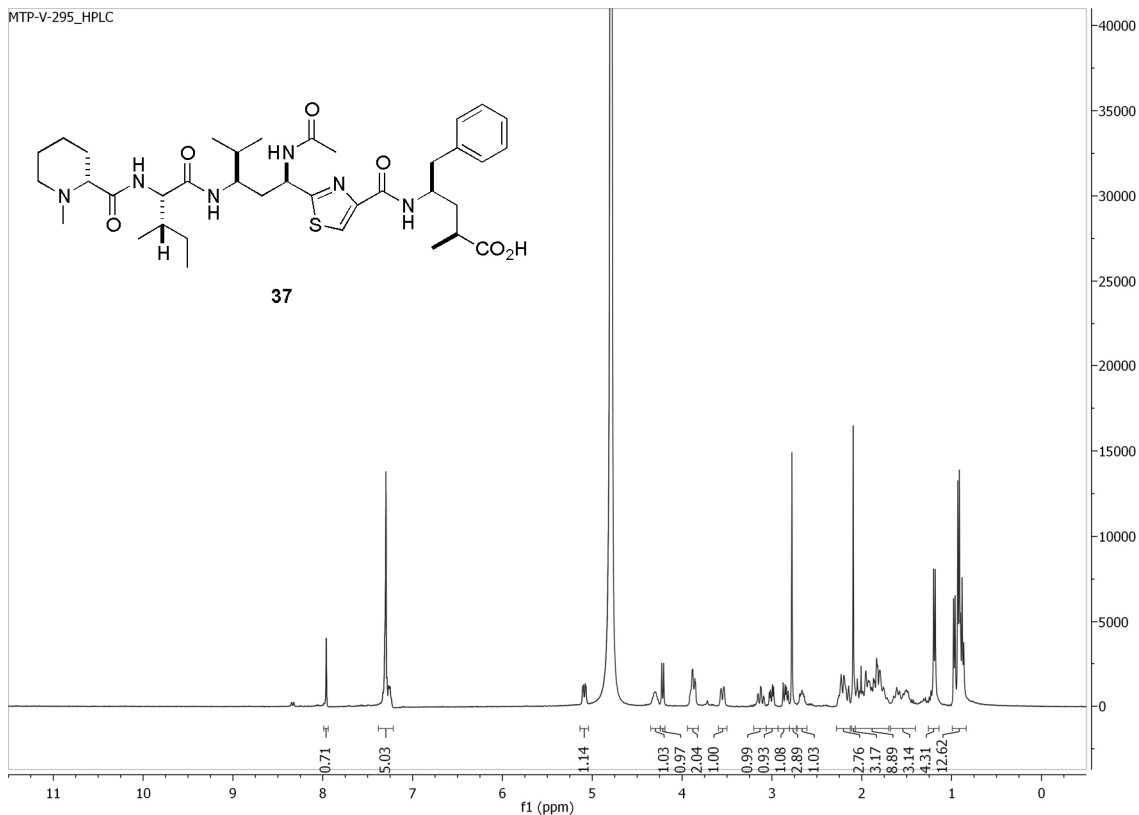
- Thompson, A. S.; Humphrey, G. R.; DeMarco, A. M.; Mathre, D. J.; Grabowski, E. J. J. Direct Conversion of Activated Alcohols to Azides using Diphenyl Phosphorazidate. A Practical Alternative to Mitsunobu Conditions. *J. Org. Chem.* **1993**, *58*, 5886–5888.
- Ullrich, A.; Chai, Y.; Pistorius, D.; Elnakady, Y. A.; Herrmann, J. E.; Weissman, K. J.; Kazmaier, U; Müller, R. Pretubulysin, a Potent and Chemically Accessible Tubulysin Precursor from *Angiococcus disciformis*. *Angew. Chem. Int. Ed.* **2009a**, *48*, 4422–4425.
- Ullrich, A.; Herrmann, J.; Müller, R.; Kazmaier, U. Synthesis and Biological Evaluation of Pretubulysin and Derivatives. *Eur. J. Org. Chem.* **2009b**, 6367–6378.
- van den Broek, L. A. G. M.; Lázaro, E.; Zylicz, Z.; Fennis, P. J.; Missler, F. A. N.; Lelieveld, P.; Garzotto, M.; Wagener, D. J. T.; Ballesta, J. P. G.; Ottenheijm, H. C. J. Lipophilic Analogues of Sparsomycin as Strong Inhibitors of Protein Synthesis and Tumor Growth: A Structure-Activity Relationship Study. *J. Med. Chem.* **1989**, *32*, 2002–2015.
- Veitía, M. S.-I.; Brun, P. L.; Jorda, P.; Falguières, A.; Ferroud, C. Synthesis of Novel *N*-protected β^3 -Amino Nitriles: Study of their Hydrolysis Involving a Nitrilase-Catalyzed Step. *Tetrahedron Asymm.* **2009**, *20*, 2077–2089.
- Vlahov, I. R.; Wang, Y.; Kleindl, P. J.; Leamon, C. P. Design and Regioselective Synthesis of a New Generation of Targeted Chemotherapeutics. Part II: Folic Acid Conjugates of Tubulysins and their Hydrazides. *Bioorg. Med. Chem. Lett.* **2008**, *18*, 4558–4561.

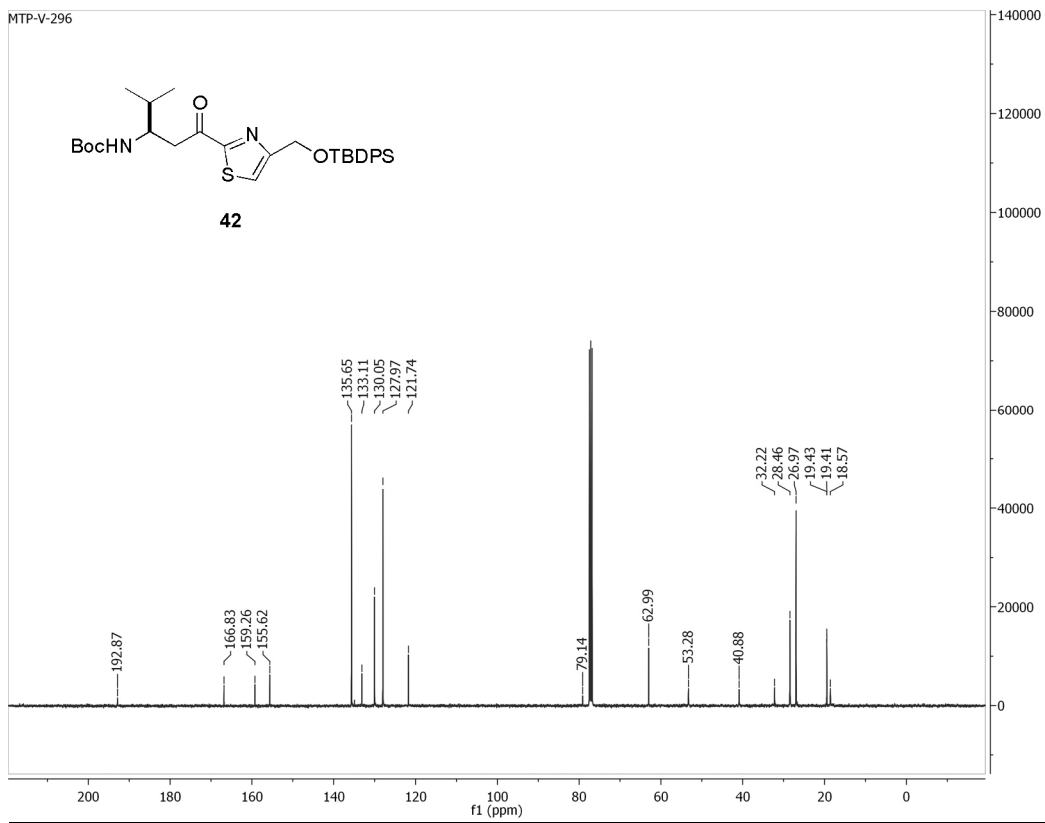
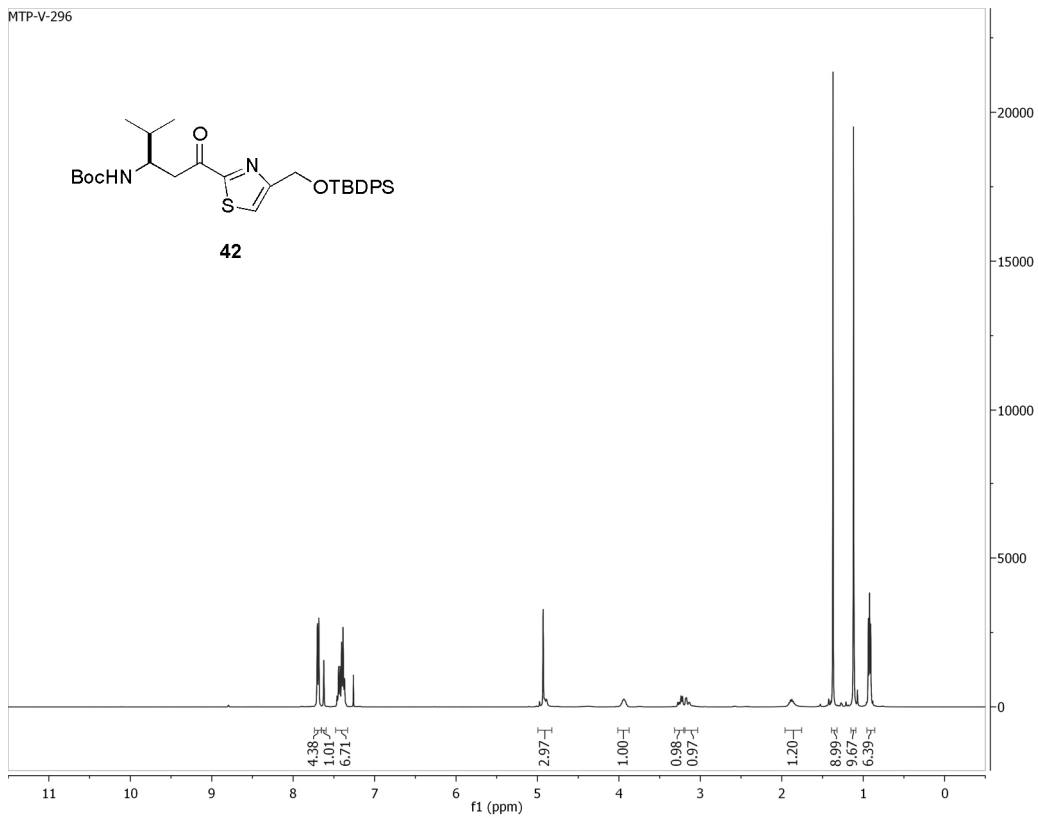
- Vlahov, I. R.; Wang, Y.; Vetzal, M.; Hahn, S.; Kleindl, P. J.; Reddy, J. A.; Leamon, C. P.;
Acid Mediated Formation of an *N*-acyliminium Ion from Tubulysins: A New
Methodology for the Synthesis of Natural Tubulysins and their Analogs. *Bioorg.
Med. Chem. Lett.* **2011**, *21*, 6778–6781.
- Wang, Z.; McPherson, P. A.; Raccor, B. S.; Balachandran, R.; Zhu, G.; Day, B. W.; Vogt,
A.; Wipf, P. Structure–activity and High-content Imaging Analyses of Novel
Tubulysins. *Chem. Biol. Drug Des.* **2007**, *70*, 75–86.
- Williams, M. W.; Young, G. T. Amino-acids and Peptides. Part XIX. The Mechanism of
Racemisation during Peptide Synthesis. “The Chloride Effect.” *J. Chem. Soc.*
1964, 3701–3708.
- Wipf, P.; Wang, Z. Total Synthesis of N¹⁴-Desacetoxytubulysin H. *Org. Lett.* **2007**, *9*,
1605–1607.
- Zhao, M. M.; Li, J.; Mano, E.; Song, Z. J.; Tschaen, D. M. Oxidation of Primary Alcohols
to Carboxylic Acids with Sodium Chlorite Catalyzed by TEMPO and Bleach: 4-
Methoxyphenylacetic acid. *Org. Synth.* **2005**, *81*, 195–203.
- Zhu, J.-L.; Lee, F.-Y.; Wu, J.-D.; Kuo, C.-W.; Shai, K.-S. An Efficient New Procedure for
the One-Pot Conversion of Aldehydes into the Corresponding Nitriles. *Synlett*
2007, *8*, 1317–1319.

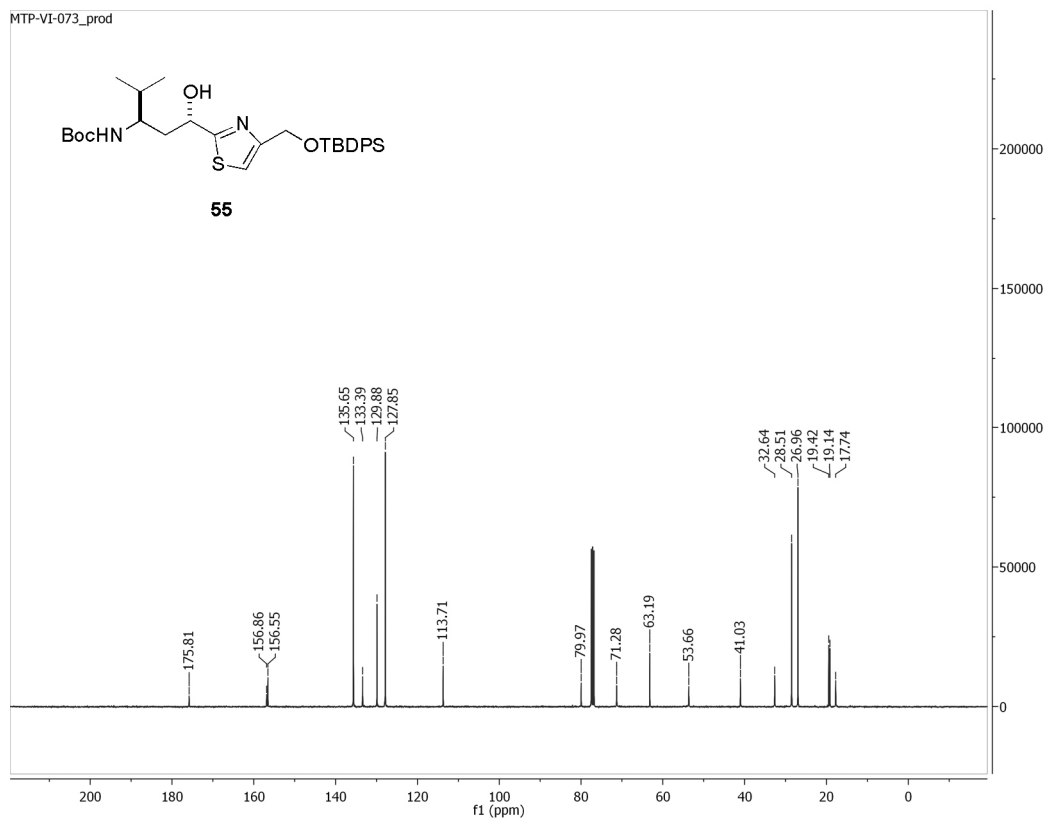
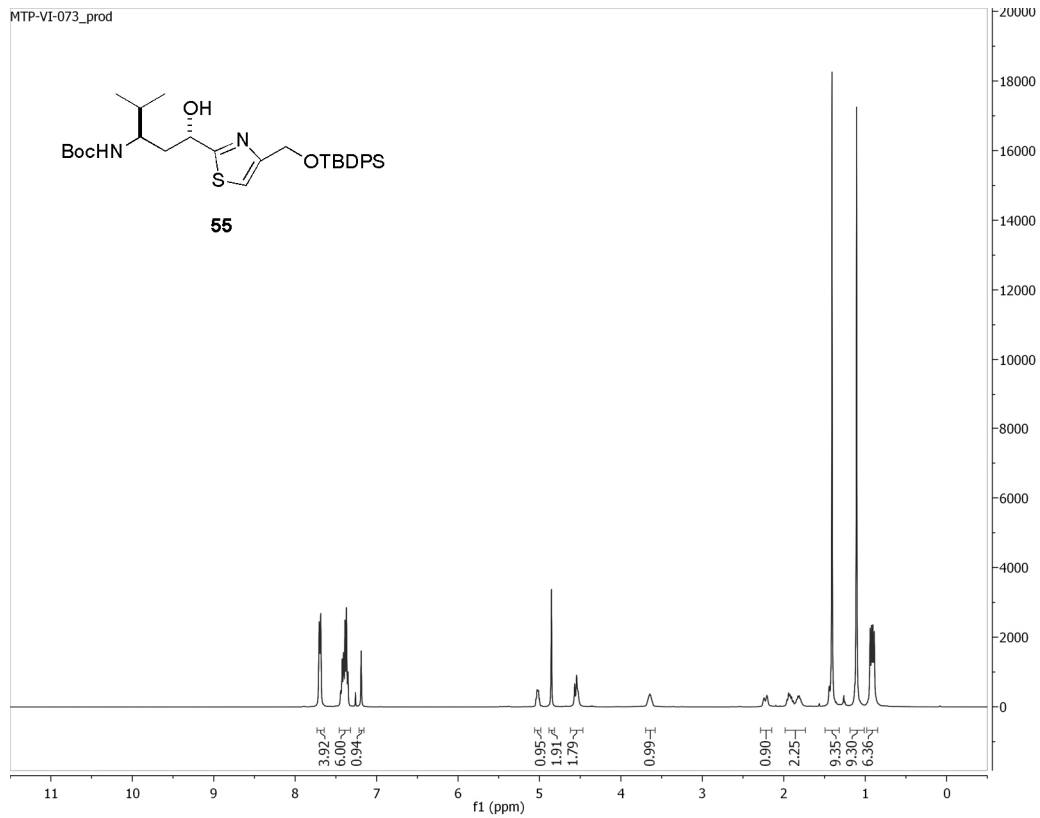
Appendix A: NMR Spectra of Key Compounds

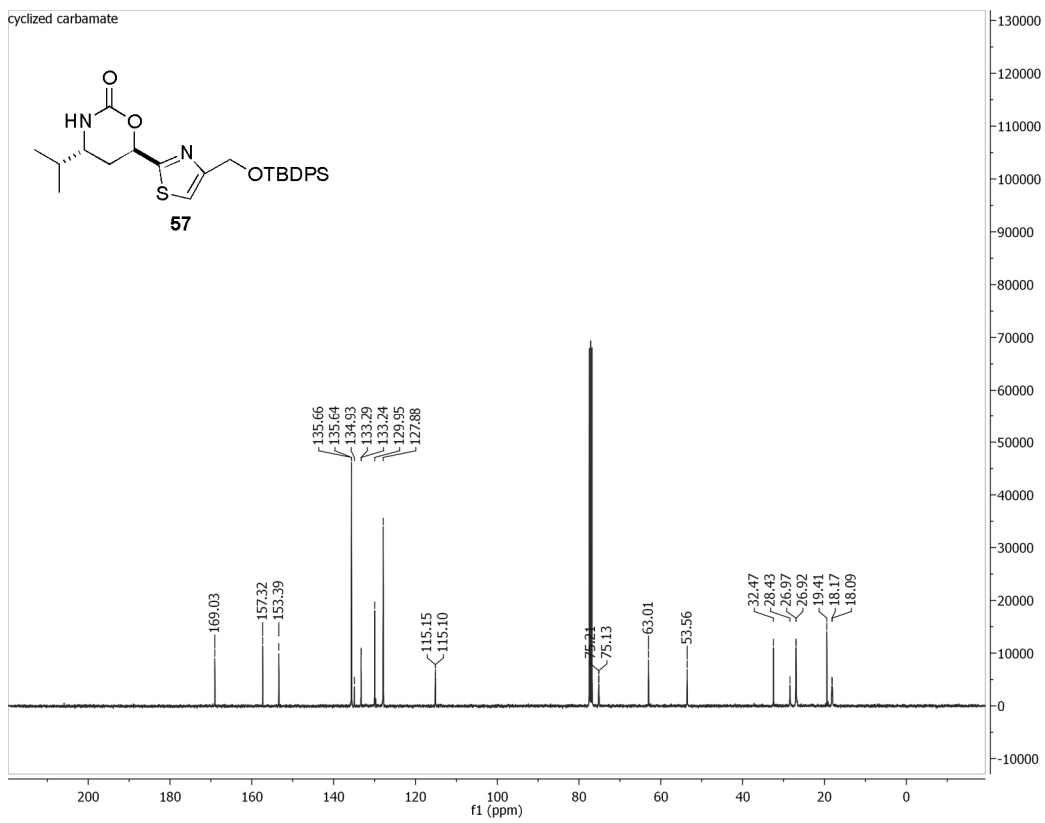
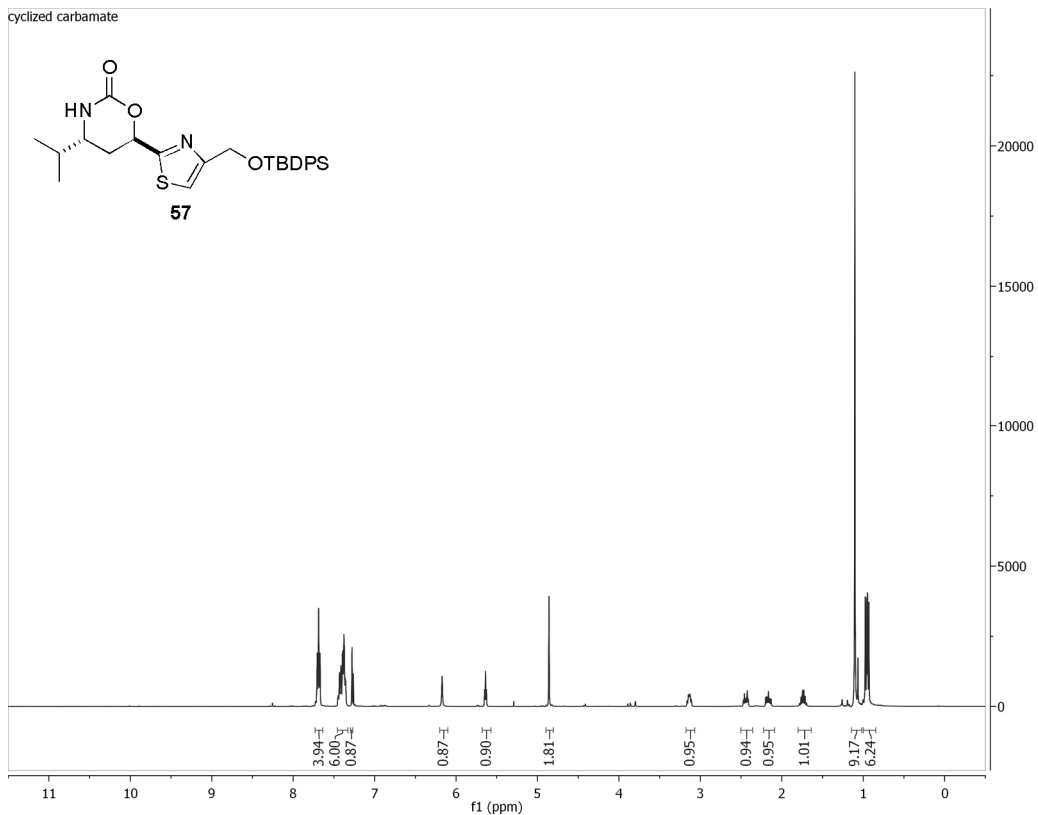


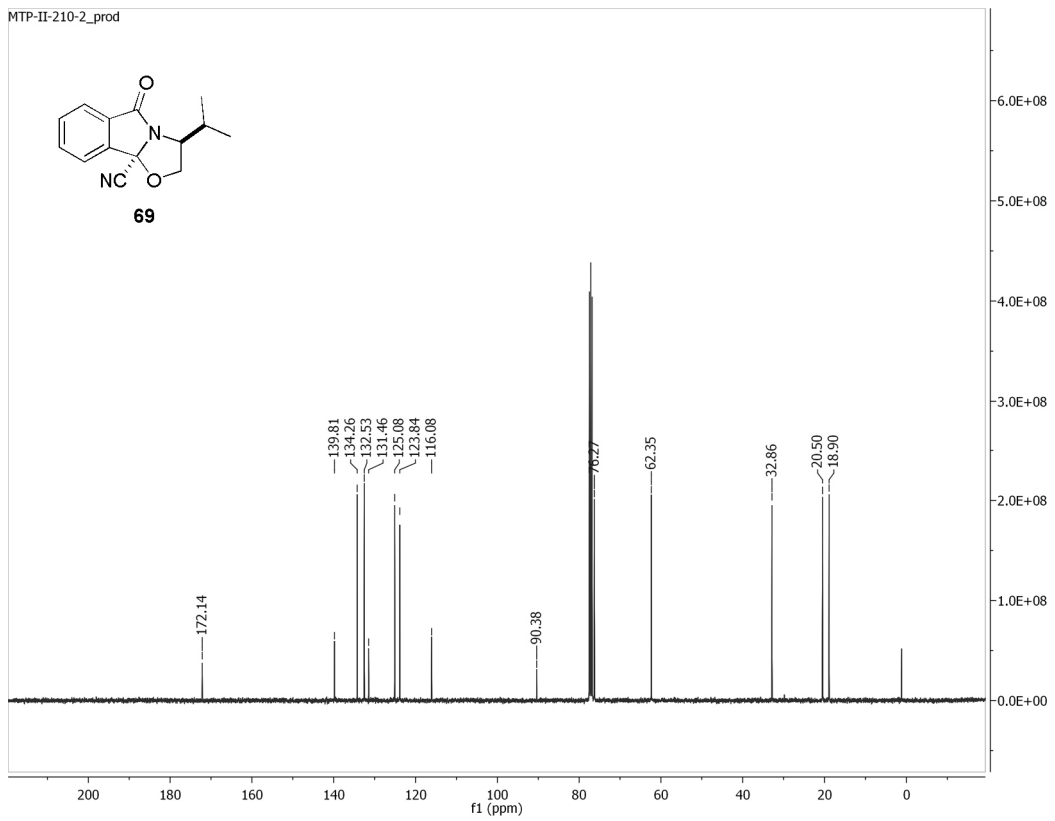
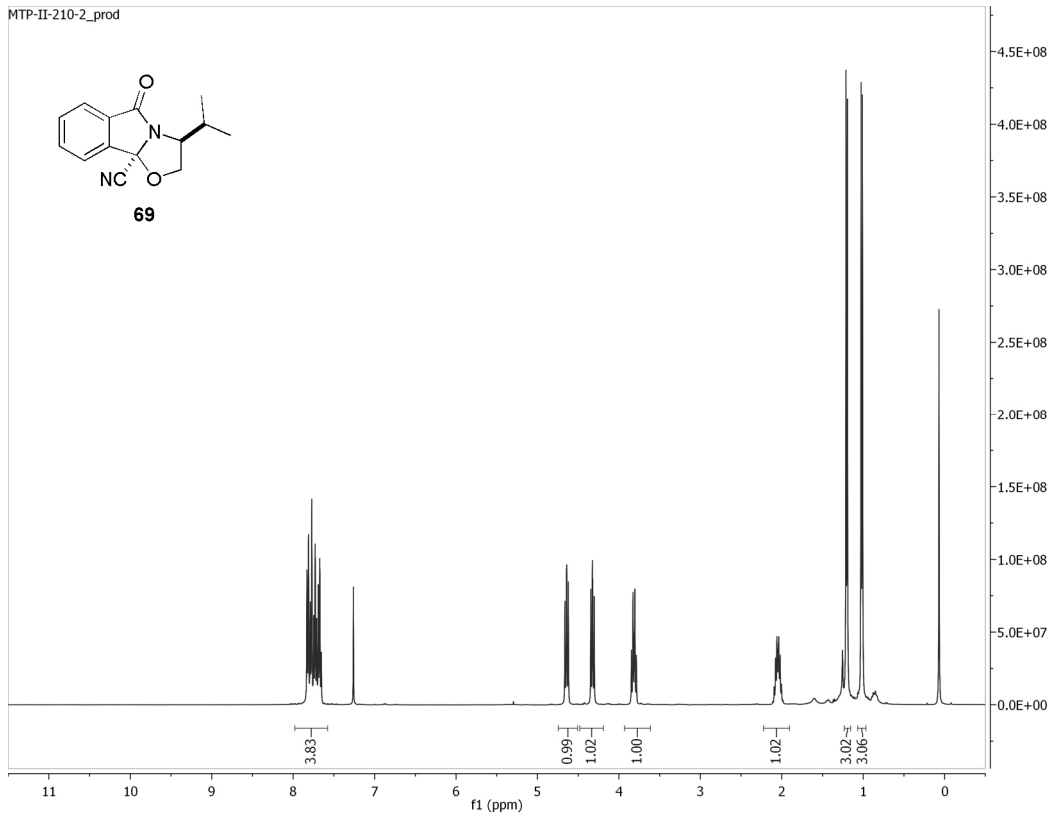


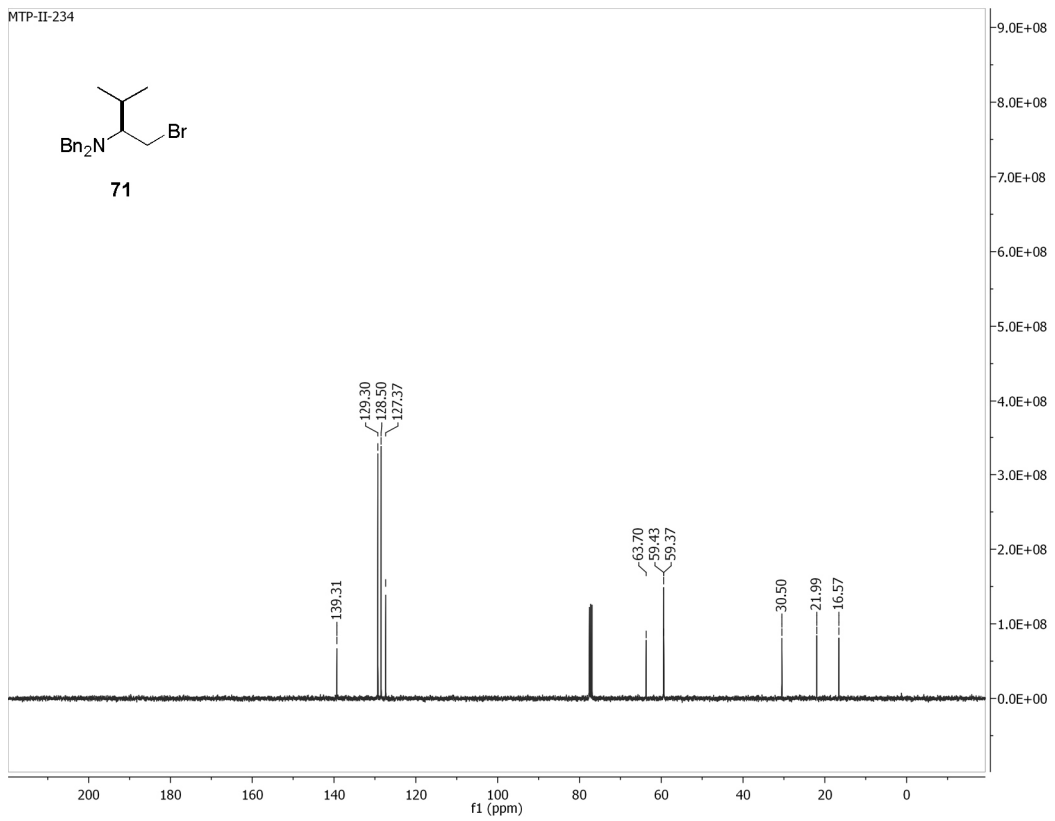
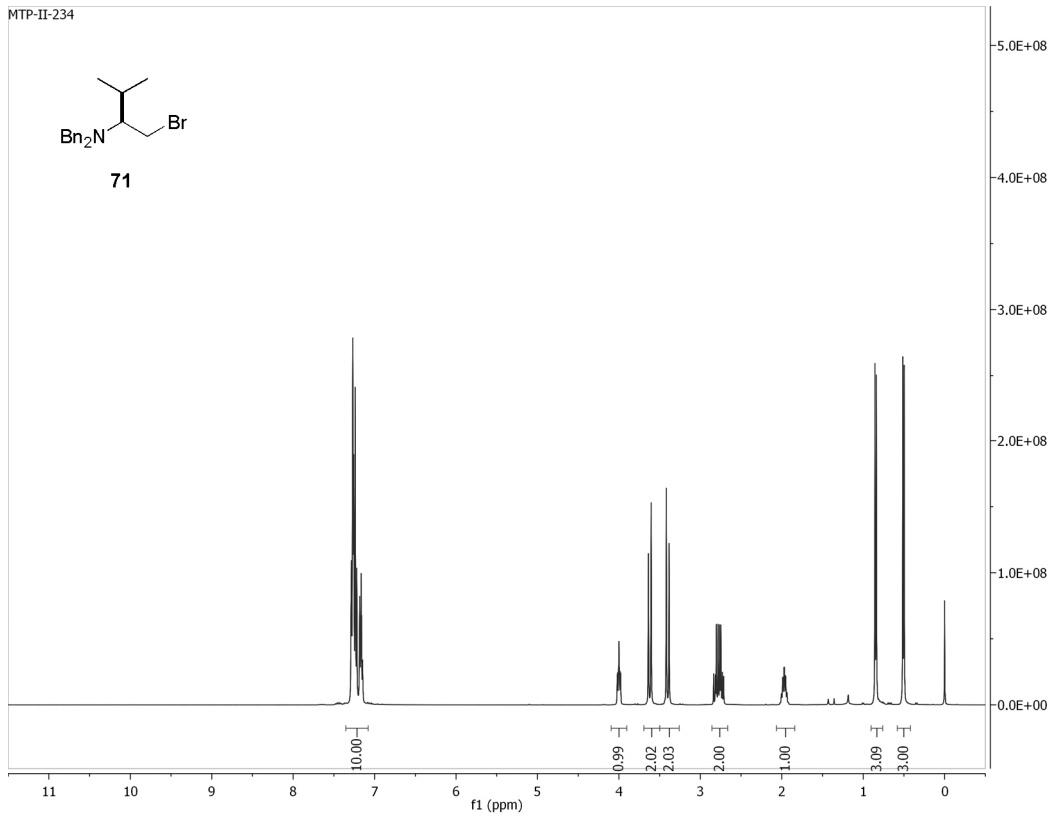


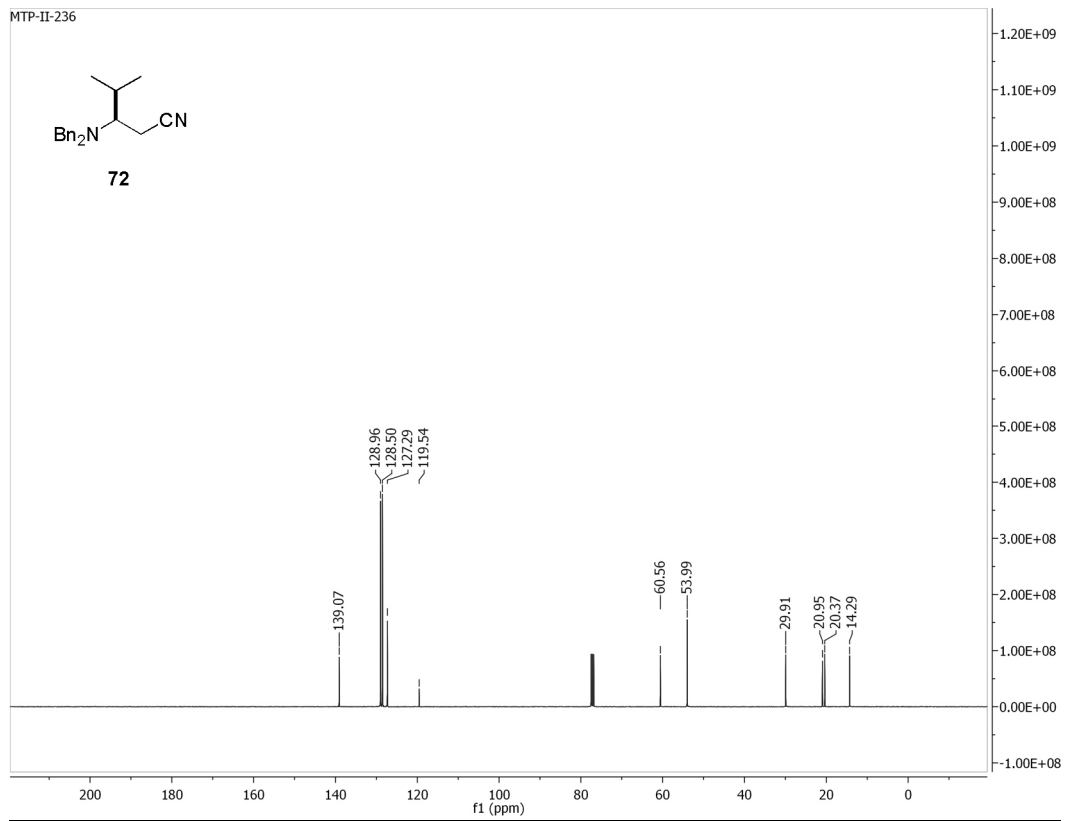
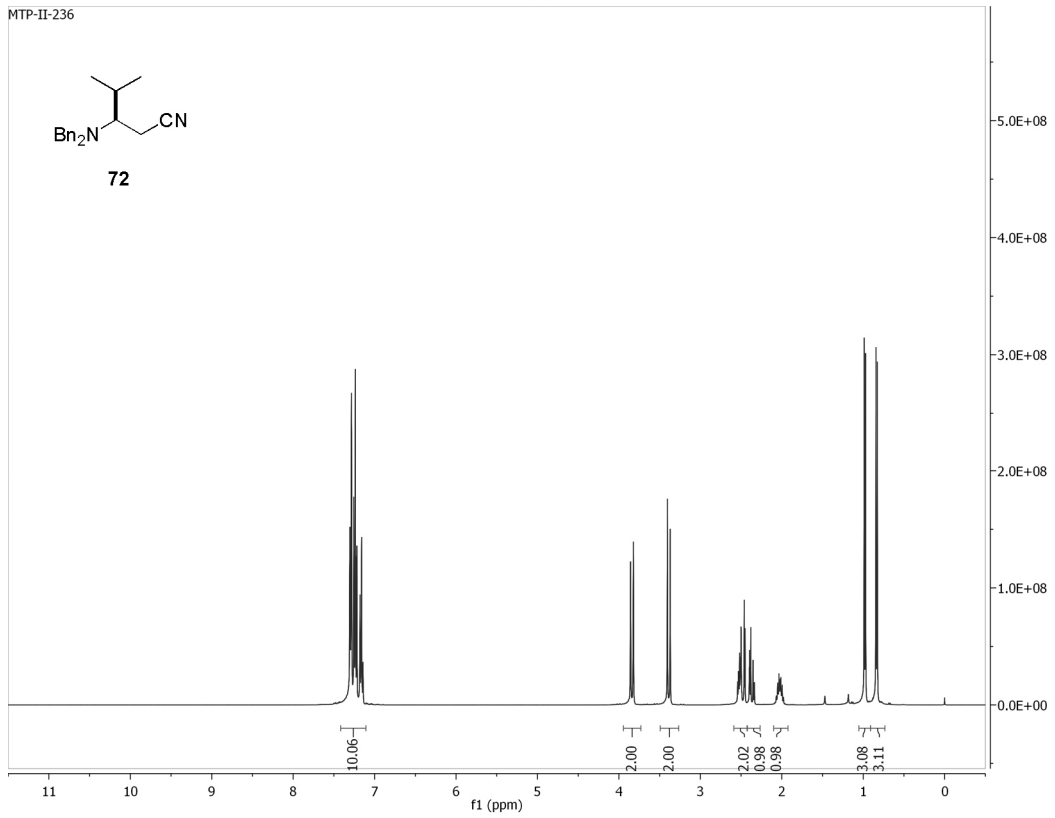


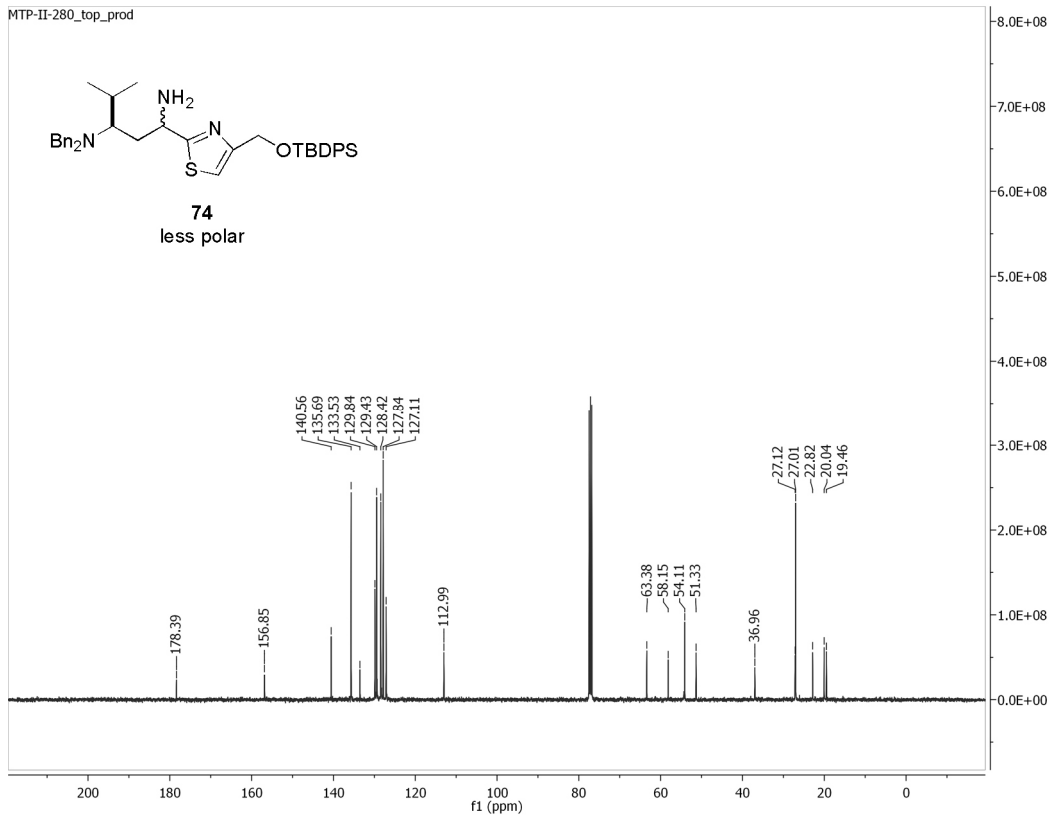
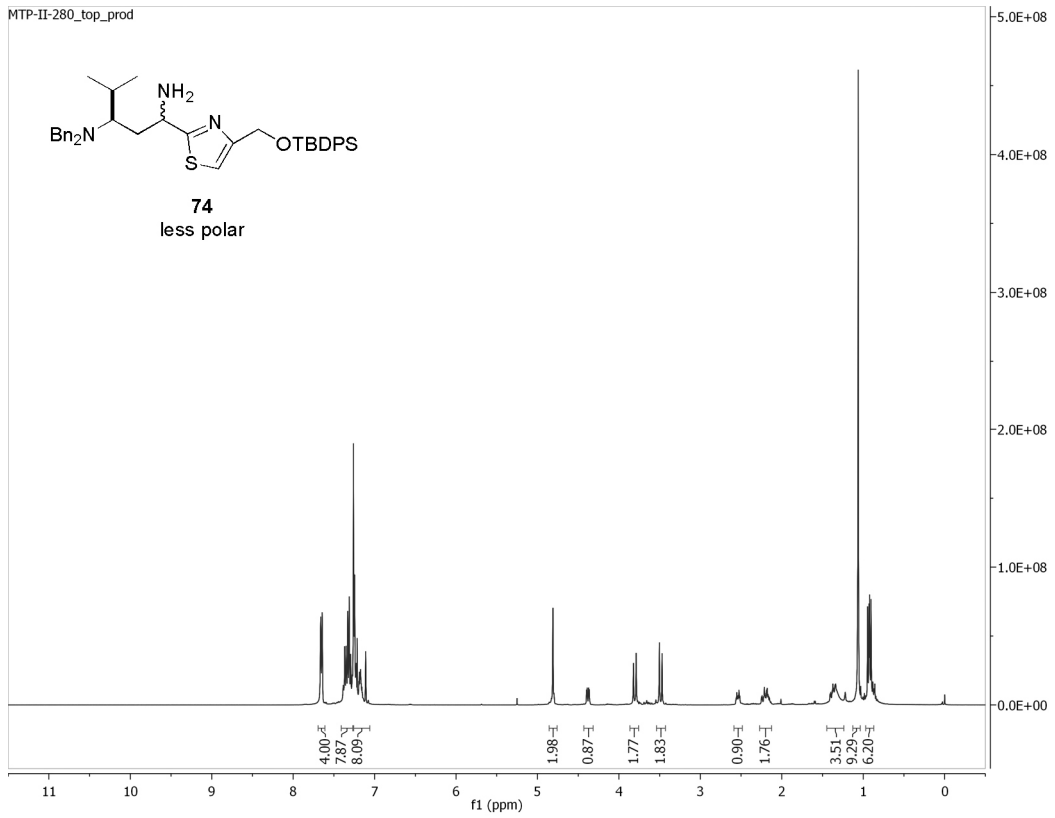


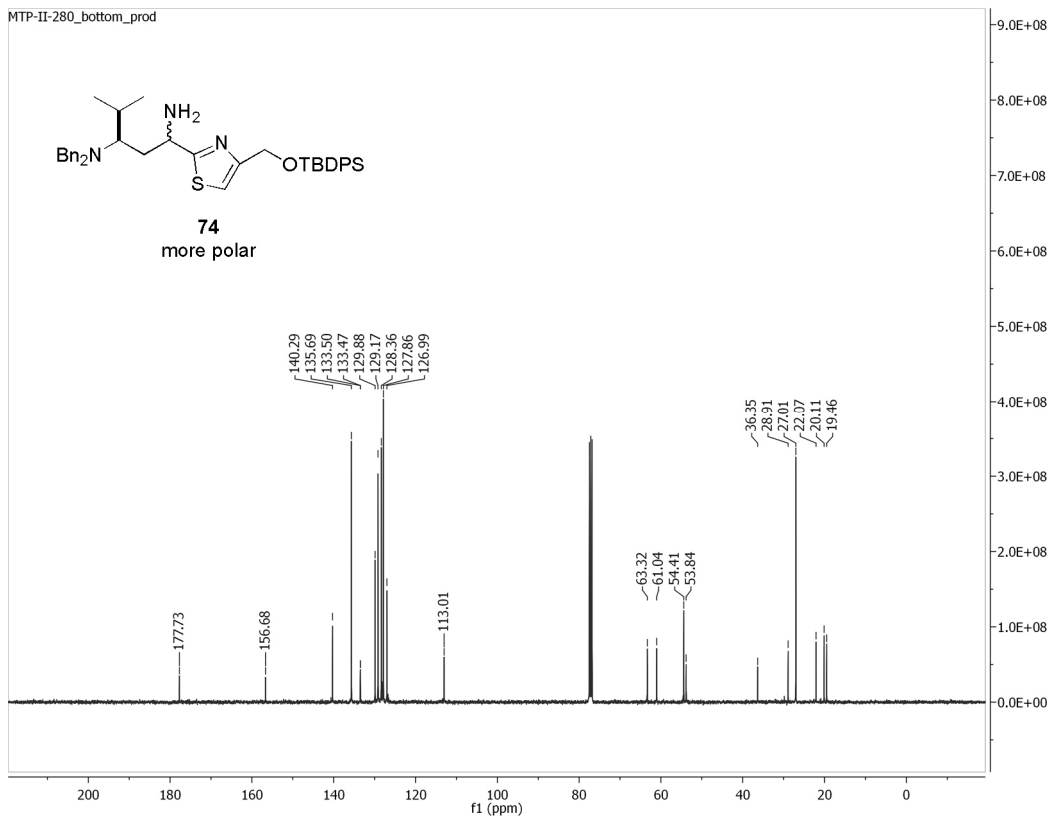
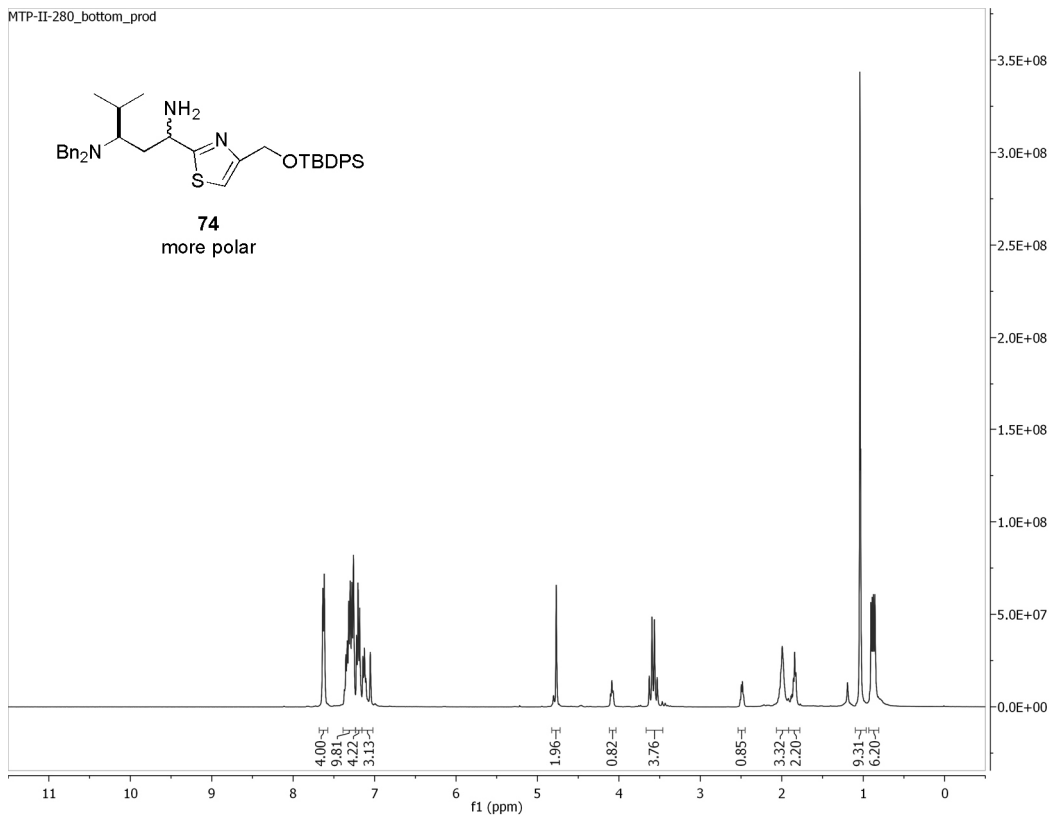


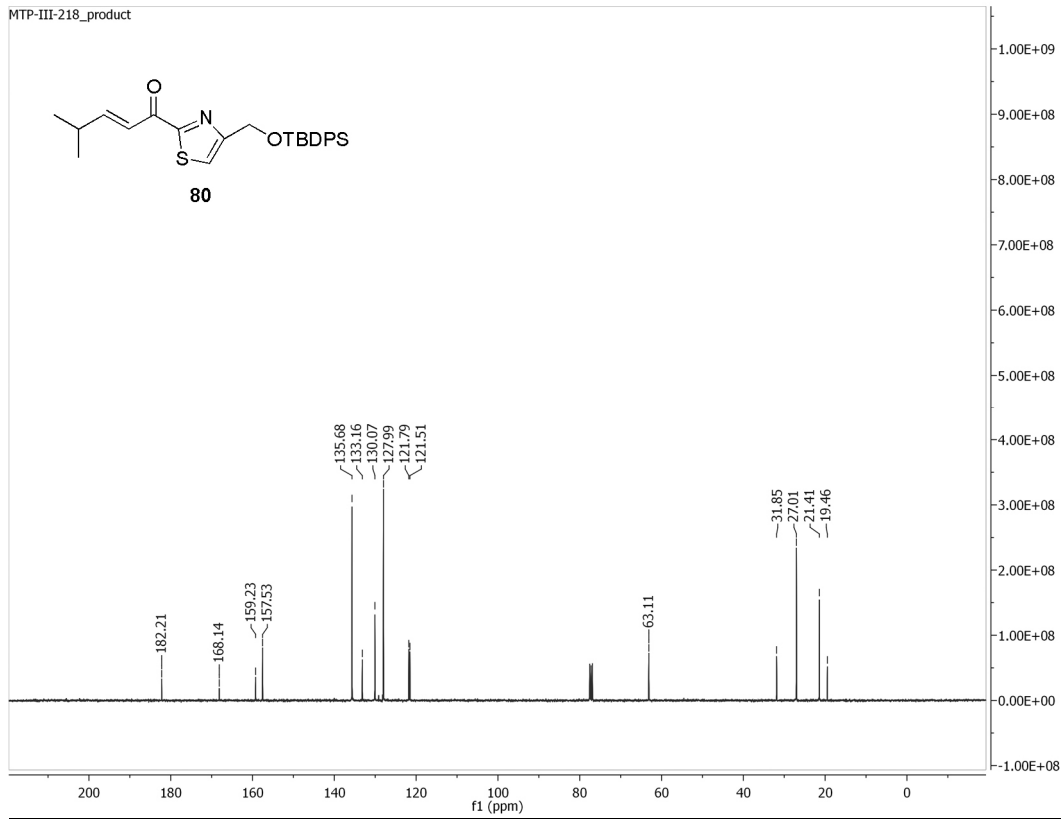
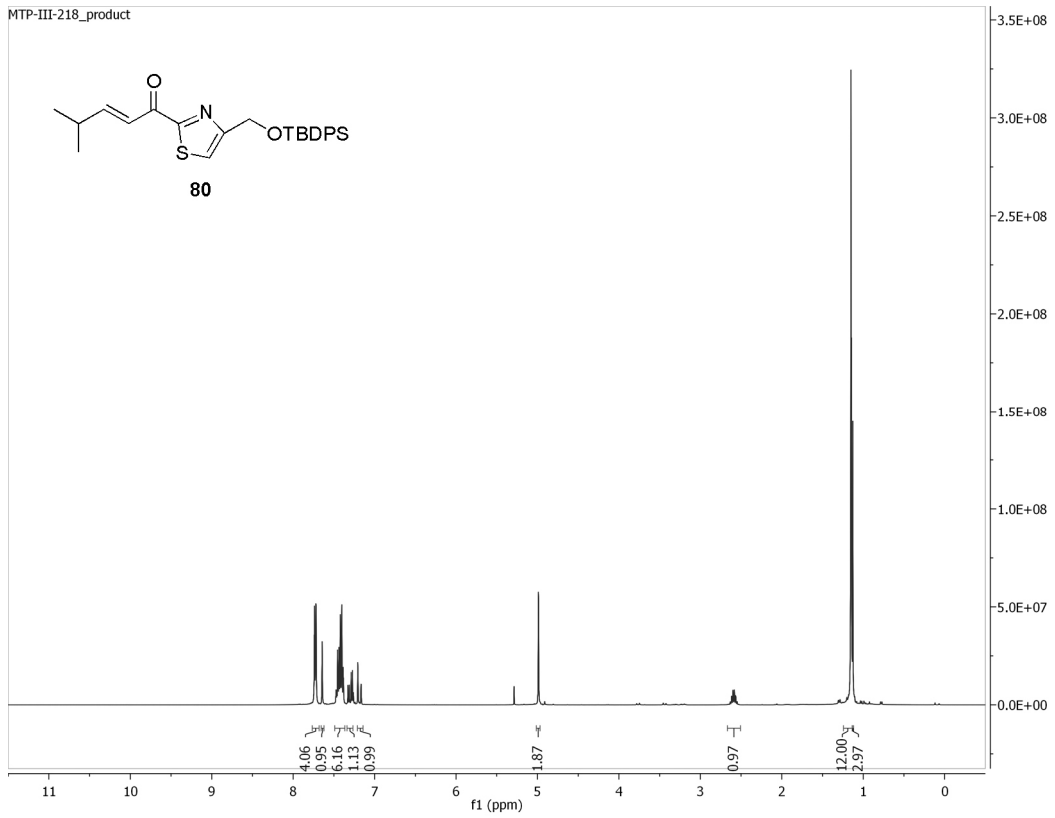


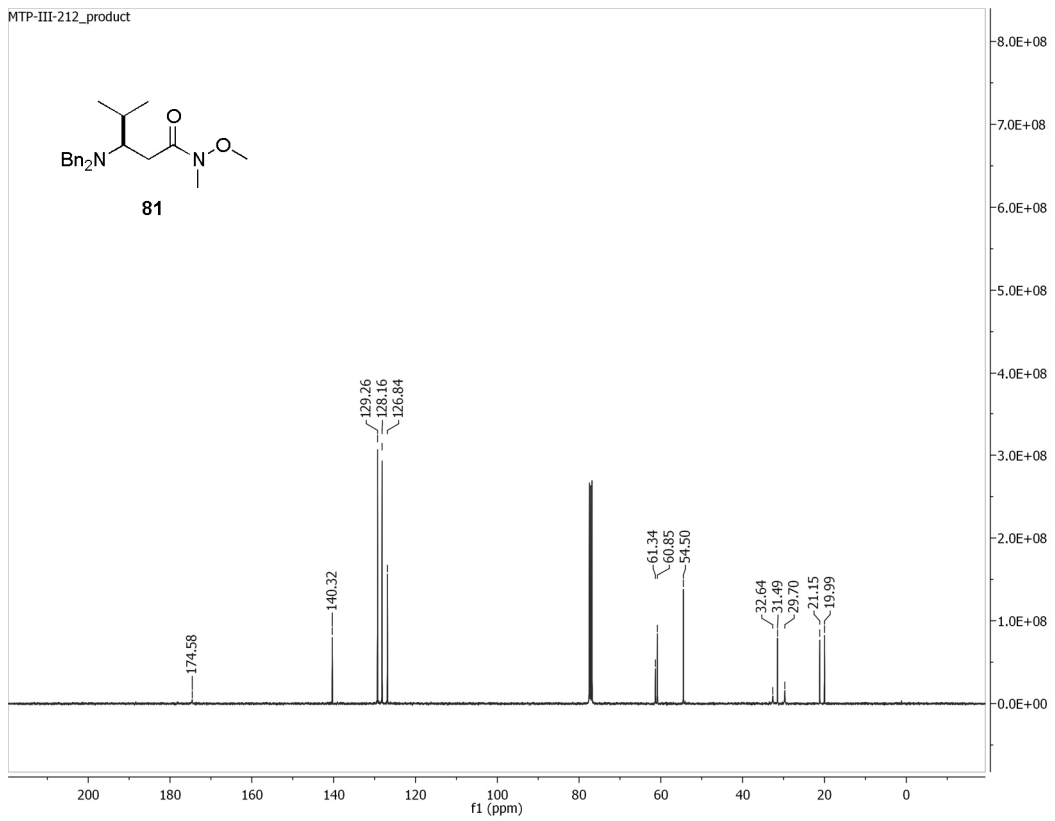
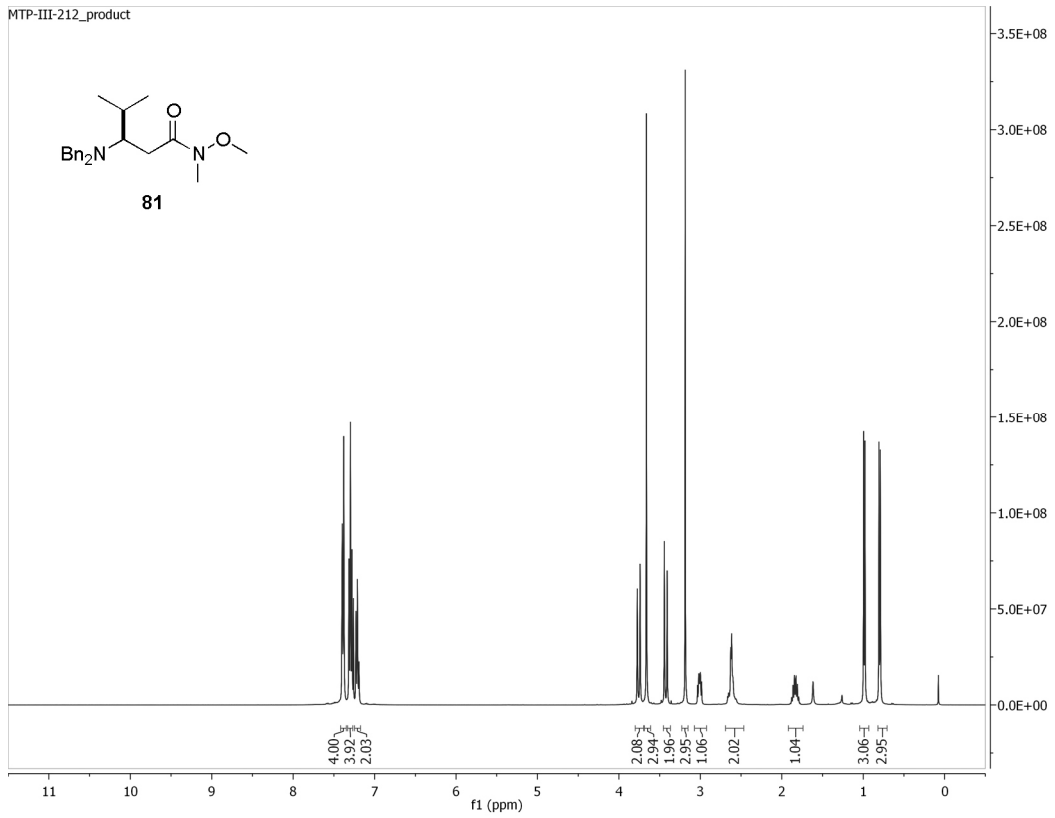




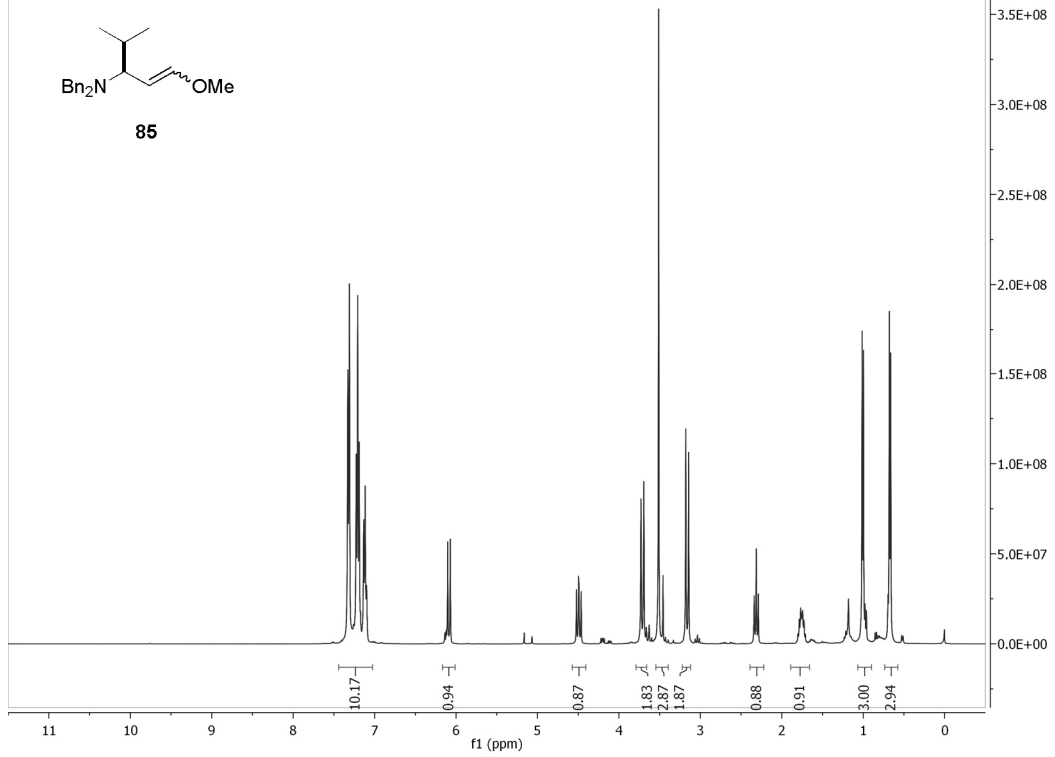
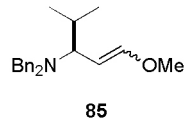




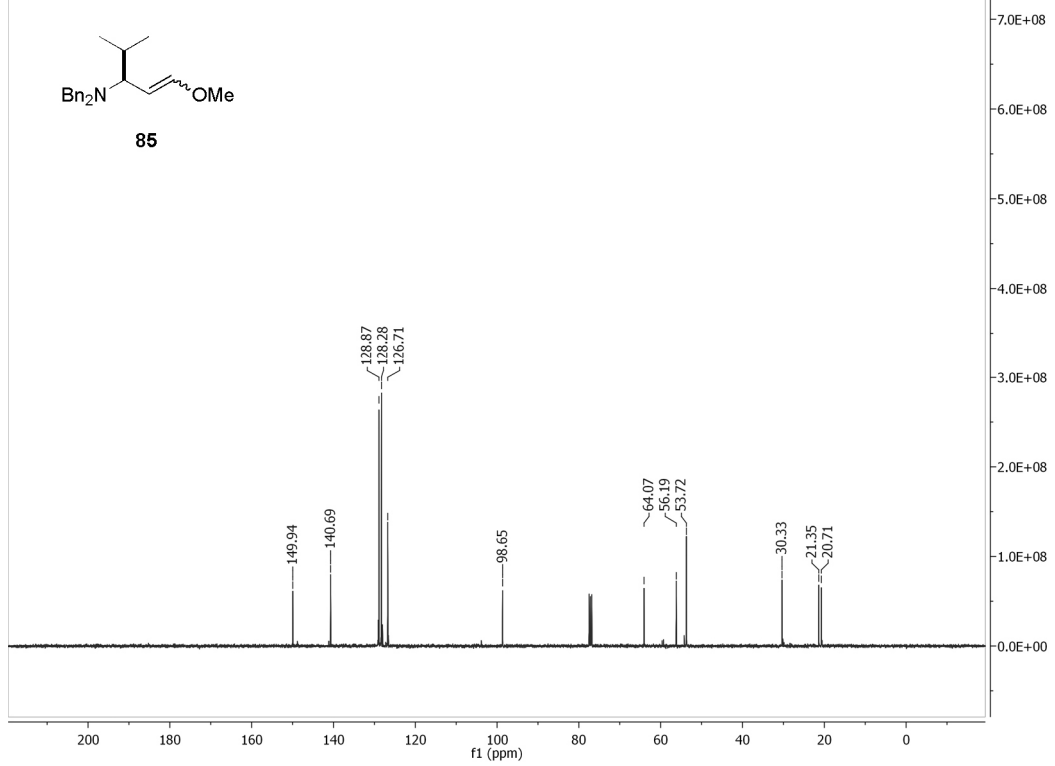
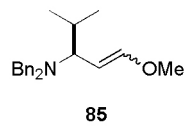


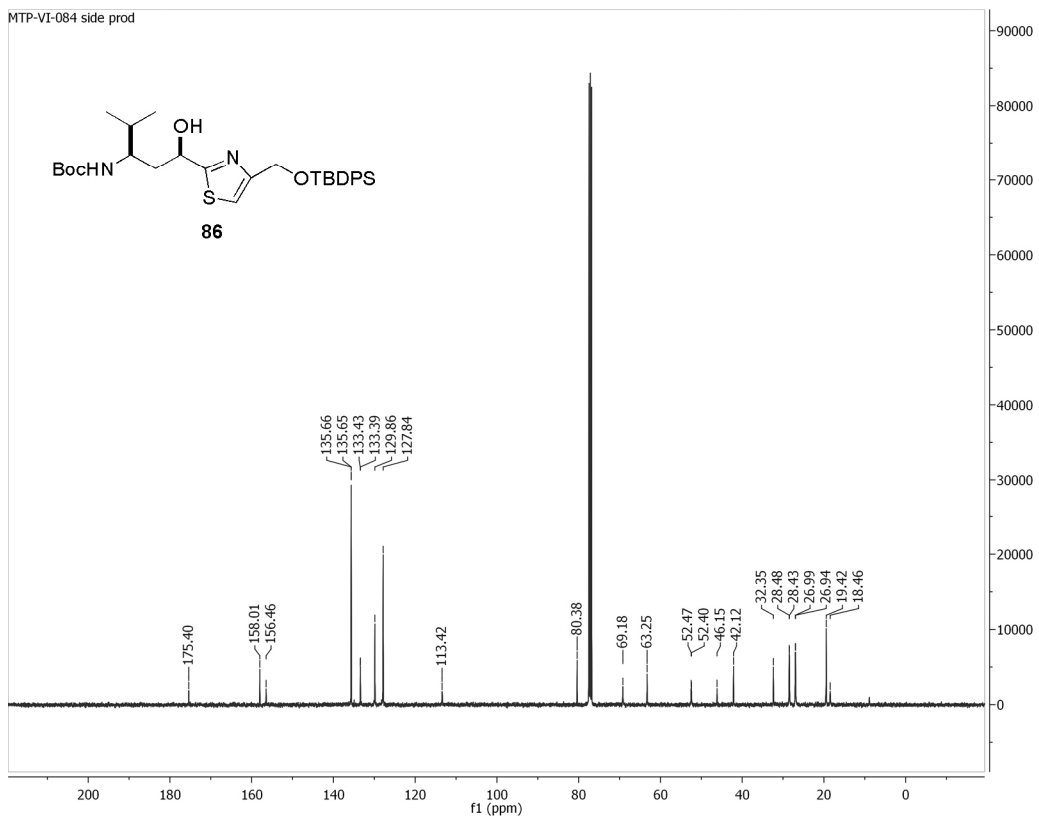
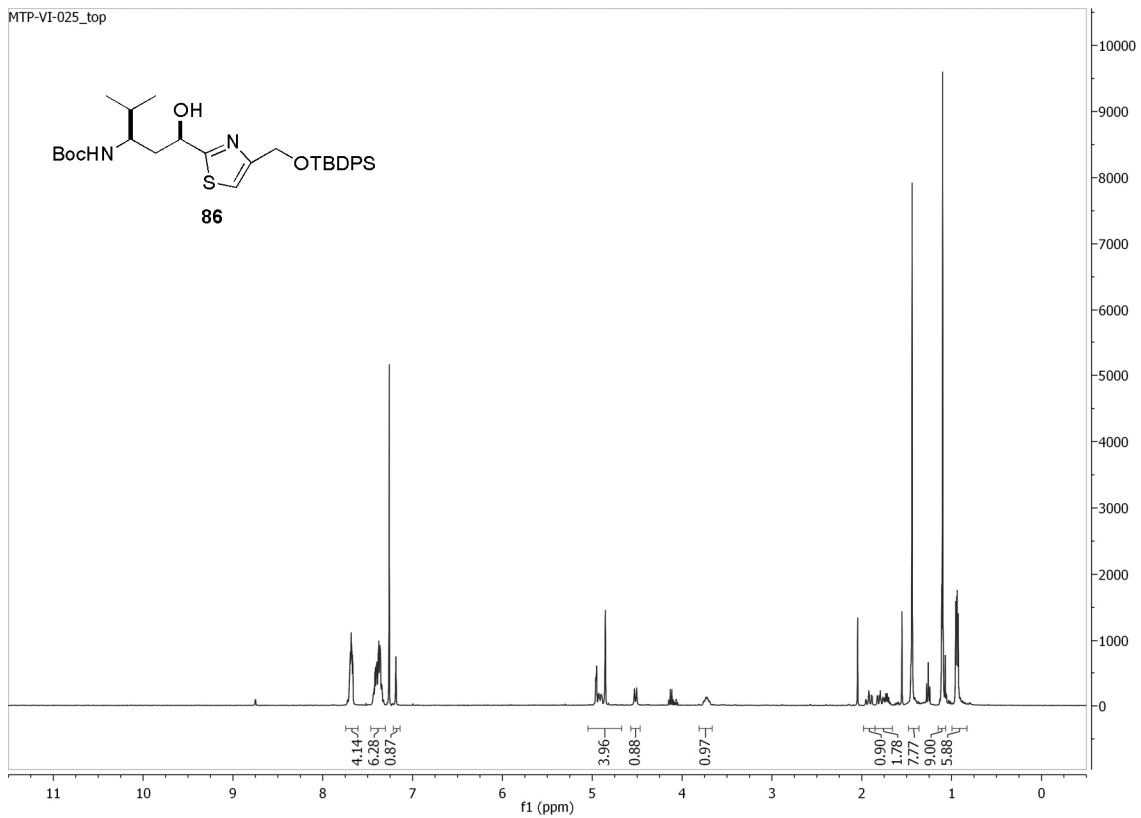


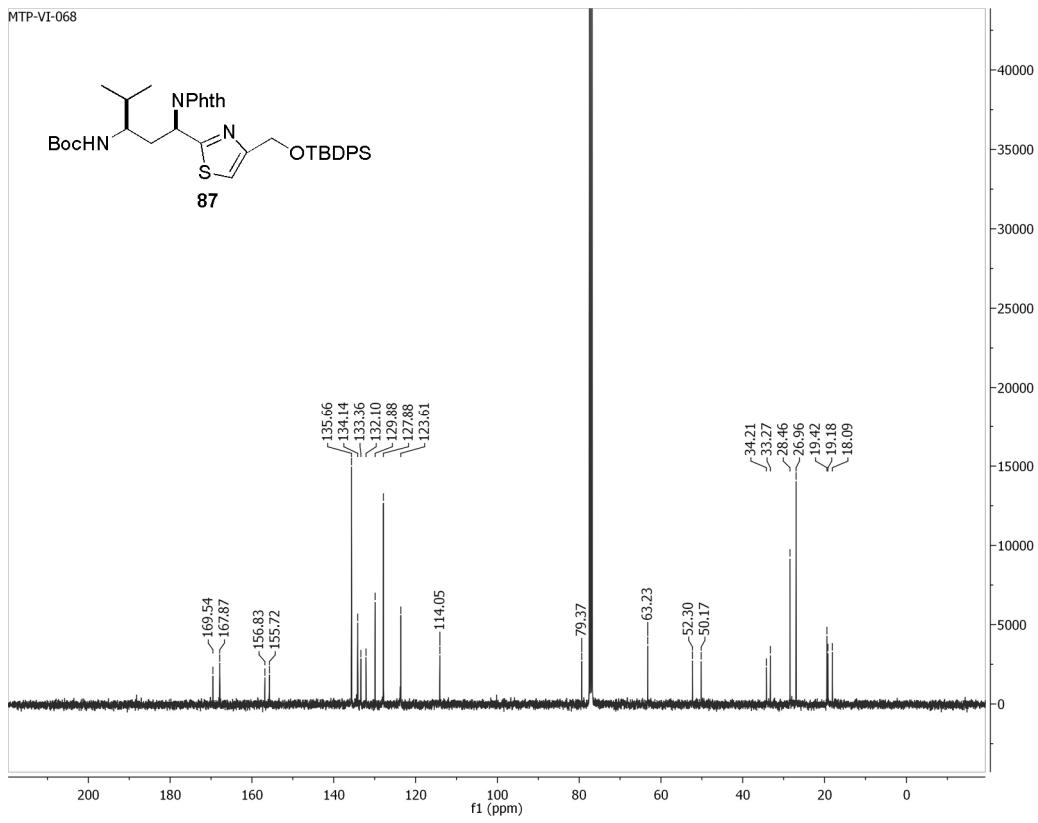
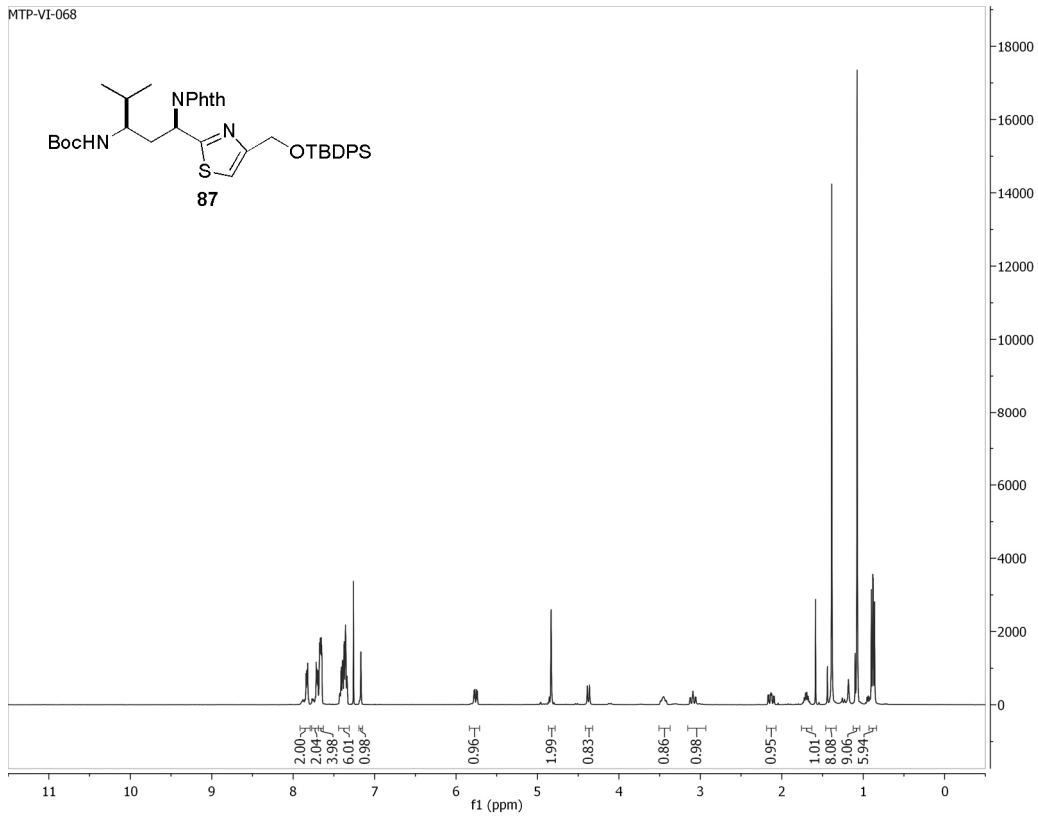
MTP-III-252

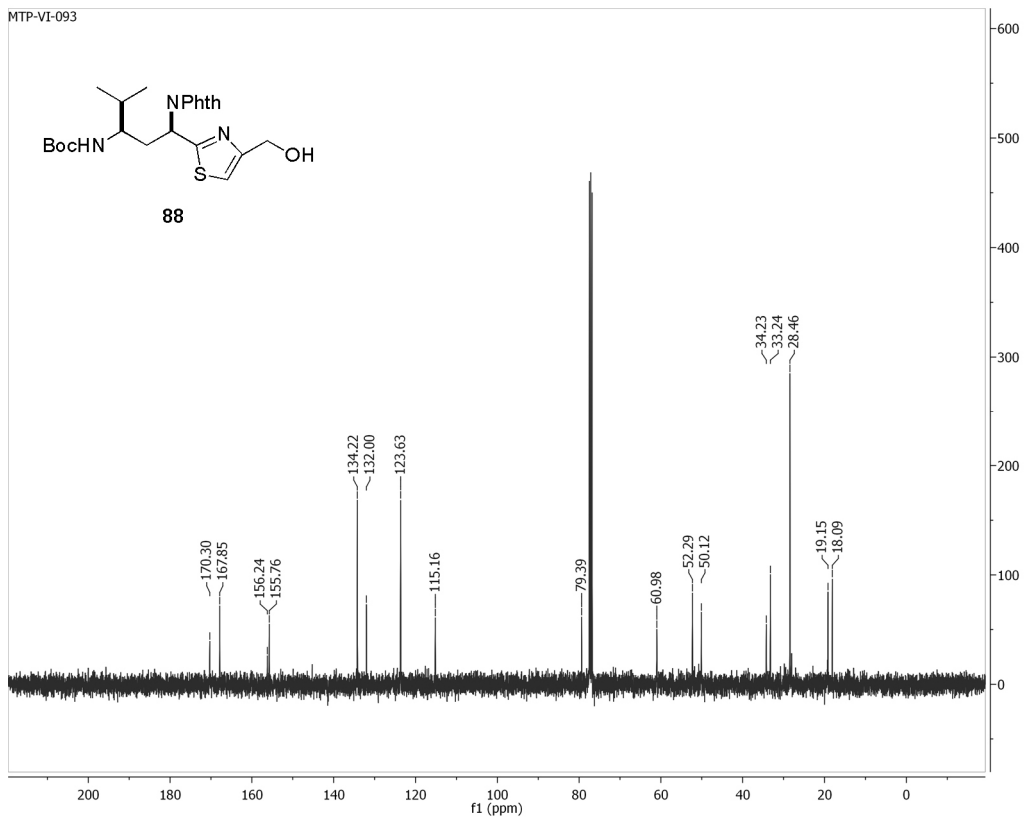
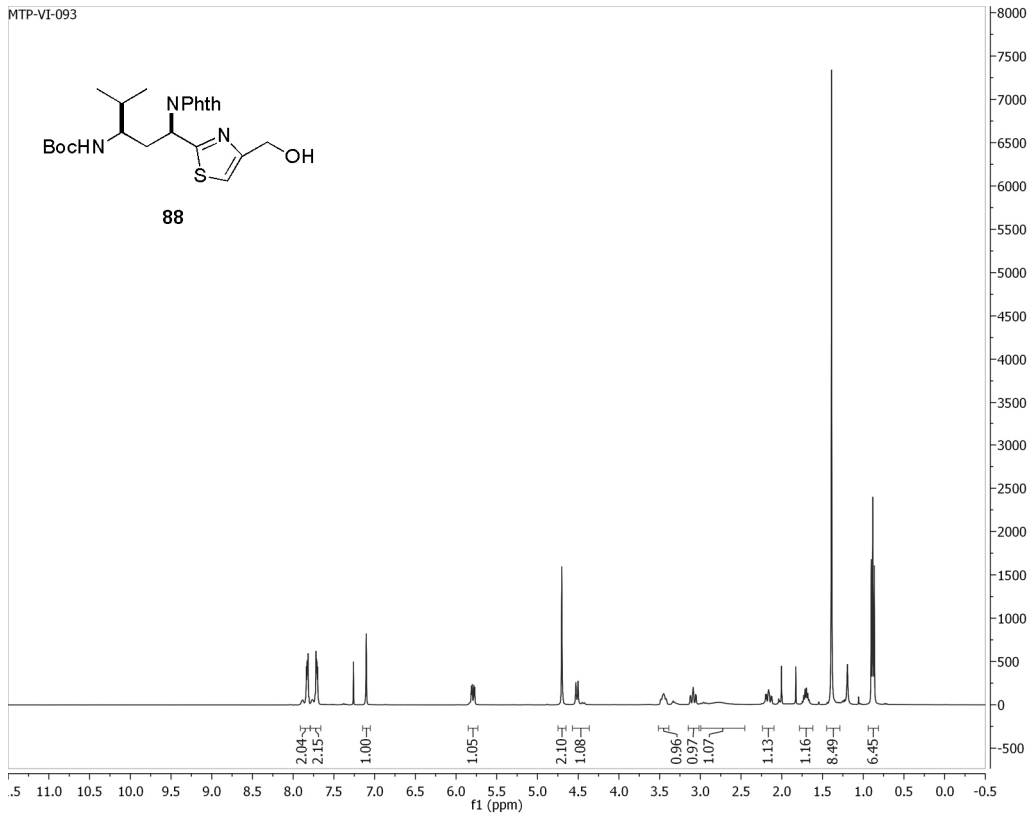


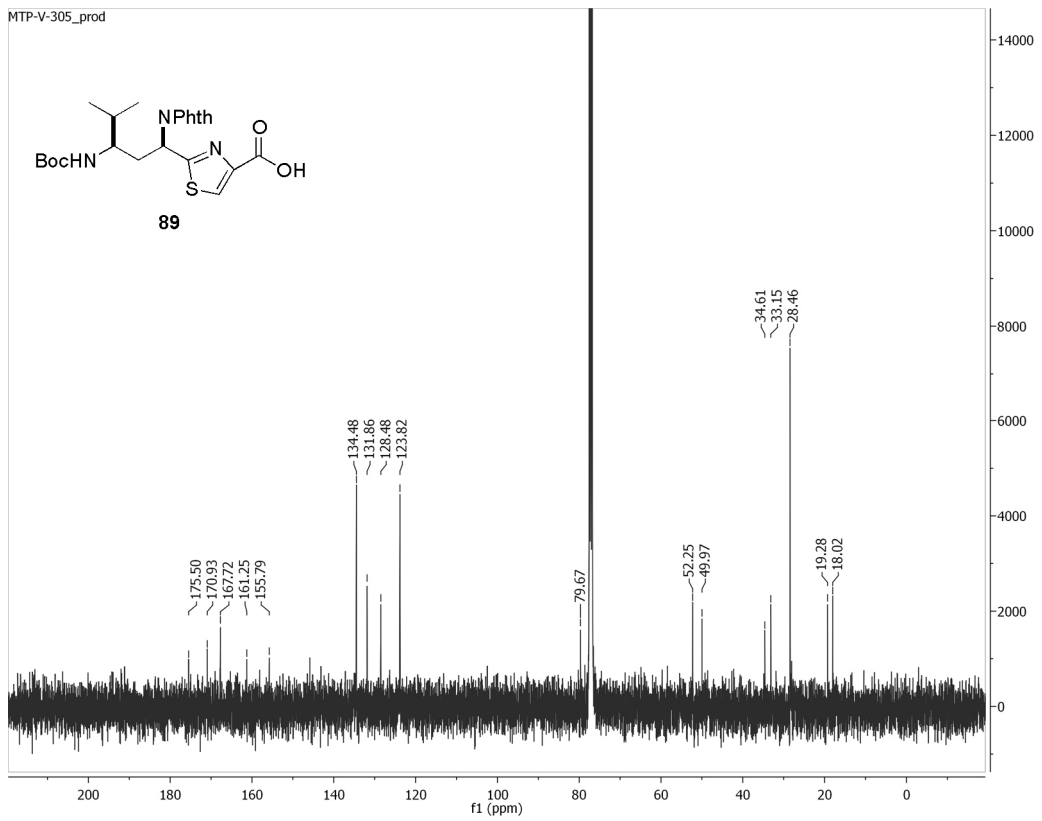
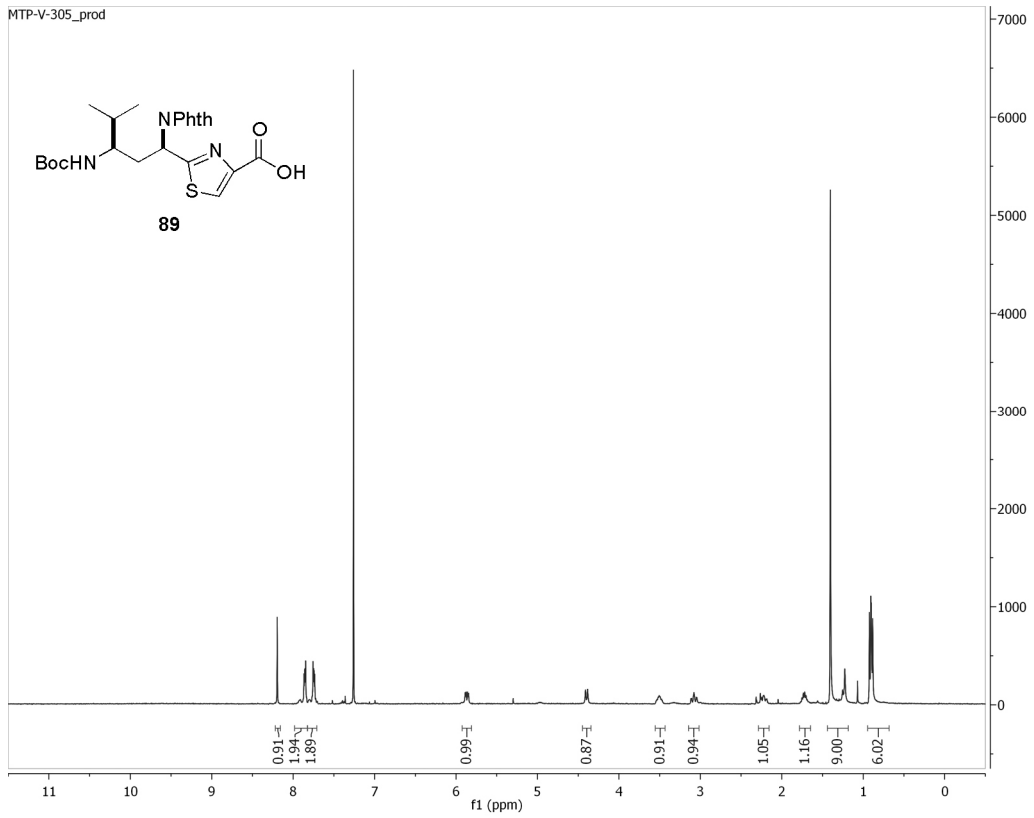
MTP-III-252

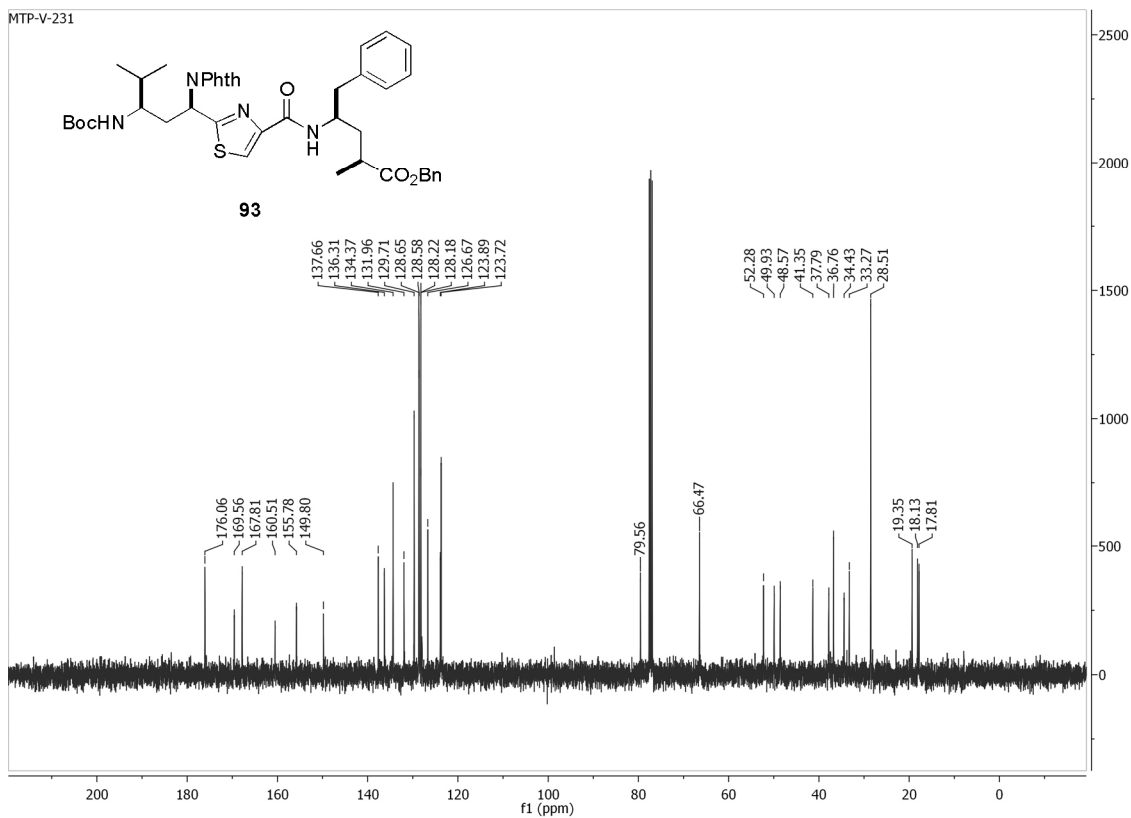
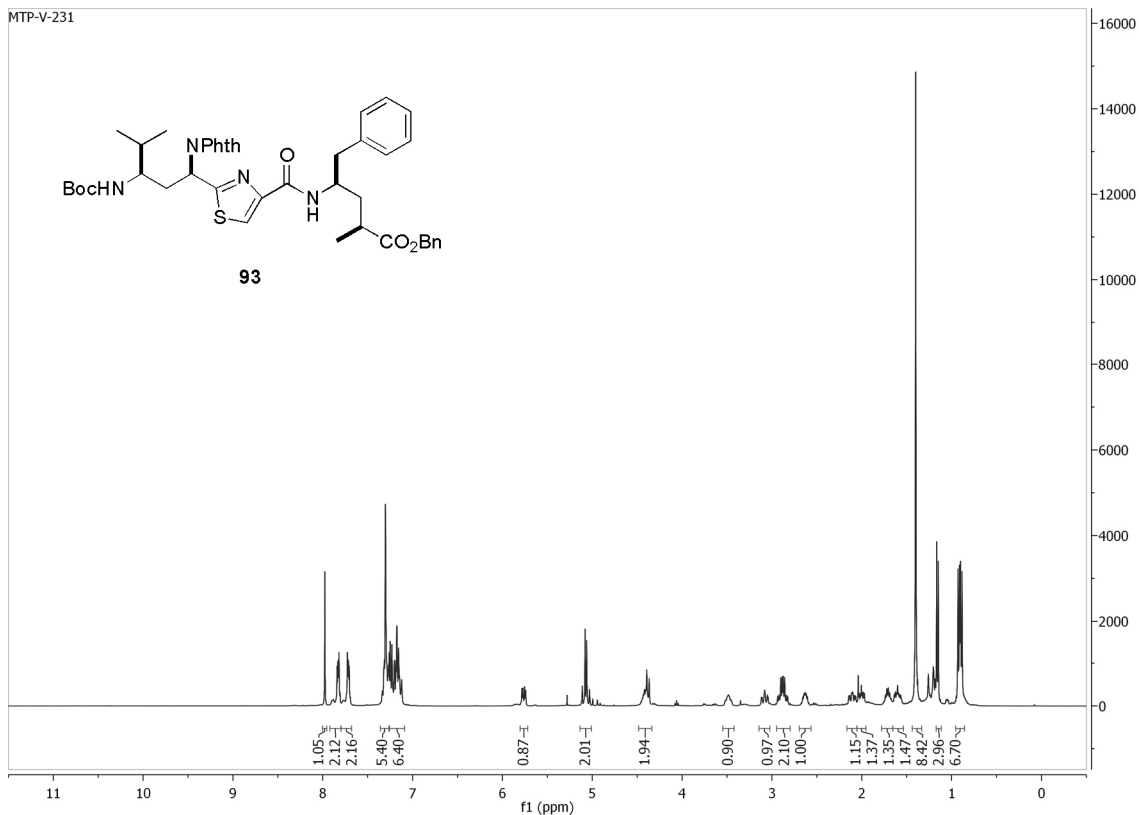


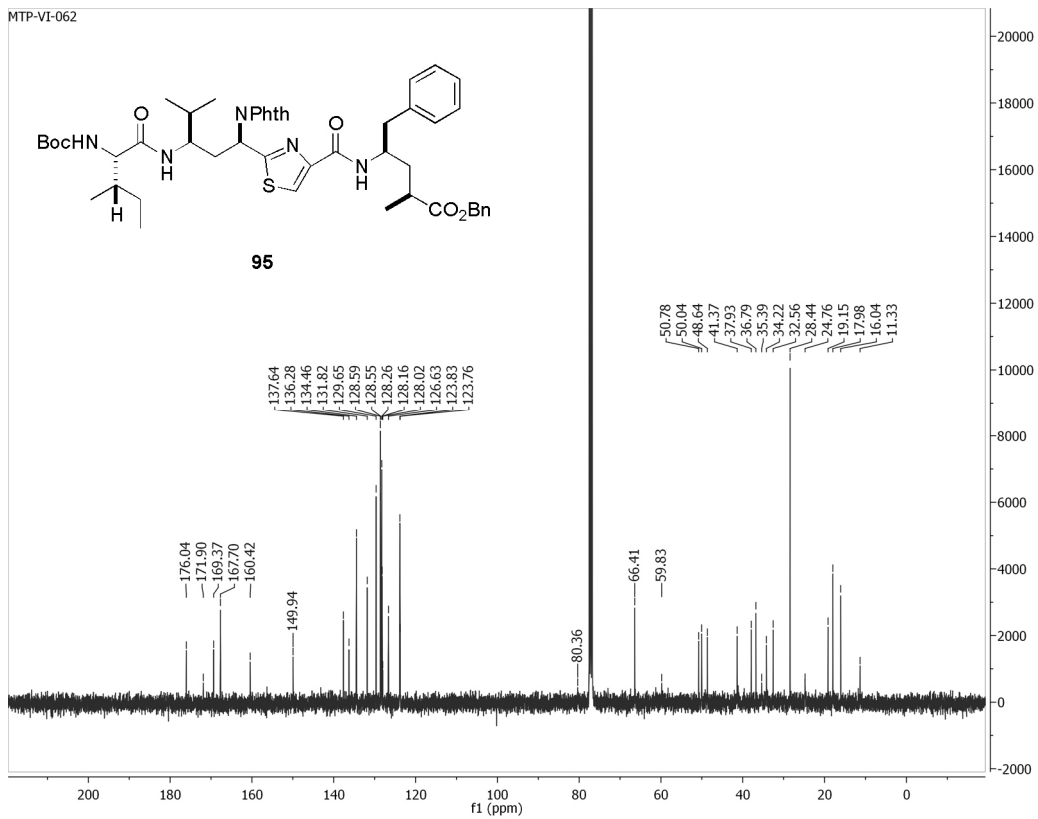
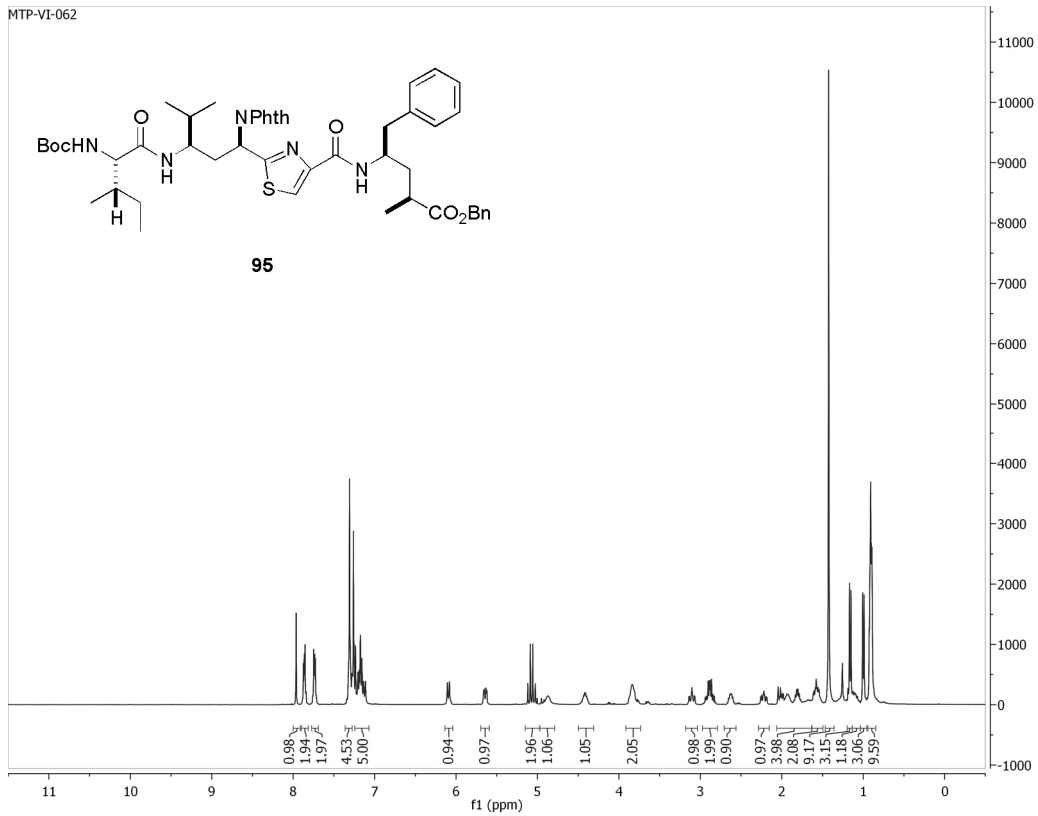


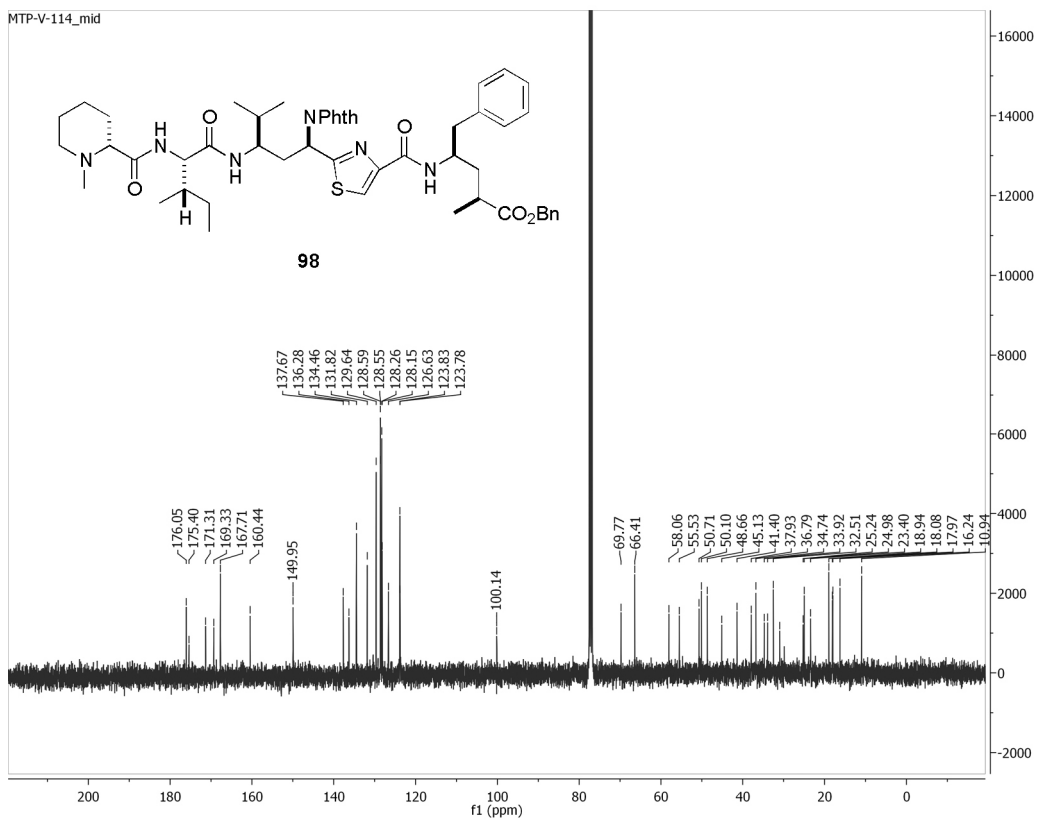
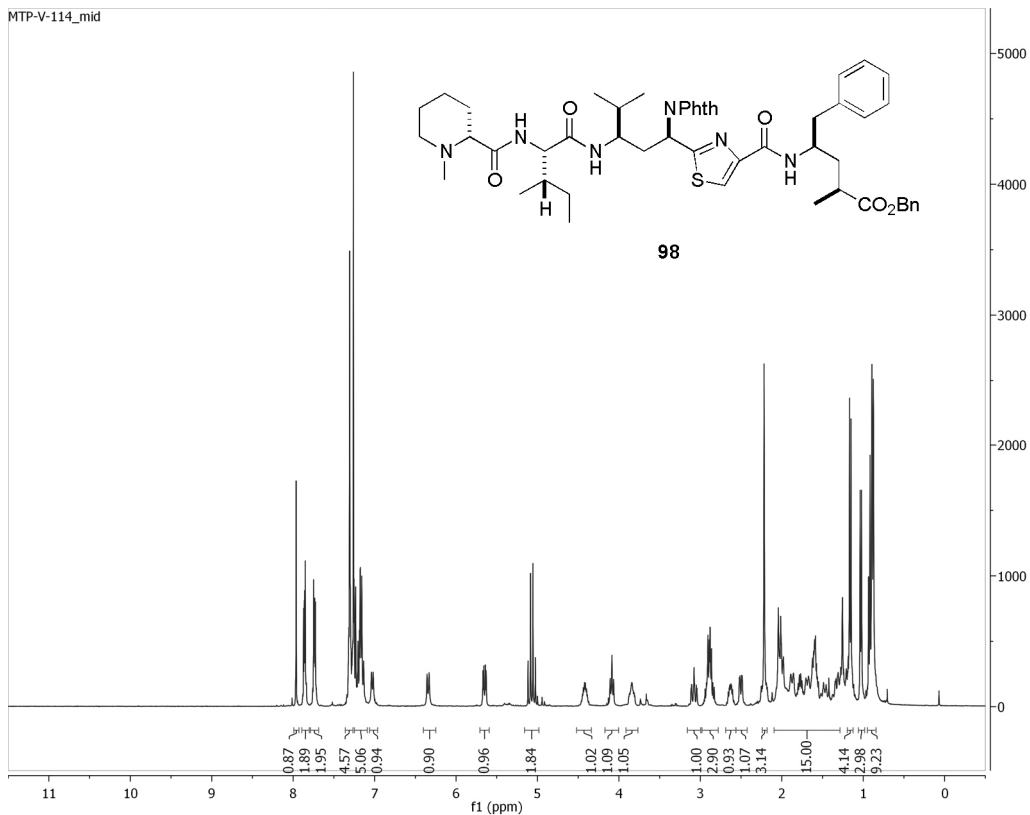


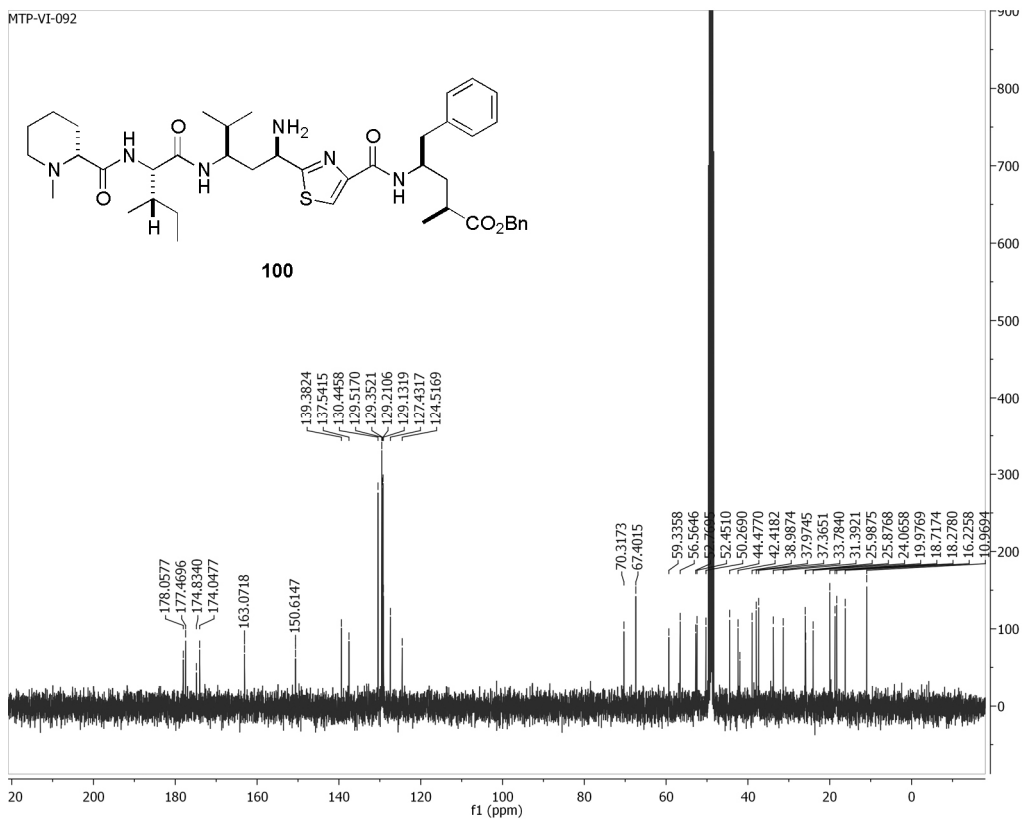
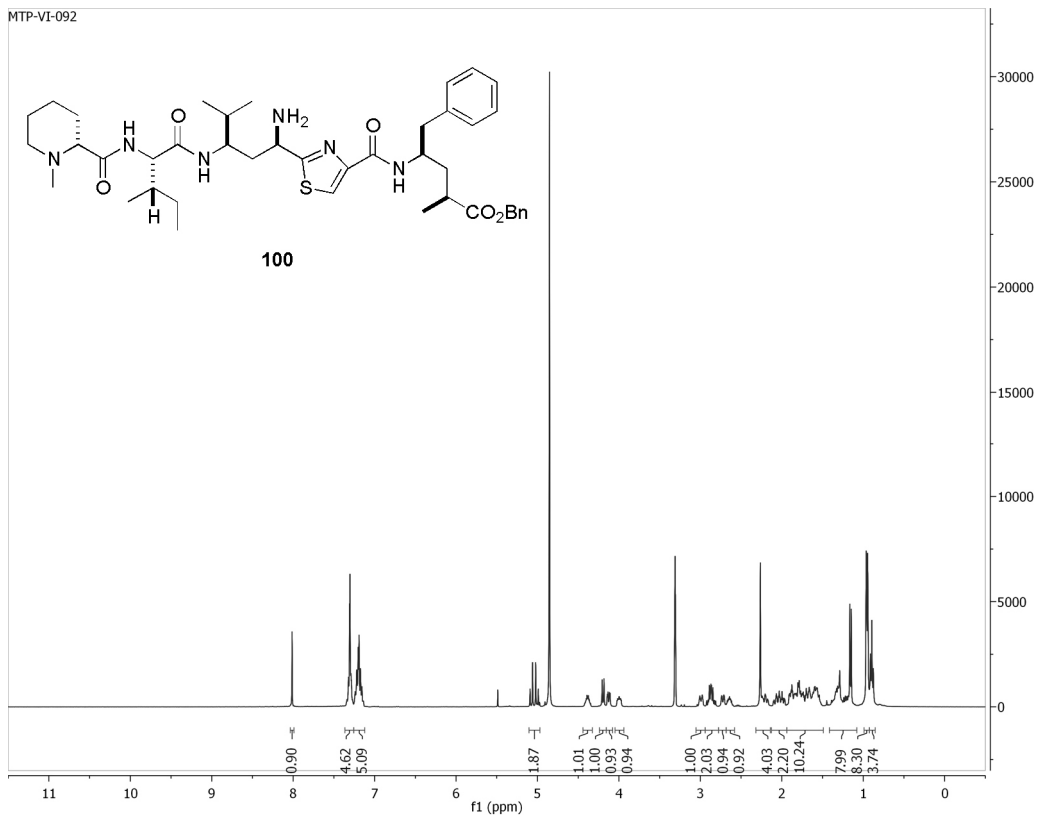


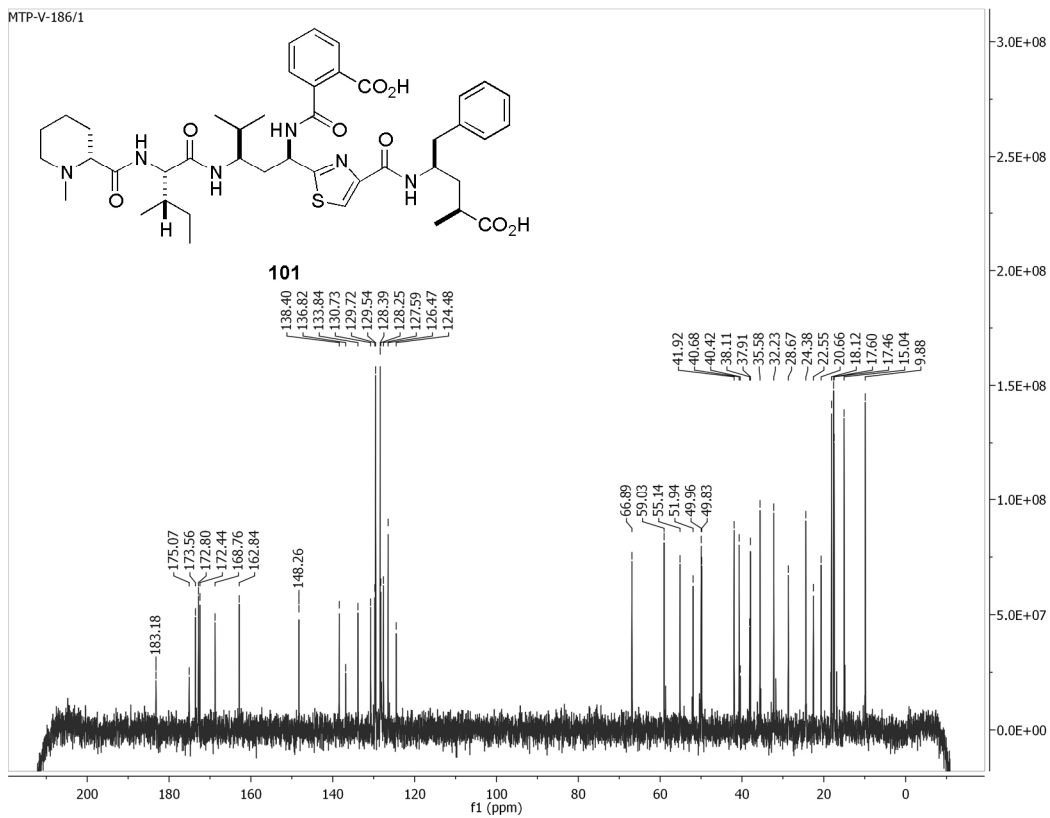
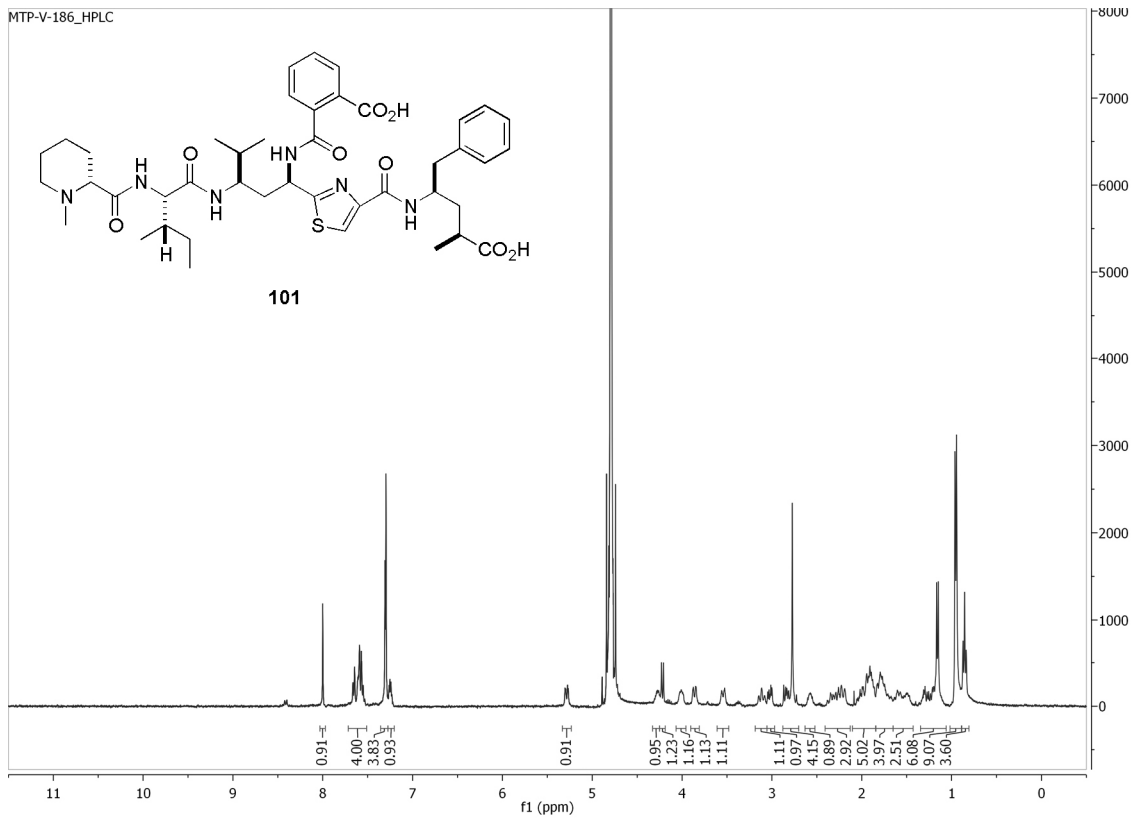


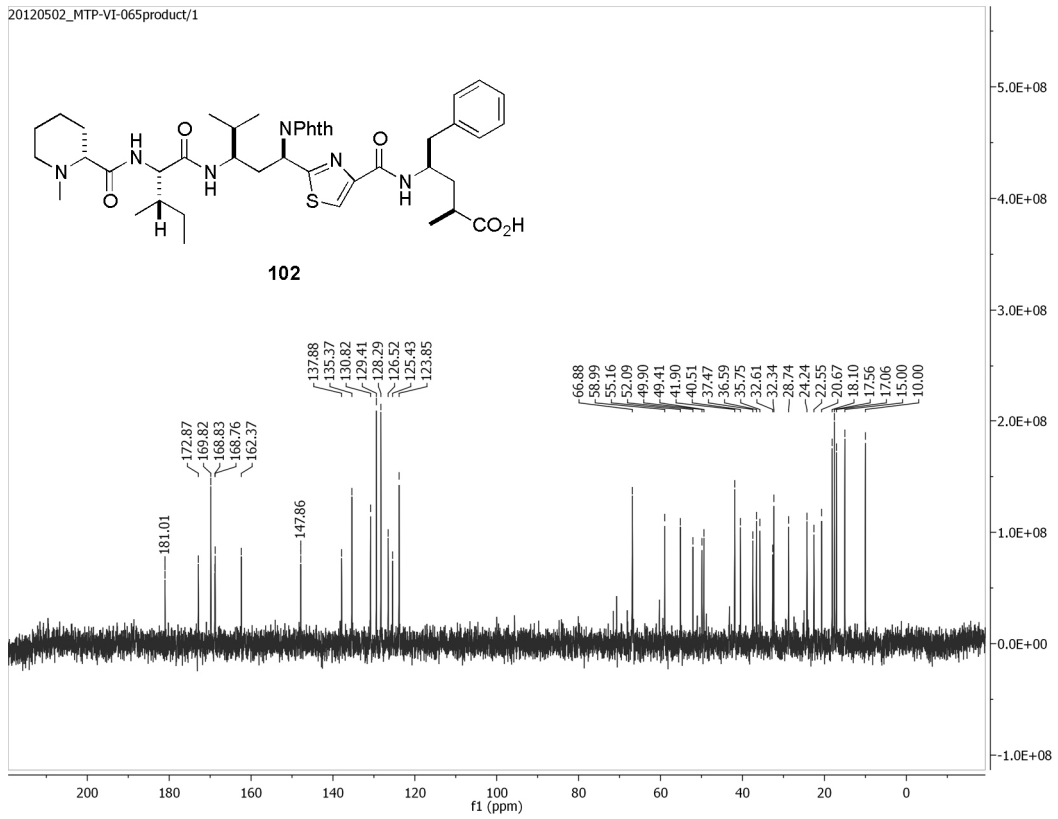
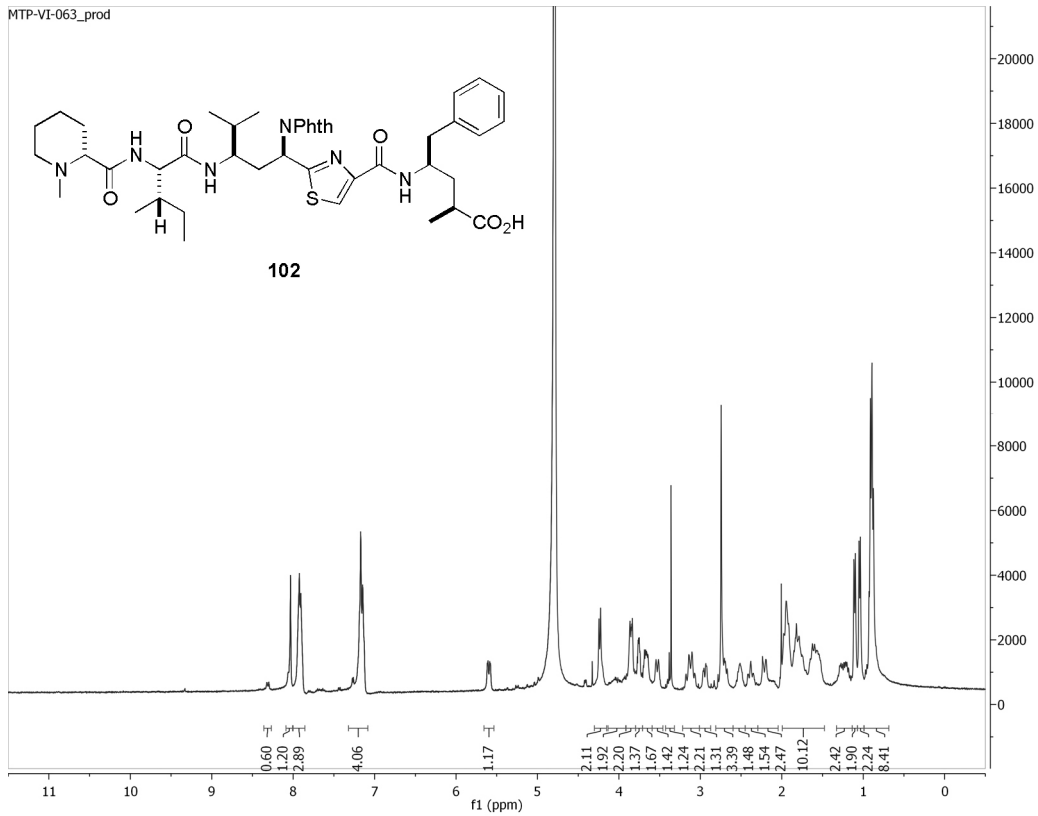


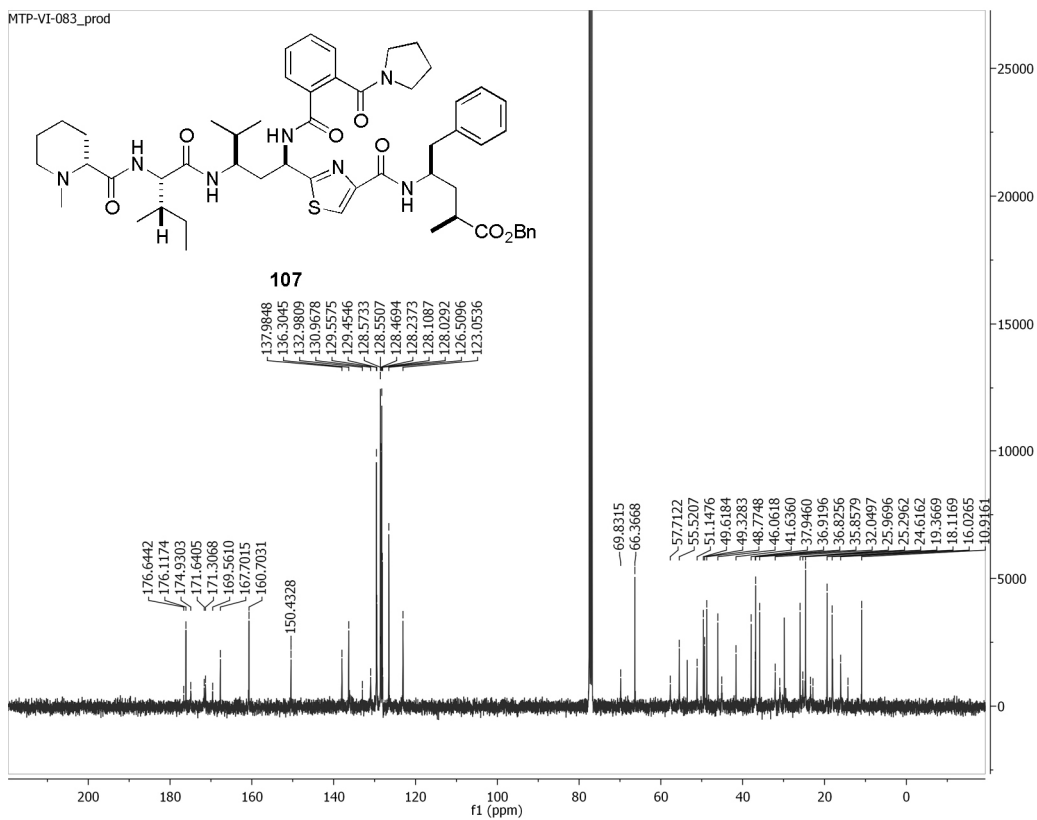
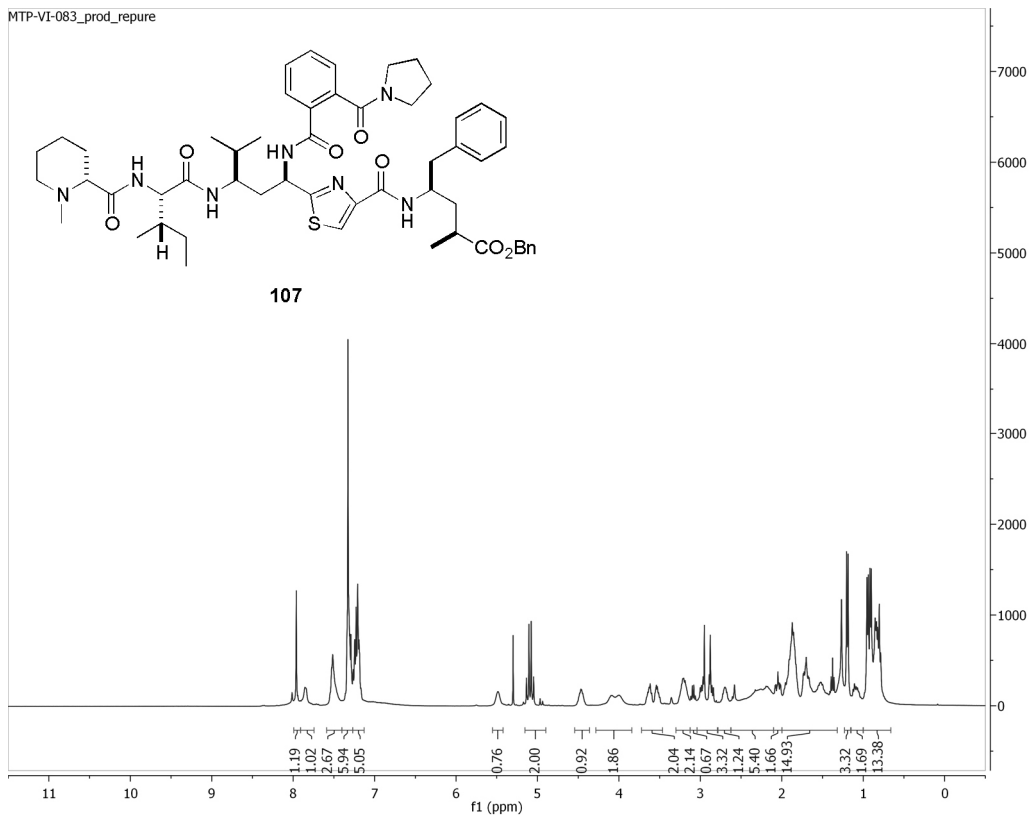


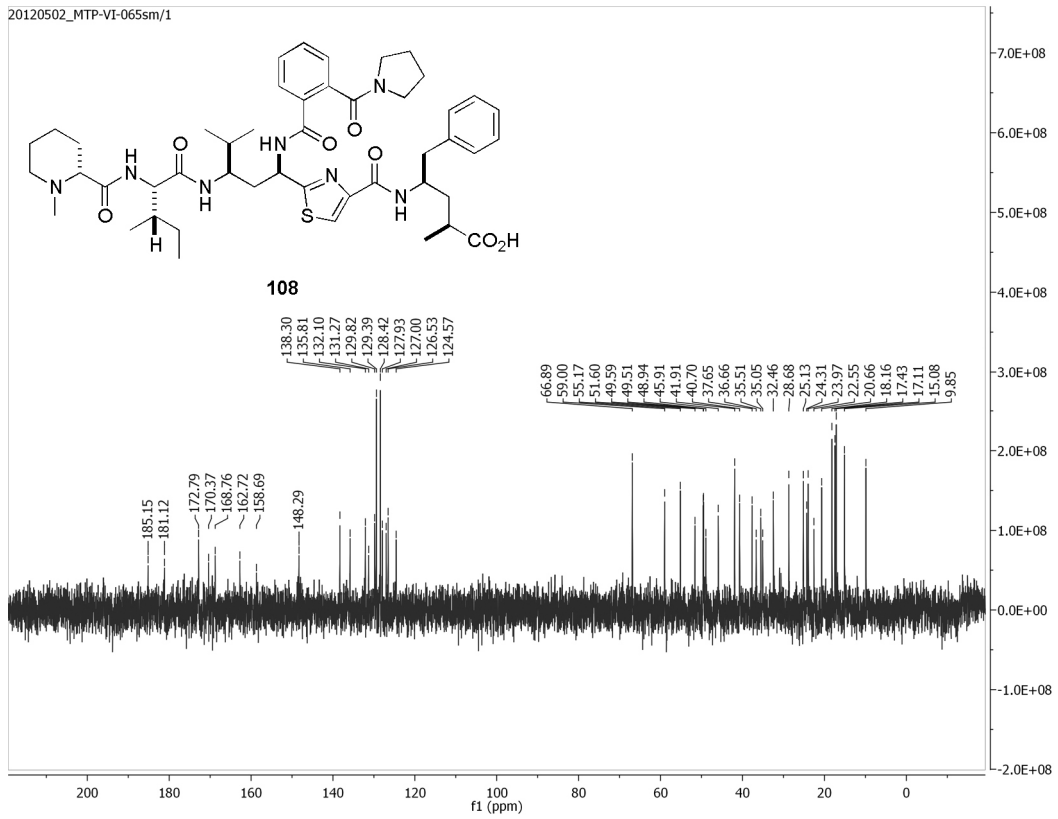
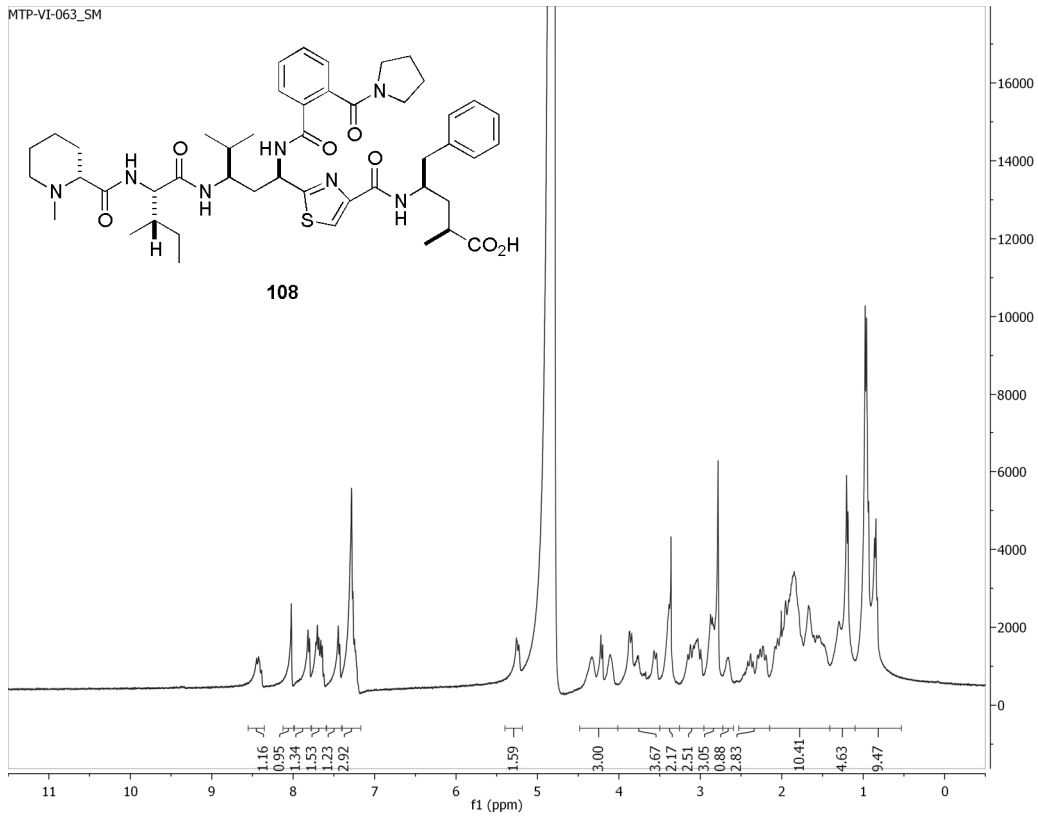




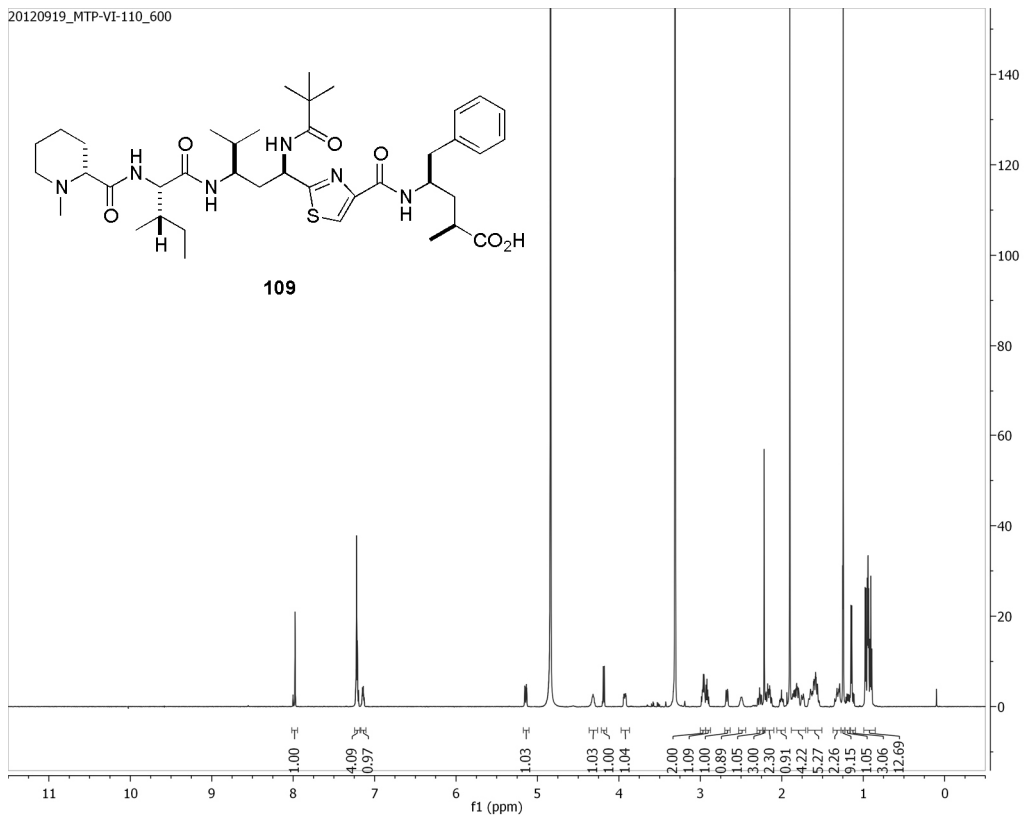




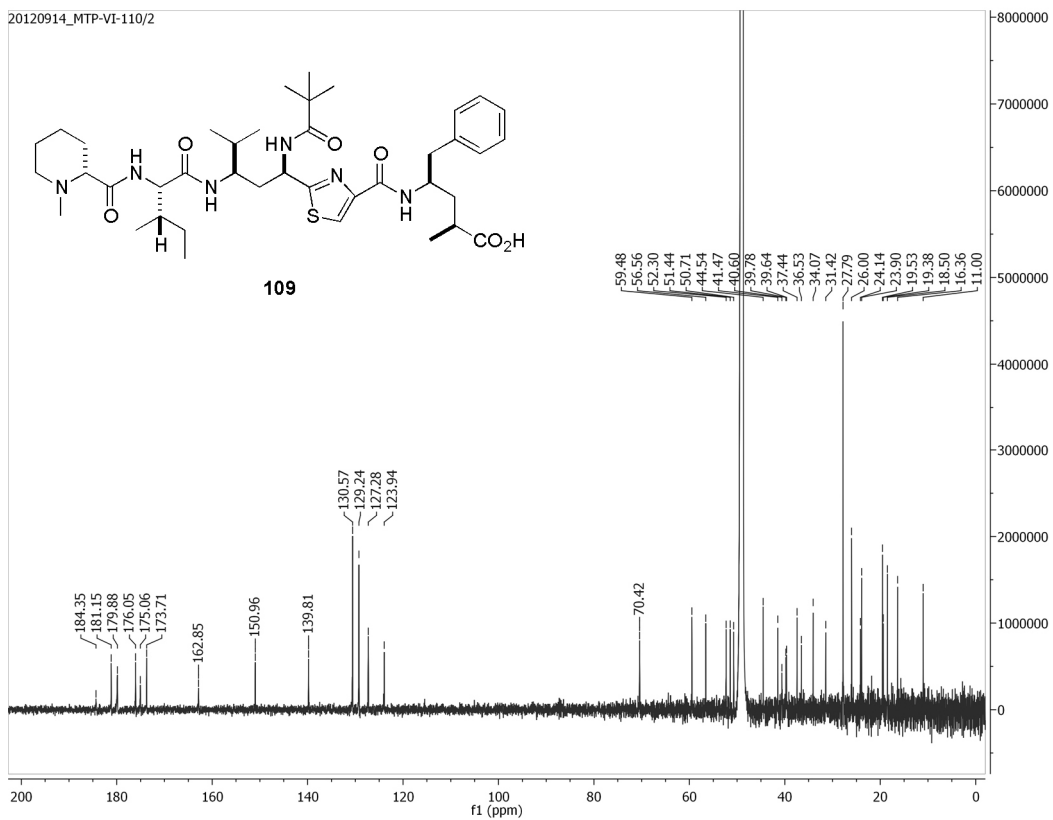


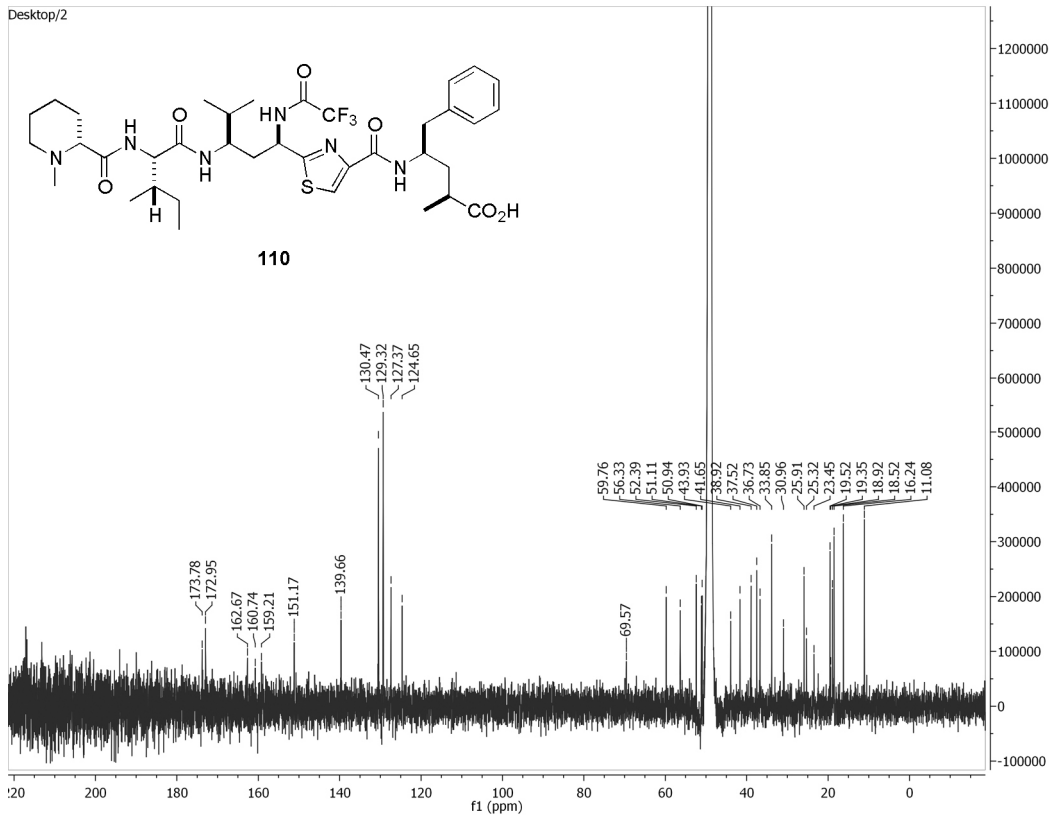
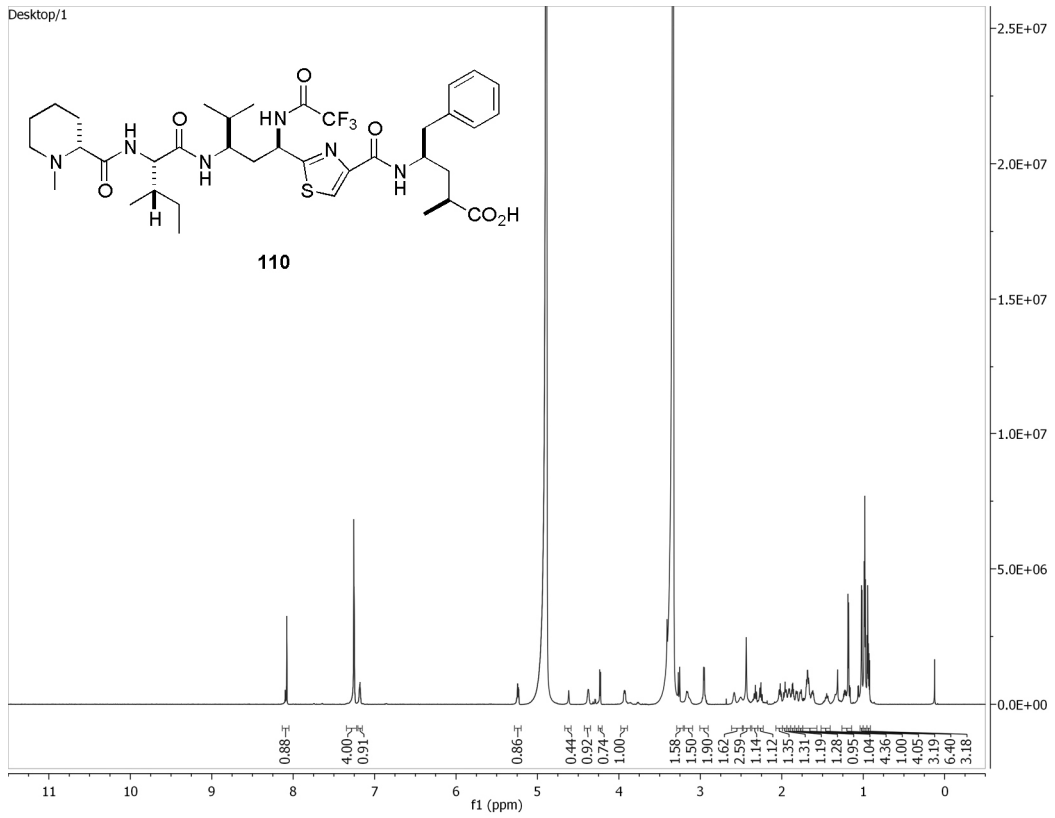


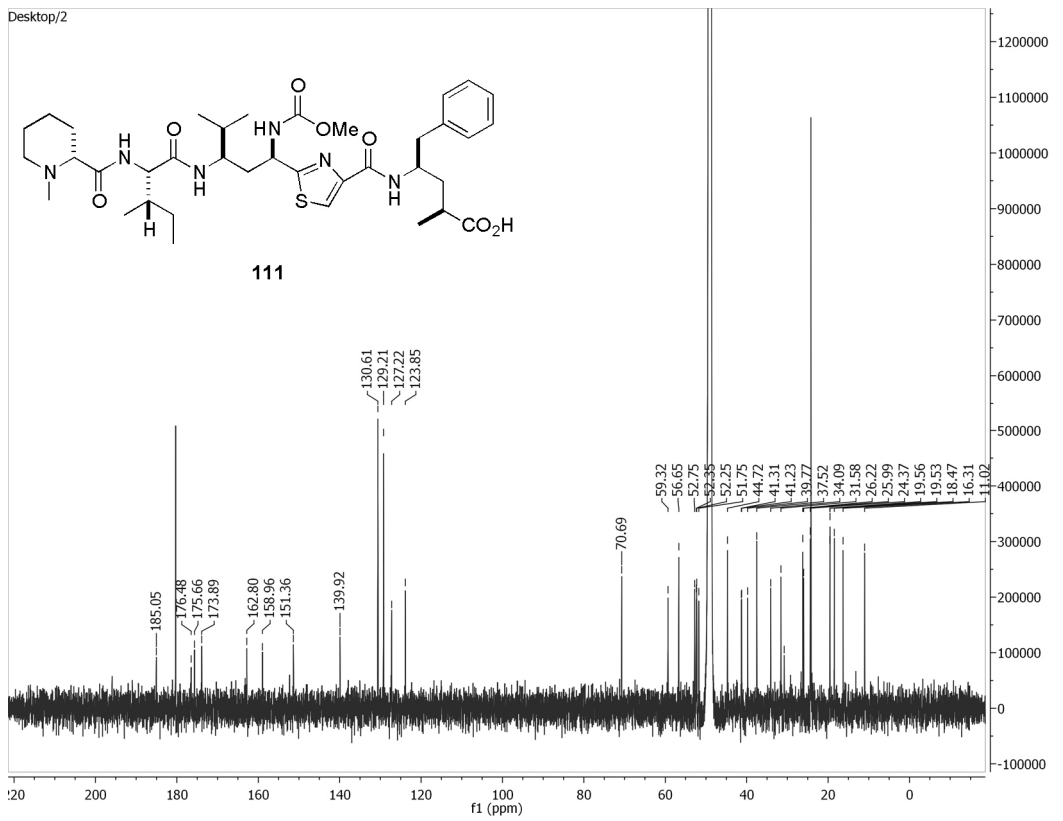
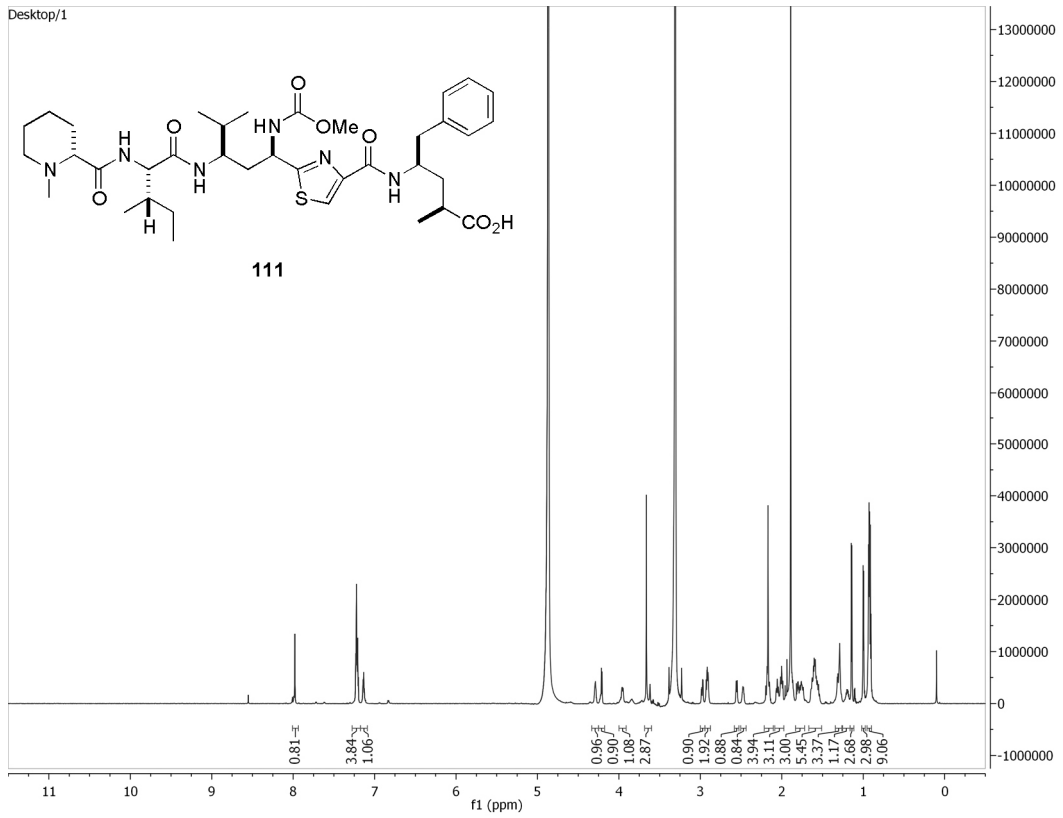
20120919_MTP-VI-110_600



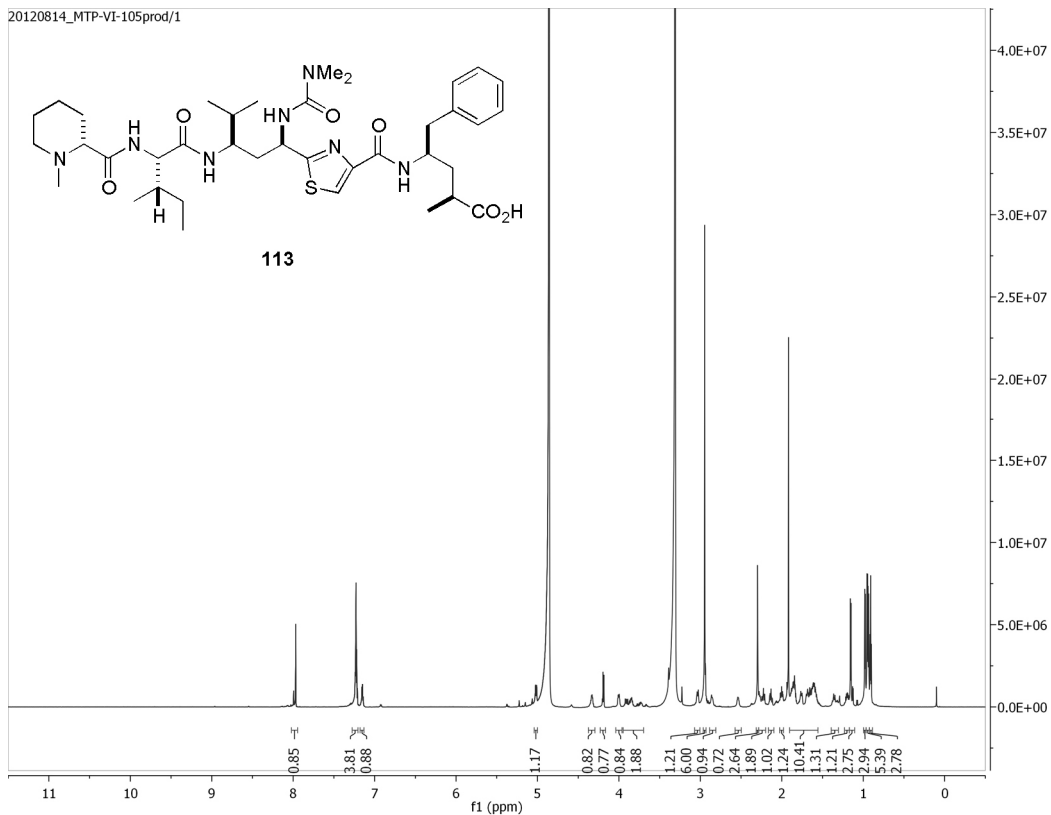
20120914_MTP-VI-110/2



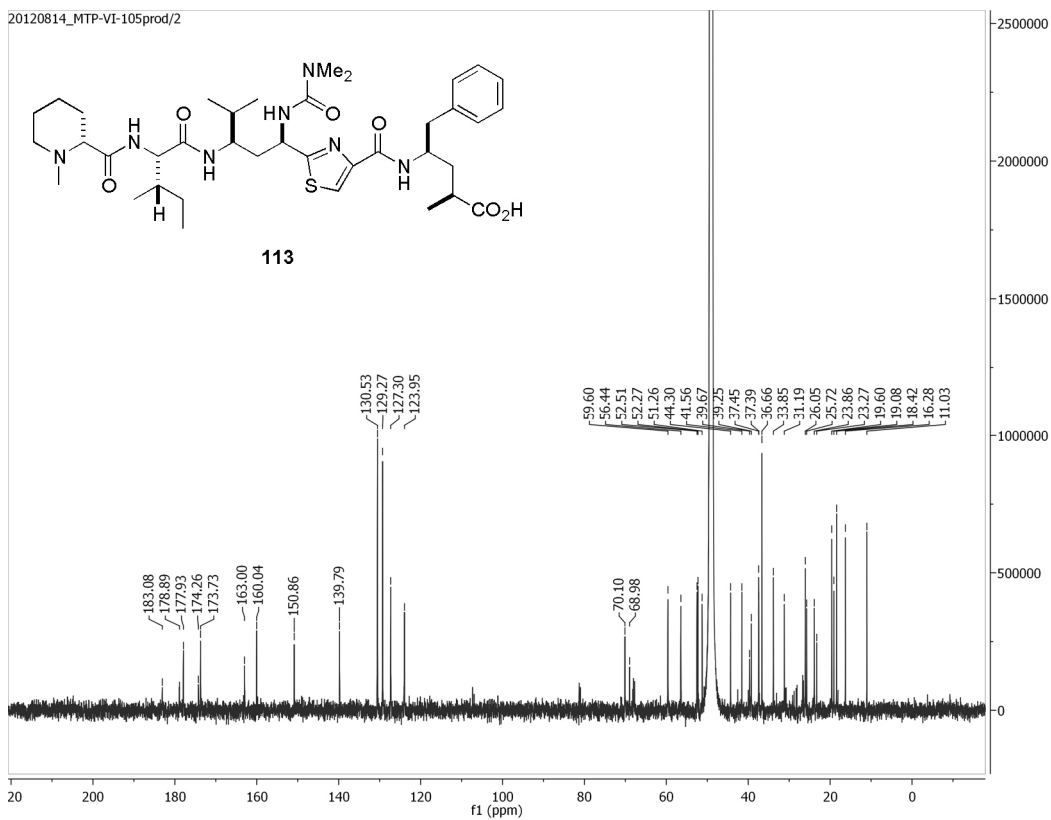


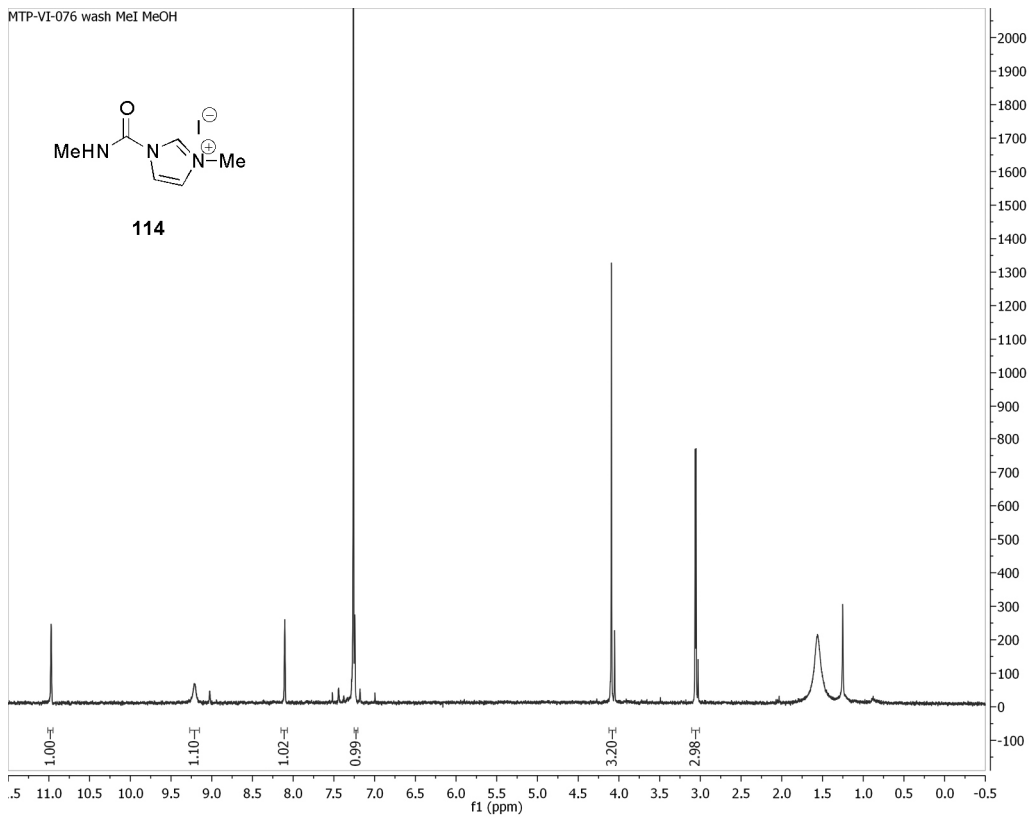


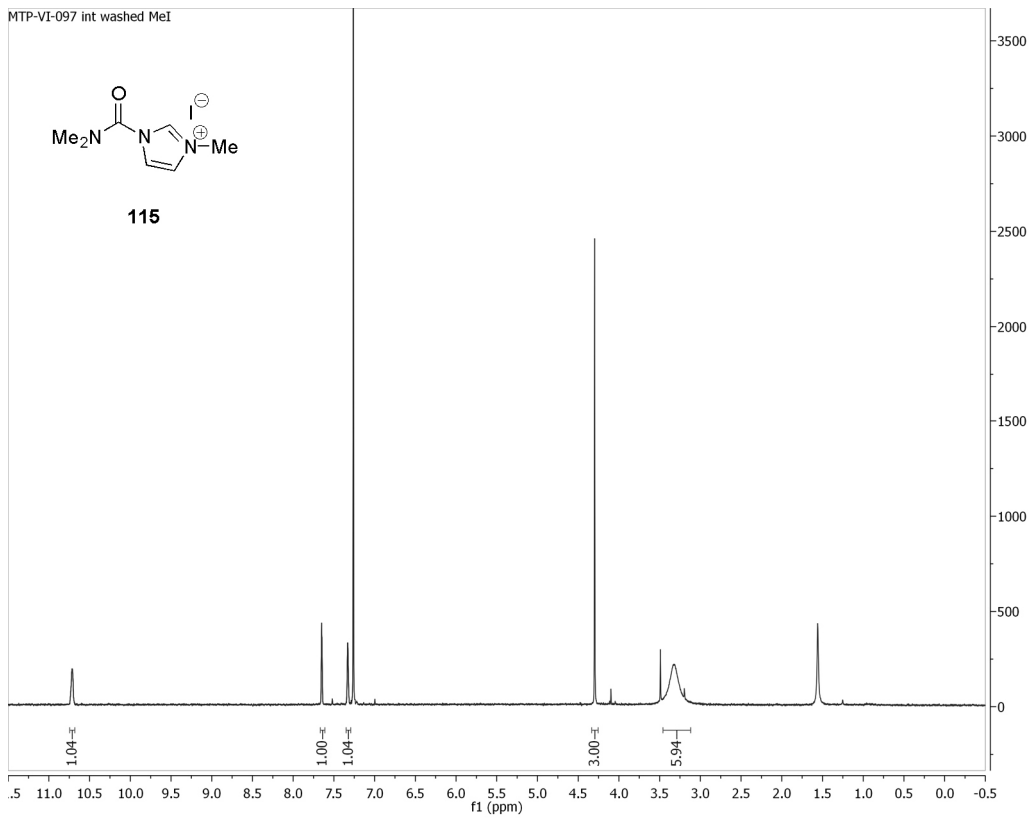
20120814_MTP-VI-105prod/1

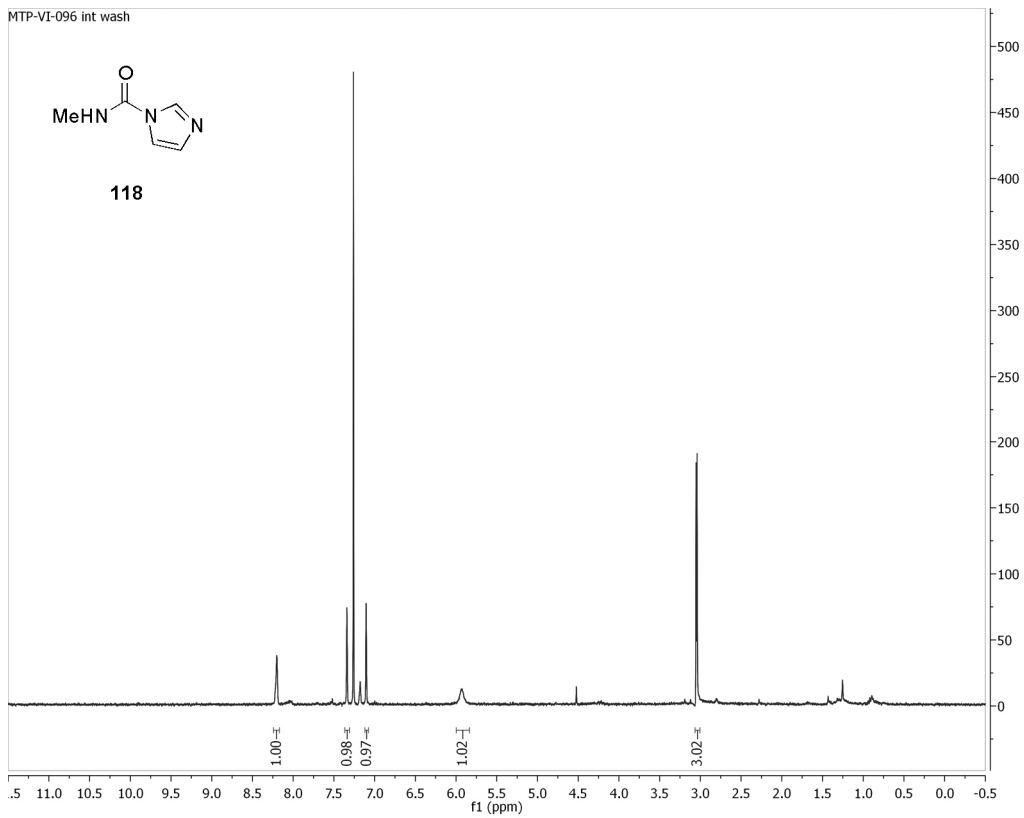


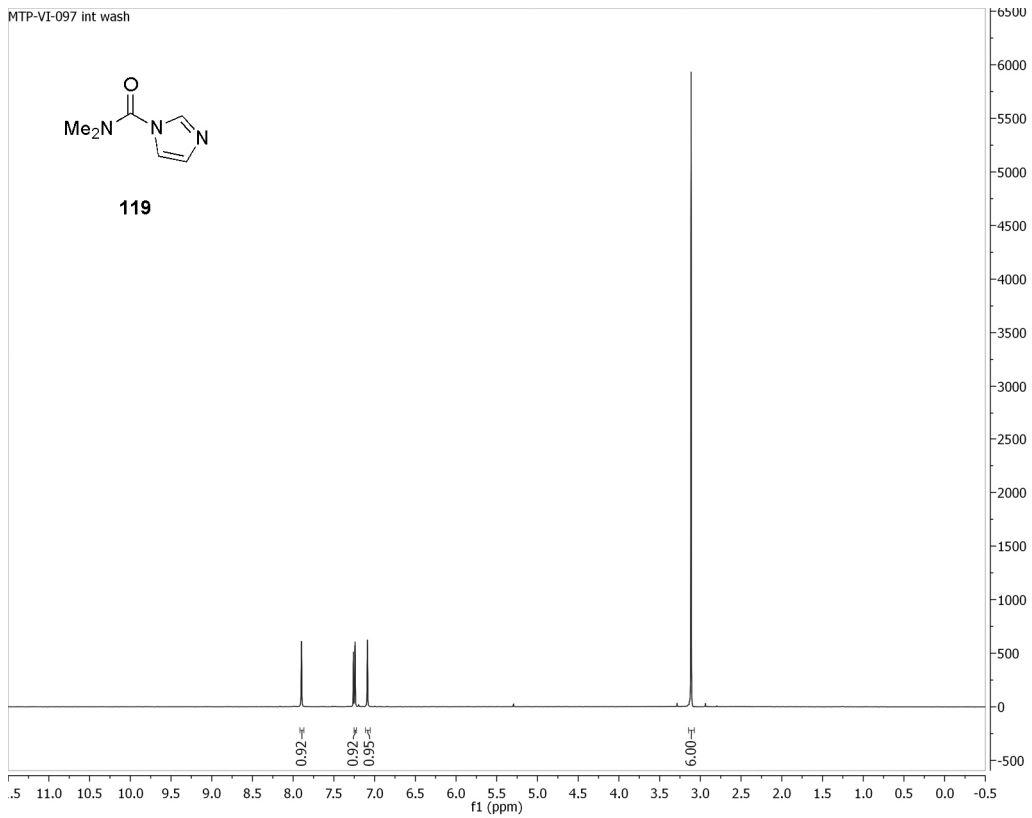
20120814_MTP-VI-105prod/2

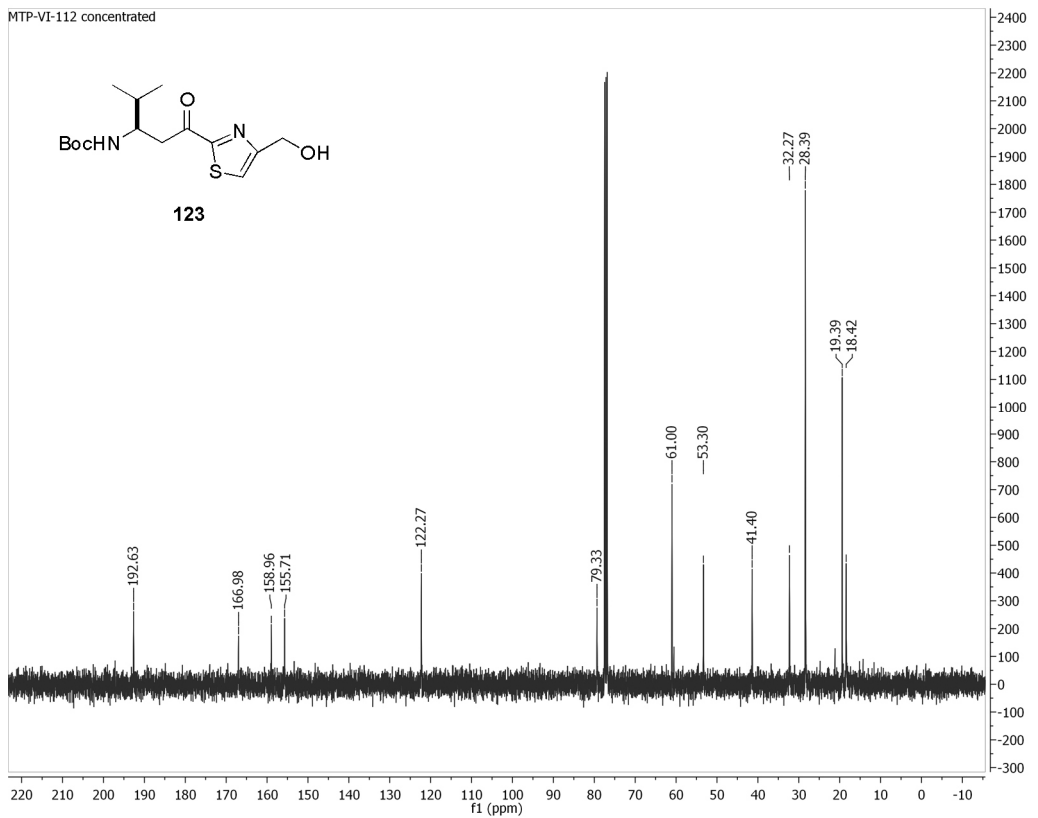
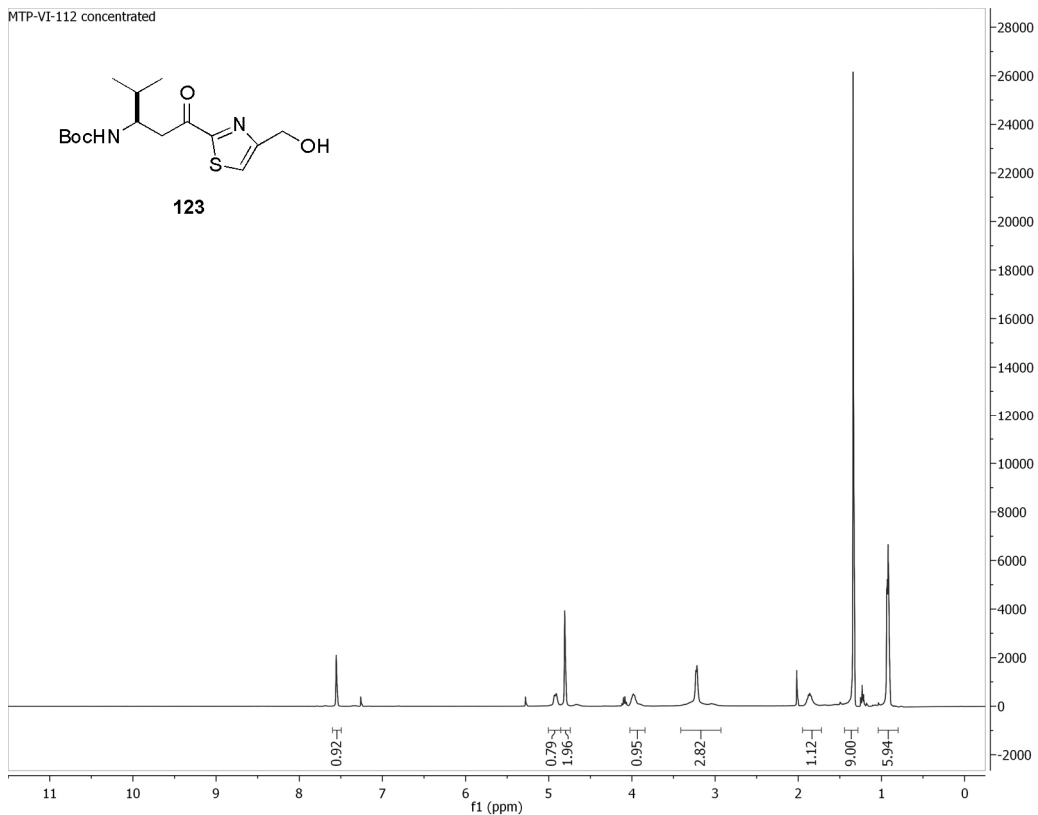




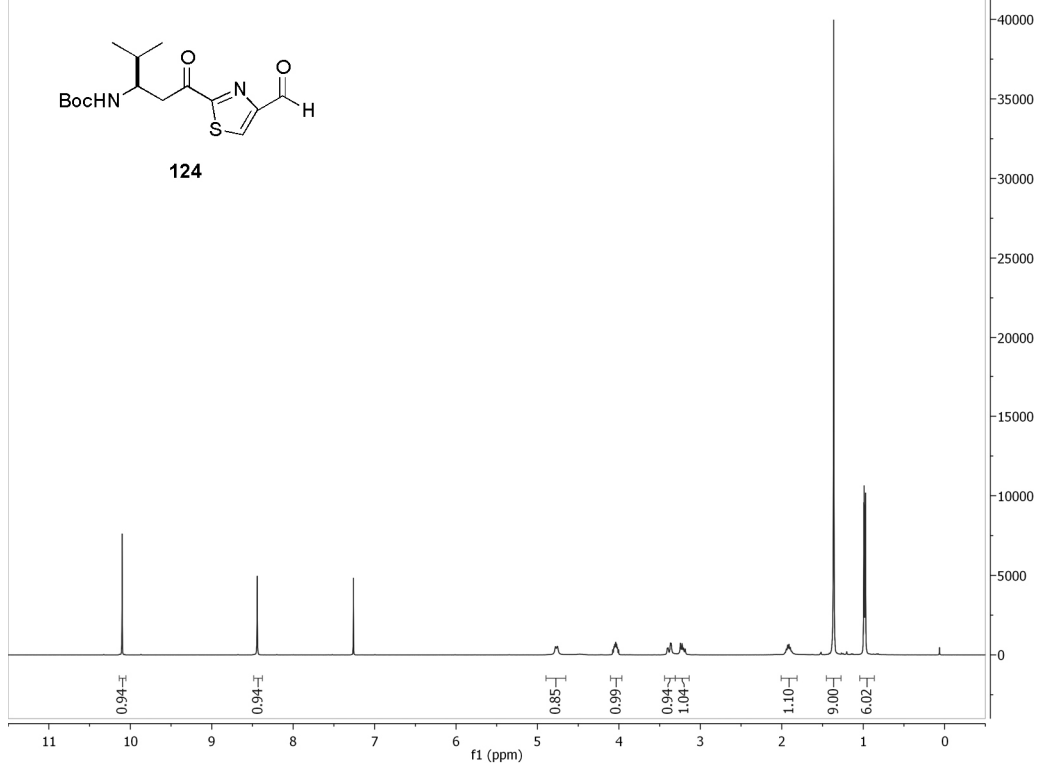




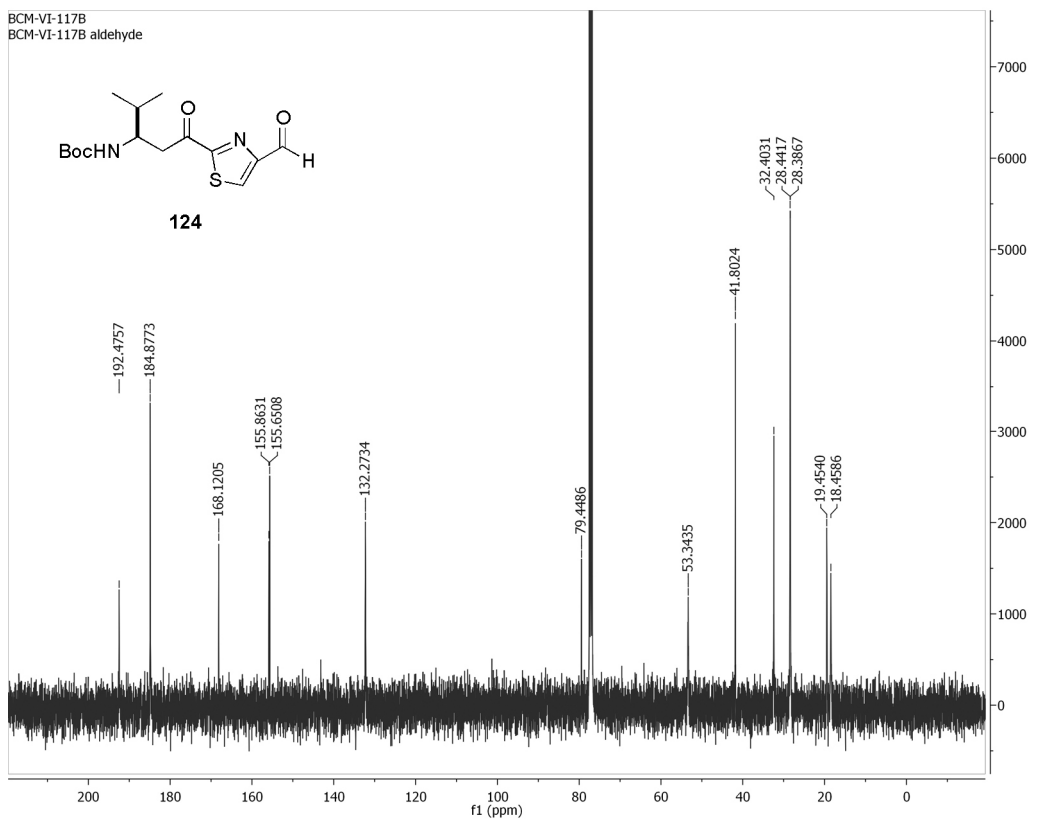


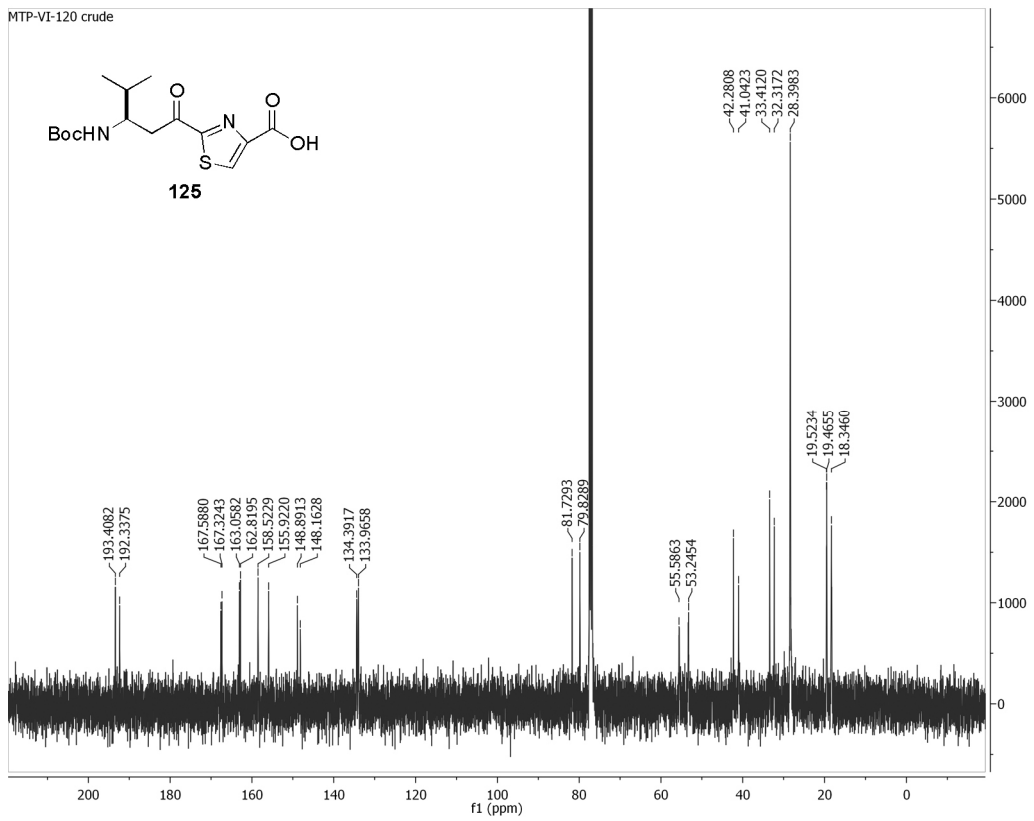
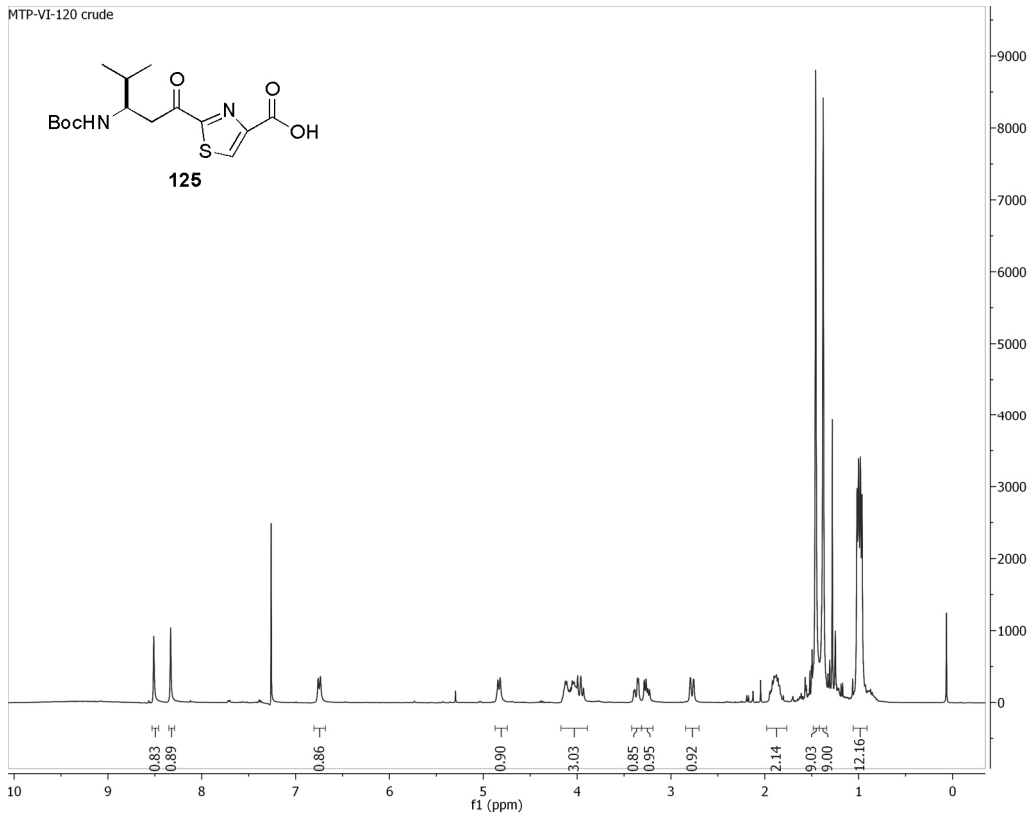


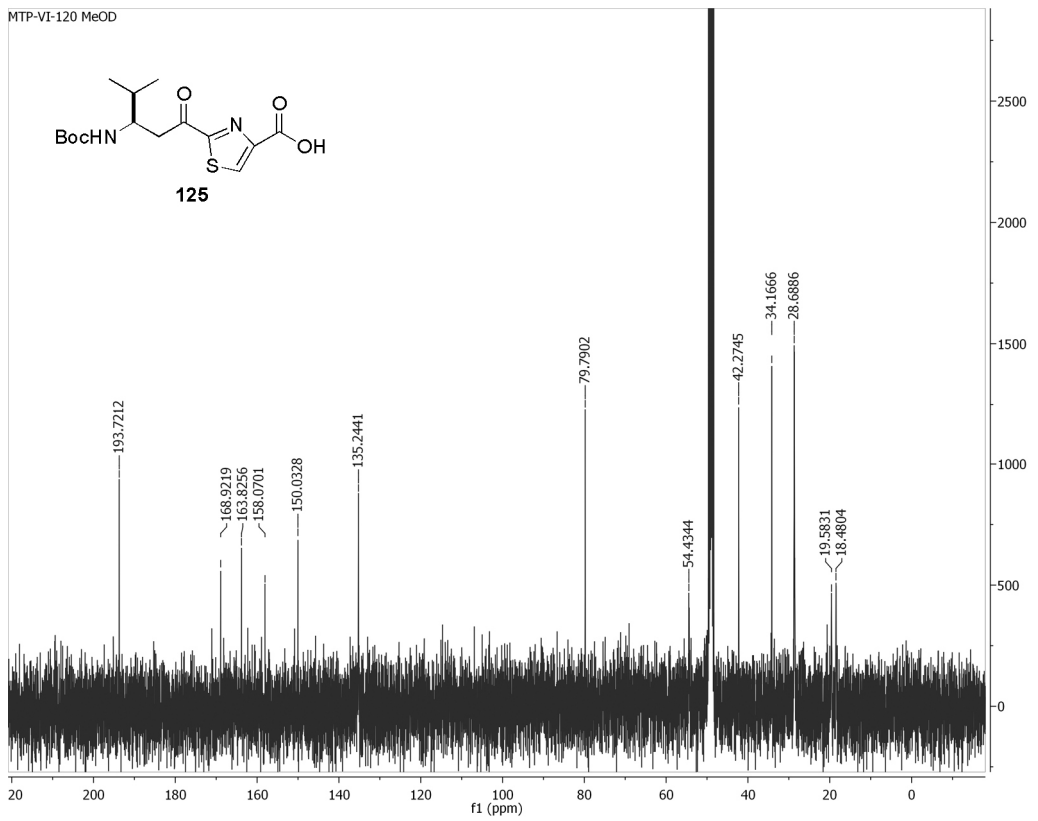
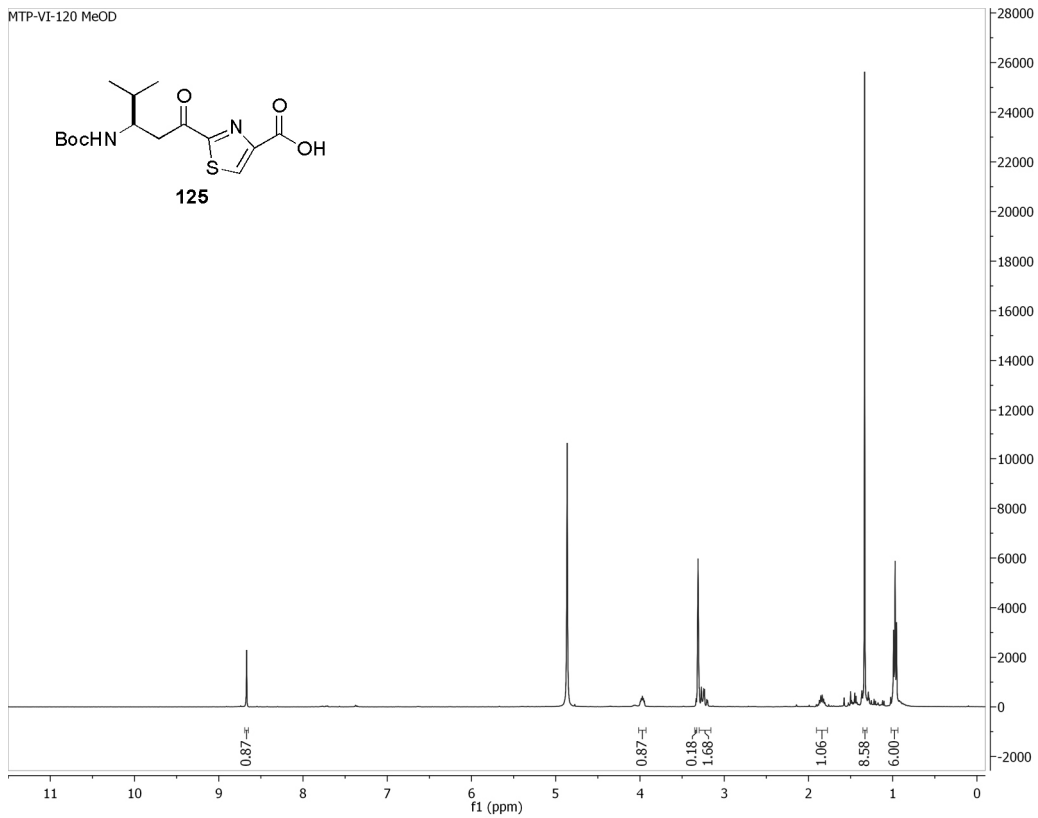
BCM-VI-117B
BCM-VI-117B aldehyde

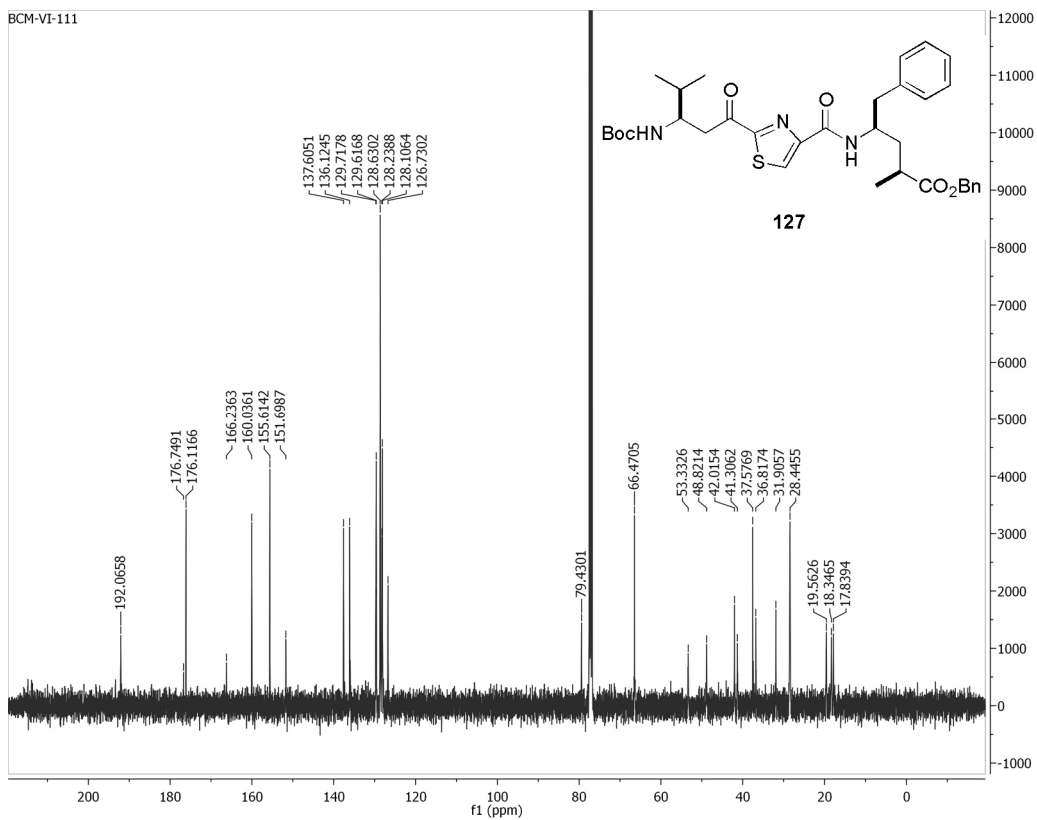
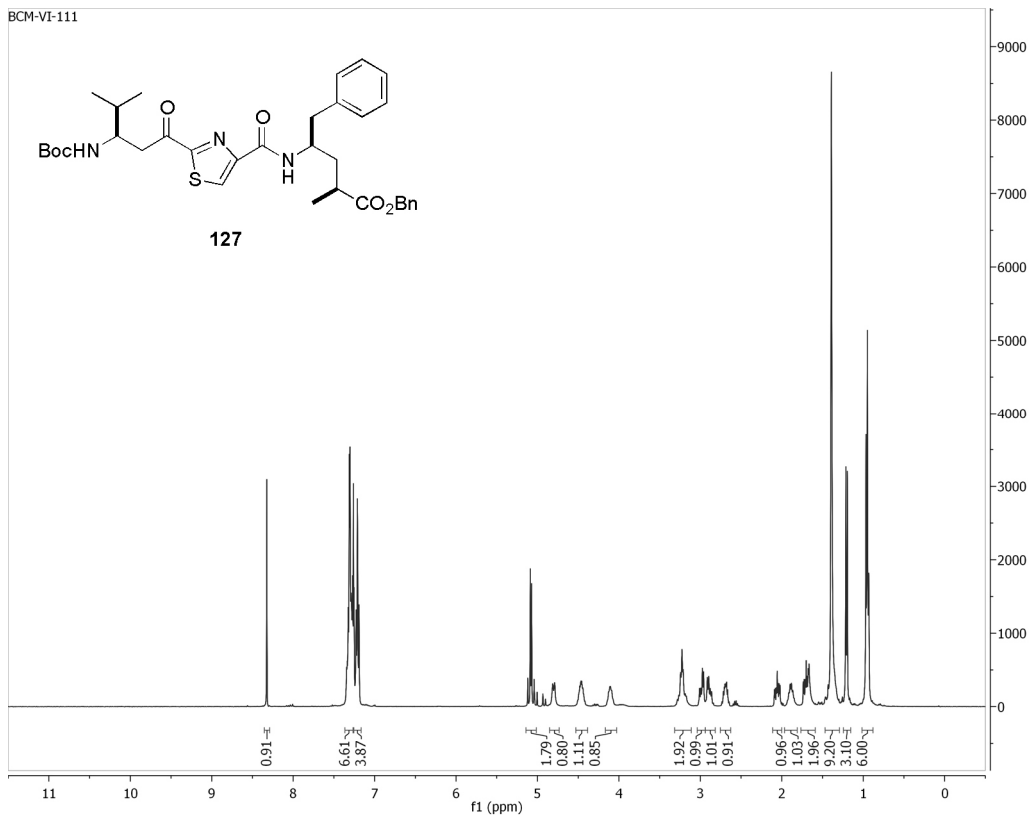


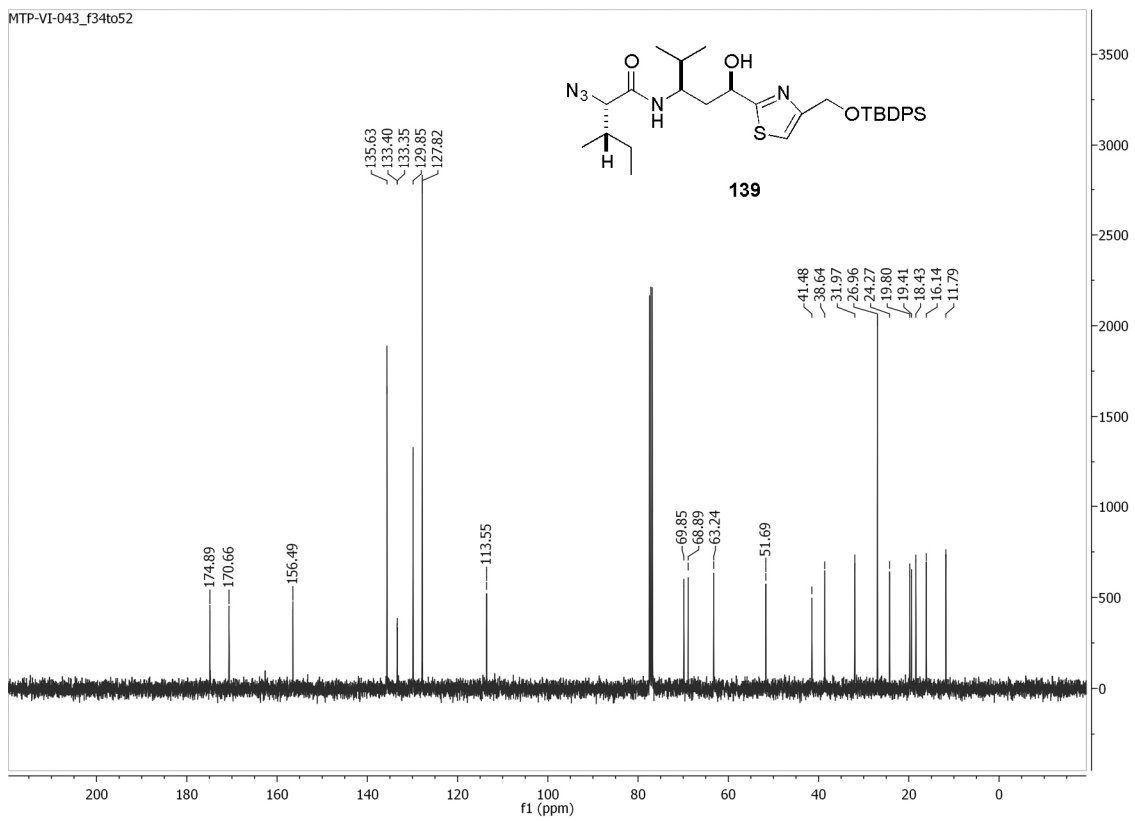
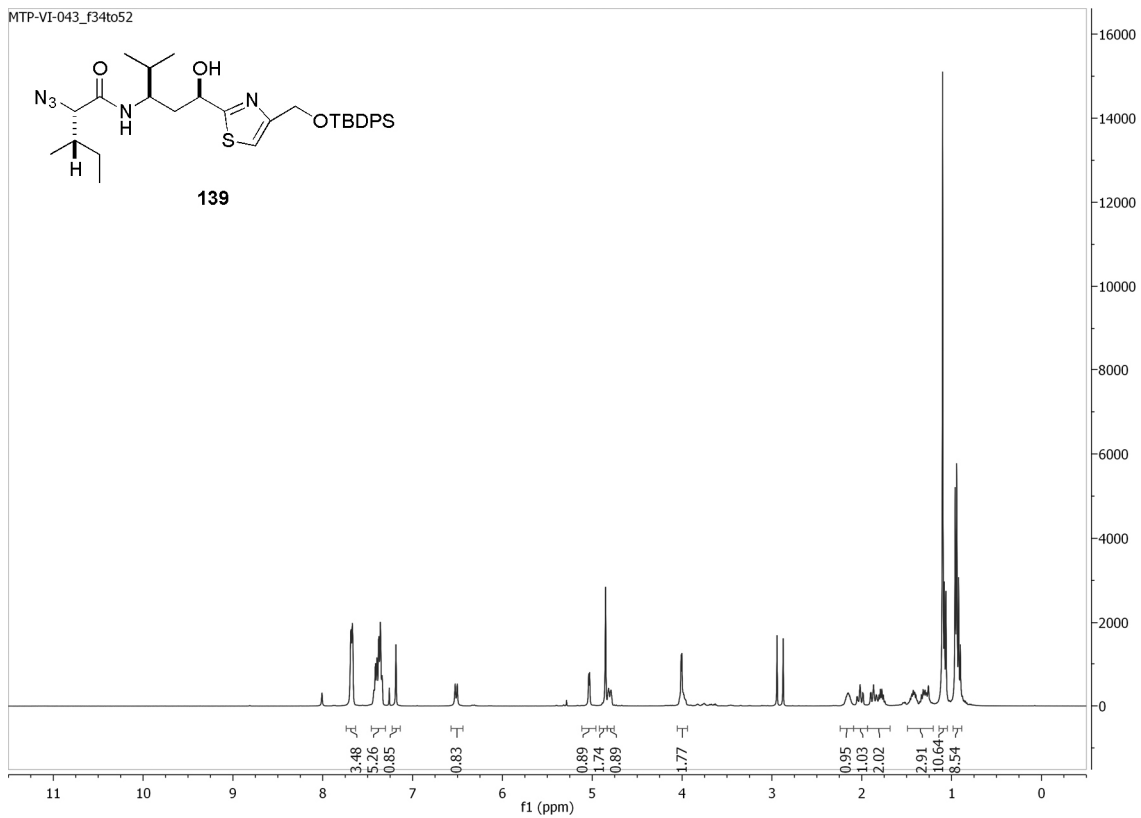
BCM-VI-117B
BCM-VI-117B aldehyde

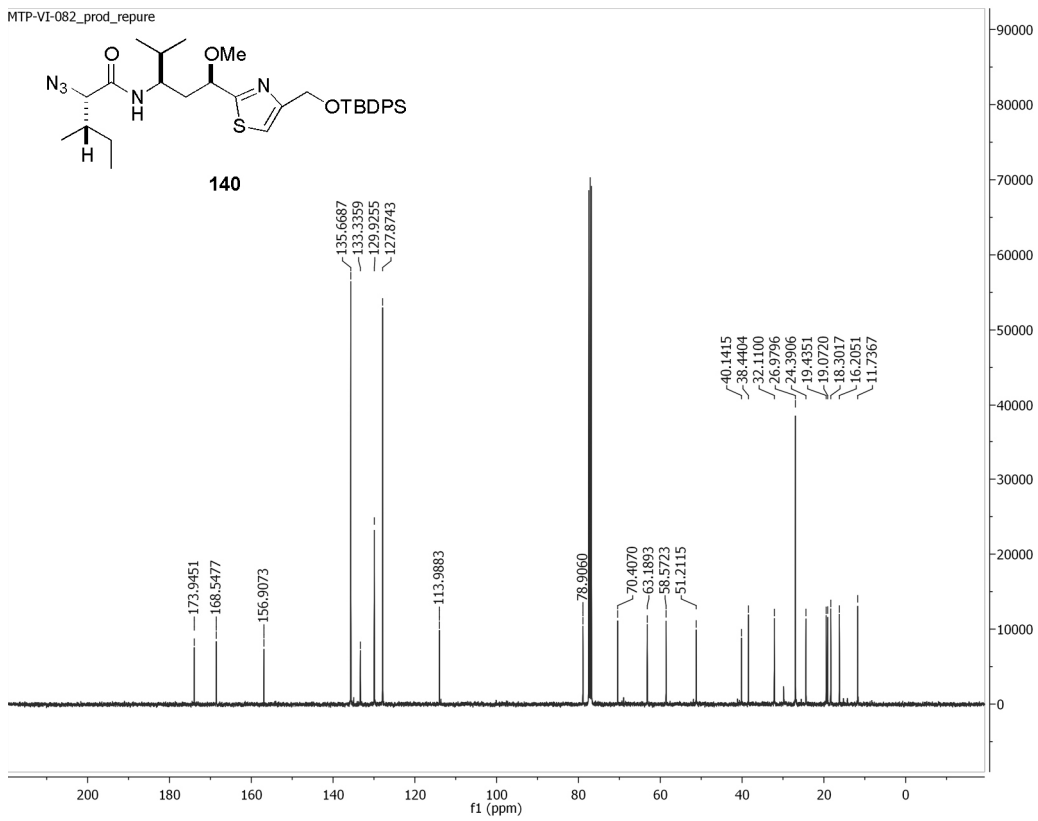
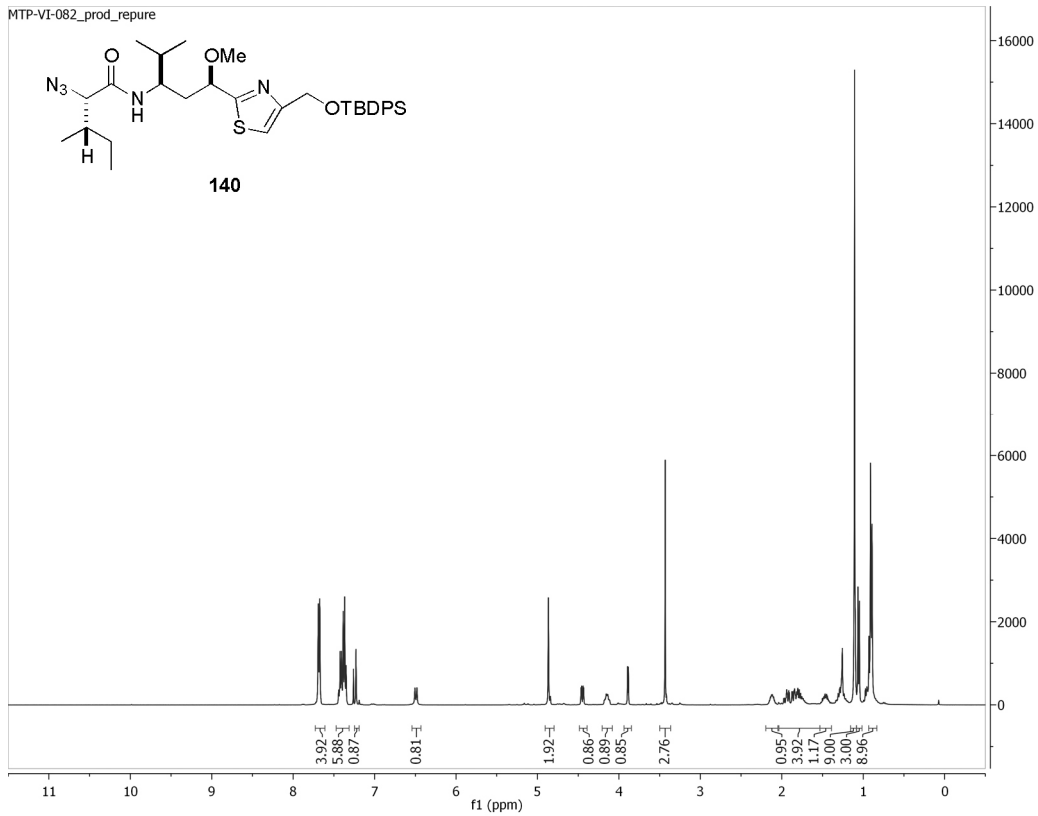


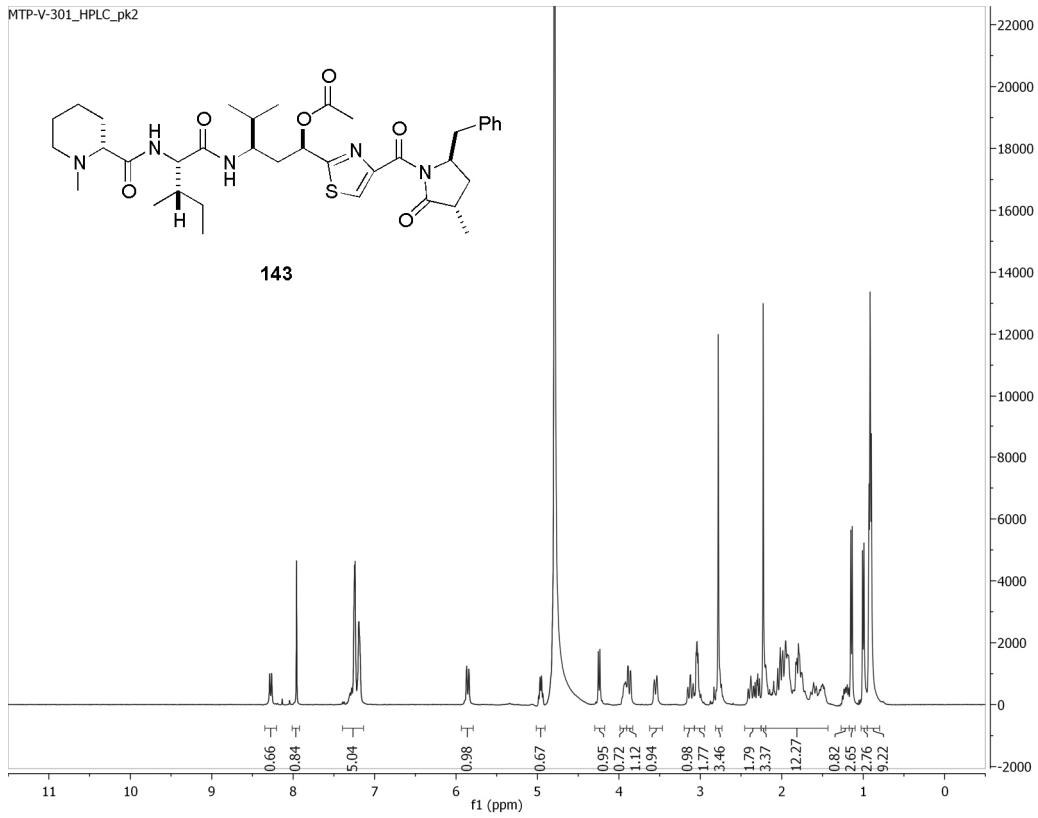


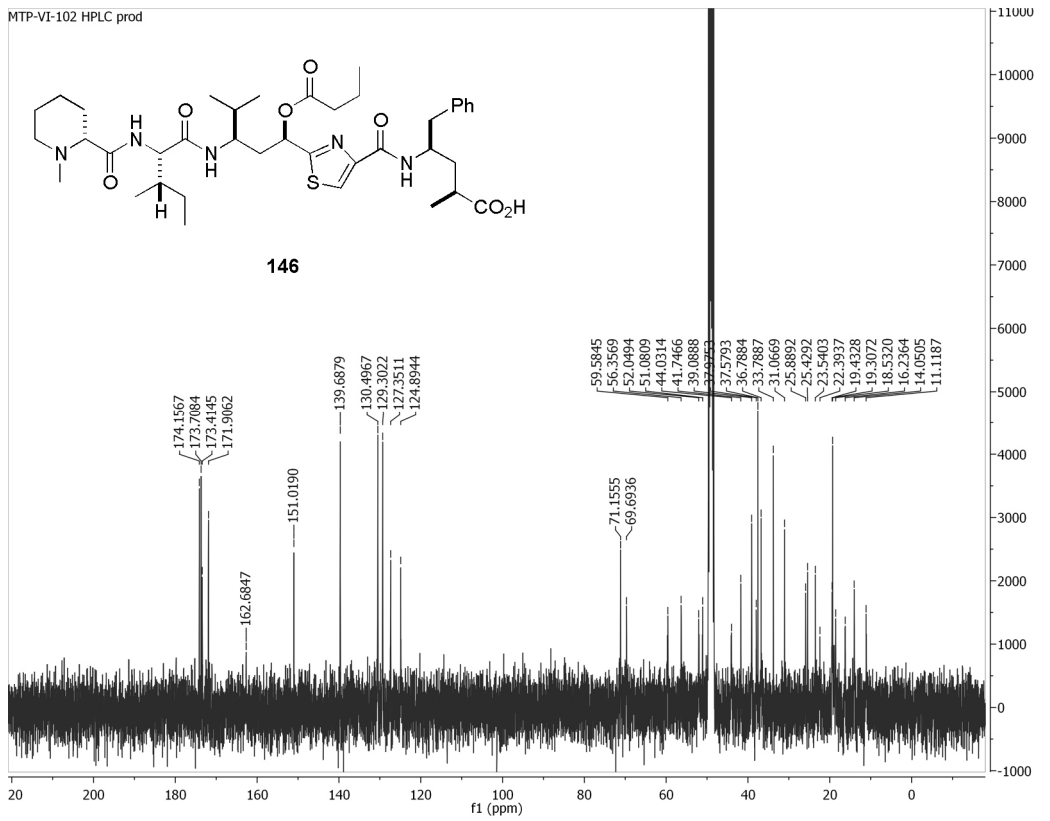
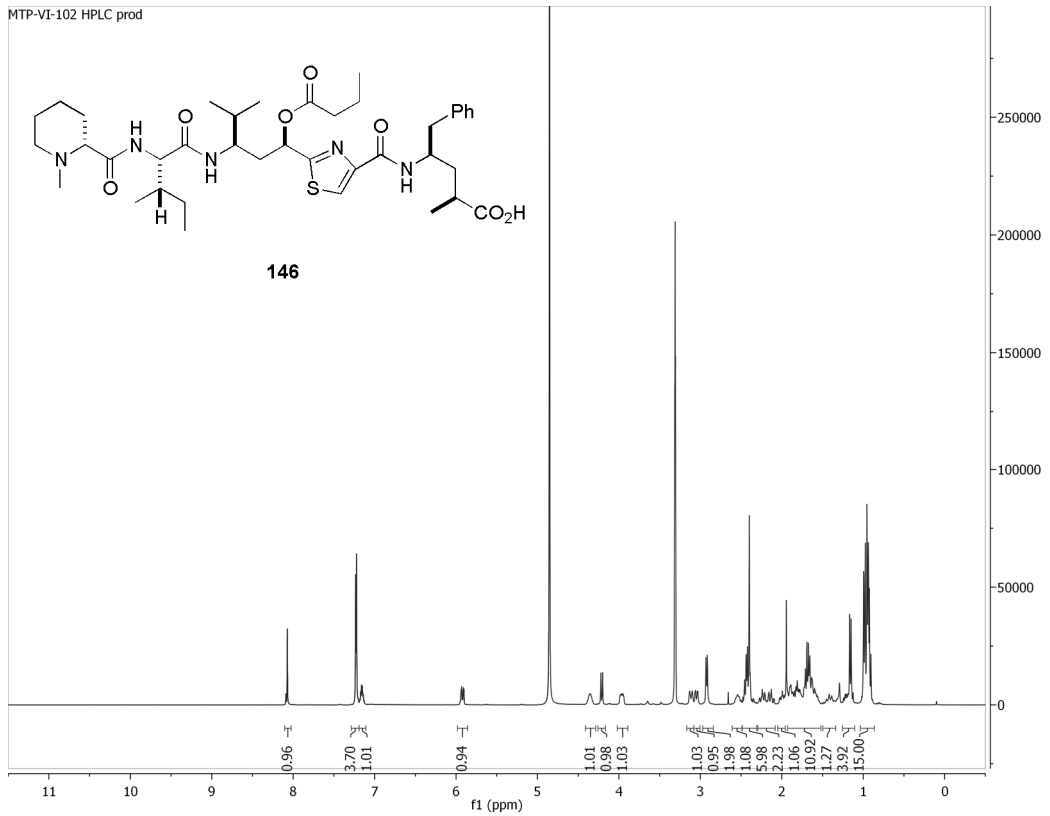




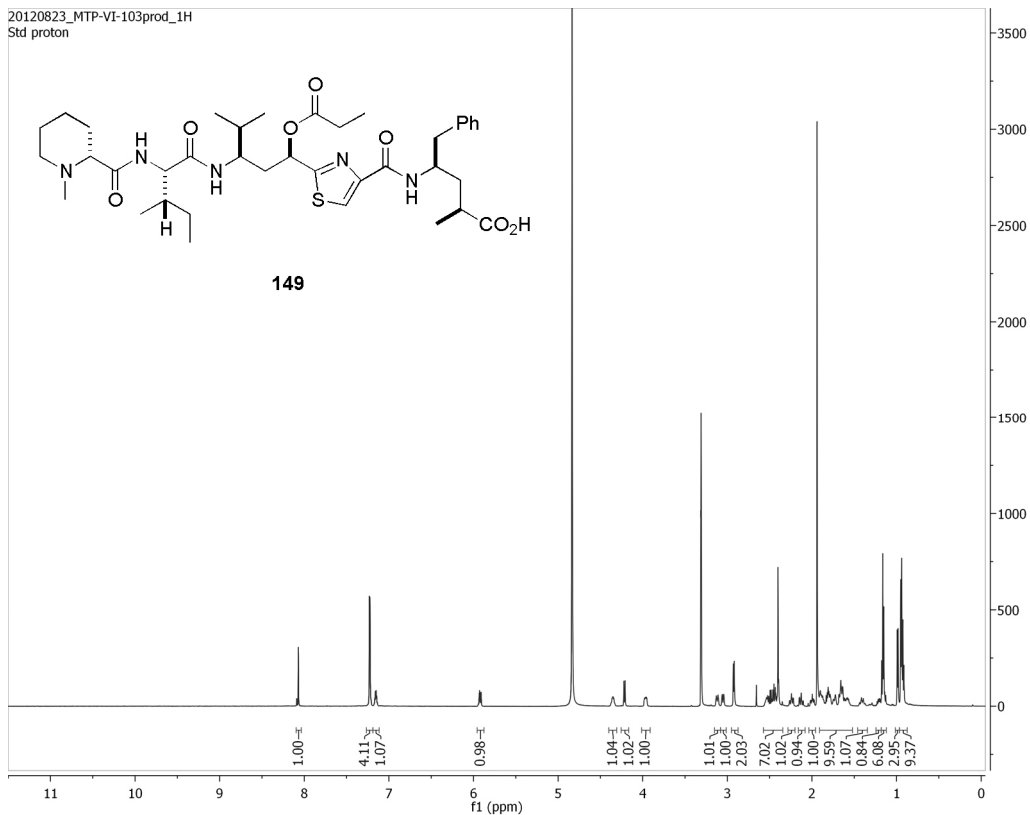








20120823_MTP-VI-103prod_1H
Std proton



20120823_MTP-VI-103prod_13C
Std carbon

